Proceedings of the Workshop on Physics at the Main Injector

May 16-18, 1989

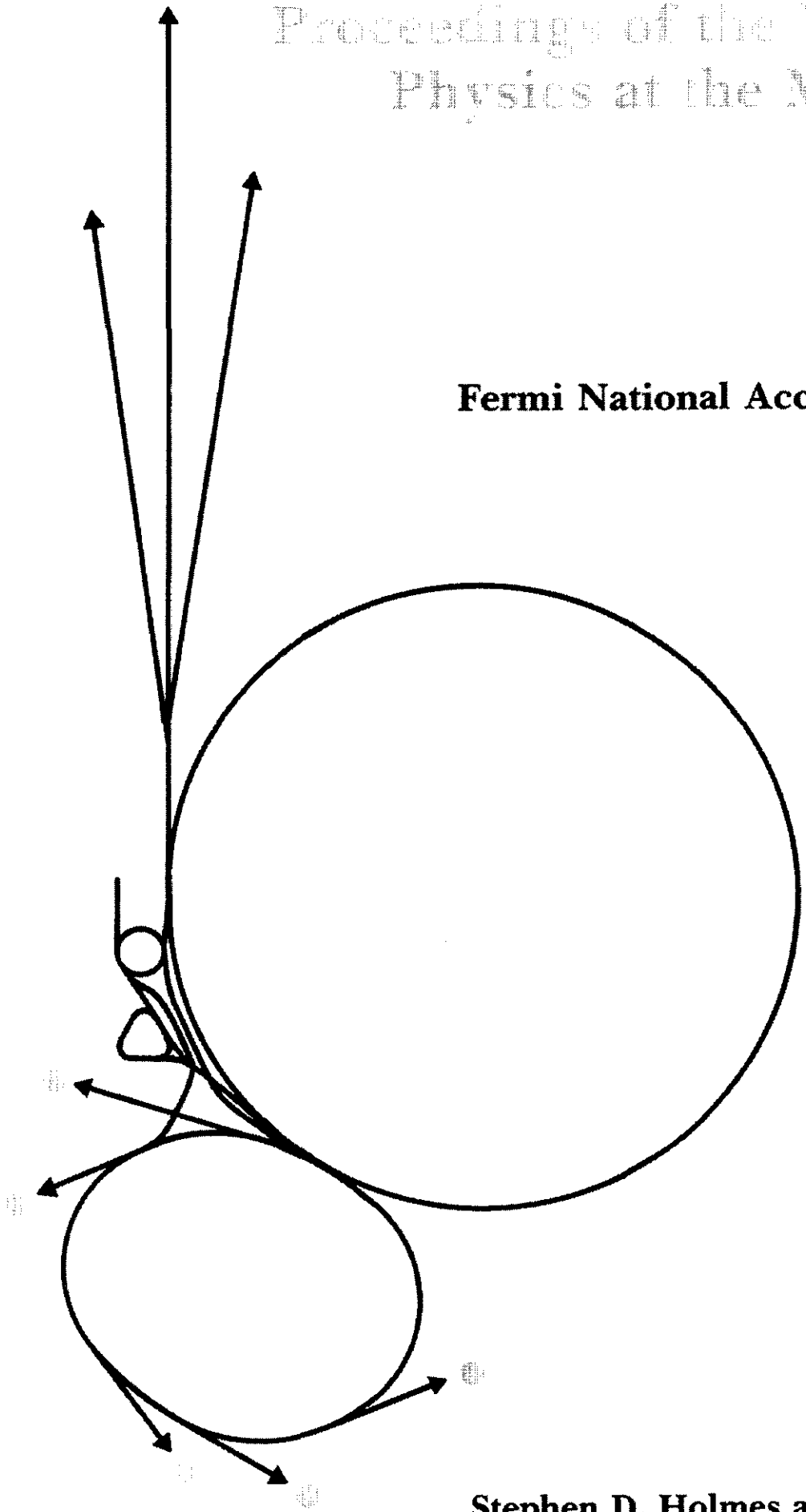

Fermi National Accelerator Laboratory
Batavia, Illinois

Edited by
Stephen D. Holmes and Bruce D. Winstein

TM-1715

Proceedings of the Workshop on Physics at the Main Injector

held at

Fermi National Accelerator Laboratory
Batavia, Illinois
May 16-18, 1989

Editors: Stephen D. Holmes and Bruce D. Winstein

Operated by Universities Research Association, Inc., under contract with the United States Department of Energy

Proceedings of the Workshop on Physics at the Main Injector

held at

Fermi National Accelerator Laboratory
Batavia, Illinois
May 16-18, 1989

PREFACE

The Fermilab Main Injector is a newly proposed accelerator to replace the existing Main Ring. Fermilab has proposed this machine primarily as a means of providing a fiftyfold increase in the luminosity available in the proton-antiproton collider. However, the high average intensity characteristics of the Main Injector (3×10^{13} extracted protons at 120-150 GeV, with a 1.5-3.0 second repetition rate) also make it a potentially attractive source of beams for certain high sensitivity K_L^0, neutrino, and antiproton experiments.

On May 16-18, 1989 a "Workshop on Physics at the Main Injector" was held at Fermilab to address such possibilities. The workshop attracted 82 registrants from the U.S., Canada, Japan, and Europe who were charged with studying the "potential uses of the newly-proposed Main Injector for very high intensity fixed target physics" and were asked to examine aspects of detector and beamline design requirements. As the initial foray into such an examination the workshop was organized in a somewhat free-for-all manner with the emphasis placed on a multitude of working groups. The working groups and their leaders are identified below:

Working Group	Group Leader(s)
Rare K Decays	
ϵ'/ϵ and $\pi^0 e^+ e^-$	J. Ritchie, H. Yamamoto
K^+ Decay in Flight	D. Marlow
CPT Tests and Flavor Violation	G. Gollin, W. Molzon
Rare K Decay Detectors	M. Schmidt
Neutral and Charged K Beams	G. Bock
Neutrinos	
$\nu_\mu \rightarrow \nu_e$ Long Baseline	M. Koshiba, K. Nishikawa
$\nu_\mu \rightarrow \nu_\tau$	N. Reay, A. Bross
$\sin^2\theta_W$ and Others	R. Bernstein, R. Brock
Antiprotons	
Experiments with Antiprotons	P. Rapidis
Polarization	
Experiments with Polarized Baryons	D. Underwood

The stage was set for the working groups by a first morning of introductory talks in which working accelerator parameters were defined, and theoretical prospects and experimental aspects were enumerated:

Main Injector Parameters	S. Holmes (Fermilab)
Prospects in K Physics	F. Gilman (Stanford)
A Detector for CP Violating and Rare K Decay Modes: Statistical and Systematic Challenges	B. Winstein (Chicago)
Neutrino Physics: A Theoretical Perspective	W. Marciano (Brookhaven)
Experimental aspects of Neutrino Physics at the Main Injector	R. Brock (Michigan State)
Antiproton Physics up to 120 GeV	G. Smith (Penn State)

The morning talks were followed by two days of working group meetings. The workshop concluded with summary reports from the working group leaders on the final afternoon.

The work of the participants is recorded in these proceedings. Included are the opening survey talks, the working group summaries, and individual contributions. In general, there was a great deal of enthusiasm for the physics reach that the Main Injector would provide, particularly in the areas of kaon and neutrino physics. Happily, during the workshop, both HEPAP and the DOE gave preliminary endorsements to the project. Many of the participants at this workshop went on to participate in the Breckenridge "Workshop on Physics at Fermilab in the 1990's" where the ideas presented here were further developed. It is hoped that these proceedings will lay the groundwork for an ongoing examination of the physics potential of the Fermilab complex over the next decade, and that five years from now experiments will be in place completing the measurements imagined in these workshops.

Stephen D. Holmes
Bruce D. Winstein

Editors

September 20, 1989

I.
Introduction

MAIN INJECTOR PARAMETERS

Stephen D. Holmes
Fermi National Accelerator Laboratory
Batavia, Illinois

Abstract

The Fermilab Main Injector is a rapid cycling, 150 GeV accelerator proposed to replace the existing Fermilab Main Ring. While designed to improve the luminosity in the p-$\bar{p}$ collider, the high average intensity capability (~2 μA) is recognized as providing an opportunity for the mounting of certain classes of High Energy Physics experiments based on beams delivered directly from the Main Injector. Performance parameters of the ring relevant to such experiments are discussed. A presently envisioned this ring could commence operations in the spring of 1994.

Overview

The Main Injector (MI) is a rapid cycling (compared to the Main Ring), 150 GeV accelerator which will replace the existing Main Ring in all its functions. The ring as proposed will be situated in its own tunnel located on the south side of the Fermilab site as shown in Figure 1. The design includes the capability of delivering slow extracted beams at 120 GeV to the switchyard area for ultimate distribution in the experimental areas.

The Main Injector is designed to enhance the luminosity achievable in the Tevatron Collider while simultaneously reducing backgrounds in the major interaction areas. The luminosity enhancement is provided by a higher antiproton productions rate, based on targetting many more protons per second, by better $\bar{p}$ transmission from large antiproton stacks, and by better transmission of high intensity proton bunches. The ring is designed to accelerate 5×10^{12} protons to 120 GeV every 1.5 seconds for $\bar{p}$ production. In this mode approximately 1/6th the circumference of the MI is filled with protons.

It has been recognized that the features of the MI which lead to enhanced luminosity in the collider also result in very high average delivered intensities which can be used directly for HEP experiments. The total intensity capability of the ring is expected to be 3×10^{13} at a cycle time of 1.9 seconds (and a 50 msec flattop). A 120 GeV slow spill capability is included in the design which would allow the 3×10^{13} protons to be spilled over 1.0 seconds with a 2.9 second cycle time. No 150 GeV slow spill capability will exist due to power and magnetic field quality constraints. However, a fast spill at 150 GeV would be possible with a cycle time of 3 seconds. The types of cycles available are summarized in Table 1.

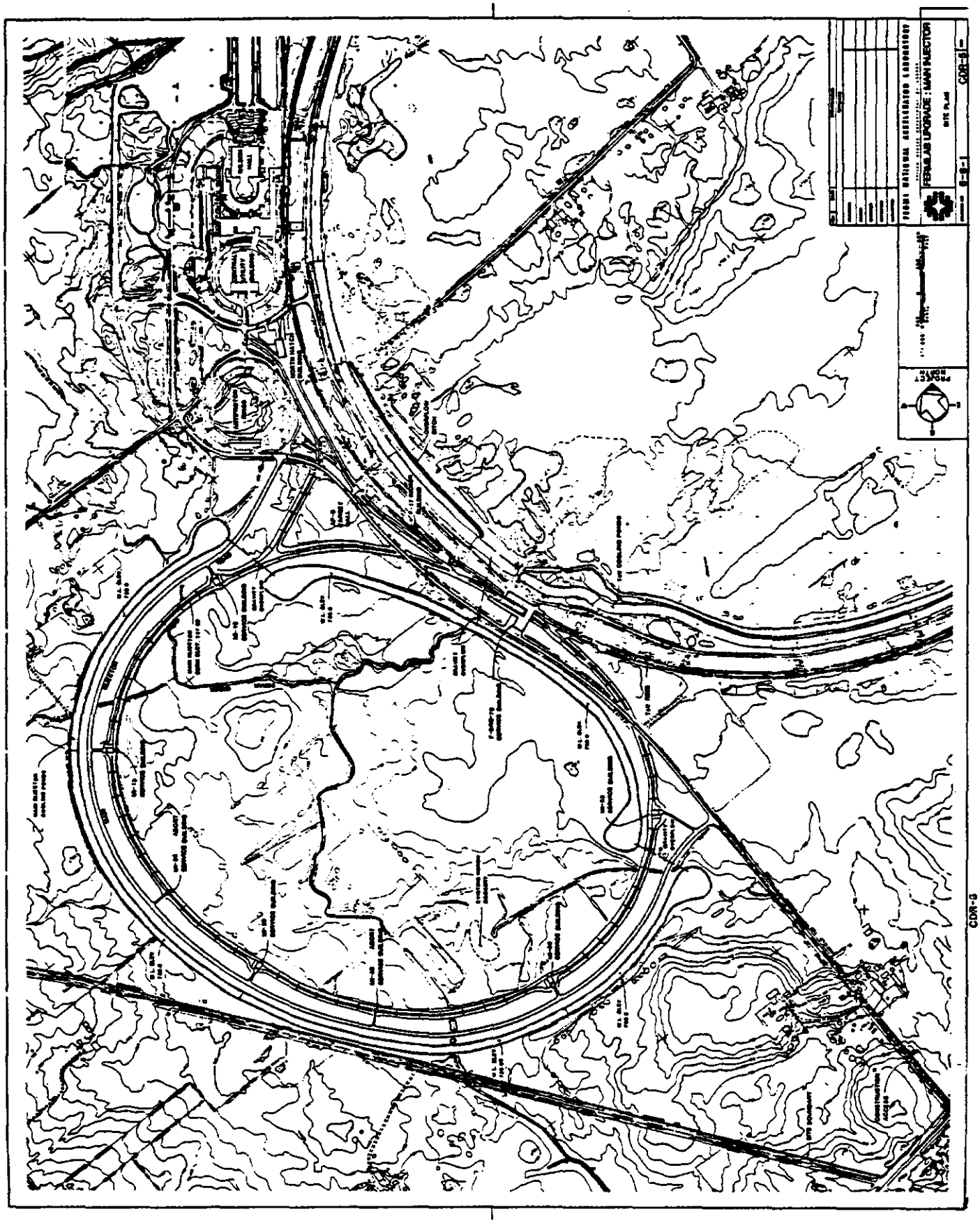
FERMILAB UPGRADE : MAIN INJECTOR
CDR-5

Table 1: Main Injector Operating Modes

Mode	Energy	Protons	Flattop	Cycle Time
$\bar{p}$ Production	120 GeV	$5x10^{12}$	0.05 sec	1.5 sec
Slow Extraction	120	$3x10^{13}$	1.0	2.9
Fast Extraction	120	$3x10^{13}$	0.05	1.9
Fast Extraction	150	$3x10^{13}$	0.05	3.0

Fermilab has requested funding for this project starting in October 1990. If funding were to commence on that date it is believed that the first beams could be delivered from the Main Injector in February of 1994.

Fixed Target Operations with the Main Injector

It is believed that beams from the Main Injector can be made available to the experimental areas simultaneous with both fixed target and collider operations of the Tevatron. Such beams could be potentially used for a wide variety of medium energy, high sensitivity experiments based on kaon, neutrino, antiproton, and/or polarized proton beams. The identification and development of scenarios for such uses is the purpose of this workshop. Up to $3x10^{13}$ primary protons are available for these experiments. Allocation of these protons to various purposes is not to be considered in this workshop--rather this task is left to future Physics Advisory Committees!

Kaons

Up to $3x10^{13}$ protons can be slow extracted over 1.0 seconds every 2.9 seconds. These 120 GeV protons can be used to produce intense secondary neutral or charged kaon beams. Higher duty factors could be made available, but at a reduced cycle rate. The primary proton beams could presumably be totally debunched before extraction.

Neutrinos

Up to $3x10^{13}$ protons can be fast extracted yielding an even higher average intensity than that described above. The cycle time depends critically on the energy of the beam. As presently designed the Main Injector will be capable of delivery of protons every 1.9 seconds at 120 GeV and every 3.0 seconds at 150 GeV.

Antiprotons

Antiprotons can also be accelerated and delivered from the Main Injector. It is expected that the antiproton accumulation rate in the Antiproton Source will be about $3x10^7$/sec following construction of the Main Injector. This would give one the ability to target 6 MI proton pulses on the antiproton production target, recover $3x10^8$ antiprotons from the Source into the Main Injector, and accelerate and extract. Obviously, an average intensity of somewhat less than $3x10^7$ antiprotons could be delivered at a specified energy in this manner. Such a scenario is incompatible with Tevatron Collider operations.

Polarized Protons

Little thought has been given to a polarized proton capability in the MI. It is hoped that workshop participants with an interest in such a capability will address not only the physics potential of such beams, but also the prospects of production and acceleration of such beams.

PROSPECTS IN K PHYSICS*

Frederick J. Gilman

Stanford Linear Accelerator Center

Stanford University, Stanford, California 94309

Abstract

Prospects for future experiments involving rare K decays are reviewed.

Introduction

The possibilities for pushing the frontier of high energy physics in K decays center on looking for processes forbidden in the Standard Model and looking for rare processes which are sensitive to the effects of virtual, heavy particles; especially those forbidden at lowest order in electroweak interactions, but allowed at one loop. It is possible now to envisage experiments with sufficient sensitivity to probe such processes at a level which will critically test the Standard Model predictions, including those that depend on the CP violating phase inherent in the three-generation quark mixing matrix.

While there is a concentration on looking for physics beyond the Standard Model, there are also interesting questions arising from the interplay of strong and electroweak interactions, and important information in pinning down the parameters inside the Standard Model from K decay experiments. As we gain knowledge about QCD corrections, hadronic matrix elements, and parameters, we can use this information to make predictions of increasing accuracy for various processes. The measurement of their rates then becomes a more sensitive test of the Standard Model or, equivalently, a search for physics outside it.

On the theoretical side, either old or new physics in K decays necessitates being acquainted with relatively few generic Feynman diagrams. There are some processes which

*Work supported by the Department of Energy, contract DE–AC03–76SF00515.

are forbidden in the Standard Model to any order. An example is leptonic flavor-changing neutral-currents. They might occur at tree-level as shown by the diagram in Fig. 1, which could represent the exchange of a flavor-changing "horizontal" gauge boson. There are also processes, which while forbidden at tree-level in the Standard Model, can occur at one-loop, as indicated by the penguin and box diagrams shown in Fig. 2. There is not much of a theoretical entry fee to understanding the basic processes, and even if you can't do the one-loop calculations yourself, you can look them up.[1]

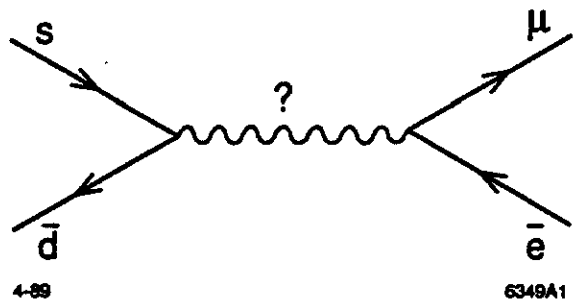

Fig. 1. Tree-level diagram involving a flavor-changing gauge boson.

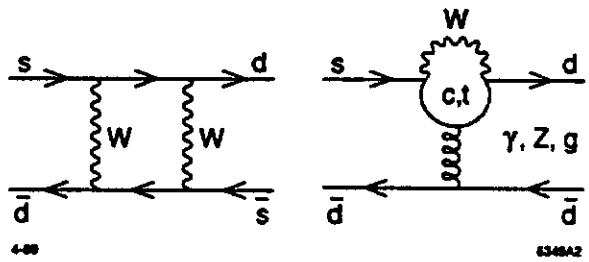

Fig. 2. One-loop diagrams giving rise to flavor-changing processes.

The "Rebirth" of K Physics

The late 1960s and early 1970s marked a peak in experiments on K decays, sparked by the discovery of CP violation.[2] This effort tailed off as many important measurements were completed and new areas of physics opened up in the 1970s at electron-positron and hadron machines.

Then, in the late 1970s and early 1980s, both theoretical and experimental developments led to a "rebirth" of K physics. On the theoretical side, the establishment of gauge theories for the strong and electroweak interactions provided a well-defined basis for calculations. The three-generation Standard Model could be used to make predictions of what, by definition, was inside, and by its complement, outside the Standard Model. The question of "who ordered the muon" was generalized to "who ordered three-generations with particular values of masses and mixing angles," and attention was directed at interactions which would connect quarks and leptons of different generations, producing flavor-changing neutral currents. It was realized that not only did the three-generation model provide an origin for CP violation in the nontrivial phase in the quark mixing matrix, but that CP violation should affect the K° decay amplitude as well as the $K^\circ - \bar{K}^\circ$ mass matrix, resulting in values of ϵ'/ϵ in the 10^{-3} to 10^{-2} range.[3] There were also predictions for short-distance contributions to a number of other rare K decay amplitudes induced at one-loop, both CP conserving and CP violating.[4]

On the experimental side, great strides were made to create high flux beams, handle high data rates, incorporate "smart triggers," improve detectors (especially for photons), and be able to analyze enormous data samples. These matched, at least to some degree, the requirements in precision and rarity being demanded by the theory for incisive tests of the Standard Model. The last few years have seen the beginning of a parade of results which are the culmination of a decade of work in perfecting and performing the needed experiments. Much more is yet to come, as one can now see the possibilities for improvements which will take us to the next generation of experiments. This indeed is the point of much of this workshop.

The Rise of the Top Quark

Over the past decade, the "typical" or "best" value of the top quark mass used in theoretical papers has risen monotonically, somehow always remaining one step, or maybe

one-and-a-half steps, ahead of the experimental then-current lower bound. Values of 15, 25, 30, 45, . . . GeV have been used in various papers (some of them mine), but all of which have fallen by the wayside as experiments have been able to search at higher and higher masses. The present lower limit is around 60 GeV, below which a top quark is said[5] to be "unlikely." It seems that lower limits even higher than this will be quoted at high confidence within a few months, as the analysis of the present round of collider data (which is still being taken as I speak) is completed. An upper limit of around 200 GeV follows from analysis of neutral and charged current data and the measured W and Z masses (*i.e.*, consistency of the ρ parameter with unity).[6] Here again, we will know much more in a few months when we have a much more accurate Z mass from electron-positron colliders. I suspect that we are headed for a lower limit (or a top mass value?!) in the neighborhood of 100 GeV later this year.

The rise of the top quark mass has important consequences when we go to calculate one-loop contributions. For the penguin diagrams in Fig. 2 involving a top and charm quark and a virtual photon (the "electromagnetic penguin"); the conserved nature of the current demands a factor of q^2, the square of the four-momentum carried by the virtual photon, be present in the numerator of the amplitude. This cancels the $1/q^2$ from the photon propagator; the leading term for small (compared to M_W^2) top mass in the coefficient of the appropriate operator behaves as $\ln(m_t^2/m_c^2)$. By contrast, the "Z penguin" or "W box" involve nonconserved currents: the factor q^2 in the numerator is replaced by the square of the quark mass in the loop, and the propagator by $1/(q^2 + M_Z^2) \approx 1/M_Z^2$ or $1/M_W^2$. The corresponding coefficient behaves like $[(m_t^2/M_W^2)\ln(m_t^2/M_W^2) - (m_c^2/M_W^2)\ln(m_c^2/M_W^2)]$ when the top mass is small. In days when $m_t^2 \ll M_W^2$, it was completely justified to throw away the Z penguin and W box contributions to such amplitudes in comparison to that of the electromagnetic penguin. Not so any more. The various graphs give comparable contributions, as we will see later in specific examples. Moreover, the contributions from the top quark become the dominant ones to various rare K decays when $m_t^2 \gg M_W^2$. In

the three-generation Standard Model, as m_t rises farther and farther above M_W, more and more of one-loop K physics is top physics and we are in the interesting situation where those working at the highest energy hadron colliders are pursuing another aspect of the same physics as those working on the rarest of K decays at low energies.

25 Years After the Discovery of CP Violation

It may be disappointing that 25 years after the discovery of CP violation[2] we have not progressed to a full understanding of its origin. Nevertheless, we have made significant theoretical progress. With the advent of the three-generation Standard Model, the question after all is not any more "why is CP violated"—it would be a surprise if CP were not violated, as it would take very special choices of the mixing angles or phase to keep CP conserved.

This can be seen very explicitly by noting that the computation of any difference of rates between a given process and its CP conjugate process (or of a CP violating amplitude) always has the form (in the three-generation case):

$$\Gamma - \overline{\Gamma} \propto s_1^2 s_2 s_3 c_1 c_2 c_3 \sin\delta_{KM} = s_{12} s_{23} s_{13} c_{12} c_{23} c_{13}^2 \sin\delta_{13} \quad , \tag{1}$$

where we express things first in the original parametrization of the quark mixing matrix[7] and then in the "preferred" parametrization adopted by the Particle Data Group,[8] using the shorthand that $s_i = \sin\theta_i$ and $c_i = \cos\theta_i$. Our present experimental knowledge assures us that the approximation of setting the cosines to unity induces errors of at most a few percent. In that case the combination of factors in Eq. (1), involving the invariant measure of CP violation,[9] becomes the approximate combination,

$$s_1^2 s_2 s_3 \sin\delta_{KM} = s_{12} s_{23} s_{13} \sin\delta_{13} \quad , \tag{2}$$

which was recognized earlier as characteristic of CP violating effects in the three-generation

Standard Model.[10] This combination of factors is (after removing s_1^2, whose value is accurately known)

$$s_2 s_3 \sin\delta_{KM} \equiv s_2 s_3 s_\delta \quad ,$$

where we have used the "old" parametrization.

The Kobayashi–Maskawa factors in the difference of rates in Eq. (1) defines the "price of CP violation" in the Standard Model. This "price" must be paid somewhere. It could be that it is paid in terms of these factors being found primarily in the decay rate for the process itself, which results in a very small branching ratio, but possibly then in a large asymmetry between particle and antiparticle. On the other hand, the price could be paid by having these factors mostly in the asymmetry between particle and antiparticle decays.

The latter situation is characteristic of K decays. The smallness of CP violation, *i.e.*, that[8]

$$|\epsilon| \approx 2.28 \times 10^{-3} \quad , \tag{3}$$

can be "naturally" understood in the three-generation Standard Model, since $s_2 s_3 s_\delta$ is of order 10^{-3}. No angle has to be fine tuned to be especially small or especially large in order to get a number of this magnitude.

This same factor of $s_2 s_3 s_\delta$ pervades all CP violation observables in the K system, so it is then not so surprising that after 25 years the total evidence for CP violation in Nature consists of a nonzero value of ϵ, and one statistically significant measurement[11] of a nonzero value of the parameter ϵ', representing CP violation in the $K \to \pi\pi$ decay amplitude itself. Experiments at Fermilab[12] and at CERN[11] are continuing with the aim of reducing the statistical and systematic errors.

Such a value[11] of ϵ' is consistent[13–15] with the three-generation Standard Model. Unfortunately, this is not a very strong statement because of our lack of knowledge both on the experimental and theoretical fronts:

- The hadronic matrix elements of the penguin operators, upon which the prediction of ϵ' depends, are fairly uncertain. Definitive results will presumably come from lattice QCD calculations which still seem several years away.
- The predictions depend on the value of $s_2 s_3 s_\delta$, which in turn depends (aside from another hadronic matrix element) on m_t through imposing the constraint of obtaining the experimental value of ϵ. Very roughly, as m_t goes up, the range allowed for $s_2 s_3 s_\delta$ goes down, and so does the prediction for ϵ'.
- Also as m_t rises, the contributions from "Z penguin" and "W box" diagrams begin to be significant. For sufficiently large m_t, a recent calculation[16] contends that most of the usual (strong) penguin contribution to ϵ' can be cancelled in this way.

There is good reason to hope that experimental and theoretical progress over the next few years will clarify these points. But even if the situation at that time is that the measured value of ϵ' is consistent with the three-generation Standard Model, it is unlikely to be regarded as conclusive. We would demand additional evidence: A single set of Kobayashi–Maskawa angles (including the phase) must be able to fit several different processes which exhibit CP violating effects, providing a redundant check on the theory.

There are several ways to get this additional evidence; none of them is easy. One is to look for CP violating effects in the B meson system. Here the CP violating asymmetries potentially can be very large—of order 10^{-1} or more in some rare modes, rather than the order 10^{-3} effects in the neutral K mass matrix. The sheer numbers of B mesons estimated to be necessary to get a statistically significant effect put this exciting possibility many years in the future.[17]

Another way is to consider other K decays where CP violating effects, although very small, may occur with a different weighting (from that in $K \to \pi\pi$) between effects originating in the mass matrix and in the decay amplitude. Although these experiments are also very difficult, there is the advantage of high intensity beams and sophisticated detectors already in existence to perform the measurements of ϵ' and search for rare K decays. Possible

K decays which come to mind include $K \to 3\pi$, $K \to \gamma\gamma$, and $K \to \pi\pi\gamma$,[18–20] and especially $K_L \to \pi^0\ell^+\ell^-$ and $K_L \to \pi^0\nu\overline{\nu}$. It is the latter route of K decays which falls within the jurisdiction of this talk and will be discussed below. If, on the contrary, the Standard Model cannot account for the results of these experiments, so much the better—we'd have evidence for physics beyond the three-generation Standard Model.

Physics Prospects for Some Rare K Decays

We will start with processes which are already measured and generally have larger rates, and move toward those with smaller branching ratios, saving the (almost?) impossible experimental measurements for the end—somehow these are also the most interesting theoretically. The decay modes discussed below are only a subset of those of interest, governed by personal prejudice and the limits of space and time. In particular, neither $K \to \mu e$ and $K \to \pi\mu e$, which involve lepton flavor-changing neutral currents and are forbidden in the Standard Model,[21] nor CP violating effects in $K \to 3\pi$, $K \to \gamma\gamma$, and $K \to \pi\pi\gamma$, are discussed here.

$K^\circ - \bar{K}^\circ$ Mixing

The grandfather of all the calculations of amplitudes which are forbidden in lowest order of the electroweak theory is that of the off-diagonal elements of the $K^\circ - \overline{K^\circ}$ mass matrix which generate the $K_L - K_S$ mass difference and ϵ. This still provides the tightest constraint on quark flavor-changing neutral currents (provided, of course, that they contribute to this process). The one-loop, short-distance contribution to ϵ has been already alluded to in our discussion of CP violation.

$K^+ \to \pi^+\ell^+\ell^-$ and $K_S \to \pi^0\ell^+\ell^-$

Both of these processes receive short-distance contributions from the "electromagnetic penguin" with a charm quark in the loop. However, there are very large QCD corrections,[22] (so big as to change the sign of the amplitude) and the result is very untrustworthy. Not

surprisingly, for the real, CP conserving, part of the amplitude which enters both these processes, it is necessary to understand significant long-distance contributions. These may be best calculable in chiral perturbation theory.[23]

The measured branching ratio for $K^+ \to \pi^+ e^+ e^-$ is[8] $2.7 \pm 0.5 \times 10^{-7}$. We may expect hundreds, if not thousands, of events from ongoing experiments, as well as some events of $K^+ \to \pi^+ \mu^+ \mu^-$. The predicted branching ratio for $K_S \to \pi^0 \ell^+ \ell^-$ is in the neighborhood of several times 10^{-9}, and will be of importance both for a check on the chiral perturbation theory calculations[23] and for CP violation in the decay, $K_L \to \pi^0 \ell^+ \ell^-$, to be discussed later.

$\underline{K^+ \to \pi^+ \nu \bar{\nu}}$

Here the short-distance contribution from charm and especially top quarks in "Z penguin" and "W box" graphs provides the dominant contribution to the amplitude: all the estimates of long distance effects show them to be negligible.[24] The QCD corrections are moderate in magnitude. They particularly need to be applied to the contribution of the charm quark. The original QCD corrections,[25] have been recently updated to the case where the top mass is comparable to M_W.[26] The resulting branching ratio for $K^+ \to \pi^+ \nu_e \bar{\nu}_e$ is shown in Fig. 3, with the dashed lines representing upper and lower bounds (given our present freedom in choosing Kobayashi–Maskawa parameters, particularly V_{td}) without QCD corrections and the solid lines giving the corresponding bounds with those corrections.[26] The branching ratio ranges between about 0.2 and 2×10^{-10} per neutrino flavor.

The upper limit on this process has recently been considerably improved to 3×10^{-8} by a dedicated Brookhaven experiment.[27] There are prospects of getting to the 10^{-9} level in the next year, and eventually reaching a sensitivity where there should be a few events if the Standard Model gives the correct rate. In the meantime there is a large window still left open for new physics between where we are now and the Standard Model prediction.

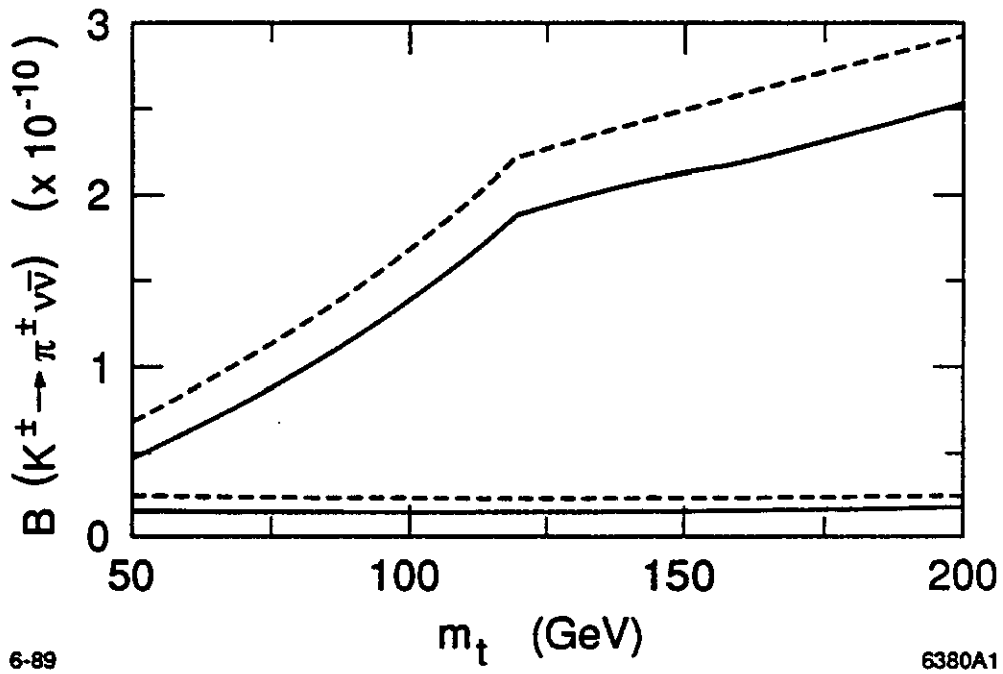

Fig. 3. The maximum and minimum of the branching ratio (per neutrino flavor) for $K^{\pm} \rightarrow \pi^{\pm}\nu\bar{\nu}$ without (dashed curve) and with (solid curve) QCD corrections ($\Lambda_{QCD} = 150$ MeV). From Ref. 26.

$\underline{K_L \rightarrow \pi^0 \ell^+ \ell^-}$

Another K decay in which it is possible to observe CP violation and which has emerged as the object of concentrated theoretical and experimental study is $K_L \rightarrow \pi^0 e^+ e^-$. If we define K_1 and K_2 to be the even and odd CP eigenstates, respectively, of the neutral K system, then $K_L \rightarrow \pi^0 e^+ e^-$ has three contributions:

(1) Through a two-photon intermediate state:

$$K_2 \rightarrow \pi^0 \gamma\gamma \rightarrow \pi^0 e^+ e^- \quad .$$

This is higher order in α, but is CP conserving.

(2) Through the small (proportional to ϵ) part of the K_L which is K_1 due to CP violation in the mass matrix:

$$K_L \approx K_2 + \epsilon K_1 \quad ,$$

$$K_1 \to \pi^0 \, \gamma_{virtual} \to \pi^0 e^+ e^- \quad .$$

We call this "indirect" CP violation.

(3) Through the large part of the K_L which is K_2 due to CP violation in the decay amplitude:

$$K_2 \to \pi^0 \, \gamma_{virtual} \to \pi^0 e^+ e^- \quad ,$$

We call this "direct" CP violation.

The question before us is the relative magnitude of these three contributions. Let us take them one at a time.

Contribution (1)

The CP conserving amplitude has a history of some uncertainty. If we consider the absorptive part of the amplitude corresponding to Fig. 4, it involves the product of the amplitude for $K_L \to \pi^0 \, \gamma\gamma$ with the QED amplitude for $\gamma\gamma \to e^+e^-$. With two real photons, there are two possible Lorentz invariant amplitudes for $K_L \to \pi^0 \, \gamma\gamma$. One is the coefficient of $F^{(1)}_{\mu\nu} \, F^{(2)}_{\mu\nu}$, which corresponds to the two photons being in a state with total angular momentum zero. Consequently, it picks up a factor of m_e when contracted with the QED amplitude, as the interactions are all chirality conserving. Its contribution to the branching ratio for $K_L \to \pi^0 e^+ e^-$ is totally negligible.[28]

The other invariant amplitude is the coefficient of a tensor which contains two more powers of momentum. One might hope for its contribution to be suppressed by angular momentum barrier factors. Because of the extra powers of momentum, in chiral perturbation

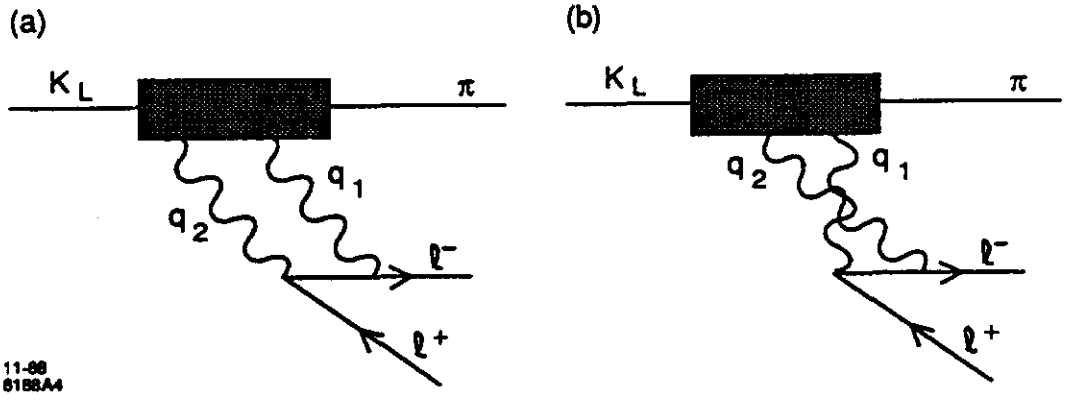

Fig. 4. Diagrams involving $K_2 \to \pi^0\gamma\gamma \to \pi^0\ell^+\ell^-$ which give a CP conserving contribution to $K_L \to \pi^0\ell^+\ell^-$.

theory this amplitude is put in by hand and its coefficient not predicted. An order of magnitude estimate may be obtained by pulling out the known dimensionful factors in terms of powers of f_π, and asserting that the remaining coupling strength should be of order one.[23] The branching ratio for $K_2 \to \pi^0\, e^+e^-$ is then of order 10^{-14}. Again, the CP conserving amplitude would make a negligible contribution to the decay rate. However, an old fashioned vector dominance, pole model predicts[29] a much bigger invariant amplitude and a consequent much bigger branching ratio of order 10^{-11}, roughly at the level as that arising from the CP violating amplitudes (see below). The applicability of such a model, however, can be challenged on the grounds that the low energy theorems and Ward identities of chiral perturbation theory are not being satisfied.[30] The consistent implementation of vector dominance with the chiral and other constraints may lead to an extra suppression

factor. The experimental upper limit on the branching ratio for $K_L \to \pi^0\gamma\gamma$ has very recently been considerably improved,[31] and now is only a few times larger than some of the predictions.[29,23] In the future, we might have not only a measurement of the branching ratio, but a Dalitz plot distribution which could help distinguish between models. The final answer for this amplitude remains to be seen both theoretically and experimentally.

Contribution (2)

We may estimate the contribution to the decay rate from the amplitude induced by "indirect" CP violation by using the identity:

$$B(K_L \to \pi^0 e^+ e^-)_{\text{indirect}} \equiv$$
$$B(K^+ \to \pi^+ e^+ e^-)\,\frac{\tau_{K_L}}{\tau_{K^+}} \times \frac{\Gamma(K_1 \to \pi^0 e^+ e^-)}{\Gamma(K^+ \to \pi^+ e^+ e^-)}\,\frac{\Gamma(K_L \to \pi^0 e^+ e^-)_{\text{indirect}}}{\Gamma(K_1 \to \pi^0 e^+ e^-)} \quad . \tag{4}$$

Experimental values[8] of 2.7×10^{-7} and 4.2 may be inserted for the first two factors on the right-hand side. The last factor is $|\epsilon|^2$ by the definition of what we mean by "indirect" CP violation in the convention where $A_0(K \to \pi\pi)$ is real. The third factor, in which $\Gamma(K_1 \to \pi^0 e^+ e^-)$ is the undetermined quantity, can be measured directly one day. As discussed previously, it has considerable theoretical uncertainties due to long-distance contributions. The ratio has a value of one if the transition between the K and the π is $\Delta I = 1/2$, as is the case for the short-distance amplitude which involves a transition from a strange to a down quark. For $\Delta I = 3/2$, the corresponding value is 4. With both isospin amplitudes present and interfering, any value is possible.[32] Eventually, an experimental measurement of $\Gamma(K_S \to \pi^0 e^+ e^-)$ will take all the present Model dependence away. For now, using a value of unity for this factor makes

$$B(K_L \to \pi^0 e^+ e^-)_{\text{indirect}} = 0.58 \times 10^{-11} \quad . \tag{5}$$

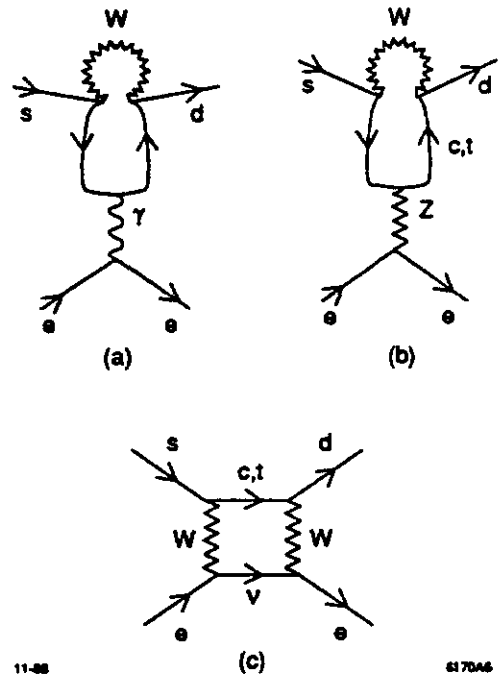

Fig. 5. Three diagrams giving a short distance contribution to the process $K \to \pi\ell^+\ell^-$: (a) the "electromagnetic penguin;" (b) the "Z penguin;" (c) the "W box."

Contribution (3)

The amplitude for "direct" CP violation comes from penguin diagrams with a photon or Z boson replacing the usual gluon and also from box diagrams with quarks (of charge 2e/3), leptons (neutrinos) and W bosons as sides, as shown in Fig. 5. For values of $m_t \ll M_W$, it is the "electromagnetic penguin" that gives the dominant short-distance contribution to the amplitude, which is summarized in the Wilson coefficient of the appropriate operator,

$$Q_{7V} = \alpha \left[\bar{s}\gamma_\mu(1-\gamma_5)d\right]\left(\bar{e}\gamma^\mu e\right) \quad ,$$

and which behaves like $\ell n(m_t^2/m_c^2)$. The Z penguin and W box graph contributions are "suppressed" by a power of m_t^2/M_W^2. Here is another example of where values of $m_t \sim M_W$ allow the "Z penguin" and "W box" contributions to become comparable to that of the "electromagnetic penguin" and to bring in another operator,

$$Q_{7A} = \alpha \left[\bar{s}\gamma_\mu(1-\gamma_5)d\right]\left(\bar{e}\gamma^\mu\gamma_5 e\right) \quad .$$

The QCD corrections are substantial for the "electromagnetic penguin" contribution and have been redone for the case[33,34] when $m_t \sim M_W$. The top quark contributions from the "Z penguin" and "W box" live up at the weak scale and get only small QCD corrections.

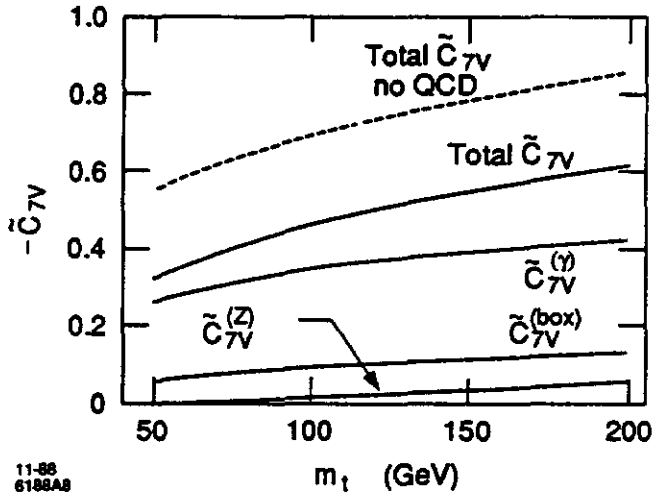

Fig. 6. Contributions to the coefficient $\tilde{C}_{7V}$ from each of its components, the "electromagnetic penguin," the "Z penguin" and the "W box" diagrams and the total $\tilde{C}_{7V}$ with QCD corrections (solid curves) with $\Lambda_{QCD} = 150$ MeV, and the total coefficient without QCD corrections (dashed curve) as a function of m_t. From Ref. 33.

The CP violating amplitude in which we are interested is proportional to the imaginary part of the Wilson coefficients and thence the difference of the contributions from the top and charm quarks:

$$ImC_7 \;=\; s_2 s_3 s_\delta \left(\tilde{C}_{7,t} - \tilde{C}_{7,c}\right) , \tag{6}$$

where the tilde indicates that the Kobayashi–Maskawa factor has been removed from the coefficient. As can be seen in Fig. 6, the coefficient $\tilde{C}_{7V}$ comes largely from the "electromagnetic penguin," even after its reduction from QCD corrections. This would not be the case if the Z couplings to charged leptons were not small due to the particular value for $\sin^2\theta_W$ chosen in Nature. On the other hand, the "electromagnetic penguin" cannot contribute to

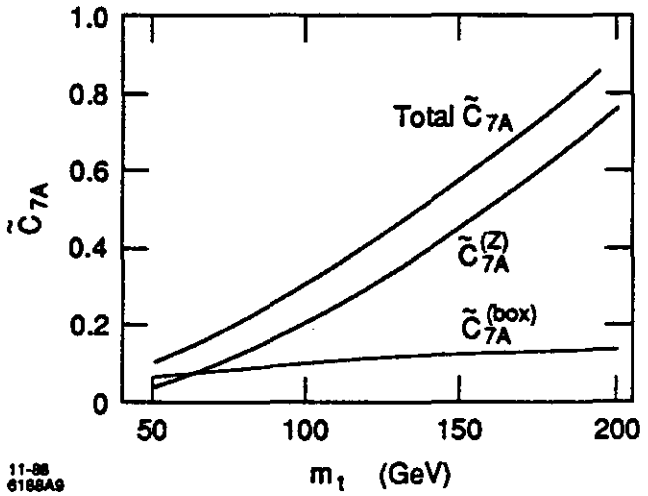

Fig. 7. Contributions to the coefficient $\tilde{C}_{7A}$ from the "Z penguin" and "W box" diagrams as a function of m_t. From Ref. 33.

C_{7A}, and here it is the "Z penguin" which gives the dominant contribution, as shown in Fig. 7.

The overall decay rate due to these "direct" CP violating amplitudes can be obtained by relating the hadronic matrix elements of the operators Q_{7V} and Q_{7A} to that which occurs in K_{e3} decay. Then, we find that

$$B(K_L \to \pi^0 e^+ e^-)_{direct} \;=\; 1.0 \times 10^{-5}\,(s_2 s_3 s_\delta)^2 \;\left[|\tilde{C}_7|^2 + |\tilde{C}_{7A}|^2\right] \quad . \tag{7}$$

The last factor ranges[33] between about 0.1 and 1.0, and as $s_2 s_3 s_\delta \leq 2.5 \times 10^{-3}$ and is typically of order 10^{-3}, the corresponding branching ratio induced by this amplitude alone for $K_L \to \pi^0 e^+ e^-$ is around 10^{-11}. Note that when $m_t \gtrsim 150$ GeV, the contribution from C_{7A} overtakes that from C_{7V}, and it is the "Z penguin" and "W box," coming from the top quark with small QCD corrections, which dominate the decay rate.

Thus it appears at this point that the contributions from the CP conserving, "indirect" CP violating, and "direct" CP violating amplitudes could all be comparable. The weighting of the different pieces in this decay is entirely different from that in $K \to \pi\pi$. The present

experimental upper limit[35,36] is 4×10^{-8}, with prospects of getting to the Standard Model level of around 10^{-11} in the next several years. Hopefully, over the next few years the CP conserving and "indirect" CP violating amplitudes will be pinned down much better, permitting an experimental measurement of this decay to be interpreted in terms of the magnitude of the "direct" CP violating amplitude.

$\underline{K_L \to \pi^0 \nu\bar{\nu}}$

Having descended to miniscule branching ratios, we now add the impossible in detection: the decay $K_L^0 \to \pi^0 \nu_\ell \bar{\nu}_\ell$ is an even more striking example of a process in which the relative size of various contributions to the decay rate are totally different[37] than in $K \to \pi\pi$. There is, of course, neither an "electromagnetic penguin" nor a two-photon, CP conserving, contribution to the amplitude. Furthermore, the "indirect" CP violation arising from the neutral K–mass matrix gives a negligible contribution to the decay rate. That leaves us with just the "Z penguin" and "W box," and the V–A character of the gauge boson couplings to neutrinos allows only the operator:

$$Q_\nu = \frac{e^2}{4\pi} \left[\bar{s}_\alpha \gamma_\mu (1-\gamma_5) d_\alpha\right] \left[\bar{\nu}_\ell \gamma^\mu (1-\gamma_5) \nu_\ell\right] \quad . \tag{8}$$

Being CP violating, it is the imaginary part of C_ν that is required:

$$Im\ C_\nu \ = \ (s_2 s_3 s_\delta)\ (\widetilde{C}_{\nu,t} - \widetilde{C}_{\nu,c}) \quad , \tag{9}$$

which is totally dominated by the top quark contribution. The branching ratio (per neutrino flavor) is

$$B(K_L^0 \to \pi^0 \nu_\ell \bar{\nu}_\ell) \ \approx \ 2.1 \times 10^{-5} \left(s_2 s_3 s_\delta\right)^2 \ |\widetilde{C}_{\nu,t} - \widetilde{C}_{\nu,c}|^2 \quad , \tag{10}$$

with the latter quantity shown in Fig. 8. Again, as $s_2 s_3 s_\delta$ is of order 10^{-3}, the branching ratio with three-generations of neutrinos is of order 10^{-11}. The QCD corrections to the t–quark contribution should be small, making this theoretically an ideal decay in which to

study CP violation in the decay amplitude. Experimentally, the problems are perhaps best represented by the statement that nobody has yet shown that a measurement of this decay is absolutely impossible.

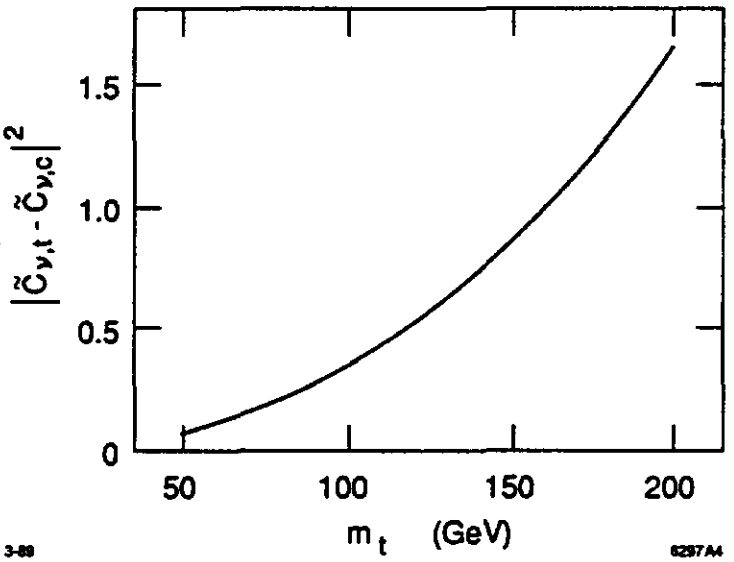

Fig. 8. The quantity $|\widetilde{C}_{\nu,t} - \widetilde{C}_{\nu,c}|^2$, which enters the branching ratio for the CP violating decay $K_L \to \pi^0 \nu_\ell \bar{\nu}_\ell$, as a function of m_t. From Ref. 26.

References

1. T. Inami and C. S. Lim, Prog. Theor. Phys. **65** (1981) 297 and *Erratum*, **65** (1981) 1772.
2. J. H. Christenson, J. W. Cronin, V. L. Fitch, and R. Turlay, Phys. Rev. Lett. **13** (1964) 138.
3. F. J. Gilman and M. B. Wise, Phys. Lett. **83B** (1979) 83;
   Phys. Rev. **D20** (1979) 2392.
4. See, for example, the recent review of J. S. Hagelin and L. S. Littenberg, MIU–THP–89/039 (1989), to be published in Prog. Part. Nucl. Phys.
5. UA1, UA2, and CDF, any talk in early 1989.
6. U. Amaldi *et al.,* Phys. Rev. **D36** (1987) 1385;
   G. Costa *et al.,* Nucl. Phys. **B297** (1988) 244.
7. M. Kobayashi and T. Maskawa, Prog. Theor. Phys. **49** (1973) 652.
8. Particle Data Group, Phys. Lett. **204B** (1986) 1.
9. C. Jarlskog, Phys. Rev. Lett. **55** (1985) 1839;
   Z. Phys. **29** (1985) 491.
10. L.-L. Chau and W.-Y. Keung, Phys. Rev. Lett. **53** (1984) 1802.
11. H. Burkhardt *et al.,* Phys. Lett. **206B** (1988) 169.
12. M. Woods *et al.,* Phys. Rev. Lett. **60** (1988) 1695
13. M. A. Shifman, Proceedings of the 1987 International Symposium on Lepton and Photon Interactions at High Energies, Hamburg, July 27–31, eds. W. Bartel and R. Ruckl, (North Holland, Amsterdam, 1988) p. 289.
14. F. J. Gilman, International Symposium on the Production and Decay of Heavy Flavors, Stanford, September 1–5, 1987, eds. E. Bloom and A. Fridman (New York Academy of Sciences, New York, 1988), vol. 535, p. 211.

15. G. Altarelli and P. J. Franzini, CERN preprint CERN–TH–4914/87 (1987), unpublished.

16. J. M. Flynn and L. Randall, Phys. Lett. **224B** (1989) 221.

17. For reviews of the theoretical estimates of CP violation in B decay and the experimental possibilities, see K. J. Foley *et al.*, Proceedings of the Workshop on Experiments, Detectors, and Experimental Areas for the Supercollider, Berkeley, July 7–17, 1987, eds. R. Donaldson and M. G. D. Gilchriese (World Scientific, Singapore, 1988), p. 701; and Proceedings of the Workshop on High Sensitivity Beauty Physics at Fermilab, Fermilab, November 11–14, 1987, eds. A. J. Slaughter, N. Lockyer, and M. Schmidt (Fermilab, Batavia, 1988).

18. L.-F. Li and L. Wolfenstein, Phys. Rev. **D21** (1980) 178.

19. L.-L. Chau and H.-Y. Cheng, Phys. Rev. Lett. **54** (1985) 1768, and Phys. Lett. **195B** (1987) 275;
J. O. Eeg and I. Picek, Phys. Lett. **196B** (1987) 391.

20. G. Ecker, A. Pich, and E. de Rafael, Nucl. Phys. **B303** (1988) 665.

21. See the discussions in Ref. 4 and in other papers in these proceedings, and references therein.

22. F. J. Gilman and M. B. Wise, Phys. Rev. **D21** (1980) 3150.

23. G. Ecker, A. Pich, and E. de Rafael, Phys. Lett. **189B** (1987) 363;
Nucl. Phys. **B291** (1987) 691, and **B303** (1988) 665.

24. See, for example, D. Rein and L. M. Sehgal, Phys. Rev. **D39** (1989) 3325, and references therein.

25. J. Ellis and J. Hagelin, Nucl. Phys. **B217** (1983) 189.

26. C. O. Dib, I. Dunietz, and F. J. Gilman, SLAC preprint SLAC–PUB–4840 (1989), unpublished.

27. D. Marlow, talk at the Twelfth International Workshop on Weak Interactions and Neutrinos, Ginosar, Israel, April 6–14, 1989.

28. J. F. Donoghue, B. R. Holstein, and G. Valencia, Phys. Rev. **D35** (1987) 2769.

29. L. M. Sehgal, Phys. Rev. **D38** (1988) 808;
T. Morozumi and H. Iwasaki, KEK preprint KEK–TH–206 (1988), unpublished;
J. Flynn and L. Randall, Phys. Lett. **216B** (1989) 221.

30. E. de Rafael, private communication.
See also G. Ecker *et al.,* Nucl. Phys. **B321** (1989) 311;
G. Ecker *et al.,* Phys. Lett. **223B** (1989) 425.

31. V. Papadimitriou *et al.,* Phys. Rev. Lett. **63** (1989) 28.

32. In a chiral perturbation theory calculation, G. Ecker, A. Pich, and E. de Rafael (Ref. 23) obtain two values: 0.25 and 2.5 .

33. C. Dib, I. Dunietz, and F. J. Gilman, Phys. Lett. **218B** (1989) 487;
Phys. Rev. **D39** (1989) 2639.

34. Another recent work on the subject is found in J. Flynn and L. Randall, LBL preprint LBL–26310 (1988), unpublished.

35. L. K. Gibbons *et al.,* Phys. Rev. Lett. **61** (1988) 2661.

36. G. D. Barr *et al.,* Phys. Lett. **B214** (1988) 1303.

37. L. Littenberg, Phys. Rev. **D39** (1989) 3322.

KAON PHYSICS AT THE MAIN INJECTOR

B. Winstein

Enrico Fermi Institute and the Department of Physics
The University of Chicago

Abstract

We explore the physics reach of the FNAL Main Injector ring for high sensitivity, high precision experiments on kaon decays, particularly those which violate CP symmetry. The considerable challenges of mounting an appropriate detector and reducing backgrounds in a very high rate environment are discussed. Comparisons with lower energy facilities are made.

I. The Current Status of Kaon Decay Experiments

The field of kaon decay physics continues to be rich and varied. Active programs are in progress at Brookhaven, CERN (fixed target and LEAR), KEK, and Fermilab, and at all of these laboratories, there are plans for extensions and major upgrades. In addition, at TRIUMF, there is a proposal for a dedicated "Kaon Factory" and at other places, there is thought of the construction of a so-called ϕ-factory for making correlated K_L-K_S pairs in abundance.

The present status of many of these experiments can be represented in a simple table (see Table 1). What is clear is that there are particular experiments which have traditionally been best executed with lower energy kaons (e.g., $K_L \to \mu e$, $K^+ \to \pi^+ \nu\nu$, and the measurement of the muon polarization in $K \to \pi\mu\nu$ decay) while there are others that benefit from the higher energy beams available (e.g., ϵ'/ϵ, $K_L \to \pi^0 e^+ e^-$, and $K_S \to 3\pi$).

TABLE 1 RARE K DECAY SEARCH STATUS

MODE	EXPERIMENT	RESULT	EXPECTED SENSITIVITY	COMMENTS
$K^+ \to \pi^+ +$ nothing	BNL E787	$<3\times10^{-8}$ (2 weeks)	10^{-10}	Detector works well
$K^+ \to \pi^+ \mu^+ e^-$	BNL E777	$<1.1\times10^{-9}$	1.5×10^{-10}	Limited by beam halo May pursue $K^+ \to \pi^+ e^+ e^-$ (357 events in hand) $\pi^0 \to \mu e < 8\times10^{-8}$
$K_L \to \mu e$	BNL E780	$<1.9\times10^{-9}$		Limited by beam halo
$K_L \to ee$		$<1.2\times10^{-9}$		Will pursue
$K_L \to \pi^0 e^+ e^-$		$<3.2\times10^{-7}$		$K_L \to \pi^0 e^+ e^-$ (10^{-10}) in E845
$K_L \to \mu e$	BNL E791	$<3.0\times10^{-10}$	$\sim2\times10^{-11}$	Limited by accidentals from K_L decays. May pursue $K_L \to \pi^0 e^+ e^-$. Will measure BR($K_L \to \mu\mu$)
$K_L \to \mu e$	KEK E137	$<4\times10^{-10}$	$\sim2\times10^{-11}$	Will pursue
$K_L \to ee$				$K_L \to \pi^0 e^+ e^-$ (10^{-10}), in E162
$K_S \to \pi^+ \pi^- \pi^0$	FNAL E621	$\lesssim1.5\times10^{-7}$	$\sim3\times10^{-9}$	Expected rate $\sim1.2\times10^{-9}$ Proposal for upgrade
$K_L \to \pi^0 e^+ e^-$	FNAL E731	$<4.2\times10^{-8}$	$\sim1\times10^{-8}$	
	NA31	$<4\times10^{-8}$		
$K_L \to \pi^0 e^+ e^-$	KEK 162		10^{-10}	
$K_L \to \pi^0 e^+ e^-$	FNAL P799		10^{-10} - 10^{-11}	

Note: Some results are preliminary while others are published.

II. The Case for High Energy

One could perhaps draw the conclusion that those modes with π^0's in the final state are best done at high energies and this is natural in that electromagnetic energy resolution invariably has a dominant term with a dependence of $E^{-1/2}$.

There are other reasons for higher energy beams which further thought reveals. For the measurement of ϵ'/ϵ, the most difficult mode is $K_L \to 2\pi^0$ which has as a background the copious $K_L \to 3\pi^0$ mode where one or two γ's either are missing or fuse with other γ's. The ammunition that one can bring to bear on this problem consists in good resolution, ability to reject extra "soft" γ's, and high acceptance; since the "soft" γ's are boosted to a higher laboratory energy (and in particular higher with respect to the copious minimum-ionizing backgrounds which do not scale with energy), they are easier to detect. This is illustrated in Figure 1 which displays the cleanest $K_L \to 2\pi^0$ signal to date (FNAL E731),[1] the background being less than 0.4%.

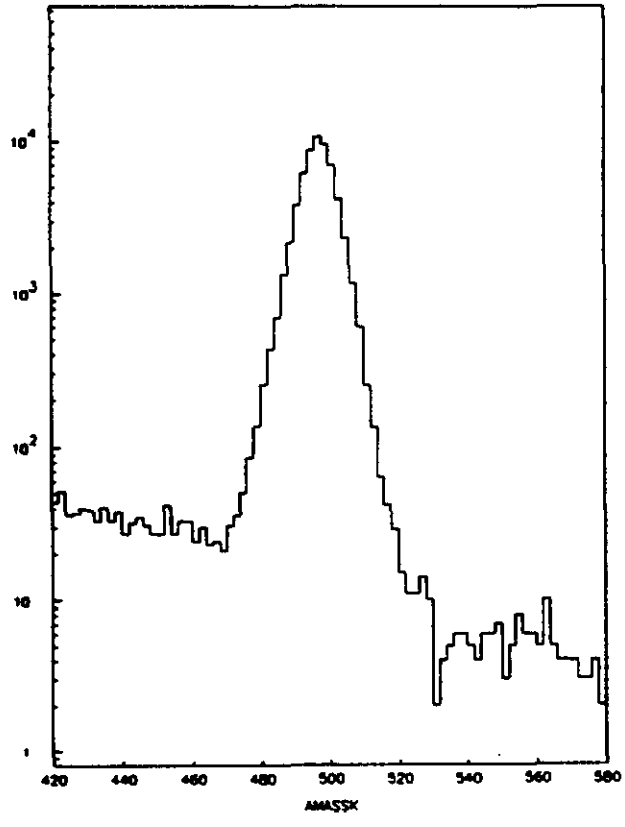

Figure 1 $M_{\pi^0\pi^0}$ for E731 (20% data analysis) for K_L decays. The background is less than 0.4%.

For the measurement of the rare mode $K_L \to \pi^0 e^+ e^-$, which is thought to be dominated[2] by direct CP violation, the major backgrounds tend to involve accidental γ's which are nearly coincident with the copious Ke_3 or $Ke_3\gamma$ decay modes. For these backgrounds, the ammunition consists in again good (energy and time) resolution, high acceptance (to recognize the other particles in an accidental event) and excellent particle identification (to reject the rate of pions faking electrons). The high energy is an advantage for the particle identification as well since TRD's are effective and they take up less valuable space thus compromising the acceptance relatively little.

III. The Near Future

At present, for the modes in question, we have the NA31 result[3] for ϵ'/ϵ; direct CP violation is claimed at the 3 sigma level. This result obviously needs confirmation and the E731 collaboration has the data in hand to determine this parameter with a statistical precision of 0.0005, enough to settle the question if indeed NA31 is correct. In addition, NA31 has completed another run in 1988 and will run again in 1989.

For the parameter η_{+-0} which governs CP Violation in 3π decays, the present sensitivity is of the order of about 10ϵ; data on tape from E621[4] will allow a determination at the level of about ϵ itself.

For the $\pi^0 e^+ e^-$ decay mode, the best limits come from FNAL[5] and CERN[6] at the 10^{-8} level. P799 at FNAL[7] should be able to reach a level between 10^{-10} and 10^{-11} in the 1992 running period.

IV. The Physics Demands

Now, we will look at what the physics demands for these modes are: we consider that "Standard-Model" sensitivities are required; however, there is always the possibility of new physics showing up at even greater levels.

Why are we considering an even more accurate determination of ϵ'/ϵ? In the case where E731 and NA31 disagree or the answer is consistent with zero, then there is a clear case for another generation of experiment. CP non-conservation is an important issue and we would not be able to say that the standard model could easily accommodate it within the Kobayashi-Maskawa framework. In parallel, we will be looking for CP violating effects with heavy

quarks but such experiments, in spite of the possibly large asymmetries, are most difficult.

Even if the experiments agree to the degree that we can say that there is an established non-zero effect, there is still an argument for doing even better. It is true that today theory can calculate the value of ϵ'/ϵ with very large uncertainty. However, with further advances on the theoretical side (lattice gauge theory, etc.) and on the experimental side (top quark mass, $b \to u$ transition) the "predictive power" will be greatly enhanced. Since we believe that CP non-conservation is a good window on physics at a very high mass scale, beyond the Standard Model, more precise measurements are clearly in order. The "Cabibbo angle" is known to about 1% and it is this precision that enables us to establish the consistency of the 3x3 weak-coupling charged current matrix. The situation in CP violation would be perhaps similar to the one concerning parity violation if the only manifestation were in the mixing of atomic energy levels: in such a case, clearly more and more refined measurements would be called for. The goal for precision on ϵ'/ϵ should be on the order of 5×10^{-5}.

For the parameter η_{+-0}, it would be satisfying to be able to establish this quantity to the level of about 10% of ϵ: at such a level of accuracy, one can begin to be sensitive to certain non-Standard Model effects.

Finally, the decay $K_L \to \pi^0 e^+ e^-$ is expected to occur at the level of about 10^{-11}. In order to effectively untangle the contributions from direct and indirect CP Violation and from the possible CP conserving $\pi^0 2\gamma$ final state, a sensitivity on the order of 10^{-13} is required.

V. The Next Step: The FNAL Main Injector

In order to reach the required level of sensitivity, especially for the $\pi^0 e^+ e^-$ decay, much more flux than is available at the Tevatron is required. The Main Injector ring can provide more than enough flux to reach these goals while maintaining a relatively high energy secondary kaon beam. In addition, it would run year-round. Some possible parameters for the incident proton beam are shown in the following Table:

Energy	120 GeV
Intensity	3×10^{13}/spill
Spill Length	1.9 sec
Repetition Rate	3.8 sec
Structure	debunched

Care must be chosen in the design of the secondary neutral Kaon beam in particular in order to reduce the effects of neutron contamination. Here we choose to employ 12rl of lead as a gamma filter and 18" of Be as a neutron moderator: this is what is used in E731 and results in about a factor of 5 reduction in kaon flux. We also use a relatively modest 6mr x 6mr beam: this corresponds to only a ±60 MeV range in transverse momentum since the mean detected Kaon energy is about 20 GeV. Under these conditions, we have the following dependence of the fluxes[8] upon targeting angle:

θ [mr]	Kaon Flux [GHz]	Neutron Flux [GHz]	Kaon Decays [MHz/20m]
0	4.9	76	174
8	3.8	14	158
16	2.7	3.2	139
20	2.2	1.9	130
24	1.9	1.3	120
32	1.5	0.7	104

Thus we see that by choosing a targeting angle around 20mr, we can reduce the neutron flux by a factor of 40 while retaining about 75% of the available kaon decays.

With such a very high kaon decay rate - one every 7ns - it is clear that the protons should be delivered as smooth as is possible: multiple kaon decays within the resolving time of the detector, typically 1ns, will comprise the major background for very high sensitivity searches. Other considerations are: it is desirable to vary the targeting angle for optimization; the (Be) target will need to be cooled; the proton beam dump should be such that the μ rate at the detector is $<10^{-7}$ per incident proton; and the neutral beam dump should be able to handle 4×10^{9} Hz of roughly 50 GeV hadrons.

VI. The Detector

We now briefly consider a model detector capable of exploiting the very high intensities available at the Main Injector. Of course a great deal of work will be required in order to completely specify its properties.

First of all, because of the 4 GHz of hadrons in the neutral beam, it is clear that there can be no detector element directly in the beam and hence there must be a vacuum pipe through the apparatus.

We will concentrate upon the higher energy part of the kaon spectrum (>15 GeV) for the reasons given above. High acceptance will dictate a large "collapsed" spectrometer. Such a detector, with active elements being 3m x 3m, is shown schematically in Figure 2. A possible configuration for the electromagnetic calorimeter is shown in Figure 3: because of the requirements of radiation hardness and precision, it appears that a highly segmented BaF_2 array is the best choice although other (less expensive) materials should be considered.

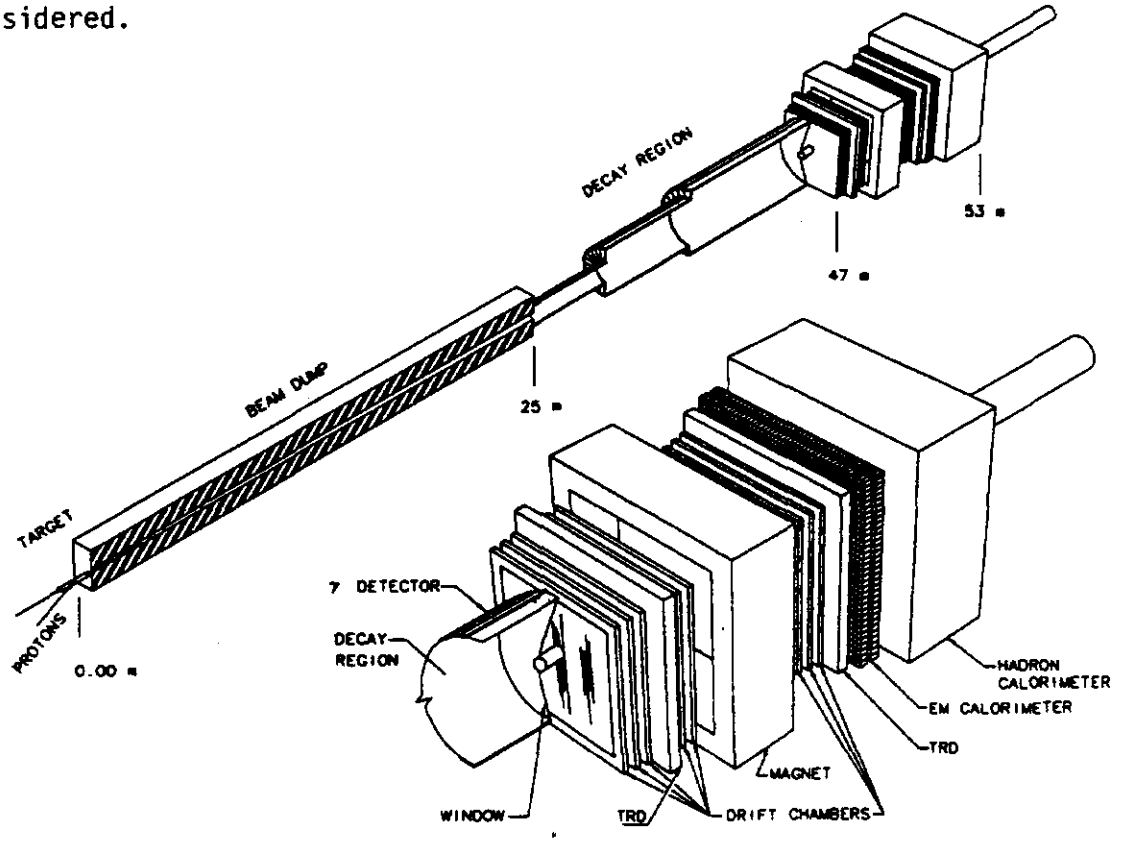

Figure 2 Model Kaon Facility at the Main injector

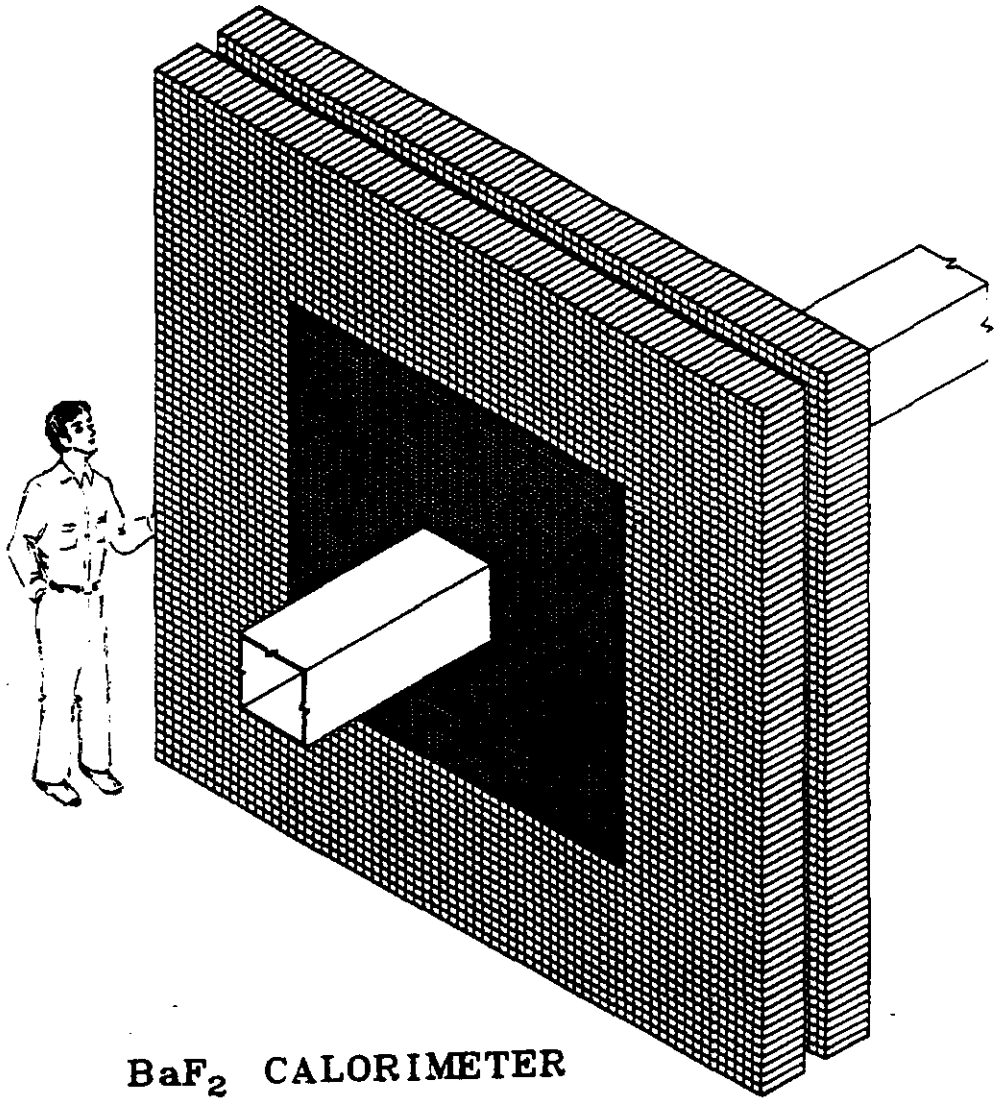

Figure 3 Possible new calorimeter for Main Injector.

This model detector has a high acceptance for four body decays; for the $\pi^0 e^+ e^-$ mode, it is 16% for decays over a 20m decay region ($P_K > 15$ GeV) where a 1 GeV γ threshold energy is assumed.

VII. Rates

The major difficulty in reaching high sensitivity will be the operation of such a detector in a very high rate environment. The singles rate in the first chamber, from Kaon decays alone, will be about 160 MHz; the rate on the hottest wire (assuming a 3mm pitch) will be about 660 KHz. Small detectors

have operated under such high rate conditions before so that it looks likely that such a detector is possible, but much work and optimization is required.

One advantage of the higher energy incident beam can be seen in that about 1/3 of the singles rates actually arise from the kaon decays of interest, namely those with momentum above 15 GeV; with a lower energy primary beam, such a favorable ratio can only be obtained by accepting lower energy kaon decays, thereby giving up the significant advantages of energy resolution and ability to reject additional decay products from either potential background or accidental events.

VIII. Sensitivity

Under the conditions outlined above, the sensitivity to the four body decay $\pi^0 e^+ e^-$ would be about 10^{-10} per hour of running. This sensitivity (for 1 hour) equals that of the best kaon experiment to date (for 1000 hrs) and thus presents over a factor of 1000 improvement, allowing for a measurement in the range of 10^{-13} to 10^{-14}. Such a sensitivity should be enough for a definitive observation of direct CP violation. Of course much work is required to convince oneself that the backgrounds, particularly from accidental kaon decays, can be reduced at this level.

For the $2\pi^0$ mode necessary for an ϵ'/ϵ determination, clearly one would not need to run under these conditions: current experiments have collected in the range of a few hundred thousand events so that a new experiment might have as a goal of order 10^7 - 10^8 events, corresponding to a sensitivity of "only" 10^{-11}. Thus one can take advantage of the greater proton flux at the Main Injector to build very small, clean, well-defined beams thereby significantly reducing a variety of systematic effects.

IX. Related Issues

Here we mention some related issues which need further work. First, it is desirable to consider a variety of measurements with K_S beams. In particular, determining the parameters governing CP violation in 3π decays, η_{000} and η_{+-0}, requires a K_S beam. In addition K_S decays to πee and $\pi\mu\mu$ are needed to disentangle the direct and indirect CP violation contributions to K^0 decay and in fact there is much to be learned from a study of the interference

between K_S and K_L decays. The beam design is most important, particularly in that one wants to be situated far closer to the production target. Second, the possible use of regenerators needs study; at 4 GHz, this is not practical but at reduced intensities (for the ϵ'/ϵ measurement), this may be the best alternative. Third, can we make use of the very large flux of charged kaons, particularly for a study of the decay $K^+ \to \pi^+\nu\nu$ "in flight?" Forth, is a sensitive search for $K_L \to \mu e$ feasible? Finally, the Main Injector opens up the possibility for far more precise tests of CPT symmetry, both in the mixing (through precise measurements of Δm, Γ_S, δ, and η_{+-}) and in the decay (Φ_{00} and Φ_{+-}) of the neutral kaon.

X. Conclusion and Experimental Challenges

The Main Injector clearly offers unique capabilities in the field of precise, high sensitivity kaon decay experiments. Such experiments provide a window on physics at very very high mass scales which in many cases are out of reach even at the SSC. However, in order to effectively exploit this capability, there are significant experimental hurdles or challenges that must be met. We close with a necessarily partial list of some of the questions that must be addressed.

1. Beam design: muons, hadronic punch through, γ filtering, soft halo particles, etc., must all be significantly reduced over levels in current neutral beams.

2. Rates and radiation damage: both calorimetry and tracking devices must be able to perform with high precision under "SSC-like" conditions.

3. Particle identification: can TRD's work reliably at more than 10^8 Hz?

4. Backgrounds: those from other decays and those from an overlap of two or more events within the resolving time of the detector need to be simulated (and eliminated!) at the 10^{-14} level.

5. Systematics: for high statistics, high precision measurements (ϵ'/ϵ and CPT symmetry tests), these will be the dominant source of uncertainty.

6. Triggering and data acquisition: tremendous rejection factors will be required.

REFERENCES

1. FNAL E731: Chicago, Elmhurst, Fermilab, Princeton, Saclay collaboration.

2. See F. Gilman, these proceedings, and references therein.

3. CERN NA31 collaboration, H. Burkhardt et al., Phys. Lett. B206, 169 (1988) ($\epsilon'/\epsilon = 0.0033 \pm 0.0011$).

4. FNAL E621: Michigan, Minnesota, Rutgers collaboration.

5. L.K. Gibbons et al., Phys. Rev. Lett. 61, 2661 (1988).

6. G.D. Barr et al., Phys. Lett. B214, 303 (1988).

7. Chicago, Elmhurst, Fermilab, Princeton collaboration.

8. A.J. Malensek, Fermilab Report FN-341.

A Theoretical Perspective on Neutrino Physics

William J. Marciano

Brookhaven National Laboratory
Upton, New York 11973

ABSTRACT

A survey of $\sin^2\theta_W$, ρ, CKM matrix, and axial-isoscalar neutral current measurments via neutrino scattering is presented. Loop effects due to heavy top or a fourth generation are described. Neutrino oscillations are discussed in a three generation mixing framework and some motivation for $\nu_\mu \to \nu_\tau$ oscillation searches is given.

Accelerator based neutrino experiments fall into two categories: 1) accurate measurements of standard model parameters and structure functions, 2) searches for neutrino oscillations. The first is part of a broad program of many diverse weak neutral and charged current measurements designed to test the validity of the standard $SU(3)_C \times SU(2)_L \times U(1)$ model. The hope is to eventually see a deviation from theory which would signal "new physics." So far, no deviation has been found; but high precision measurements still have a long way to go before many hypothetical new interactions are expected to become observable. Such tests have also become an important indirect probe of the top quark mass, since its contribution through quantum loop corrections grows like m_t^2 and we now know m_t is large. Neutrino oscillation experiments are more in the way of high payoff longshots. The standard model does not predict oscillations, but they can be readily accommodated by giving neutrinos small masses and mixing them, in analogy with quarks. There are some theoretical reasons for favoring oscillations, in particular grand unified models naturally support very small neutrino masses. In addition, neutrino mass could close the universe or

This manuscript has been authored under contract number DE-AC02-76CH00016 with the U.S. Department of Energy.

be the dark matter seeds for galaxy formation, exciting possibilities. However, at present there is no compelling experimental evidence for neutrino oscillations. The long standing solar neutrino puzzle[1] is our best observational hint in favor of oscillations, but it may merely indicate deficiencies in the solar model used to predict solar neutrino fluxes.[2] In any case, that problem has heightened our interest in neutrino mass, mixing and oscillations. It also inspired some beautiful ideas such as the MSW effect in which matter enhances oscillations.[3] The physics of neutrino oscillations is so intellectually stimulating, that it would be a shame if nature did not use it at some level.

In this talk, I will focus on those aspects of neutrino physics which fall under the domain of accelerator based experiments, particularly those that can be carried out at Fermilab. The possibility of much higher intensities due to a new main injector means one must now seriously consider another round of neutrino experiments. My discussion will include $\sin^2\theta_W$, ρ, the CKM matrix elements V_{cd} and V_{cs}, and axial-isoscalar neutral current effects. The last of these has recently aroused interest because of an EMC polarized μp scattering result that calls into question the proton's spin distribution among its constituents.[4] I will also briefly mention how "new physics" might enter into precision tests of the standard model. In the case of neutrino oscillations, I favor pushing all types of searches as far as possible. A good experiment that can genuinely extend oscillation bounds on the mixing parameter $\sin^2 2\theta$ or the mass difference parameter Δm^2 that governs oscillatory behavior by at least an order of magnitude deserves serious consideration. However, my personal view favors $\nu_\mu \to \nu_\tau$ oscillation experiments. I will outline below, some reasoning behind that theoretical prejudice.

The weak mixing angle θ_W is very special. It enters in weak neutral current couplings, gauge coupling ratios such as $e = g \sin\theta_W$, and the natural mass relation $m_W = m_Z \cos\theta_W$. The ρ parameter is 1 in the standard model, but could deviate if the Higgs scalar sector is enlarged. It could also "appear" to deviate from 1 if "new physics" enters either at the tree or loop level and disturbs the standard model's predictions. We test the standard model by precisely measuring $\sin^2\theta_W$ and ρ in as many ways as possible. A deviation in one experiment as compared with others would signal new physics.[5]

Radiative corrections must, of course, be included in any precise comparison of different experiments; otherwise, loop effects might be interpreted as new physics. One of the most

interesting examples of important radiative corrections occurs in the relation[6]

$$m_W = m_Z \cos\theta_W = \left(\frac{\pi\alpha}{\sqrt{2}G_F}\right)^{1/2} \frac{1}{\sin\theta_W (1-\Delta r)^{1/2}} = \frac{37.281 \text{ GeV}}{\sin\theta_W (1-\Delta r)^{1/2}} \tag{1}$$

where Δr embodies electroweak radiative corrections to Thomson scattering (α), muon decay (G_F) and gauge boson masses. In addition, if $\sin^2\theta_W$ is extracted from a neutral current experiment, that data must separately be corrected for loop effects. The quantity Δr is particularly sensitive to a large top quark mass or fourth generation isodoublet mass splitting. That feature is illustrated in table 1 where values of Δr are given for different m_t, using the recent MARK II - CDF average[7]

$$m_Z = 91.1 \pm 0.1 \text{ GeV} \tag{2}$$

central value as input in (1). That table shows how a precise determination of $\sin^2\theta_W$ or m_W would pinpoint m_t (always assuming no cancellation by additional "new physics").

The present world average value of $\sin^2\theta_W \equiv 1 - m_W^2/m_Z^2$ extracted from deep-inelastic $\nu_\mu N$ scattering, in particular $R_\nu \equiv \sigma_{NC}(\nu_\mu N)/\sigma_{CC}(\nu_\mu N)$ is (after accounting for radiative corrections)[5]

$$\sin^2\theta_W = 0.232 \pm 0.003 \pm 0.005 \tag{3}$$

where the second error is theoretical in that a model is used to correct for charm threshold effects. A rather unique nice feature of determining $\sin^2\theta_W$ from R_ν is that the radiative corrections are quite insensitive to m_t changes due to a fortunate cancellation.[6] All other determinations of $\sin^2\theta_W \equiv 1 - m_W^2/m_Z^2$ depend sensitively on m_t through loop corrections. (Of course, measurements of both m_W and m_Z directly give $\sin^2\theta_W \equiv 1 - m_W^2/m_Z^2$ with no need to correct. At present, the CDF masses directly give $\sin^2\theta_W = 0.226 \pm 0.015$.) Comparing the results in (2) and (3) via table 1, gives

$$\left.\begin{array}{l} \Delta r \gtrsim 0.20 \\ m_t \lesssim 200 \text{ GeV} \end{array}\right\} 95\%\text{CL.} \tag{4}$$

with a value of m_t around 90 GeV favored. A global fit to m_W, m_Z and all neutral current data favors $m_t \simeq 130 \sim 140$ GeV but the errors are still large. To determine m_t

Table 1: Predictions for $\Delta r, \sin^2\theta_W$, m_W and $m_Z - m_W$ as a function of m_t, using $m_Z = 91.1$ GeV as input. (The Higgs mass has been set at 100 GeV, but the results are not terribly sensitive to reasonable changes. For $m_H \simeq 1\text{TeV}, \Delta r$ increases by +0.009.)

m_t (GeV)	Δr	$\sin^2\theta_W$	m_W (GeV)	$m_Z - m_W$ (GeV)
75	0.066	0.234	79.7	11.4
90	0.060	0.232	79.8	11.3
105	0.056	0.230	79.9	11.2
120	0.051	0.229	80.0	11.1
135	0.046	0.227	80.1	11.0
150	0.041	0.225	80.2	10.9
165	0.035	0.224	80.3	10.8
180	0.029	0.222	80.4	10.7
195	0.023	0.220	80.5	10.6
210	0.017	0.218	80.6	10.5
225	0.010	0.216	80.7	10.4
240	0.002	0.213	80.8	10.3
255	-0.006	0.211	80.9	10.2
270	-0.014	0.209	81.0	10.1
285	-0.023	0.206	81.2	9.9

to ± 15 GeV would require a 1% measurement of $\sin^2\theta_W$ or a ± 100 MeV measurement of $m_Z - m_W$. (At that level, the Higgs mass uncertainty is not negligible.)

The m_t example nicely illustrates the desirability of measuring $\sin^2\theta_W$ to $\pm 1\%$ via R_ν. Of course, a new experiment would have to accumulate very high statistics and find a way to overcome the dominant uncertainty from charm threshold effects.[5] (See R. Brock's talk.) The new main injector could provide a more intense beam and large event rates. To overcome the charm problem, one must either be able to reliably estimate or directly measure

the charm production cross-section. (Alternatively, a different flux normalization could be used.) A more reliable theoretical estimate can be made be restricting the analysis to very high energy data, say $E_\nu \gtrsim 150$ GeV. Alternatively, one can use dimuon data to directly measure charm production. Both methods should of course be used as a consistency check. Given the importance of $\sin^2\theta_W$ and unique features of determining it in R_ν, a new round of experiments should be seriously considered. If a genuine 1% measurement of $\sin^2\theta_W$ is possible, it should be undertaken.

Comparison of $\nu_\mu N$ and $\overline{\nu}_\mu N$ deep-inelastic scattering data (both neutral and charged current cross-sections) also provides a sensitive means of measuring the ρ parameter. Such a comparison presently gives[5]

$$\rho = 0.999 \pm 0.015 \qquad \left(\overset{(-)}{\nu}_\mu N \text{ data}\right) \tag{5}$$

which dominates the world average determination of that parameter $\rho = 0.998 \pm 0.009$. A very heavy top quark would effectively give[8]

$$\rho^{eff} = 1 + \frac{3}{8\sqrt{2}\pi^2} G_F m_t^2 \simeq 1 + 0.002 \frac{m_t^2}{m_W^2} \tag{6}$$

The data on ρ show no hint of a very large m_t or a large fourth generation mass splitting for which

$$m_t^2 \to (m_{t'} - m_{b'})^2 + 2m_{t'}m_{b'} + 4\frac{m_{t'}^2 m_{b'}^2}{m_{t'}^2 - m_{b'}^2} \ell n \frac{m_{b'}}{m_{t'}} \tag{7}$$

in (6).

A determination of ρ to within 0.25% could pinpoint m_t to within 40-20 GeV for m_t in the range 100-200 GeV but would also start to encounter Higgs mass sensitivity. Alternatively, if $\sin^2\theta_W$ were determined to $\pm 1\%$ via R_ν alone and compared with $\sin^2\theta_W$ measured elsewhere with smaller errors, say by gauge boson masses, ρ is effectively determined to $\pm\frac{1}{4}\%$ in the comparison.

Another way to measure $\sin^2\theta_W$ is using $\nu - e$ scattering. An ongoing CHARM II experiment[9] aims for ± 0.005 (statistical) in $\sin^2\theta_W$ via $\sigma(\nu_\mu e)/\sigma(\overline{\nu}_\mu e)$. At issue will be the relative normalization of ν_μ and $\overline{\nu}_\mu$ fluxes. A proposed LCD experiment[10] at LAMPF would measure $\sin^2\theta_W$ and be sensitive to ρ by measuring the ratio $R' = \sigma(\nu_\mu e)/[\sigma(\nu_e e) + \sigma(\overline{\nu}_\mu e)]$. The goal is a 2% measurement of R' which gives $\sin^2\theta_W$ to

± 0.002. An appealing feature of that experiment is freedom from flux normalization uncertainties. Although comparing R' with m_Z is not very sensitive to m_t, it does provide an important probe of new interactions. For example, in $SO(10)$ models with an extra neutral gauge boson Z_χ, one finds that R' is decreased by[11]

$$R' \simeq R'_{\substack{Standard \\ Model}} \left(1 - 1.3 \frac{m_Z^2}{m_{Z_\chi}^2}\right) \tag{8}$$

So, a 2% measurement of R' gives a sensitivity to m_{Z_χ} at the level of 750 GeV. At present, the bound $m_{Z_\chi} \gtrsim 300$ GeV comes from the atomic parity violation.[5] Similarly, such an experiment would reduce the laboratory bound on the muon neutrino's dipole (or transition) moments by an order of magnitude to $10^{-10} e/2m_e$. Such a moment would increase the $\nu_\mu - e$ cross-section.

Neutrino scattering cross-sections have also been used to determine CKM quark mixing matrix elements. CDHS dimuon data gives[12]

$$\begin{aligned} \mid V_{cd} \mid &= 0.207 \pm 0.024 \\ \mid V_{cs} \mid &= 0.95 \pm 0.15 \end{aligned} \tag{9}$$

One might be able to improve the determination of $\mid V_{cd} \mid$ by studying charm production in deep-inelastic $\nu_\mu N$ scattering (and $\overline{\nu}_\mu N$) at low energies. For $E_\nu \sim 10 - 20$ GeV, almost all charm is produced by scattering off d quarks; so $\mid V_{cd} \mid$ is isolated. The low energy neutrino oscillation emulsion experiment proposed for the new main-injector may be ideal for a study of $\mid V_{cd} \mid$. Charm decays may be better suited to determine the ratio $\mid V_{cd} \mid / \mid V_{cs} \mid$ where theoretical uncertainties tend to cancel. That ratio could then be used to obtain $\mid V_{cs} \mid$ from $\mid V_{cd} \mid$.

Another interesting reaction to study with low energy neutrinos is elastic $\overset{(-)}{\nu}_\mu p$ scattering. The standard model predicts no axial-isoscalar weak neutral current in the lowest order $SU(2)$ limit. Strange quark sea and gluon loops,however, induce an axial-isoscalar component. Results from BNL E734 indicate their effect to be about 10-20% of the axial-isovector amplitude.[13] That finding is consistent with EMC results for polarized μp scattering.[4] In both cases there is an ongoing debate as to whether strange quarks or gluons are responsible.[14] By precisely measuring $d\sigma/dQ^2$ for $\nu_\mu p$ and $\overline{\nu}_\mu p$, one could study the axial-isoscalar form factor and attempt to sort out strange quark and gluon effects. The

axial-isoscalar neutral current plays a special role in QCD, it is not conserved because of instantons; so, its study is clearly warranted.

I come now to the subject of neutrino oscillations. The present experimental bounds

$$\begin{aligned} m_{\nu_e} &< 12 \text{ eV} \\ m_{\nu_\mu} &< 0.25 \text{ MeV} \\ m_{\nu_\tau} &< 35 \text{ MeV} \end{aligned} \tag{10}$$

leave considerable room for speculation that neutrinos possess mass. Such speculations are fueled by grand unified theories, astrophysics, and cosmology. Grand unified models favor very light Majorana neutrino masses proportional to m_f^2/M_R where M_R is a very heavy right-handed neutrino mass scale and m_f is a typical fermion mass (the see-saw mechanism[15]). Given that relation one might expect a hierarchical mass ordering among the three neutrino masses $m_3^2 >> m_2^2 >> m_1^2$ or

$$m_1^2 : m_2^2 : m_3^2 :: m_u^4 : m_c^4 : m_t^4 \tag{11}$$

If that is the case, then one might approximately expect

$$m_1^2 : m_2^2 : m_3^2 :: 1 : 10^{10} : 10^{17} \tag{12}$$

That hierarchy would have important consequences for neutrino oscillations. Of course, at issue is what M_R value sets the overall mass scale? If any neutrino has mass $20 \sim 50$ eV, it could provide the missing mass necessary to close the universe and be a dark matter candidate. On the other hand, the MSW solution to the solar neutrino flux depletion favors some neutrino mass in the $10^{-2} \sim 3 \times 10^{-4}$ eV range.

If neutrinos have mass, then one expects them to mix. In analogy with quarks, the weak interaction states ν_e, ν_μ and ν_τ will be related to the mass eigenstates ν_1, ν_2 and ν_3 by

$$\begin{pmatrix} \nu_e \\ \nu_\mu \\ \nu_\tau \end{pmatrix} = \begin{pmatrix} c_1 c_3 & s_1 c_3 & s_3 e^{-i\delta} \\ -s_1 c_2 - c_1 s_2 s_3 e^{i\delta} & c_1 c_2 - s_1 s_2 s_3 e^{i\delta} & s_2 c_3 \\ s_1 s_2 - c_1 c_2 s_3 e^{i\delta} & -c_1 s_2 - s_1 c_2 s_3 e^{i\delta} & c_2 c_3 \end{pmatrix} \begin{pmatrix} \nu_1 \\ \nu_2 \\ \nu_3 \end{pmatrix}$$
$$c_i = \cos\theta_i, \ s_i = \sin\theta_i, \ i = 1, 2, 3 \tag{13}$$

If the quark analogy holds, one expects small θ_i. Indeed, the CKM matrix has $s_1 \simeq 0.2$, $s_2 \simeq 0.05$ and $s_3 \simeq 0.005$. However, one should keep an open mind about the magnitude of neutrino mixing.

Neutrino mixing and masses will lead to oscillations which in the general 3×3 case can be quite complicated. A hierarchical mass relationship as in (12), however, simplifies things. In that case, the relevant mass squared differences $\Delta m^2_{ji} = m^2_j - m^2_i$ are effectively reduced from 3 to 2 independent parameters since $\Delta m^2_{31} \simeq \Delta m^2_{32}$. Also, the hierarchy implies

$$\Delta m^2_{21} << \Delta m^2_{31} \simeq \Delta m^2_{32} \tag{14}$$

with Δm^2_{21} entering only for very long distance phenomena and Δm^2_{31} important for shorter distances. (I use Δm^2_{31} and Δm^2_{32} interchangably.) So, for example, Δm^2_{21} may be important for the solar neutrino problem while Δm^2_{31} and Δm^2_{32} may be relevant for laboratory or terrestrial experiments. The MSW solution would correspond to $\Delta m^2_{21} \simeq 10^{-4} \sim 10^{-7}$ eV^2 which translates via (12) into $\Delta m^2_{31} \simeq \Delta m^2_{32} \simeq 10^3 \sim 1$ eV^2. That domain is readily accessible in oscillation experiments at accelerators. Of course, that estimate is meant to be very rough. I would suggest pushing neutrino oscillations studies to $\Delta m^2_{31} \simeq 10^{-2}$ eV$^2 \sim 10^4$ eV^2 at accelerators and covering the smallest mixing angles possible.

In the hierarchy case, the neutrino oscillation problem reduces to 2×2 mixing with effective mixing parameters. The relevant Δm^2 will depend on R/E_ν where R is the distance traversed by neutrinos and E_ν is their energy. For example, the case $R/E_\nu \sim O\left(1/\Delta m^2_{31}\right) << 1/\Delta m^2_{21}$ relevant for terrestrial experiments at accelerators has oscillation probabilities governed by[15]

$$\begin{aligned} P(R)_{\nu_\mu \to \nu_e} &\simeq \sin^2\theta_2 \sin^2 2\theta_3 \sin^2\left[\frac{\Delta m^2_{31} R}{4E_\nu}\right] \\ P(R)_{\nu_\mu \to \nu_\tau} &\simeq \sin^2 2\theta_2 \cos^4\theta_3 \sin^2\left[\frac{\Delta m^2_{31} R}{4E_\nu}\right] \\ P(R)_{\nu_e \to \nu_\tau} &\simeq \cos^2\theta_2 \sin^2 2\theta_3 \sin^2\left[\frac{\Delta m^2_{31} R}{4E_\nu}\right] \end{aligned} \tag{15}$$

If we assume CKM mixing, those oscillation probabilities become

$$\begin{aligned} P(R)_{\nu_\mu \to \nu_e} &\simeq 2.5 \times 10^{-7} \sin^2\left[\frac{\Delta m^2_{31} R}{4E_\nu}\right] \\ P(R)_{\nu_\mu \to \nu_\tau} &\simeq 0.01 \sin^2\left[\frac{\Delta m^2_{31} R}{4E_\nu}\right] \\ P(R)_{\nu_e \to \nu_\tau} &\simeq 10^{-4} \sin^2\left[\frac{\Delta m^2_{31} R}{4E_\nu}\right] \end{aligned} \tag{16}$$

In such a scenario, $\nu_\mu \rightarrow \nu_\tau$ oscillations is clearly the "best bet."

N. Reay and collaborators are examining the feasibility of doing a $\nu_\mu \rightarrow \nu_\tau$ appearance experiment with the new main injector using an emulsion target. They would push the effective $\sin^2 2\theta$ bounds to 2.5×10^{-4} for $\Delta m^2_{31} > 10\ \mathrm{eV}^2$ and about 10^{-2} for $\Delta m^2_{31} \gtrsim 1\mathrm{eV}^2$. Such a study is extremely interesting . It probes a mass range relevant for astrophysics and cosmology at very small mixing. If they find oscillations, it would revolutionize neutrino physics.

In conclusion, I see an important role for the next generation of Fermilab's accelerator based neutrino experiments. A well supported deep-inelastic $\nu_\mu N$ scattering initiative at the Tevatron could determine $\sin^2 \theta_W$ to $\pm 1\%$ and ρ to $\pm 0.25\%$ when compared with m_W and m_Z. High intensity lower energy neutrino beams made possible by the advent of a new main injector could push $\nu_\mu \rightarrow \nu_\tau$ oscillation appearance studies into exciting new domains. A $\nu_\mu \rightarrow \nu_\tau$ emulsion experiment would have the side benefit of determining $\mid V_{cd} \mid$ to high precision via charm production. Other possibilities such as elastic $\overset{(-)}{\nu}_\mu p$ and $\overset{(-)}{\nu}_\mu e$ scattering measurements would also be interesting initiatives that should be considered. Neutrinos are very special particles, so we should strive to understand their role in nature as well as possible.

REFERENCES

1. J.K. Rowley, B. Cleveland, and R. Davis, Am. Inst. Phys. Conf. Proc. 126, 1 (1985).
2. J. Bahcall and R. Ulrich, Rev. Mod. Phys. 60, 297 (1988).
3. P. Mikheyev and A. Yu Smirnov, Nuovo Cimento C9, 17 (1986); L. Wolfenstein, Phys. Rev. D26, 1662 (1982).
4. J. Ashman *et al.*.
5. U. Amaldi, A. Böhm, L.S. Durkin, P. Langacker, A. Mann, W. Marciano, A. Sirlin, and H.H. Williams, Phys. Rev. D22, 2695 (1987).
6. See talks at the Lepton-Photon Symposium - SLAC (1989).
7. M. Veltman, Nucl. Phys. B123, 89 (1977).
8. CHARM II Collaboration.
9. LCD proposal LA-11300, D.H. White, spokesman.

10. S. Godfrey and W. Marciano, proceedings of the 1987 BNL neutrino workshop, edited by M.Murtagh, p. 195.

11. H. Abramowicz, *et al.*, Z. Phys. C15, 19 (1982); W. Marciano and Z. Parsa, Ann. Rev. Nucl. Part. Sci. 36, 171 (1986).

12. L.A. Ahrens *et al.*, Phys. Rev. D35, 785 (1987).

13. D. Kaplan and A. Manohar, Nucl. Phys. B301, 527 (1988).

14. M. Gell-Mann, P. Ramond, and R. Slansky in "Supergravity" (1979).

15. W. Marciano, proceeding of the 1987 BNL neutrino workshop, edited by M. Murtagh, p. 1.

SOME IDEAS FOR NEUTRINO PHYSICS WITH THE PROPOSED FERMILAB MAIN INJECTOR

Raymond BROCK

Department of Physics and Astronomy
Michigan State University, East Lansing, MI 48824

A review is given of some possible physics opportunities available from neutrino beams produced by the proposed Fermilab Phase II upgrade which would incorporate extraction at high repetition rate of the Tevatron 150 GeV proton injection beam.

Introduction

Of the possible accelerator upgrades for Fermilab, the construction of the so-called Main Injector holds intriguing possibilities for neutrino physics. There are two obvious features of this proposal that are relevant:

1. *High Rate* - The high rate comes from the likelihood of large numbers of extracted protons (2×10^{13} per extraction) and the high repetition rate of every 3 seconds. Further, the possibility of fixed target running during colliding beam periods could also be an important feature.
2. *Unique energy regime* - The energy of neutrinos from the 150 GeV proton beam would be intermediate to the traditional beams of the past. This could be important for some physics, such as low Q^2 processes.

The beams that could be built at this facility for neutrino physics are conventional wide-band beams (WBB), conventional narrow band beams (NBB), multi-flavored beams such as those derived from K^0_L, and beams from a muon storage ring.

The physics topics of interest derive from the unique features of these beams. In this note, some of the possible opportunities will be outlined with some given detailed examination and others only suggested. For the topics chosen, an attempt will be made to indicate where the challenges lie: with detectors and/or beams. It is hoped that some of these ideas will be further examined during the Physics of the 1990's Workshop to be held in the summer of 1989.

Beams and Rates

Muon Neutrino Beams

Conventional beam possibilities follow along familiar lines of producing focussed secondary beams without momentum selection as well as momentum-selected beams.

Wide-Band Beam (WBB) The flux for the wide band beam (WBB) was calculated by the Research Division[1] and is modelled on a conventional two-horn focussing system. The layout is for a 400m tunnel, 110m shield, and a 10m recess with the production spectrum from the Malensek-modified Atherton Model[2]. Experience suggests that this model is optimistic and so it is traditional to take 70% of the results[1]. Experience also shows that one can roughly estimate the bare-target result for comparison by taking 4% of the perfect focussing result. The fluxes from perfect focussing, bare target, and the modified-production model are shown in Figure 1. The expected "realistic" flux values are shown in Table 1.

Various flux integrals are will be required below. For the energy-independent and linearly-dependent cross sections those integrals are:

$$\int_3^{120} \frac{dN_\nu}{dE_\nu} dE_\nu = 1.6\text{x}10^{-3} \text{ neutrinos} / \text{m}^2 \cdot \text{pot}$$

$$\int_3^{120} E_\nu \frac{dN_\nu}{dE_\nu} dE_\nu = 2.0\text{x}10^{-2} \text{ neutrinos} \cdot \text{GeV} / \text{m}^2 \cdot \text{pot}$$

The integral distributions for flux and energy-weighted flux are shown in Figure 2.

Narrow-Band Beam (NBB) In order to estimate the prospects for a narrow-band beam, general results of an old 150GeV proposal[3] were used. The proponents of this proposal calculated a 2-horn beam for 150 GeV protons as well as a narrow band beam which used the focussed horn beam of their WBB proposal directed onto a conventional series of bending/focussing elements giving a momentum bite of $3<p<18$ GeV. This gave a spectrum with was roughly 3 GeV wide (FWHM), centered on the same energy at which the wide-band flux peaked with half of the WBB intensity at that energy. Using these parameters, a Narrow Band Beam (NBB) spectrum has been approximated for this study. Figure 3 shows this spectrum (compared with the WBB). The kaon peak has been ignored as it is quite small relative to the already small pion peak. The FWHM of this beam is roughly 2 GeV, although the effective width in a detector might be smaller due to the nominal *E-r* correlation. The integrals for this beam are:

$$\int_3^{120} \frac{dN_\nu}{dE_\nu} dE_\nu = 2.1\text{x}10^{-4} \text{ neutrinos} / \text{m}^2 \cdot \text{pot}$$

$$\int_3^{120} E_\nu \frac{dN_\nu}{dE_\nu} dE_\nu = 1.3\text{x}10^{-3} \text{ neutrinos} \cdot \text{GeV} / \text{m}^2 \cdot \text{pot}$$

The flux of the NBB is roughly 10% of the total WBB flux rate, as was stated in reference 3. It should be stressed that these parameters for a potential NBB are for estimation purposes only. Should serious interest develop in the physics possibilities of such a beam, a design effort should be undertaken[4]. There are some precedents for (un-built) high-flux NBBs both for Fermilab and Los Alamos[5].

Speciality Neutrino Beams. Other beam possibilities include ν_μ and ν_e beams from muon storage rings and from K^0_L beams. Bernstein has estimated the rates from a K^0_L beam[6] while the properties of a muon storage ring facility were recently considered elsewhere[7].

The unique physics possibilities are driven by the enormous rates available with 150 GeV beam extraction. For the purpose of calculating realistic rates, the following will be defined as a fixed target **RUN**:

- 70 hour weeks
- 9 month duration
- 1m radius detector
- 110m shield
- 70% detector "on-time" efficiency

For a typical Fermilab fixed-target running period of 9 months of 70 hour weeks (roughly a 42% efficiency which is consistent with recent neutrino running), the number of protons which could be delivered to a neutrino experiment during a **RUN** is:

$$2.0\times10^{13}(\text{protons}/3s)\cdot(70\,\text{h}/\text{wk})\cdot(3600s/\text{h})\cdot(36\,\text{wks}/\text{run})=6\times10^{19}\,protons/\textbf{RUN}$$

which is a factor of 120 more integrated proton intensity delivered in either of the last two fixed target runs. While the cross sections are lower by roughly a factor of 10 because of the lower energies, the overall gain in data-collection would still be an order of magnitude more.

As a benchmark, prior to the actual physics discussion, a set of fiducial reactions for rate comparisons are considered below. The physics interest in a selection of these reactions will be considered in separate sections. These fiducial reactions are "regular" deep-inelastic charged current events, $\nu+N\rightarrow\mu+X$; neutrino electron scattering, $\nu_\mu+e\rightarrow\nu_\mu+e$; the quasi-elastic charged current process, $\nu+p\rightarrow\mu+p$; the elastic neutrino scattering reaction, $\nu+p\rightarrow\nu+p$; and the trident process, $\nu+Z\rightarrow+Z+\mu+\mu$. For these different processes, the cross sections may have various energy dependences. The general cross section for all of the processes which we will consider can be written in the following general form:

$$\sigma(E_\nu)=[a+bE_\nu+c\cdot E_\nu\ln(eE_\nu)]$$

where the table below shows the appropriate values of the constants appearing above. The cross sections are in cm^2 and an isoscalar target is assumed for the actual calculations. The cross sections are shown in Figure 4 (normalized to the quasi-elastic cross section of about $1\times10^{-38}cm^2$).

process	*a*	*b*	*c*	*e*
$\nu N\rightarrow\mu X$	0	0.62×10^{-38}	0	0
$\nu p\rightarrow\mu n$	1×10^{-38}	0	0	0
$\nu_\mu e\rightarrow\nu_\mu e$	0	2×10^{-42}	0	0
$\nu Z\rightarrow Z\mu\mu$	0	0	$\frac{4.2\times10^{-45}Z^2}{A^{1/3}}$	$\frac{6.1}{A^{1/3}}$
$\nu p\rightarrow\nu p$	0.15×10^{-38}	0	0	0

Under these beam conditions the number of deep-inelastic charged current events available in this period would be considerable. The calculations in Table 1 show the number of events/proton/ton and events/ton•**RUN** (including a 70% data-taking/live-time efficiency factor) for each possible 150 GeV beam as well as a comparison with the existing detectors in the world which have the characteristics most relevant to the study of each fiducial reaction: the Lab E 500t iron detector (for the $\nu_\mu N\rightarrow\mu X$ reaction), CHARM II fine-grained 700t glass detector (the $\nu_\mu e\rightarrow\nu_\mu e$ reaction), the BNL E734 fine-grained 170t detector (the $\nu p\rightarrow\mu n$ and $\nu p\rightarrow\nu p$ reactions), and Lab C fine-grain 100t sand/steel-shot detector ($\nu Z\rightarrow Z\mu\mu$ reaction). We would expect the total samples for these benchmark reactions in the above **RUN** (times a 70% running efficiency) as shown in Table 2. The largest event samples for these same reactions in the world today are (or soon will be) shown in Table 3.

It should be stressed that for each of these calculations, the rates include 2 efficiency factors of nearly 50% for the accelerator and 70% for the experiment: these are realistic rates and compete very favorably with the potential of higher energy machines.

Physics Issues

The most interesting physics issues which appear to be the best match for the accelerator capabilities are broadly divided into 2 classes: Oscillations and Standard Model tests.

Oscillations

The obligatory relationship for the mixing of two neutrino species is

$$\mathcal{P}(\nu_i \rightarrow \nu_j) = \sin^2 2\vartheta \sin^2(1.27\Delta m^2 \frac{L}{E_\nu})$$

which leads to two possible experimental techniques:

Appearance experiment - performed with one detector in which a search is mounted to look for the presence of something that shouldn't be there. Typically, (in the absence of backgrounds) the results of the search are reported as $\mathcal{P}(\nu_\mu \rightarrow \nu_x) = \frac{N_x}{N_\mu}$ with null results leading to the assignment of $N_x = 2.3$ for a 90% C.L. upper limit.

Disappearance experiment - performed with two detectors or more in which a search is mounted to look for the absence of something that should be there. Here, the searches have been traditionally $\mathcal{P}(\nu_x \rightarrow \nu_x) = 1 - \mathcal{P}(\nu_x \rightarrow \nu_y)$, where x=e,μ and $y \neq x$.

One immediately sees that a feature of the Appearance sort of experiment is that it can be the *discovery* channel for a new type of neutrino, rather than "just" a limit.

The rules-of-thumb for where concentration of effort pays off in the traditional Δm^2 vs $sin^2 2\vartheta$ exclusion plots are: a small mixing limit requires high statistical precision while a small mass limit requires a large distance. In point-of-fact, the inevitable presence of background complicates this somewhat. The sensitivities are[8]:

Large Δm^2 $sin^2 2\vartheta \propto \frac{1}{N_i}$ without backgrounds

$sin^2 2\vartheta \propto \sqrt{\text{background fraction}}\sqrt{\frac{1}{N_i}}$ with backgrounds

Small Δm^2 $\Delta m^2 sin^2 2\vartheta \propto \frac{E}{L}\sqrt{\frac{1}{N_i}}$ without backgrounds

$\Delta m^2 sin^2 2\vartheta \propto \frac{E}{L}\sqrt{[\sqrt{\text{background fraction}}\sqrt{\frac{1}{N_i}}]}$ with backgrounds

Generally, the channels for $\nu_i \rightarrow \nu_e$ have backgrounds which are > a few % and the channels $\nu_i \rightarrow \nu_\tau$ have backgrounds which are < a few %.

It appears to be a matter of taste at present as to which is the most fruitful expenditure of effort: small mixing angle (perhaps at the expense of mass-sensitivity) or the ever-popular push to the lowest possible mass limit. Proponents of both viewpoints have as their prime motivation the standard cosmological interest in understanding the potential for there being enough mass in the Universe to affect geometry toward eventual closure. Generally, it seems that those who are concerned about galactic formation problems tend toward a view with the following features:

- neutrinos of a light sort (<70eV) cannot satisfy criteria for galaxy formation
- The **theoretical prejudice** is that new particles are required (generically, weakly-interacting-massive-particles, WIMPs)

- Therefore, there is no prediction for just how light neutrinos might be

Those whose concern is for Big Bang neutrinos tend toward a view with the following features:

- light neutrinos could serve well, since they are abundant
- The theoretical prejudices are that there is a mass hierarchy $m(\nu_t)>>m(\nu_\mu)>>m(\nu_e)$ and that the magnitude of quark mixing should be similar to that for lepton mixing, which in some models[9] leads to the prediction that $\vartheta_{q\mu} \approx \vartheta_{23}$ so that $sin^2 2\vartheta_{q\mu} \approx$ few 10^{-4}
- The mass, therefore, necessary to close is ≤ 65 eV and it should be associated with the difference between the heaviest known neutrino (τ) and the middle neutrino (μ).

This last view has the feature that no new particles are required and that there is an actual prediction for the ranges of interest for mass and mixing angle. The former view makes no prediction and requires new particles. Regardless of one's allegiance, certainly all gains in mass and mixing are potentially interesting, and it is a matter of gain vs $ (¥, DM, or £).

Two groups have expressed interest in the Main Injector for the purpose of studying neutrino oscillations and both have sensitivities which match the two views described above. Both of these designs will be reported on in the papers presented to the sessions and therefore only summary is presented here.

1. Ohio State, Carnegie Mellon, Fermilab, Nagoya University, Kobe University, and Osaka City University

- Short baseline (100m), appearance experiment $\nu_\mu \rightarrow \nu_\tau$

$$\nu_\mu \rightarrow \nu_\tau + N \rightarrow \tau + X$$

$$\tau \rightarrow \textit{muonless final states}$$

- search strategy: identify kinks in neutral current-appearing events
- hybrid emulsion-electronic spectrometer
  fully magnetic
  similar in spirit to E531
- concentration on small mixing angle with sensitivity to $sin^2 2\vartheta$ at the level of few x 10^{-4}
- WBB from horn focussing

2. Tokai University, INS University of Tokyo, Kobe University, Tokyo Institute of Technology

- long baseline (stage I, 50-100km; stage II, 500-1000km), disappearance experiment for $\nu_\mu \rightarrow \nu_\tau, \nu_e$

$$\nu_\mu \rightarrow \nu_\tau + n \rightarrow \tau + p$$

$$\tau \rightarrow e + \nu_\tau + \nu_e$$

- search strategy: identify electrons
- H_2O Cerenkov detector
  similar in spirit to Kamiokande II
- concentration on small mass with sensitivity eventually to
  $\Delta m^2 > 10^{-3}$ for $\nu_\mu \rightarrow \nu_e$ and $\Delta m^2 > 3\text{x}10^{-3}\text{eV}^2$ for $\nu_\mu \rightarrow \nu_\tau$

It should be noted that both groups are experienced in this field and these designs are following previous successful experiments. Figure 5 shows the exclusion plots with the present limits contrasted with those of the proponents for above designs. Also shown on the figure are the limits

for oscillations for the disappearance sort proposed at Brookhaven National Laboratory of a 10km long baseline experiment.

The challenges:

Detector challenge

- come to grips with the question of scale! (especially in the case of the long baseline detector)
- backgrounds
- is there additional physics possible with an oscillation experiment?

Beam Challenge

- are the two proposals compatible with one another?
- beam contaminants are potentially a problem, especially $\overline{\nu}_\mu$, $\overline{\nu}_e$, and ν_e

Standard Model Tests

There are a number of ways to confront the Standard Model using a high-rate low energy neutrino beam. These include detailed studies of measurements of the Weinberg Angle, determination of hadronic structure through Structure Functions (both elastic and inelastic), certification of neutrino identity, and Universality. Here, a sampling of issues is summarized, with more detail left for working group summaries.

sin²ϑW One of the most important of all programmatic studies in electroweak physics is the testing of the Standard Model through precision measurements of $\sin^2\vartheta_W$ determined in different reactions. By applying the necessary higher-order corrections (in the spirit of the traditional g - 2 tests) the field theory is directly tested. The standard observations of higher order effects come from comparing the masses of the actual intermediate vector bosons (IVB), Z and W, with the determination of $\sin^2\vartheta_W$ from some other source or sources.

The most precise determinations of $\sin^2\vartheta_W$ come from the comparison of deep-inelastic neutrino charged current scattering with that of neutral current scattering. The charged current reaction provides the necessary normalization and the ratio of the two is then a function of $\sin^2\vartheta_W$. While there are considerable benefits associated with this technique (chiefly, the large cross section), the desired precision is such that very small systematic uncertainties become the major limitations. Presently, the measurements are largely limited by the theoretical uncertainty associated with the charged current process $\nu_\mu q \rightarrow c\mu$ where q represents a light quark and c represents a produced heavy quark, such as charm. The parton model is ill-equipped to deal with such a non-scaling process since an undesirable length scale associated with the charm quark mass is introduced. The deep inelastic scattering measurements all use a modification of the parton model called "Slow Rescaling" which parameterizes this modification in terms of a single parameter, m_C. The uncertainty in $\sin^2\vartheta_W$ can then be represented as a function of m_C as roughly $6\%\cdot(m_C - 1.5)\cdot\sin^2\vartheta_W$, which is large on the scale of the required precision.

The capability of testing the Standard Model to a precision of a few percent through this particular measurement has presently reached an impasse due to the systematic errors associated with the neutrino determinations and the calorimetric uncertainties in the IVB mass determinations. The deep-inelastic measurements are largely complete from precision determinations at the 400 GeV-era narrow-band neutrino experiments at Fermilab and CERN and that experimental chapter appears to be closed.

The world's data from deep inelastic neutrino scattering leads to the following result[10]:

$$\sin^2\vartheta_W = 0.233\pm0.003\pm \textit{theory}$$

where the first error is the quadrature combination of statistical and experimental uncertainties and *theory* is the theoretical uncertainty which ranges from 0.006-0.007 depending upon the degree of skepticism assigned to the parton model uncertainties. The question for proponents of the Main Injector is twofold: can an experiment at the MI reduce the uncertainty on $\sin^2\vartheta_W$ through a separate measurement *or* can an experiment at the MI with a different agenda incidentally yield information regarding the theoretical uncertainties to retroactively lend support for a reduced value of *theory* .

Elastic Scattering. Obvious ways to avoid the above theoretical issues would be to perform the measurement of $\sin^2\vartheta_W$ on a leptonic target or to forego flavor-changing normalization reactions. The former approach is usually to rely on the purely leptonic reaction $\nu_\mu + e \rightarrow \nu_\mu + e$, plus the antineutrino analogue reaction. Here, the physics is somewhat cleaner at the expense of an extremely small cross section: approximately 10^{-4} of the normal rates. This reaction has a noble history with largely two groups (CHARM at CERN using the 400GeV SPS and E734 at Brookhaven using the 32 GeV AGS) dominating the world's data in both statistical precision and systematic understanding. The combination of results from these two collaborations gives[11]

$$\sin^2\vartheta_W = 0.201\pm0.021$$

which, for its purity of interpretation is lacking in statistical precision in order to play the role of the crucial comparison reaction to the IVB mass measurements.

The CHARM II collaboration has, for the past few years, been pursuing high precision measurements of this reaction in an attempt to gather 2000 of both neutrino and antineutrino events. In this way, it is hoped that the ratio $R = \dfrac{\sigma(\bar{\nu}+e\rightarrow\bar{\nu}+e)}{\sigma(\nu+e\rightarrow\nu+e)}$ can be determined to 2%. To accomplish this an heroic effort on determining the relative fluxes must be successful, as knowledge of that quantity to ±2% is required[12].

As Table 1 shows, an enormous number of events are possible in the WBB, unlike any previous situation in which a paucity of events is typically a problem. Therefore, systematic uncertainties will be the major concern. Given the head start by the CHARM II experiment and the certainty that an R measurement at the MI would be dominated by the flux systematics, another technique should be considered which would exploit the high rates, but be cleaner experimentally. The obvious possibility would be to determine the y distribution.

For the standard model (with only V and A contributions), the cross section is:

$$\frac{d\sigma^{\nu,\bar{\nu}}}{dy} = \rho^2\frac{G^2 m_e E_\nu}{2\pi}\left\{A + B(1-y)^2\right\}$$

where A and B are functions of $\sin^2\vartheta_W$ and y is defined in the laboratory as $y = \dfrac{E_e}{E_\nu}$. By exploiting the two-body kinematics, it can be expressed in terms of the outgoing angle of the electron:

$$y = 1 - \frac{\theta_e^2 E_e}{2m_e}$$

Because of the quadratic dependence of y on angle, the angular resolution is the limiting factor in resolution at low y. Also, since the angle depends inversely on neutrino energy, large angles are more likely at lower energy accelerators and this might be more manageable at the MI than at a conventional 400 GeV era machine. This has been attempted in a significant way, at a lower energy accelerator, only by the Brookhaven experiment which had an angular resolution which was

impressive but sufficient only to separate the two terms in a likelihood fit in θ_e and not y. Nonetheless, they measured $\sin^2\vartheta_W = 0.195 \pm 0.018 \pm 0.013$ using this technique[13].

Two possible methods might be employed in an effort at determining y: both of which are possible only because of the impressive flux of the MI:

1. Because of the enormous rates, a fairly modest sized detector is sufficient to collect a significant number of events: 1000 events could be collected in a RUN with only 30 tons. Improving upon the Brookhaven angular resolution in a conventionally sized neutrino detector (>100 tons) might be very difficult. However, perhaps in such a small detector, it might be financially feasible to exploit the advances made in modern designs of tracking devices (silicon strips, scintillating fibers, etc.).
2. While all experiments have been performed in a wide-band beam to date, the intensity of the MI might make a narrow band neutrino beam and a conventionally sized neutrino detector (300 tons) feasible. In that way, the neutrino energy could be determined by exploiting the (hopefully) narrow spread of neutrino energies around a well-determined mean (using charged current events, for example).

This latter possibility is considered as a part of the neutrino working group and possible rates from such a beam appear in Tables 1 and 2.

The challenges for a y measurement are:

Detector challenge

- integrate sufficient size (>200 tons) with modest angular resolution in a single detector[14] (narrow band beam possibility).
- greatly improve present electron angular resolution performance to a few mrad in a small-sized detector (wide band beam possibility).

Beam Challenge

- design a narrow band beam with a narrow π band (≤ 5 GeV) width and high rate

Inelastic Scattering. While charm production is the limiting factor in the deep-inelastic measurements, the MI beam has the unique feature of being just at threshold for charm production and as such might provide a fruitful laboratory for a study of this process. An understanding of charm production in a region which is far from scaling and at low Q^2 is not available and there is little data from which one might construct a phenomenology of this process. Should, however, such an understanding become available it might be possible to apply it to the analyses of the older deep-inelastic experiments and argue convincingly for a reduction in the theoretical error.

The cross section for the *light quark→ heavy quark* transition can be obtained through some simple extensions to the naive parton model where the introduction of a heavy quark final state having mass m_c comes from a replacement of the scaling variable x_{Bj} by $\xi = x_{Bj} + \frac{m_c^2}{2M\nu}$. The only parameter is then the "mass", m_c. All of our understanding of this process comes from the observation of opposite sign dimuon production in neutrino and antineutrino scattering where the cross section is in fact:

$$\underset{a}{\left[U_{qc}\right]}\cdot\underset{b}{\left[(1-y+\frac{xy}{\xi})\right]}\cdot\underset{c}{\left[\xi q(\xi)\right]}\cdot\underset{d}{\left[\sum_i D_c^{h_i}\right]}\cdot\underset{e}{\left[BR_i(h_i\rightarrow\mu)\right]}$$

where each factor is:

- *a* Kobayashi-Maskawa mixing parameter
- *b* kinematical suppression factor related to the V,A character of the matrix element
- *c* quark distribution function for the struck parton
- *d* fragmentation function for the final heavy quark, c, to produce a charmed hadron, h_i
- *e* branching ratio for h_i to decay semi-leptonically to a muonic final state

a-e are each, to some degree, unknown. Certainly knowledge of any one of these factors is highly correlated with most of the others. For example, the determination of the strange quark sea (*c*) comes from just this process and an adjustment of any of the other quantities (especially *d* and *e*) will affect this result.

Should an experiment run at the MI in which charm could be detected (such as the hybrid emulsion experiment mentioned above in the context of neutrino oscillations) one or both of two possible outcomes could occur:

1. Many hundreds or possibly a few thousands of charm events could be measured (in the form of D^0 inclusive states) thereby providing a unique data set for understanding the production process for $\nu N\rightarrow\mu+D+X$ at low Q^2 and low ν. This understanding could be retroactively applied for an overall reduction in the uncertainty in $\sin^2\vartheta_W$. It is also possible that such a study might yield better information on $xs(x)$ and/or U_{cd}.

2. By actually studying charm in such a detector, it might be possible to decouple the correlations in the quantities *a-d* (*e* would not be relevant) and actually measure $R=\frac{\sigma(NC)}{\sigma(CC)}$ with internally-calibrated determinations of the theoretical uncertainties.

The challenges are:

Detector challenge

- understand whether the hybrid-emulsion design can be optimized for superior muon detection and moderate calorimetry in order to identify charged and neutral current events and measure p_μ and ν
- understand the uncertainties in low Q^2 production of heavy quarks in order to decide on the feasibility of contributing retroactively to the theoretical uncertainties in the world's data on $\sin^2\vartheta_W$

Beam Challenge

- understand the antineutrino and ν_e flux contaminations

Hadronic Structure

The oldest of all measurements in deep-inelastic scattering is the determination of the nucleon constituent content and momentum fractions - the structure functions. While our theoretical understanding has matured over the years to our present-day appreciation of QCD, the measurements have also progressed in the degree to which small effects are becoming apparent. The best example of this is the variation of the singlet structure function, F_2 with atomic number, the so-called EMC effect.

While quite mature in many ways, there are still a number of annoying problems with the interpretation of the world's results:

1. $F_2(x,Q^2)$. This quantity is difficult to interpret in QCD and involves an understanding of the neutral parton distribution. At the same time, it is the simplest quantity for the experimenters: high statistics are possible from ν, μ, and e beams and the comparisons among them have led to nice parton model tests, such as the classical 5/18 comparison showing that the charged partons indeed carry fractional charges. However, while there is broad agreement from one experiment to another in the overall level of $F_2(x,Q^2)$ in Q^2 bins, the first logarithmic derivative $\frac{\partial \ln F_2}{\partial \ln Q^2}$ as a function of x_{Bj} is disturbingly poor in comparison with the QCD prediction and the agreement between iron target experiments and light target experiments is likewise not good (see Figure 6)[15]. These examples of poor agreement have led some to speculate as to the possibility of a Q^2 dependence of the EMC effect[16]. More experimentation is likely required. In addition, there is recently a "crisis" in the determination of the proton structure function as determined in μ scattering experiments.
2. $xF_3(x,Q^2)$. This quantity, while easier to interpret in QCD because it requires no knowledge of the gluon distribution, is much more difficult to measure. Indeed, measurement of xF_3 is the source of the best understanding of the scale parameter, Λ. However, here too, we have a rather disturbing situation experimentally. The participation of the charged lepton experiments in the measurement of $xF_3(x,Q^2)$ comes from the expectation that at high x there should be no difference between this and $F_2(x,Q^2)$, hence the latter is used above the region of the sea, typically x greater than about 0.25. Indeed, the statistical imprecision inherent in neutrino experiments, which have direct access to $xF_3(x,Q^2)$, has forced them to take the same approach. The determination of Λ and the quality of the fits are shown in Figure 7 for a variety of experiments[15]. Clearly, the there is a clustering of iron experiments and lighter targets, with the former giving much less likely fits than the latter.
3. R_L. This quantity, the ratio of the longitudinal to transverse cross sections, is simple to interpret and very difficult to measure. Part of the difficulty, at least, is the strong Q^2 dependence and the large corrections required for target mass effects. This mapping in Q^2 is only successfully done through the combination of experiments from different laboratories with the neutrino experiments contributing only asymptotically and the rest of the mapping governed by the SLAC electron experiments.
4. High twist. Our understanding of nucleon structure is not complete until there has been a satisfactory description and systematic-free determination of that structure at Q^2 only a few times the scale of the nucleon itself. The passage of the elastic region into the scaling region has for many years been a source of interest and surprise at the early onset of scale-free behavior (remember "precocious scaling"?). There have been theoretical attempts at understanding the higher twist effects over the years[17], but the experimental situation is very confused. Figure 8 shows a combination of data for a combination electron/muon analysis and two separate neutrino experiments where the fit is to a parameterization of the "twist-4" contribution to F_2 of the form

$$F(x,Q^2) = F_{lowest\ twist}(x,Q^2)\cdot(1+\frac{\mu^2}{Q^2})$$

What is actually plotted is $\mu^2 \equiv H_4(x)$[18].

What are the solutions to the above problems? Obviously, comparisons and combinations of data from different experiments is a possible problem, as is the limited statistical precision. Further, the possibility exists that the gluon distribution may be stiffer in heavy targets thereby dooming the use of F_2 as an approximation to $xF_3(x,Q^2)$. Or, higher twist might be stronger in heavy targets[15]. The only uncomplicated way to solve this is to collect enough data to convincingly use $xF_3(x,Q^2)$ to measure $xF_3(x,Q^2)$! Recently[19], it has been argued that determination of the helicity structure functions would be extremely useful for a convincing determination of the parton distribution functions. This too would require fitting as a function of x,Q^2, and y, and therefore requires very large amounts of data.

It is entirely conceivable that only additional experimentation will solve the above problems - or convincingly exacerbate them, thereby leading us to new physics. Such a third generation experiment could be designed for Fermilab (and nowhere else) and should have the following two characteristics:

1. *Interchangeable target planes*. This would allow for separate experiments to be performed on different nuclei with identical acceptances, thereby eliminating possible systematic biases in attempts to combine data from different experiments. Because of the rate capabilities, the possibility of collecting >1M events on different targets in one RUN is very real. [Problems 1 and 2.]
2. *Exposure to both Tevatron and MI neutrino beams*. This would allow for an extremely large range of $Q^2$to be explored with very high statistical precision, perhaps (depending on various resolution and acceptance limitations) covering SLAC to Tevatron ranges. Simultaneous (within the same accelerator cycle) Tevatron and MI running would be desirable, although there is no indication that such extraction gymnastics are feasible. [Problems 3 and 4.]

Any future plans for neutrino experiments should take these two features seriously.

Detector challenge

- Design a detector with different, interchangeable targets
- Study the resolution and acceptance characteristics of such a detector to optimize use at both the MI and the Tevatron

Beam Challenge

- study simultaneous extraction of fast spill for both 150GeV and 900GeV running

Other Issues

In addition to the above standard physics topics, at least two additional issues could be addressed only at a high rate facility such as the MI.

Neutrino Identity. A long-standing question involves whether the identity of the outgoing neutrino in a neutral current interaction is as expected from the standard model. A sure way to check this is to look for the interference terms arising from the amplitude sum between charged and

neutral currents in $\nu_e+e\rightarrow\nu_e+e$ scattering. This has been seen by the group at Los Alamos and is consistent with the standard model prediction that a) there should be interference =>identical neutrinos and b) that this interference should be destructive. There is, however, no similar test for ν_μ. There are two ways to check for ν_μ identity.

The possibility of a helicity flip can be checked for by again fitting for the y distribution in $\nu_\mu+e\rightarrow\nu_\mu+e$ scattering. A helicity flip, (such as might occur from a large magnetic moment, introducing a $\sigma_{\mu\nu}$-like term in the matrix element) not allowed in the V, A model of Weinberg and Salam would manifest itself in a term proportional to $1/y$ which would ride on top of the standard model distribution[20]. Superior low-y resolution would be required to detect such a disturbance and so this measurement is consistent with the demands made of the narrow band beam discussion above. Of course, searches of the classic sort for additional spacetime terms such as S,P, and T contributions have not been performed for this reaction and would contribute terms proportional to (1-y) to the cross section.

Another means by which neutrino identity could be studied is again by an interference method, although this time through the "trident" reaction $\nu_\mu+Z\rightarrow\nu_\mu+\mu^+\mu^-+Z$ which occurs coherently from the nuclear Coulomb field through either charged or neutral current channels. Recently, the CCFR collaboration has reported an observation of 10.9±3.8 events where the standard model predicts 5.0±1.5 for this reaction and they concluded at that time that the interference predicted by the standard model is not confirmed by this measurement, although certainly not ruled out.[21] Since, through the early beautiful measurement using both the CDHS and CHARM detectors, we learned that the helicity of the muon is as expected in charged current interactions this would be a test of the neutral current channel alone. The cross section for this reaction was listed above and is proportional to $Z^2E\ln E$. Hence, there is a premium on the use of a heavy target. The really interesting feature of this reaction is that measurement of the interference in either angle or momentum is equivalent to a single measurement for one or the other of two impossible reactions:

$$\nu_\mu+\mu^+\rightarrow\nu_\mu+\mu^+$$

$$\nu_\mu+\mu^-\rightarrow\nu_\mu+\mu^-$$

The interference between the momentum of the μ^+ and μ^- is shown in Figure 9 for 50 GeV neutrinos. Clearly, the interference is large, but at very low values.

Right-handed W. The best limit for right handed W bosons comes from muon decay experiments and an early CDHS experiment[22]. This is shown in Figure 10 and comes from fitting for y at low x. The limitation in sensitivity to θ is statistical. Here the analysis is for a model of two charged intermediate vector bosons, W_1 and W_2 which mix in $SU(2)_L\otimes SU(2)_R\otimes U(1)$ according to

$$W_L\propto W_1\cos\theta+W_2\sin\theta$$

Clearly, the structure function experiment suggested above could improve this limit over a large energy range.

Conclusions

The potential of a high-intensity, low energy proton accelerator for providing a new tool for studying neutrino interactions is very promising. While typical progress in High Energy Physics traditionally fol'ows the highest energy reaches, often important issues requiring study can only be adequately addressed through high rate devices with low backgrounds. In this regard, the neutrino beams available from the Main Injector are unique in their potential - intermediate in a poorly-studied energy regime and unparalleled in intensity. In this review, only a few of the many possible issues in neutrino physics have been covered. Many more topics could have been discussed such as exclusive final states, elastic neutral current processes, and Universality.

Should this unique facility be built, increased attention will certainly be given to a new generation of neutrino experiments.

---

[1] I am grateful to Linda Stutte of the Fermilab Research Division for information on fluxes.

[2] H.W. Atherton *et al.* CERN 80:07, 1980, A. Malensek, Fermilab Technical Report FN-341, 1981.

[3] L.G.Hyman for a 1977 ANL,CMU,UK,MSU,NDU, and PU collaboration proposal.

[4] An attempt has been made to simulate a NBB for the MI and it was preliminarily found that the total flux as indicated in the text might be obtained but at the expense of an energy spread which could easily be twice that of the Argonne proposal and asymmetric. No attempt has been made to exploit the vertex position as a means of limiting the energy spread. (Linda Stutte, private communication.)

[5] For a 300GeV NBB horn design, see Baltay and Cohen Columbia memo *Two Horn Narrow Band Neutrino Beams* , un-numbered memo circa 1975. For a design for Los Alamos (29GeV , NBB system for LAMF II) see Wang *et al.* in *Physics with Lampf II* , LA-9798-P Los Alamos National Laboratory, page 237).

[6] R. Bernstein, contribution to this Workshop.

[7] See W.Y.Lee, in Proceedings of the New Directions in Neutrino Physics at Fermilab Workshop, September, 1988. To be published.

[8] M. Shaevitz in Proceedings of the New Directions in Neutrino Physics at Fermilab Workshop, September, 1988. To be published.

[9] H. Harari, Phys. Lett. **216B** (1989) 413.

[10] U. Amaldi *et al*, Phys. Rev. **D36** (1987) 1385 , R. Brock, "Deep Inelastic Neutrino Measurements of $\sin^2\vartheta_W$", to be published in *Proceedings of the New Directions in Neutrino Physics at Fermilab*, September, 1988.

[11] CHARM: F. Bergsma *et al.*, Phys. Lett. **117B** (1982) 272, Phys. Lett. **147B** (1984) 481; E734: L.A. Ahrens *et al.*, Phys Rev. Lett. **51** (1983)1514, Phys. Rev. Lett. **54** (1985) 18.

[12] V. Zacek for CHARM II in Proceedings of the XXIV International Conference on High Energy Physics, R. Kotthaus and J.H. Kuhn, eds., Springer-Verlag, Berlin, p917.

[13] K. Abe, *et al.* Phys. Rev. Lett. **62** (1989) 1709.

[14] See R. Brock, contribution to this Workshop.

[15] G.A. Voss in Proceedings of the 1987 International Symposium on Lepton and Photon Interactions at High Energies, W. Bartel and R. Ruckl, eds., North Holland, Amsterdam, 1988, p 581.

[16] See, for example, F.E. Taylor, in Proceedings of Neutrinos '88, June, 1988. To be published.

[17] R.L. Jaffe and M. Soldate, Phys. Rev. **D26** (1982) 49, R.K. Ellis, W. Furmansky, and R. Petronzio Nucl. Phys. **B212** (1983) 29, Jianwei Qiu, Argonne report ANL-HEP-PR-88-10.

[18] The only neutrino experiment to successfully fit for both Λ and a non-zero Twist 4 contribution simultaneously is BEBC WA 59 experiment at CERN; K. Varvell, *et al.*, Z.Phys. C36 (9187) 36. Figure 8 is derived from Figure 8 in reference 15.

[19] W.K. Tung et al. Argonne report ANL-HEP-CP-89-01.

[20] For a recent discussion of this issue as well as Universality, see J. Rosen to be published in *Proceedings of the New Directions in Neutrino Physics at Fermilab*, September, 1988.

[21] M. Oreglia for CCFR in Proceedings of the XXIV International Conference on High Energy Physics, R. Kotthaus and J.H. Kuhn, eds., Springer-Verlag, Berlin, p924. The only previous report is from the CHARM collaboration, with an observed 1.7±1.7 events in wide band running F. Bergsma *et al.*, Phys. Lett. **122B** (1983) 185.

[22] H. Abramowicz *et al.*, Z. Phys. C12 (1982) 225, J.M. Frere, private communication.

WBB RUN $\nu_\mu N \rightarrow \mu X$		
events/proton/ton	*events/ton*	*comparison with Lab E (500t, Tevatron QT beam)*
7.4×10^{-15}	280,000	6,000 events/ton
NBB RUN $\nu_\mu N \rightarrow \mu X$		
events/proton/ton	*events/ton*	*comparison with Lab E (500t, Tevatron NBB)*
4.3×10^{-16}	17,850	500 events/ton

WBB RUN $\nu_\mu e \rightarrow \nu_\mu e$		
events/proton/ton	*events/ton*	*comparison with CHARM II (700t, CERNPS horn beam)*
1.2×10^{-18}	36	2.8 events/ton
NBB RUN $\nu_\mu e \rightarrow \nu_\mu e$		
events/proton/ton	*events/ton*	*comparison with CHARM II (700t, CERNPS horn beam)*
8×10^{-20}	3.2	2.8 events/ton

WBB RUN $\nu p \rightarrow \mu n$		
events/proton/ton	*events/ton*	*comparison with BNL E734 (700t, BNL horn beam)*
5×10^{-16}	14,500	2.8 events/ton
NBB RUN $\nu p \rightarrow \mu n$		
events/proton/ton	*events/ton*	*comparison with BNL E734 (700t, BNL horn beam)*
6×10^{-17}	2600	2.8 events/ton

WBB RUN $\nu p \rightarrow \nu p$		
events/proton/ton	*events/ton*	*comparison with BNL E734 (700t, BNL horn beam)*
7.4×10^{-17}	2000	2.8 events/ton
NBB RUN $\nu p \rightarrow \nu p$		
events/proton/ton	*events/ton*	*comparison with BNL E734 (700t, BNL horn beam)*
9×10^{-18}	390	2.8 events/ton

WBB RUN $\nu Z \rightarrow Z\mu\mu$ (Fe target)		
events/proton/ton	*events/ton*	*comparison with Lab C (100t, Tevatron QT beam)*
4.9×10^{-20}	2	0.02 events/ton

Table 1. Rates for fiducial reactions of interest.

WBB	$\nu_\mu N \rightarrow \mu X$ events/run	$\nu_\mu e \rightarrow \nu_\mu e$ events/run	$\nu_\mu Z \rightarrow Z\mu\mu$ events/run
Lab E detector	70M (E_ν>10GeV)	-	1000
Lab C detector	14M (E_ν>10GeV)	2900 (E_ν>10GeV)	200
15' BC (light mix)	3.2M (E_ν>5GeV)	400 (E_ν>10GeV)	28
280*liters* emulsion	220K (E_ν>5GeV)	30 (E_ν>10GeV)	2

Table 2. Rates per RUN for the MI for typical detectors.

$\nu_\mu N \rightarrow \mu X$	3M	Lab E E744
$\nu_\mu e \rightarrow \nu_\mu e$	2000	CHARM II
$\nu_\mu Z \rightarrow Z\mu\mu$	2	CHARM

Table 3. Existing samples from the highest rate detectors.

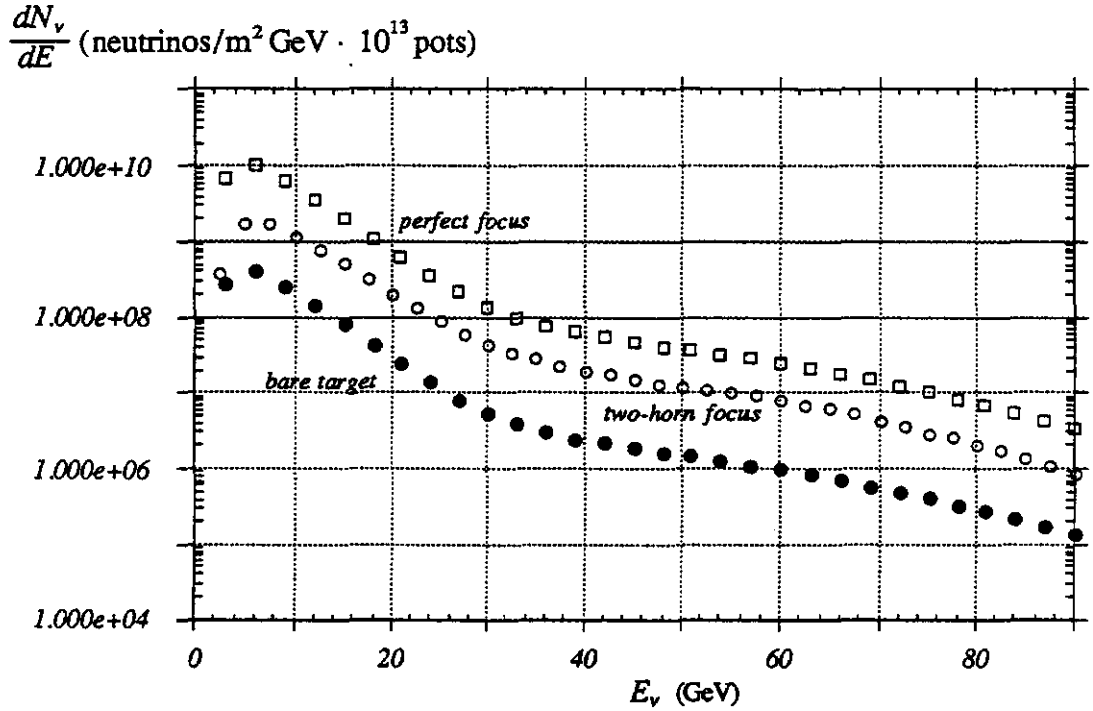

Figure 1. Flux predictions for 150 GeV protons.

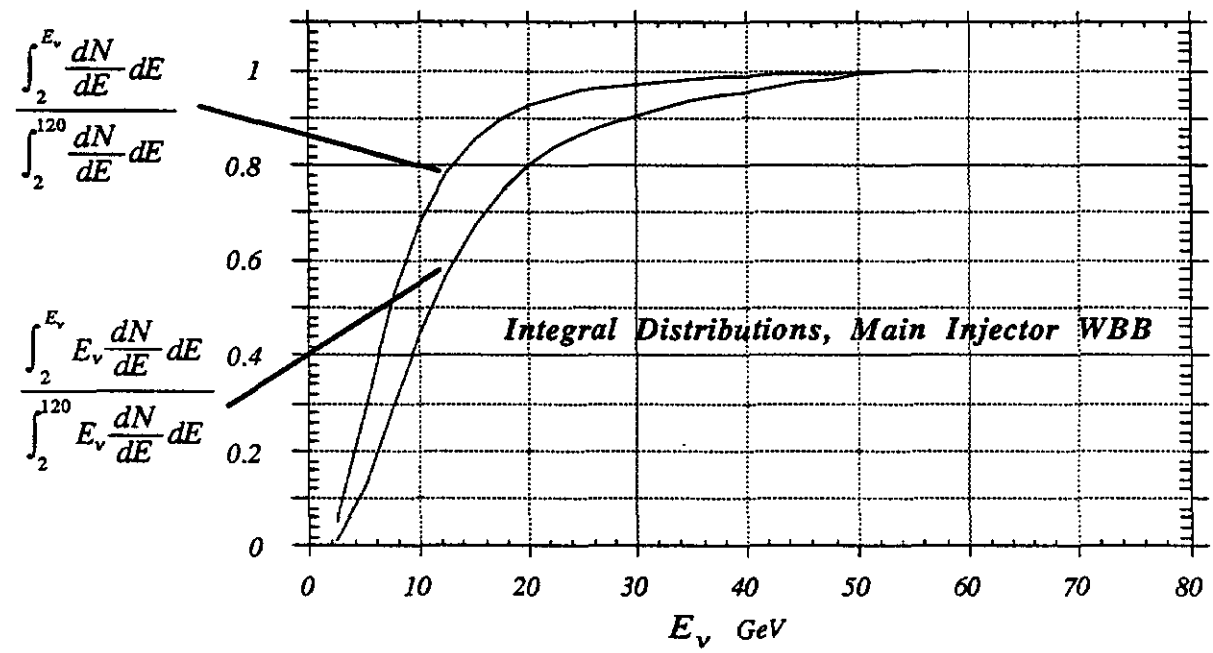

Figure 2. Integral distributions for the two-horn Wide Band Beam flux at 150 GeV primary momentum.

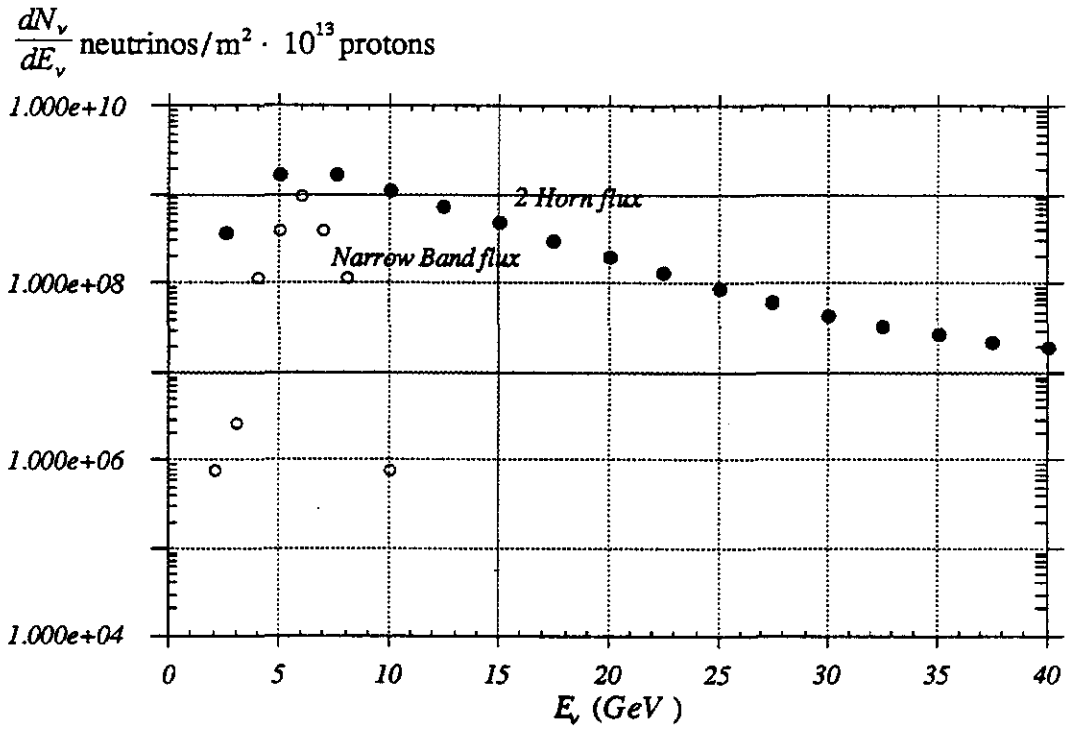

Figure 3. Optimistic Narrow Band Beam flux.

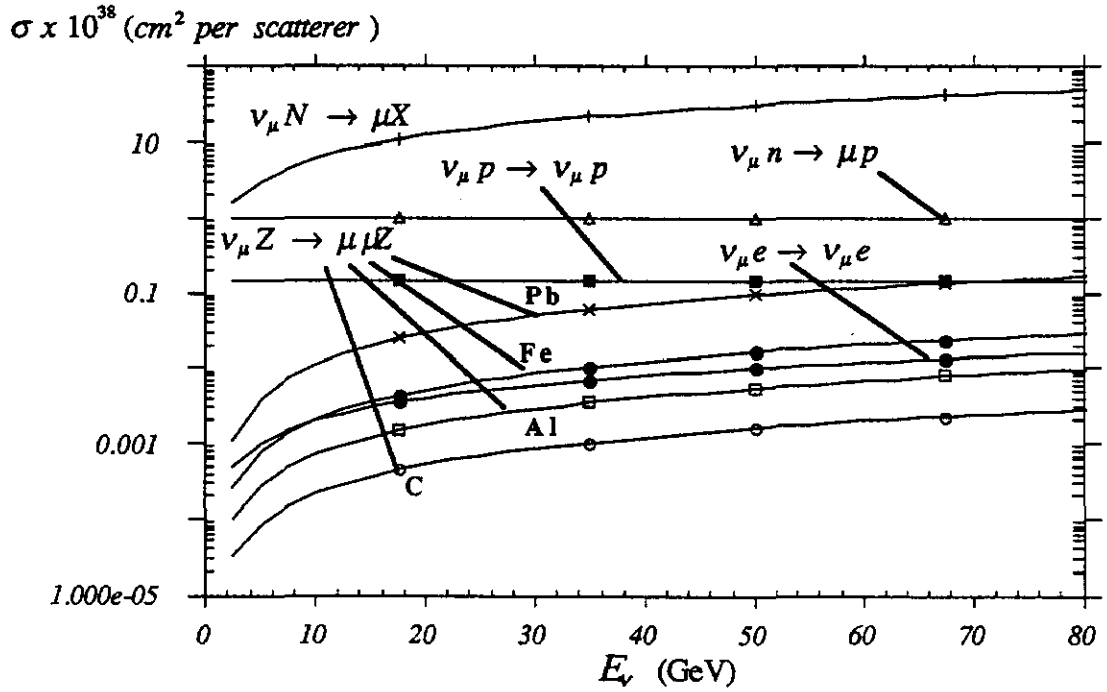

Figure 4. Cross sections for Main-Injector-relevant process.

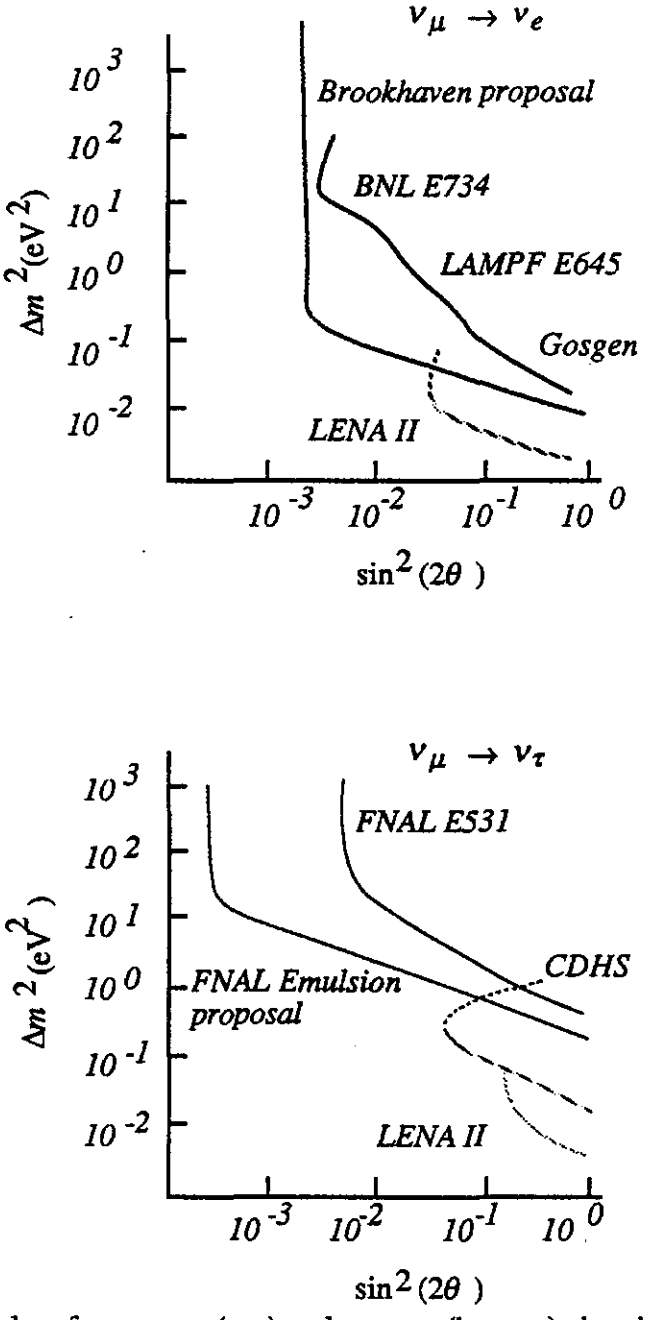

Figure 5. Exclusion plots for $\nu_\mu \rightarrow \nu_e$ (top) and $\nu_\mu \rightarrow \nu_\tau$ (bottom) showing the existing limits and the expectations from the Fermilab proposals referred to in the text as well as the BNL proposal.

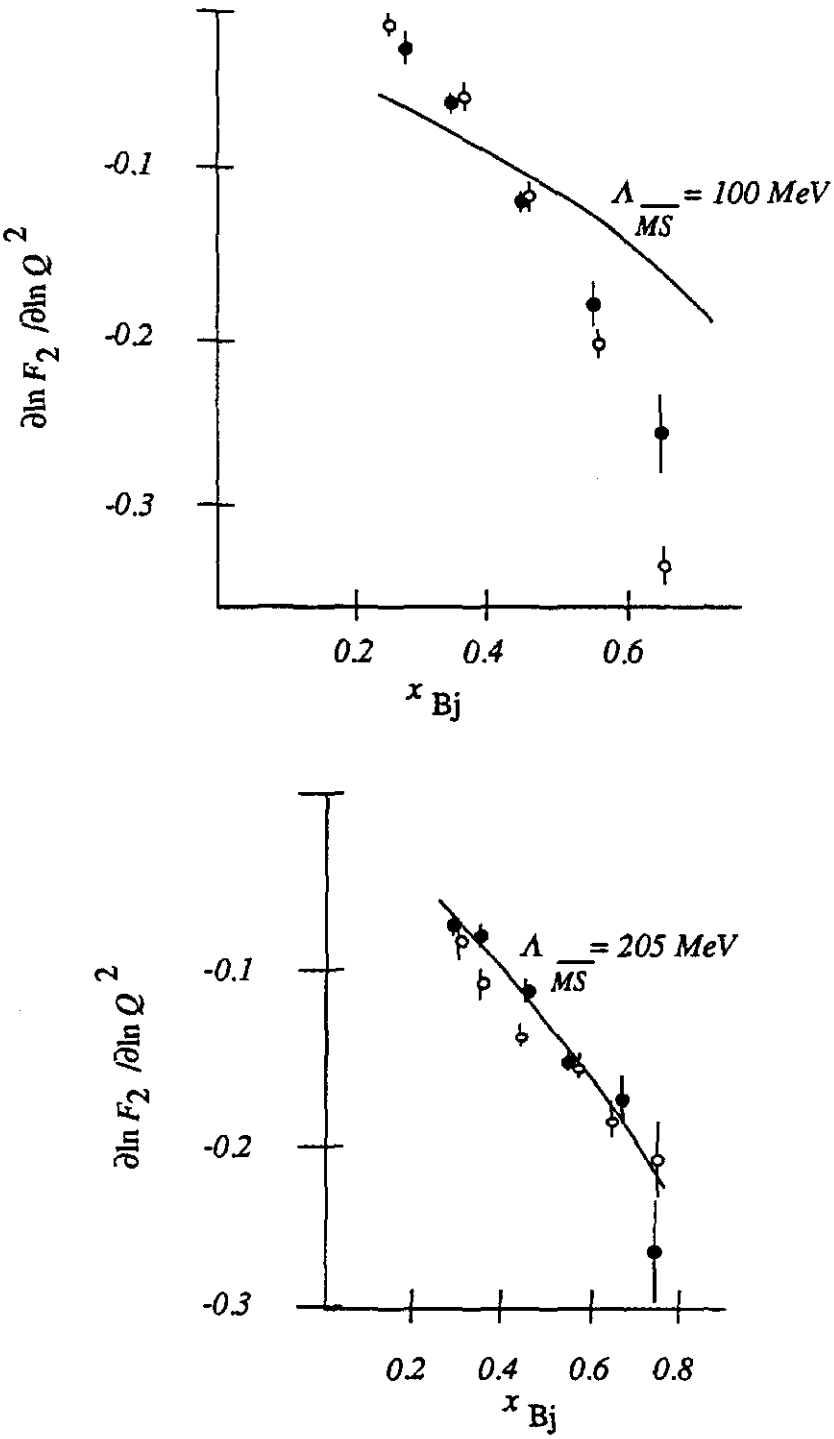

Figure 6. Slope of F_2 with Q^2 versus x for Fe targets (top: EMC, closed circles; CDHS, open circles) and BCDMS (bottom: H_2, open circles; C, closed circles).

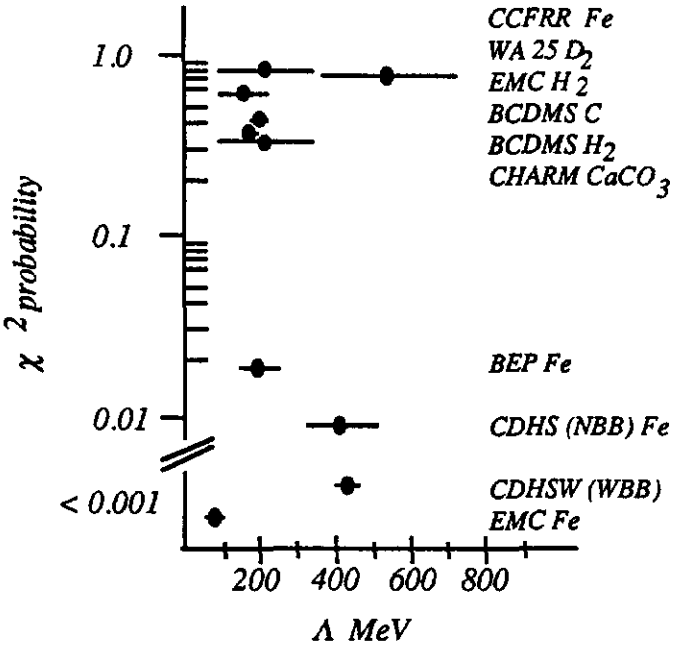

Figure 7. Fit probability versus Λ for various experiments from non-singlet measurements. For the muon data, F_2 used for $x > 0.25$. For the neutrino data, xF_3 used for $x < 0.4$ and F_2 used for $x > 0.4$.

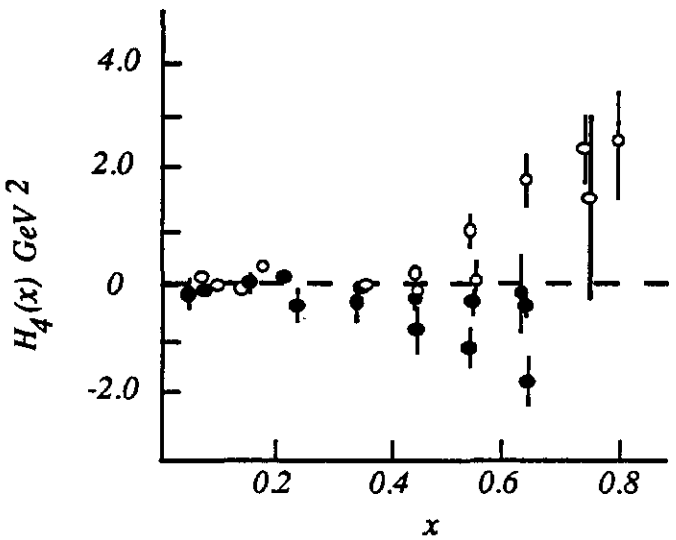

Figure 8. Twist 4 contribution from a variety of charged lepton experiments (open circles) and neutrino experiments (closed circles).

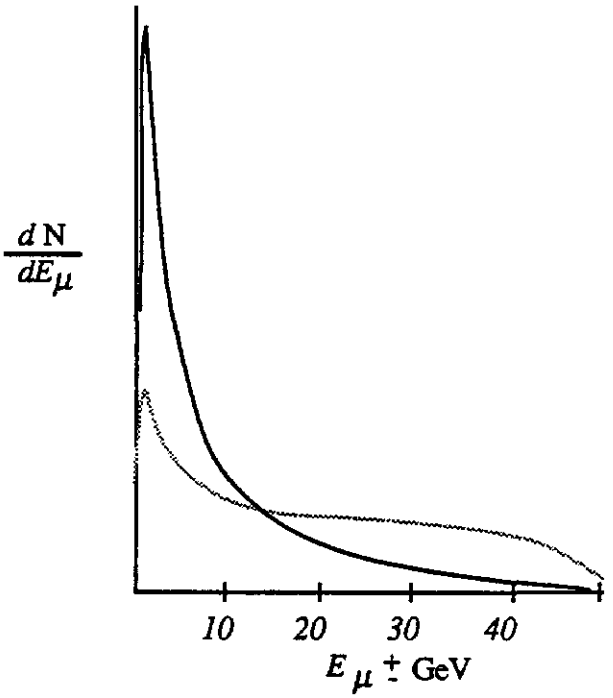

Figure 9. Énergy distribution of μ^+ (solid) and μ^- (gray) from tridents at a neutrino energy of 50GeV.

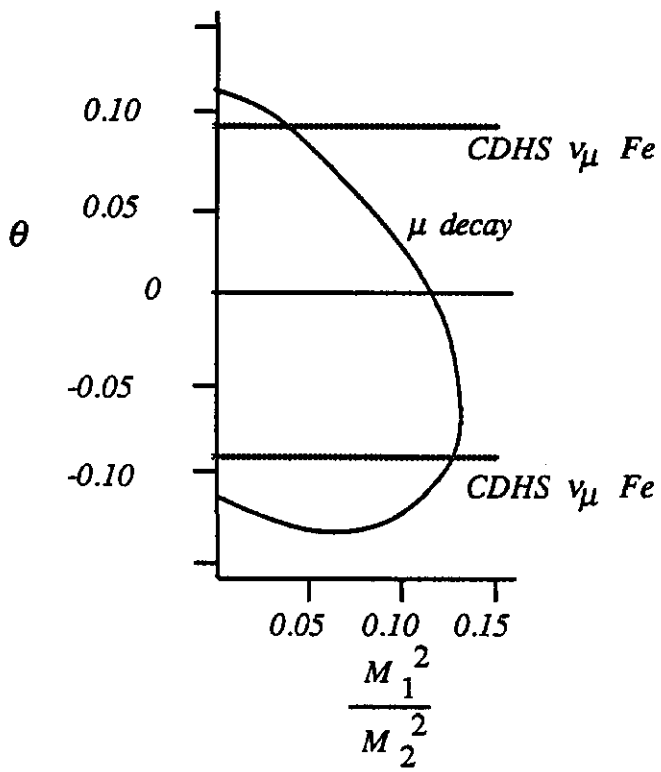

Figure 10. Limits on extra charged gauge bosons from neutrino interactions (CDHS) and μ decay.

ANTIPROTON PHYSICS UP TO 120 GeV*

Gerald A. Smith
Laboratory for Elementary Particle Science
Department of Physics
Pennsylvania State University
University Park, PA 16802

I. Summary

Many excellent opportunities exist for new and exciting physics utilizing antiprotons at the proposed Main Injector at Fermilab. High luminosity is a key ingredient for experiments involving charmonium, CP-violation in hyperon-antihyperon decay and charmed baryon properties where cross sections and symmetry violating effects are small. These experiments can be best done at momenta below ~ 25 GeV/c. Important experiments on searches for exotic meson states, color transparency effects in nuclei and the time-like form factor of the proton can also be done in this momentum range. Possibilities exist for experiments at higher momenta, including spin effects with polarized beams and tests of QCD effects in nuclear targets.

II. Introduction

The Main Injector offers numerous possibilities for new physics with pure, intense antiproton beams up to 120 GeV. For this brief review, I have chosen to illustrate this by discussing three well-defined experiments, plus mentioning briefly several other possibilities which could be further explored in detail at the Breckenridge Workshop. In advance, I wish to acknowledge an important source of information which has its origins in the CERN Super-Lear proposal.[1]

*Work supported in part by the US National Science Foundation.

III. Charmonium Physics

Experiment E760[2] in the existing Fermilab Antiproton Accumulator illustrates in many ways the unique capabilities of intense, cooled antiproton beams and related technologies (i.e. gas jet targets). The physics goals of E760 parallel closely those of R704, a first generation experiment performed at the CERN ISR in 1984. For reference, I show the basic features of charmonium spectroscopy in Fig. 1. Due to the shutdown of the ISR, only limited results were achieved, such as observation of the J/ψ, $\chi_{1,2}$ and η_c and a hint of the $^1P_1$ state.[3-7] Even so, the advantages of $\bar{p}p$ formation of charmonium states with cooled antiprotons were dramatically proven as illustrated in Fig. 2, which shows signals for $\chi_{1,2} \rightarrow J/\psi\gamma \rightarrow e^+e^-\gamma$ from R704, compared to those from the Crystal Ball. The full effects of beam resolution in formation, in contrast to final state photon spectroscopy resolution in the decay $\psi' \rightarrow \chi\gamma$, is very apparent. And, of course, electron-positron collisions can only directly access states with $J^{PC} = 1^{--}$ by photon exchange, whereas proton-antiproton collisions can directly access all states by two or three gluon exchange processes.

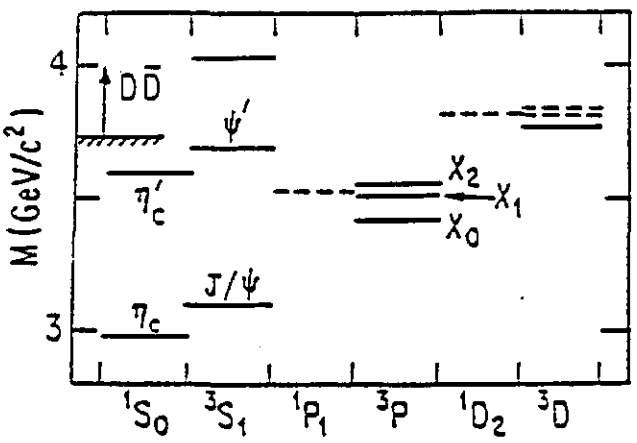

Fig. 1 - Low-lying charmonium states.

With a factor of fifty more rate (five times more acceptance, ten times more luminosity) than R704 and excellent mass resolution (300 KeV rms) in the 3-7 GeV/c range, the following physics goals appear within reach:

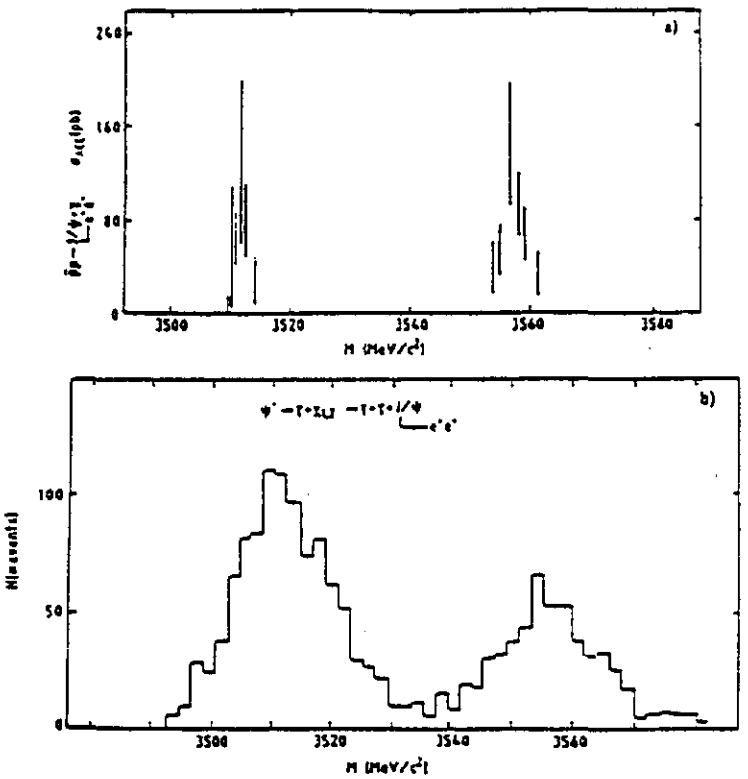

Fig. 2 – Results on $\chi_{1,2}$ states from (a) R704 and (b) Crystal Ball.

- Discover 3 previously unknown narrow states:

  1) $^1P_1$ or 1^{++} (charmonium analog of B-meson): Search for

     $^1P_1 \rightarrow J/\psi + \gamma$ (forbidden by C)

     $^1P_1 \rightarrow J/\psi + 2\pi$ (suppressed by P-wave phase space)

     $^1P_1 \rightarrow J/\psi + \pi^0$ (isospin violating (S-wave)): (remember that $\omega \rightarrow \pi^0\eta$ @ 8.7%)

  2) $^1D_2$ or 2^{-+} (predicted by models): Note that $2M_D < M(^1D_2) < M_D + M_{D^*}$ and decay to $D\bar{D}$ is forbidden by parity, so it's likely to be narrow, i.e. $^1D_2 \rightarrow J/\psi + \gamma$ ($\Delta L = 2$ M1 transition).

     $\rightarrow J/\psi + \rho^0$ (isospin violating (S-wave))

  3) $^3D_2$ or 2^{-+} ($\bar{c}c$ state mass close to $^1D_2$): Cascade decays to J/ψ will likely be strong, i.e.

$^3D_2 \rightarrow \chi + \gamma \rightarrow J/\psi + \gamma\gamma$ (both allowed E1 transitions)

$^3D_2 \rightarrow J/\psi + \pi^0$ (isospin violating (P-wave))

- Confirm weak η'_c
- Accurately measure masses of $^1P_1$, $^3D_2$, $^1D_2$: These are sensitive to spin, spin-orbit, tensor and relativistic terms in the charmonium potential.
- Accurately measure total widths for all narrow $c\bar{c}$ states: Presently total widths are poorly known (except for $^3S_1$). Total widths are predicted in QCD via 2 or 3 gluon annihilation diagrams.
- Measure helicity amplitudes in $\bar{p}p$ production: In perturbative QCD, calculations of 2 or 3 gluon annihilation diagrams coupled to $\bar{p}p$ with massless quarks give a helicity selection rule $\lambda_{c\bar{c}} = \lambda_p - \lambda_{\bar{p}} = \pm 1$, which forbids states with $0^{-+}(\eta_c)$, $0^{++}(\chi_o)$ and $1^{+-}(^1P_1)$.[8,9] However, it is known from studies of η_c decay that $BR(J/\psi \rightarrow \bar{p}p) \simeq 2\ BR(\eta_c \rightarrow \bar{p}p)$, so the rule is broken. Therefore, it is of interest to actually measure the ratios of all helicity amplitudes, 0 and ± 1, to further probe spin effects in QCD.
- Unravel multipoles: Radiative decays of $c\bar{c}$ states often allow competing multipoles, e.g. $2^{++} \rightarrow 1^{--}$ via E1, M2 or E3 transitions, $2^{-+} \rightarrow 1^{--}$ via M1, E2 or M3 transitions.[10] Multipoles are sensitive to high momentum components in the wavefunction $(M_2/E_1)^2 \sim v^2/c^2$, etc., and probe the regime where relativistic corrections are small.

I show in Fig. 3 a schematic layout of the detector. Details of the silicon detector array which monitors luminosity via $\bar{p}p$ diffractive elastic scattering are not shown. Particles produced in the intersection of the $\bar{p}$ beam and the gas jet emerge through an inner tracking system comprised of layers of drift tubes and a radial projection chamber. The next layer is a

gaseous threshold counter, comprised of two polar and eight azimuthal sectors, which identifies $e^{\pm}$ from J/ψ decay. The cerenkov system is followed by an outer and forward tracking system comprised of limited streamer tubes and proportional chambers.

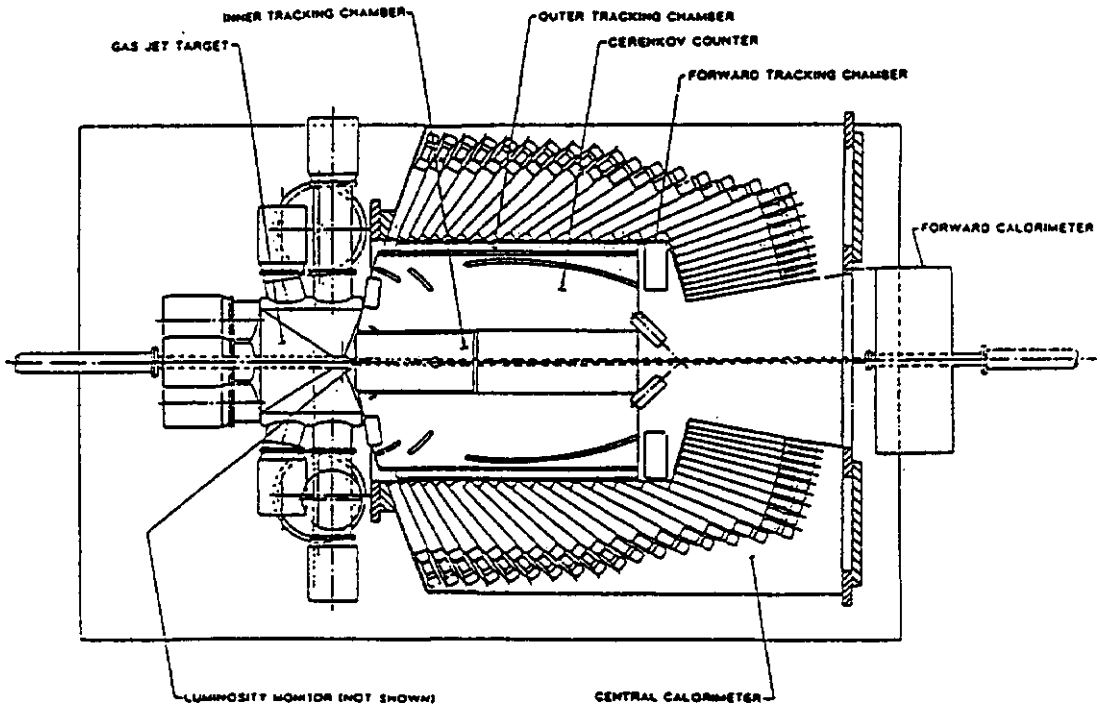

Fig. 3 - E760 Detector

The central electromagnetic calorimeter is comprised of 1280 lead glass modules with pointing geometry. The modules are organized into 64 azimuthal "wedges", each containing 20 modules. The number of radiation lengths per module varies from 16(70°) to 24(15°). The forward calorimeter closes the end-cap region down to ~ 2° around the beam pipe. It consists of 144 modules (non-pointing) of ~ 15 radiation lengths each, constructed in a lead-scintillator sandwich format.

IV. Search for CP-Violation in Hyperon-Antihyperon Decay

After 25 years CP violation has only been observed in the neutral kaon system. Why this is so no one knows, but surely it would be most exciting

and rewarding to observe it in another system. Recently it has been pointed out that it may be possible to observe CP-violation in $\Delta S=1$ non-leptonic hyperon decays by comparing the decay of hyperon-antihyperon pairs produced in antiproton-proton interactions.[11-14] Employing the usual decay parameters, $\alpha = 2ReS^*P/|S|^2+|p|^2$ and $\beta = 2ImS^*P/|S|^2+|p|^2$, it is argued that CP-violation will be manifest as non-zero values of $\alpha+\bar{\alpha}$ and $\beta+\bar{\beta}$ as shown in Table 1.[15]

Table 1 – Predictions of CP-violation in hyperon-antihyperon decay.

Model	$\beta+\bar{\beta}$	$\alpha+\bar{\alpha}$	$\beta+\bar{\beta}/\alpha+\bar{\alpha}$
KM Standard	2×10^{-4}	-0.7×10^{-4}	– 3
Weinberg-Higgs	1×10^{-3}	-3×10^{-4}	– 3
L-R Symmetric	-0.6×10^{-4}	2×10^{-5}	– 3

These are small numbers and present a serious challenge to experimentalists. Because β seems to be more sensitive than α, one would want to study $\Xi\bar{\Xi}$ decays, which are fully self-analyzing in terms of α and β (second scatter experiments following hyperon decay seem to be out of the question). One could produce $\Xi\bar{\Xi}$ paris at about 3.5 GeV/c antiproton momentum, which is ~ 0.9 GeV/c above threshold, where the cross-section peaks at ~ 2-4 μb based on scant bubble chamber data. Unfortunately there is no information available on the $\Xi,\bar{\Xi}$ polarization (which must be equal due to C-invariance in the strong interaction). Therefore, a preliminary experiment is required in which the cross section and polarization are accurately mapped out from threshold up to ~ 4 GeV/c.

Assuming a polarization of 30%, it has been estimated that 10^8 events are required to measure β to 10^{-3} accuracy.[16] With a luminosity of $5\times10^{31}cm^{-2}sec^{-1}$ using a gas jet in the Antiproton Accumulator,[17] a 3 μb cross-section and

including only charged decays $\Lambda(\bar{\Lambda}) \rightarrow p(\bar{p}) + \pi^-(\pi^+)$, it would take ~ 10^7sec of live beam, assuming a 33% data collection efficiency, to accumulate 10^8 events. This is not an unreasonable amount of time considering the importance of the measurement. The real challenges arise when one considers how to trigger on the exclusive reaction and deal with systematic errors. These will receive careful attention at the Breckenridge Workshop.

V. Charmed Baryons

From the previous section we see that the symmetric production of hyperon-antihyperon pairs with well understood properties in antiproton-proton interactions can be exploited to test a fundamental symmetry principle. Therefore, why not turn this around and use this symmetry to learn more about the basic properties of charmed baryons?[18] There are fifteen predicted low-lying charmed baryons shown in Fig. 4. Of these fifteen, only five rate at least one star in the Review of Particle Properties[19]. Hence,

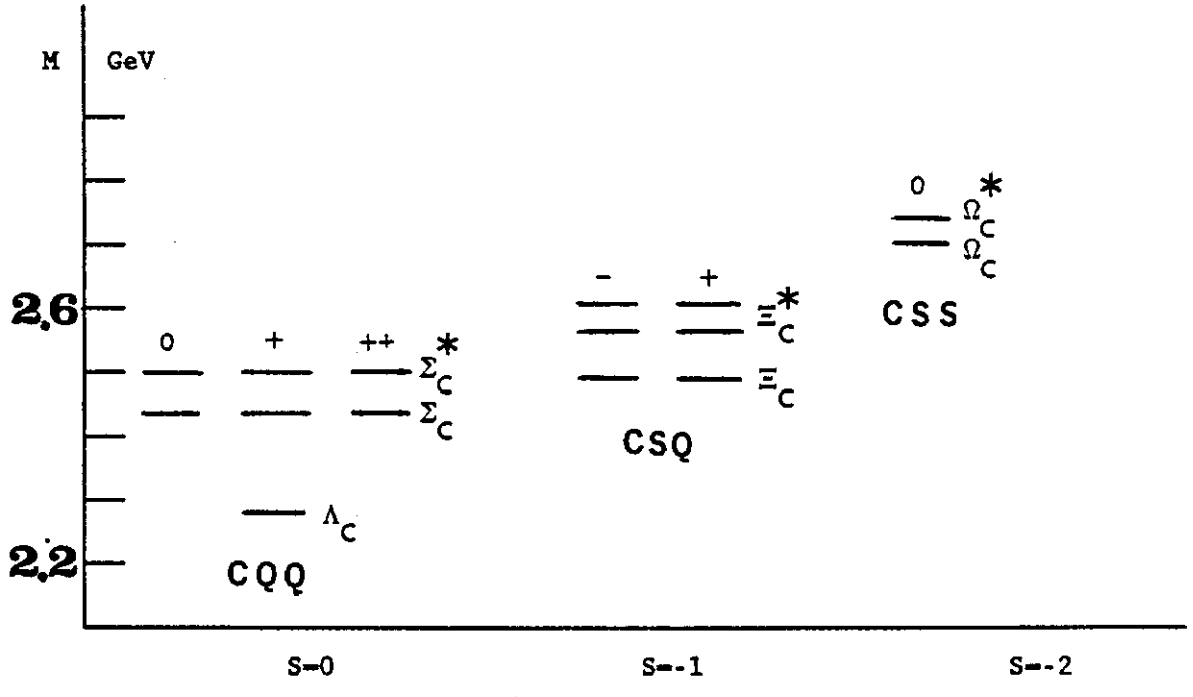

Fig. 4 – Low-lying charmed baryons.

this is a wide-open field which, incidentally, will be the subject of a future major experiment at Fermilab.[20] The goals of such investigations are precise measurements of masses, lifetimes, decay branching ratios and production dynamics, including polarization.

As in the CP experiment, the best way to do this is to produce exclusive pairs (i.e. $\Lambda_c\bar{\Lambda}_c$) of hyperons so that one has very strong kinematic constraints and a handle on systematic errors. Using QCD as a guide ($\sigma \propto m_q^{-8}$) and scaling from $\Lambda\bar{\Lambda}$, the cross section for $\Lambda_c\bar{\Lambda}_c$ is estimated to be ~ 200 nb.[18] As with $\Lambda\bar{\Lambda}$, one would sit slightly above threshold (10 GeV/c), perhaps at 15 GeV/c. To access the heaviest charmed baryons, a beam momentum of ~ 20-25 GeV/c would be appropriate. Suppose, for example, one were interested in studying rare semi-leptonic decays $\Lambda_c^+ \rightarrow \Lambda_s^0 e^+\nu$ (~ 2% est.), $\Lambda_s^0 \rightarrow p\pi^-$ (64%). Then, with a luminosity of $10^{31}cm^{-2}sec^{-1}$, one would collect exclusive pairs of semi-leptonic decays at a rate of ~ 20-30 per day. Requiring only one semi-leptonic decay per event would increase this yield by perhaps a factor of five. Therefore, in one year of running one could accumulate ~ 50K semi-leptonic decays and perhaps ~ 250K analyzable hadronic decays. The logical place to do this is in the Main Injector itself, using it as a storage ring with a gas jet target. Although this possibility is not described within the boundaries of the present Main Injector plan,[17] I recommend that it get serious consideration at the Breckenridge Workshop.

VI. Other Physics Possibilities

Numerous other ideas have either crossed my mind or been brought to my attention. They are (in arbitrary order):

1) Spin physics (polarized beams via Stern-Gerlach, Siberian snake, or spin filter techniques).

2) Drell-Yan, EMC physics with nuclear targets.

3) Color transparency effects with nuclear targets.[21]

4) Time-like proton form factor, G_E vs G_M in $\bar{p}p \rightarrow e^+e^-$.

5) Dimensional counting rules, QCD in $\bar{p}p \rightarrow ab$ at 90°.[22]

6) Glueball searches using $\bar{p}p$ annihilation (with and without polarized $\bar{p}$'s).

7) Searches for cryptoexotic mesons (Q^2Q^2).[23]

It is planned that each of these gets special attention at the Breckenridge Workshop.

VII. References

1. P. Dalpiaz et al, "Physics at Super-Lear," CERN/EP-87-27, Feb. 12, 1987.
2. "A Proposal to Investigate the Formation of Charmonim States Using the Antiproton Accumulator Ring," Fermilab-Ferrara-Genoa-Irvine-Northwestern-Penn State-Torino Collaboration, approved December 1985.
3. C. Baglin et al, Phys. Lett. 172B, 455 (1986).
4. C. Baglin et al, Phys. Lett. 171B, 125 (1986).
5. C. Baglin et al, Phys. Lett. 187B, 191 (1987).
6. C. Baglin et al, Nucl. Phys. B286, 592 (1987).
7. C. Baglin et al, Phys. Lett. 195B, 85 (1987).
8. S. Brodsky and P. Lepage, Phys. Rev. D24, 2848 (1981).
9. A. Andrikopoulou, Z. Phys. C22, 63 (1984).
10. M. Olsson, Phys. Rev. D31, 1759 (1985).
11. J.F. Donoghue, Workshop on Antimatter Physics at Low Energy, (FNAL, April, 1966) p. 241.
12. J.F. Donoghue and S. Pakvasa, Phys. Rev. Lett. 55, 162 (1985).
13. J.F. Donoghue et al, Phys. Rev. D34, 833 (1986).
14. J.F. Donoghue et al, Phys. Lett. 178B, 319 (1986).

15. Courtesy of A. Nathan, Univ. of Illinois.

16. D.C. Peasle, Univ. of Maryland, "Search for CP-Violation in Hadronic Decay," Feb. 20, 1989.

17. The Fermilab Upgrade – An Overview, Jan. 9, 1989, p. 36.

18. S. Brodsky et al, "QCD Prospects in Antiproton-Proton Interactions at Super-Lear," to appear in Proc. IX European Symposium on Antiproton-Proton Interactions and Fundamental Symmetries, Mainz, FRG, Sept. 5-10, 1988.

19. M. Aguilar-Benitez et al, Phys. Lett. 204B, 1 (1988).

20. Fermilab experiment #781 – Carnegie Mellon-Fermilab-Beijing-Leningrad-Iowa-Sao Paulo-Yale Collaboration.

21. S. Heppelmann and G.A. Smith, "Color Transparency and J/ψ Production in Antiproton-Nucleus Collisions," AIP Conf. Proc. No. 185, ed. S.U. Chung, p. 581.

22. See C. Baglin et al, "Precision Measurements of the Antiproton-Proton Elastic Scattering Cross-Section at 90° in the Incident Momentum Range Between 3.5 GeV.c and 5.7 GeV/c," CERN EP/89-60, April 25, 1989, submitted to Phys. Lett.

23. J. Rosen, "Heavy Hadronic Molecules," AIP Conf. Proc. No. 185, ed. S.U. Chung, p. 611.

II.
Working Group Summaries

CP VIOLATION AT THE MAIN INJECTOR: Report of the Working Group on CP Violation Experiments

J. L. Ritchie*
University of Texas at Austin, Austin, TX 78712

G. J. Bock	*Fermilab*
G. B. Thomson	*Rutgers University*
K. Lang	*Stanford University*
L. S. Littenberg	*Brookhaven National Lab*
R. Rameika	*Fermilab*
Y. W. Wah	*University of Chicago*
B. Winstein	*University of Chicago*
H. Yamamoto*	*University of Chicago*
T. Yamanaka	*Fermilab*

Introduction

CP violation was discovered 25 years ago, yet remains one of the most profound mysteries of particle physics. The Standard Model allows CP violation through a non-zero value of the complex phase of the Kobayashi-Maskawa (KM) matrix, but does not require it; experiments so far cannot distinguish between this hypothesis, the superweak hypothesis of Wolfenstein, or a variety of other potential mechanisms. More incisive experiments are needed.

The goal of this working group was to assess the potential for CP violation experiments at the proposed Main Injector. The 3 days of the workshop were too short to carry out detailed studies, but clear progress was made toward identifying major areas for future work. Also, some of the contributed papers to this proceedings report on studies which continued beyond the workshop itself.

We focused on two areas: (1) issues associated with modes of the type $K_L \to \pi^\circ \ell^+ \ell^-$, where ℓ represents either e or μ, and (2) the potential for improved measurements of the

* Group leaders

parameter $\frac{\epsilon'}{\epsilon}$. Other interesting topics, such as CP violation in the decay $K_L \to \gamma\gamma$ or the prospects for a search for $K_L \to \pi^\circ\nu\bar{\nu}$, received less attention than we would have liked, due to the short time available.

Direct CP Violation in the Decay $K_L \to \pi^\circ e^+e^-$

The decay amplitude for $K_L \to \pi^\circ e^+e^-$ receives contributions from (1) direct CP violation, (2) $K_L - K_S$ mass mixing, and (3) a CP conserving 2-γ process. The theoretical complexities of this decay were described at this workshop by Gilman and will not be discussed here. The experimental problem is to isolate the direct CP violating amplitude because it is the part which can be calculated in the Standard Model with reasonable confidence as a function of KM angles and the mass of the top quark.

Three possibilites for isolating the direct amplitude present themselves. The first is a separate measurement of the branching ratios $Br(K_L \to \pi^\circ e^+e^-)$, $Br(K_S \to \pi^\circ e^+e^-)$, and $Br(K_L \to \pi^\circ\gamma\gamma)$; it is at least possible that this would be sufficient, although it would depend on the mixing contribution and the CP conserving part (which can be estimated once the $K_L \to \pi^\circ\gamma\gamma$ rate is known) being small compared to the direct amplitude. This approach is experimentally the least challenging and is clearly the natural first step, which is already under way. Experiment 845 at BNL, with an ultimate expected sensitivity for $K_L \to \pi^\circ e^+e^-$ of 10^{-10}, has already taken data, and a new effort at Fermilab with a projected sensitivity of 10^{-11} has been proposed. (Subsequent to the workshop, the experiment, E799, was approved.) Also, considerable progress in a search for $K_L \to \pi^\circ\gamma\gamma$ has been made by FNAL E731, which was described at the workshop. The E731 limit is 2.7×10^{-6} (90% confidence level). While this is a difficult mode, the prospects appear very good that E799 can observe it.

The other two possible approaches, measuring the structure of the Dalitz plot and measuring the interference between K_L and K_S into $\pi^\circ e^+e^-$ as a function of proper time, both require enormous improvements in sensitivity over presently planned experiments. It is in the context of such experiments, which depend on amassing a large sample of decays which occur at the 10^{-11} level, that a new facility such as the Main Injector becomes important.

By measuring the structure of the Dalitz plot, we mean observing a large sample of $K_L \to \pi^\circ e^+e^-$ decays in an experiment running in a K_L beam and comparing the Dalitz plot distribution of the events with those expected from different underlying mechanisms.

This is the experimental set-up proposed in the early discussion of CP violation experiments at the Main Injector.[1] While there is reason to believe that there may be striking Dalitz plot asymmetries due to interference between the CP violating and CP conserving amplitudes if their magnitudes are similar,[2] this measurement appears still to require an independent measurement of the $K_S \to \pi^\circ e^+ e^-$ rate to fully isolate the direct amplitude. A measurement of the interference between K_L and K_S versus proper time would not preclude using the Dalitz plot distributions as supplimentary information. The key difference is that the experiment would have to be situated in a beam with a significant K_S component. Normally, this would mean the experiment would have to be close to the K° production target. Therefore, the beam-associated problems of adequate shielding make this the more difficult experiment.

We conclude that the power of Main Injector experiments to study direct CP violation in $K_L \to \pi^\circ e^+ e^-$ depends critically on the ability to measure $K_S \to \pi^\circ e^+ e^-$. Therefore, much of the effort at the workshop was concentrated on addressing this issue. It has led us to consider a K° beam which is much shorter than the one originally discussed.[1] Understanding whether an experiment can actually live in this short beam is one of the main questions which demands future study. The K_S beam will be discussed later in this report. Another prominent question is whether the high energy of the Main Injector (compared to other kaon sources, such as the AGS) provides an intrinsic advantage in doing this physics. Finally, there is the question of background rejection. We address these below.

Interference between K_L and K_S in $K^\circ \to \pi^\circ e^+ e^-$

The $K_L - K_S$ interference formalism will not be described here in the interest of brevity; it has been worked out in a form appropriate for this decay by Littenberg and is presented elsewhere.[3] The maximum interference between K_L and K_S into $\pi^\circ e^+ e^-$ should occur at about 10 K_S lifetimes. On a plot of distance (z) from the production target versus K° momentum, a fixed proper time is represented by a straight line eminating from the origin, as shown in Figure 1. One can see from such a plot that AGS energies are poorly matched to this measurement. K° flux at the AGS is peaked between 2 and 4 GeV, depending on production angle, with only a small tail of the distribution extending above 10 GeV. In order to utilize the majority of the flux at low momentum, it would be necessary to define the neutral beam in only a couple of meters, which is not possible. At

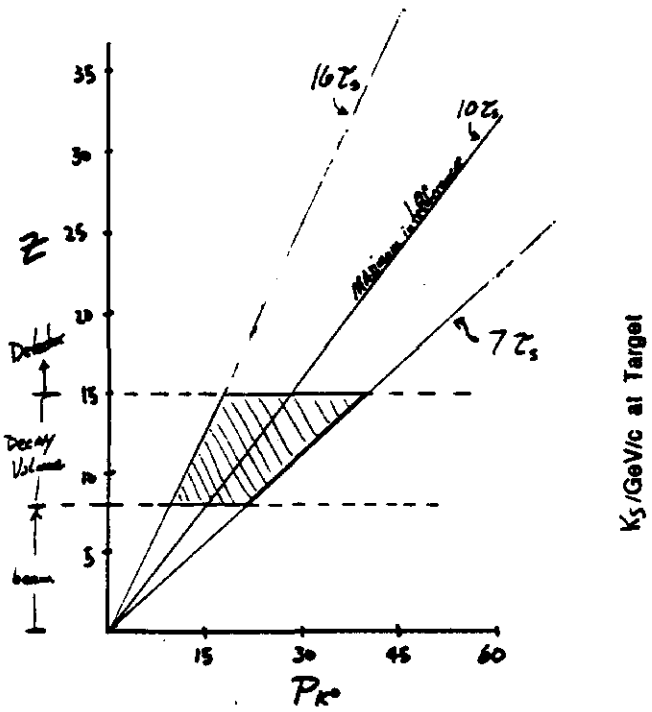

Figure 1 ⊢ 10 to 40 GeV ⊣ - useful momentum range
⊢ 15 to 25 ⊣ - sensitive region for max. interference

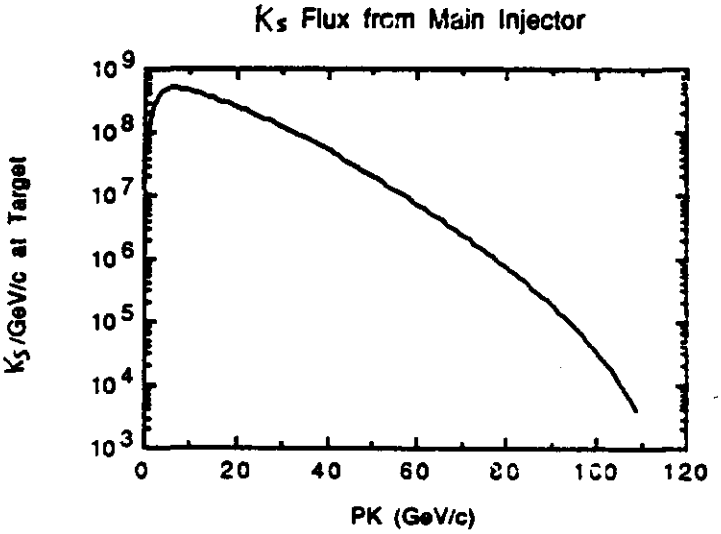

Figure 2

the Main Injector, the K° momentum spectrum, shown in Figure 2, is much more favorable. Approximately 40% of the flux is between 10 and 40 GeV. If a neutral beam can be defined in 8 meters, then this large fraction of the kaons fall into the interference region between about 7 and 16 K_S lifetimes. Two different experimental scenarios were considered at the workshop. G. Thomson has described one of these in a separate contributed paper. The result of the other is shown in Figure 3, with the input assumptions listed; the error bars on the interference curve show the statistical error from the number of expected events in each K_S lifetime bin. The two curves are for the case of no direct CP violation and the case of $\frac{\text{direct}}{\text{mixing}} = \sqrt{3}$, both in the presense a fixed CP conserving contribution.

It should be noted that a pure K° initial state has been assumed in these analyses. A useful improvement in future considerations would be to include a realistic estimate of the effect of the "dilution factor," which comes about because of the presence of a $\overline{K^\circ}$ admixture in the initial state.

A K_S Beam

The neutral beam proposed for the interference experiment is not a straightforward extrapolation of current experience. The nearest equivalent beam presently in operation

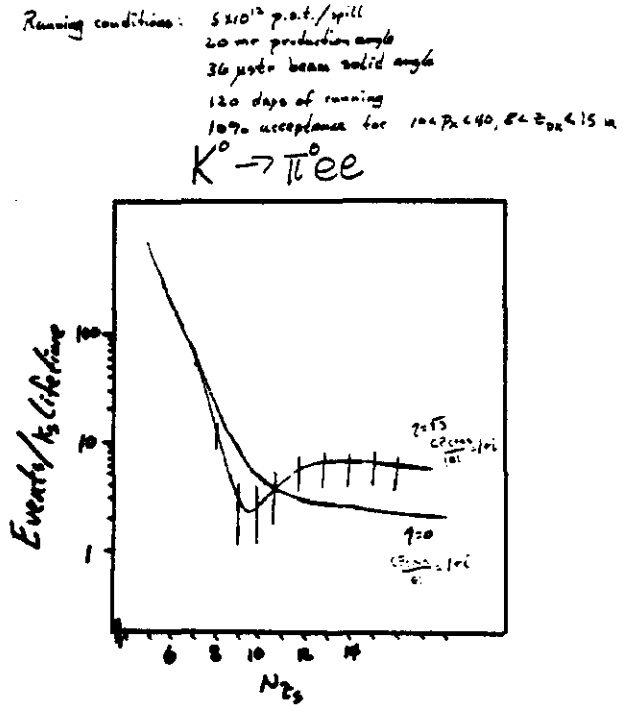

Figure 3

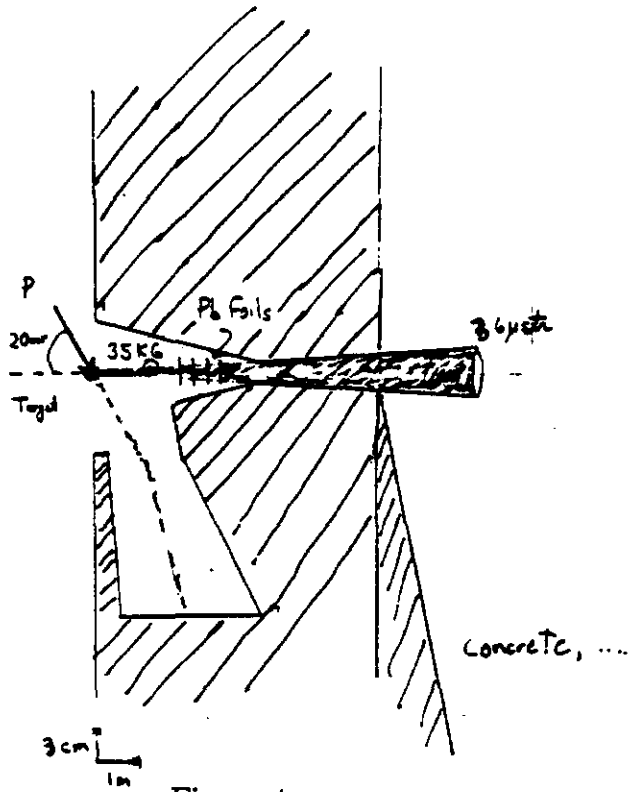

Figure 4

seems to be the E791 beam at BNL, where 5×10^{12} protons are routinely targeted and the decay volume begins 9.5 meters from the production target. The primary beam energy at BNL is only 24 GeV, however. Even if hadronic debris is not a problem at the higher Main Injector energy, a naive estimate suggests that muons probably will be. Therefore, very careful shielding calculations and optimization of the shielding design must be carried out. The basic concept of the proposed beam, sketched in Figure 4, is to follow the "hyperon magnet" style of neutral beam (see G. Thomson's paper also) by magnetizing the entire collimation channel with a 35 kilogauss field. This would be a major improvement over E791. The following table compares the two beams:

	E791/BNL	Main Injector
Protons on target/spill	5×10^{12}	5×10^{12}
Proton energy	24 GeV	120 GeV
Production angle	48 mrad	20 mrad
Solid angle	70 μstr	36 μstr
$\int B \cdot d\ell$ (target to dump)	26 kG × 2 m	35 kG × 4 m
$\int B \cdot d\ell$ (target to decay region)	26 kG × 2 m + 17 kG × 2 m	35 kG × 7 m
Distance - target to decay region	9.5 m	7.5 m

Backgrounds in $K_L \to \pi^\circ e^+ e^-$

Several experimental groups have performed background calculations for this decay, including E791 at BNL, E845 at BNL, and E799 at Fermilab, as described in the proposals for these experiments. However, the energy is different at the Main Injector. Typically, the region of low ee invariant mass (below m_{π°) is abandoned because of the severe backgrounds from π° Dalitz decays. The major remaining backgrounds are then believed to be an overlap of two decays. One scenario is $K_L \to \pi e \nu$ and two photons from $K_L \to \pi^\circ \pi^\circ \pi^\circ$ reconstructing as a π°; if the charged pion is misidentified as an electron, then the event can fake $K_L \to \pi^\circ e^+ e^-$. A related process is $K_L \to \pi e \nu \gamma$ with one accidental photon from another decay. Such considerations emphasize the importance of good photon energy resolution, good timing resolution, good $\pi : e$ discrimination, and large acceptance for accidental γ's. The Main Injector should provide an advantage in acceptance for accidental γ's over lower energy machines (such as the AGS), principally because the γ's are boosted to energies well above the scale set by minimum ionizing particles registering in an electromagetic calorimeter. T. Yamanaka has investigated the backgrounds in the case of the Main Injector and his conclusions are contained in a separate contributed paper.

The Decay $K_L \to \pi^\circ \mu^+ \mu^-$

The decay $K_L \to \pi^\circ \mu^+ \mu^-$ has received less attention than $K_L \to \pi^\circ e^+ e^-$ from experimentalists because it appears to have much more serious backgrounds. This can be seen by considering one of the major backgrounds to $K_L \to \pi^\circ e^+ e^-$, namely the overlap of $K_L \to \pi e \nu$ with two accidental photons. Here, the ability to discriminate between the π and a second e is critical. In the $K_L \to \pi^\circ \mu^+ \mu^-$ case, the corresponding backgound would be $K_L \to \pi \mu \nu$ with two accidental photons. Here the problem is to discriminate between the π and a second μ, which is much harder. There is the additional problem that the π and μ masses are closer together than the π and e masses, so that the effect of misidentification (or decay) on the final reconstructed K_L mass is much less. Therefore, a process such as $K_L \to \pi^\circ \pi^+ \pi^-$ is clearly not a problem for $K_L \to \pi^\circ e^+ e^-$, but may be for $K_L \to \pi^\circ \mu^+ \mu^-$. However, these general considerations have not been quantified prior to this workshop. K. Lang and Y. Wah have made progress toward putting these ideas in quantitative terms and their work is described in a separate contributed report.

Direct CP Violation in the Decay $K_L \to \pi\pi$

Measurement of the parameter $\frac{\epsilon'}{\epsilon}$, which characterizes the strength of direct CP violation in the decay $K_L \to \pi\pi$, has been the major thrust of CP violation experiments in the kaon system for many years, with major efforts currently underway at both Fermilab (E731) and CERN (NA31). The key issue is whether $\frac{\epsilon'}{\epsilon}$ can be distinguished from zero; a clearly non-zero value would finally discredit the superweak hypothesis. Even though the CERN experiment has reported a result 3 σ from zero,[4] recent indications from FNAL E731 suggest that an experimental concensus may be elusive. Independent of the immediate situation, it is worthwhile to consider whether a facility such as the Main Injector will permit a significant improvement in the precision of these experiments.

In a double beam experiment such as FNAL E731, the dominant statistical error comes from the number of observed $K_L \to \pi^\circ\pi^\circ$ decays; the full E731 sample contains roughly 300K such decays. It seems clear that the extra flux available at the Main Injector should remove any statistical limitation. However, the additional complexity of the events caused by the higher instantaneous rates in the detector may lead to unforeseen systematic problems. Some of the familiar systematic problems can be improved at the Main Injector. For example, the size of the neutral beams can be reduced, owing to the greater flux per unit solid angle, which in turn reduces the probability of a $K^\circ \to \pi^\circ\pi^\circ$ decay in the K_S beam appearing to originate in the K_L beam due to scattering in the regenerator. However, other sources of systematic error, such as the equality of the energy scale for the charged and neutral modes, has no particular dependence on the parameters of the accelerator. Significant improvements may (or may not) be possible, but are not intrinsic to the Main Injector. These studies have been pursued mainly by H. Yamamoto and are described in a separate contributed paper.

Conclusion

We have found that the unusual combination of high energy and high flux offered by the Main Injector holds considerable promise in the study of CP violation in the kaon system. The energy appears to be well suited to a measurement of the interference of K_L and K_S into $\pi^\circ e^+ e^-$, provided an experiment can function sufficiently close to the production target. A careful study of the short beam and muon shielding are clearly of the

highest priority in assessing the reality of this promise. Other critical uncertainties concern the detector problems of coping with the flux available and rejecting subtle backgrounds in a high rate environment which has no precident. These are difficult problems, but the prospect of a qualitative improvement in CP violation experiments is a strong incentive.

References

1. B. Winstein, G. J. Bock, and R. Coleman, "CP Violation in the Kaon System with the Fermilab Upgrade," EFI 89-01, January, 1989.
2. L. M. Sehgal, Phys. Rev. **D38**, 808(1988).
3. M. Atiya *et al.*, "Kaon Physics in the 1990's: Rare Decays and CP Violation," FERMILAB-CONF-89/56, March, 1989; report for Snowmass 1988.
4. H. Burkhardt *et al.*, Phys. Lett. **206B**, 169(1988).

REPORT OF THE WORKING GROUP ON K^+ DECAY IN-FLIGHT

H.S. Collins, D.R. Marlow, and F.C. Shoemaker
Princeton University, Princeton, NJ 08544

T.F. Kycia and L.S. Littenberg
Brookhaven National Laboratory, Upton, NY 11973

D.A. Bryman
TRIUMF, Vancouver, BC, CANADA V6T 2A3

Introduction

The study of rare kaon decays has enjoyed considerable attention over the past few years.[1] Decays of both charged and neutral K's have been studied, the latter including such modes as $K^+ \to \pi^+ \nu\bar{\nu}$, $K^+ \to \pi^+ \gamma\gamma$, $K^+ \to \pi^+ e^+ e^-$, and $K^+ \to \pi^+ \mu^+ e^-$. The focus of this study is the $K^+ \to \pi^+ \nu\bar{\nu}$ reaction, or more generally, the $K^+ \to \pi^+ + \textit{nothing}$ reaction.

In the Standard Model (SM), the decay $K^+ \to \pi^+ \nu\bar{\nu}$ is forbidden to first order by the GIM mechanism, but is allowed to proceed via higher order diagrams with internal charm and top quark lines. The resulting three-generation SM prediction lies in the range $\mathrm{BR}(K^+ \to \pi^+ \nu\bar{\nu}) \simeq (1-8) \times 10^{-10}$, depending on m_t and the Kobayashi-Maskawa mixing angles. Although study of the SM rate is interesting in itself, the $K^+ \to \pi^+ + \textit{nothing}$ reaction is also a good place to look evidence of physics beyond the SM.

The Stopped K^+ Technique

The most sensitive experimental searches for $K^+ \to \pi^+ \nu\bar{\nu}$ to date[2,3] have been carried out using stopped K^+'s. This technique has the advantage of eliminating uncertainties associated with the measurement of the initial state (i.e. $E_{\mathrm{initial}} = M_K$ exactly), and results in decay π^+'s having kinetic energies, ranges, and momenta of about 100 MeV, 40 cm, and 200 MeV/c, respectively. Since resolutions of a few percent are achieved in the measurement of each of these quantities, the characteristics of the decay π^+ can be well determined. Finally, the energy of the final state π^+ is low enough that it can be stopped in scintillator, allowing it to be tagged through detection of the $\pi \to \mu \to e$ decay sequence.

The primary disadvantage of the stopped K^+ technique is rate. Although production cross-section and decay-length considerations point to high K^+ beam momentum, the effects of out-scattering and nuclear interactions in the degrader used to stop the incoming K^+ call for a lower momentum. The inevitable compromise ($P_K \simeq 800$ MeV/c) leads to significant losses on all scores. Even the simple expediant of increasing the proton beam intensity is not entirely straightforward, since one needs to contend with the large singles rates that result from fully absorbing the energy of the $\sim 10^7$ particles (π^+'s and K^+'s) that enter the detector each second.

Despite these difficulties, the sensitivities achieved using stopped K^+'s have continued to improve over the years. Brookhaven Experiment 787 hopes to achieve a sensitivity at the $\mathrm{BR}(K^+ \to \pi^+ \nu\bar{\nu}) \sim$ few $\times 10^{-9}$ level from their 1989 data.

Overview of the In-Flight Technique

The design considered in this report is but one of a number of alternatives. In particular, the choice of beam momentum was somewhat arbitrary and deserves further study. Furthermore, the detector geometry has not been optimized. Nonetheless, to facilitate background and rate estimates that are at least partially quantitative, it is useful to consider a specific design.

The basic layout of the detector is shown in Fig. 1. A 20 GeV/c RF-separated K^+ beam enters the $\simeq$ 10-meter long decay tank from the left after passing through beam Čerenkov detector. Each beam kaon is momentum-analyzed to an accuracy of $\Delta p/p = .5\%$ by measuring its position at a dispersed focus. The decay pions are momentum-analyzed by a 1.0 GeV/c P_T-kick bending magnet located downstream of the decay region. An electromagnetic calorimeter directly downstream of the magnet is used to veto photons from $K^+ \to \pi^+\pi^0$, $K^+ \to \pi^0\mu^+\nu$, and $K^+ \to \mu^+\nu\gamma$ decays. A notch in the bend side edge of the electromagnetic calorimeter allows beam particles to pass through the apparatus without interacting. Additional photon detectors are placed inside of and in front of the magnet and along the walls of the decay tank to catch photons emitted at large angles with respect to the beam. Sets of drift chambers located before and after the decay region measure the direction of the incoming K^+ and outgoing π^+, determining the K^+ decay angle (θ_D) with a precision of $< 100\mu$R. A third set of chambers downstream of the magnet tracks the decay π^+. The downstream charged-particle arm consists of a TRD for vetoing electrons and a finely-segmented hadronic calorimeter. The hadronic calorimeter is used primarily for $\pi/\mu/e$ separation, as described in detail below.

The basic strategy of the experiment is to exploit the two-body nature of the primary backgrounds, $K^+ \to \mu^+\nu$ and $K^+ \to \pi^+\pi^0$. Figs. 2(a-c) show θ_D, the decay angle versus vs P_π for $K^+ \to \mu^+\nu$, $K^+ \to \pi^+\pi^0$, and $K^+ \to \pi^+\nu\bar{\nu}$ decays, respectively (P_π refers to the final state charged-track, which in some cases may actually be a μ or e). Since the two-body modes fall in clearly defined bands (lines in the limit of perfect resolution), large background rejection factors can be obtained by vetoing all events in those bands. Some $K^+ \to \pi^+\nu\bar{\nu}$ events fall on or near the bands, but the three-body nature of the decay causes many to fall in the interior region, well away from the two-body bands. The portion of the $K^+ \to \pi^+\nu\bar{\nu}$ phase space thus accepted corresponds to $\nu\bar{\nu}$ effective mass values of $M_{\nu\bar{\nu}} > M_{\pi^0}$, nicely complementing the $M_{\nu\bar{\nu}}$ region covered by the stopped K^+ experiments. The approximate acceptance limit of the experiment is shown in Fig. 2(b). In addition to the angular limits, P_π is restricted to the range $8 < P_\pi < 16$ GeV/c. The lower bound eliminates events at low outgoing momentum, where π/μ separation is more difficult (see below), while the upper bound removes $K^+ \to \pi^+\pi^0$ decays where the π^0 has relatively less energy, making it harder to veto.

Statistical Sensitivity

Extrapolating[4] from the design of an RF-separated beam used at CERN ($\Delta\Omega \simeq 30\mu$sR, $\Delta p/p \simeq \pm 2\%$, $\pi : K \simeq 1 : 4$, and $L = 160$m), one expects a rate of $\sim 2 \times 10^7$ K^+ per main injector spill. Thus, in a good year one can hope for

$$N_K \simeq 2 \times 10^7/\text{spill} \times .3\ \text{spills/sec} \times 10^7\text{sec} \simeq 6 \times 10^{13}$$

The acceptance of the apparatus considered in this study is given by

$$\begin{aligned} A_{K^+ \to \pi^+ \nu\bar{\nu}} &= P_{DK} \times \varepsilon_{\mathrm{kin}} \times \varepsilon_{\mathrm{TRD}} \times \varepsilon_{\mathrm{cal}} \times \varepsilon_{\mathrm{misc}} \\ &= .07 \times .20 \times .70 \times .50 \times .30 = .0015 \end{aligned}$$

where P_{DK} is the probability that 20 GeV/c K^+ will decay in the 10-meter decay volume, $\varepsilon_{\mathrm{kin}}$ is the efficiency of the θ_D vs P_π cut (see Fig. 2), $\varepsilon_{\mathrm{TRD}}$ is the probability that the TRD *won't* accidently fire on a π^+, $\varepsilon_{\mathrm{cal}}$ is the efficiency of the calorimeter for tagging π^+'s, and $\varepsilon_{\mathrm{misc}}$ takes into account sundry trigger and analysis losses. Combining $A_{K^+ \to \pi^+ \nu\bar{\nu}}$ with the expected number of K^+'s, one arrives at a $K^+ \to \pi^+ \nu\bar{\nu}$ sensitivity of 10^{-11} per event, corresponding to between 10 and 80 events over the range of the SM prediction.

Background Rejection—General Considerations

The estimated statistical sensitivity, although encouraging, is, of course, only half of the story. In the paragraphs that follow, rejection factors for the various background modes will be considered. The list of backgrounds considered is by no means exhaustive, but those cases that are discussed are indicative of the nature of the problems that would need to be faced in a more complete design study.

Kinematic and Geometric Constraints

Although most $K^+ \to \mu^+ \nu$ and $K^+ \to \pi^+ \pi^0$ events can be eliminated via the kinematic considerations described above, any effect leading to a gross mismeasurement of the scattering angle or momentum can cause these events to spill into the signal region. Such mismeasurements can occur as the result of nuclear scattering in the windows of the vacuum tank or the drift chambers. Perhaps the most serious shortcoming of the in-flight technique is that the "0C" nature of the two-body kinematic reconstruction leaves one with no other purely kinematic indication that this has happened. However, such scatters will generally result in a poorly reconstructed vertex, and can be mostly eliminated by cutting on the distance of closest approach between the beam and decay tracks. Monte Carlo studies indicate that a cut requiring the two tracks to approach one another to within .15 cm retains approximately 90% of bona fide K decays.

Muon Rejection

The rejection of $K^+ \to \mu^+ \nu$ events depends critically on the positive identification of μ's in the downstream hadronic calorimeter. The technique[5] for doing this exploits the different pattern of energy loss expected for high-energy π's and μ's in matter. Since the range of 10 GeV muons in Fe is $\sim$ 850 cm, most muons will cleanly penetrate the ten-interaction-length-thick ($\simeq$ 160 cm) calorimeter. Most of the pions, however, will produce hadronic showers, leaving behind a large fraction of their energy in a pattern that is qualitatively different from that of the through-going muons.

In-flight π^+ decays and hadronic shower fluctuations, which are limiting factors in the usual application where one wishes to reject pions and positively tag muons, produce a loss in efficiency, but do not compromise the muon rejection capability. Rather, the limitations in muon rejection stem from (at least) three other sources; all having to do with the way muons behave. An intrinsic limitation appears to come from hadron production

from deep inelastic scattering (DIS). The cross section for this process, deduced from the parameterizations[6] of Van Ginneken, is plotted in Fig. 3 as a function of $y \equiv (E_\mu - E'_\mu)/E_\mu$, where E_μ and E'_μ are the energies of the muon before and after the interaction. The muons from events where $E'_\mu > 1$ GeV will have a 85 cm ($\sim 5\lambda_I$) range in Fe. If one assumes that such tracks can be distinguished from the secondaries of hadronic showers, then only the cross section for values of $y > 1 - 1/E$ (E in GeV) will contribute to the misidentification of muons as pions. Furthermore, since nearly all pion-induced hadronic showers will begin to develop in the first three interaction lengths of the calorimeter, one needs only to consider a "target" thickness of $\sim 3\lambda_I \simeq 50$ cm when estimating the probability of an "unrecoverable" DIS event. The results of such an estimate are shown in Fig. 4. Averaging over the energy region of interest ($8 < E_\mu < 16$ GeV), one obtains a muon rejection factor of $f_{\overline{\mu}} = 1.3 \times 10^{-6}$.

In principle, one could obtain almost arbitrarily good π/μ separation by going to higher energies.[7] However, other limitations eventually will set in. For example, in addition to DIS events, muons also suffer catastrophic energy losses from bremsstrahlung. In fact, in the $.9 < y < 1$ region of interest the bremsstrahlung cross section is considerably larger than that for DIS. However, the energy spent by the muon materializes as a photon, and these events can rejected by analyzing the pattern of energy deposition. Finally, muon decays followed by a shower of the decay positron could simulate a hadronic shower. For a 10 GeV muon, the probability of decay in the first three interaction lengths is $\simeq 8 \times 10^{-6}$. Once again, the obvious difference between the development of electromagnetic and hadronic showers can be exploited to reduce this source of background events to a level below that of DIS. Events where the muon decays upstream of the calorimeter will be rejected using the TRD.

π^0 and γ Rejection

Efficient detection of photons is crucial to the rejection of backgrounds such as $K^+ \to \pi^+\pi^0$ and $K^+ \to \mu^+\nu\gamma$. Assuming that the thickness of the photon detectors is large enough to reduce losses from escaping photons to a negligible level, two main sources of inefficiency remain. First, some photons will emerge from the decay vertex at lab angles so large that they miss the photon detection arrays while others be downshifted in energy to the point where they are very difficult detect. Second, a small ($\sim 10^{-3}$) fraction of the photons that enter the detector will be undergo photonuclear interactions instead of producing electromagnetic showers. Since the photon's energy must ultimately appear in one form or another it is reasonable to expect that a large fraction of the photonuclear interactions will produce readily detectable reaction products. Thus, above 1 GeV, single photon inefficiencies at the 10^{-4} or better level should be possible, although quantitative estimates remain to be made.

A simple (but at best approximate) model has been employed to estimate the π^0 detection inefficiency for $K^+ \to \pi^+\pi^0$ decays. At energies above 1 GeV, the inefficiency for photons striking the downstream electromagnetic calorimeter was assumed to be 10^{-4}, while the inefficiency for the presumably less-than-ideal detectors located along the decay tank was taken to be 10^{-3}. Further, the detection efficiency in both systems was assumed to steadily worsen with decreasing energy down to 10 MeV, where it dropped to zero. A Monte Carlo simulation based on the above assumptions yields an π^0 detection inefficiency

of $f_{\overline{\pi^0}} \sim 10^{-7}$. Clearly, such a crude model should not be taken too seriously, but it does indicate that extremely good detection efficiencies are at least plausible.

Some Specific Backgrounds

Armed with the above factors, one can estimate the number of background events expected from specific sources.

$K^+ \to \mu^+\nu$ Decays: The dominate mechanism appears to be the case where the K^+ scatters diffractively in the upstream window of the vacuum tank and then undergoes $K^+ \to \mu^+\nu$ decay in the fiducial volume. The magnitude of the K^+ momentum is only slightly altered in an elastic reaction and there are unlikely to be any detectable reaction products. The diffraction angle for 20 GeV/c kaons scattering from ^{12}C is $\sim$ 12 mR, which will completely throw off the kinematic reconstruction. For a .025-cm-mylar vacuum window, the probability of a nuclear interaction is $\sim 10^{-3}$. Monte Carlo indicates that the combination of requiring a good vertex and requiring the event to fall in the signal region (see Fig. 2b) yields an overall factor of $f_{\rm recon} \simeq .002$ in rejection. These factors, plus the $f_{\overline{\mu}}$ factor from the calorimeter yield an expected number of background events of

$$\begin{aligned} N_{K^+\to\mu^+\nu} = &\quad N_K \times \mathrm{BR} \times P_{DK} \times P_{\rm scat} \times f_{\rm recon} \times f_{\overline{\mu}} \\ &= (6\times10^{13}) \times .63 \times .07 \times .001 \times .002 \times (1.3\times10^{-6}) \\ &\simeq 7 \text{ events} \end{aligned}$$

to be compared with the $10-80$ legitimate $K^+ \to \pi^+\nu\overline{\nu}$ events expected at the SM rate. Improvements in $f_{\overline{\mu}}$ could probably be realized by going to higher energy.

$K^+ \to \pi^+\pi^0$ Decays: The analysis here proceeds as above, except that in this case diffractive scattering can occur in either window (i.e. both the π and the K interact strongly) and the μ veto from the hadronic calorimeter is replaced by the photon veto. Also, the kinematics cut is less effective since the $K^+ \to \pi^+\pi^0$ events start out closer to the signal region. The expected number of events is

$$\begin{aligned} N_{K^+\to\pi^+\pi^0} = &\quad N_K \times \mathrm{BR} \times P_{DK} \times P_{\rm scat} \times f_{\rm recon} \times f_{\overline{\pi^0}} \\ &= (6\times10^{13}) \times .21 \times .07 \times .002 \times .008 \times 10^{-7} \\ &\simeq 1.4 \text{ events} \end{aligned}$$

$K^+ \to \mu^+\nu\gamma$ Decays: This background requires the use of both the muon identifier and the the photon detector. Since $K^+ \to \mu^+\nu\gamma$ is a three-body mode, the μ is not constrained to lie along the $K^+ \to \mu^+\nu$ line of Fig. 2(a). However, most such events will be vetoed because of the accompanying γ. According to Monte Carlo, for a center-of-mass cutoff of $E_\gamma > 5$ MeV (corresponding to $\mathrm{BR}(K^+ \to \mu^+\nu\gamma) = .0055$) the fraction of events that fall in the signal region of Fig. 2(b) and are unaccompanied by a detectable γ (i.e. one with $E_\gamma^{\rm lab} > 10$ MeV) is $f_{\rm kin} \simeq 6\times10^{-5}$. Thus the expected number of background events is

$$\begin{aligned} N_{K^+\to\mu^+\nu\gamma} = &\quad N_K \times \text{BR} \times P_{DK} \times f_{\text{kin}} \times f_{\overline{\mu}} \\ &= (6\times10^{13}) \times .0055 \times .07 \times (6\times10^{-5}) \times (1.3\times10^{-6}) \\ &= 2 \text{ events} \end{aligned}$$

Once again, improvements in f_{kin} and $f_{\overline{\mu}}$ could probably be realized by increasing the kaon beam energy.

$K^+\to\mu^+\nu$ Decay Followed by $\mu\to e$ Decay: In this scenario, the muon from $K^+\to\mu^+\nu$ decays before leaving the fiducial volume. Since the direction of the muon is only slightly altered in the low-transverse-momentum $\mu^+\to e^+\nu\overline{\nu}$ decay, the effectiveness of the vertex cut is reduced. On the other hand, the lab momentum of the decay electron can be very different from that of the muon, making it possible for events to spill into the signal region of Fig. 2(b). Monte Carlo predicts a factor of $f_{\text{recon}} = .008$ for the combination of vertex and kinematics cuts. The downstream hadronic calorimeter is then presented with the task of e/π rather than μ/π separation. Since one can not expect to do as well in e/π separation a TRD is used to obtain additional rejection. TRD's operating over a similar momentum range have achieved e inefficiencies[8] on the order of 10^{-4}. EGS-based Monte Carlo studies have given preliminary indications that of order 10^{-3} of the showers induced by 10 GeV electrons deposit more than 1 GeV of their energy beyond the first two nuclear interaction lengths of Fe in the calorimeter. This factor can presumably be further improved by using Pb rather than Fe for the first part of the calorimeter. Combining these factors yields

$$\begin{aligned} N_{K^+\to\pi^+\pi^0} = &\quad N_K \times \text{BR} \times P_{DK} \times P_{\mu\to e} \times f_{\text{recon}} \times f_{\text{TRD}} \times f_{\overline{e}} \\ &= (6\times10^{13}) \times .63 \times .07 \times 10^{-4} \times .008 \times 10^{-4} \times .001 \\ &= .2 \text{ events} \end{aligned}$$

Window Scattering Events: The events in this class take a a number of different forms. In particular, one can have reactions of the following types: i) $K^+\to K^+ + X$, ii) $K^+\to\pi^+ + K^0 + X$, and iii) $\pi^+\to\pi^+ + X$. These backgrounds are particularly pernicious since they can yield a final state hadron without an absolute guarantee of accompanying visible energy. For .025-cm-thick mylar vacuum windows, the probability of an inelastic interaction is about $P_{\text{int}} \simeq 5\times10^{-4}$. The main weapons are the vertex cut (in this case requiring the decay vertex to lie well inside of the decay volume) and doing the best possible job on vetoing reaction products. A Monte Carlo estimate of the rejection power of the vertex requirement yields $f_{\text{vertex}} = 10^{-5}$. Unfortunately, even a qualitative estimate of the factor to be expected from vetoing the reaction products is extremely difficult. However, the requirement that P_π be less than 16 GeV/c ensures that the K must give up at least 4 GeV of energy; energy that must appear in one form or another. A factor of $f_{\text{veto}} \sim 10^{-4}$ therefore seems *plausible* for the combined probability that the K: i) is down-shifted in momentum to the 8 to 16 GeV/c range, ii) emerges with an angle falling in the signal region, and iii) is not accompanied by detectable reaction by-products. For the $K^+\to K^+ + X$ case, one can combine the factors to arrive at a predicted event yield of

$$\begin{aligned} N_{int} = & \quad N_K \quad \times P_{\rm int} \times f_{\rm veto} \times f_{\rm vertex} \\ & = (6 \times 10^{13}) \ \times \ .001 \ \times \ 10^{-4} \ \times \ \ 10^{-5} \\ & = 60 \text{ events} \end{aligned}$$

A background at this level is clearly a problem. However, the value of $f_{\rm veto}$ is highly uncertain and a careful analysis of this factor might yield a much more (or less!) optimistic estimate. Analysis of the other backgrounds in this class remains to be done. The $K^+ \rightarrow \pi^+ + K^0 + X$ case is particularly worrisome, since production of a high-momentum K_L could simultaneously satisfy strangeness conservation and fool the extra energy veto.

Summary and Conclusions

It appears that a dedicated $K^+ \rightarrow \pi^+ \nu\bar{\nu}$ apparatus operating at the Fermilab Main Injector could achieve a statistical sensitivity sufficiently good to acquire several tens, if not several hundreds, of events at the SM level. However, preliminary estimates show that a number of background problems remain to be solved. Further study may well reveal other problems.

More generally, there is lack of all-important practical experience to serve as a guide in the design of the detector components. Indeed, very little directly applicable experimental data is available to confirm estimates for muon and photon detection. Also, there is a similar dearth of experimental data that shed light on the question of nuclear interactions in the vacuum windows. Although this state of affairs is clearly less than desirable, it does leave open the possibility that background problems may be less severe than what has been estimated above.

References

1) for reviews of rare kaon decays see L.S. Littenberg, Nucl. Phys. **B279** (1987) 194; D.A. Bryman, Int'l. Jour. of Mod. Phys. **A4** (1989) 79.

2) Y. Asano *et al.*, Phys. Lett. **107B** (1981) 159.

3) I-H. Chiang *et al.*, AGS Experiment #787 proposal (1983).

4) we thank G. Bock and A. Malensik for providing estimates of the K^+ yield at the main injector.

5) we thank J. Ritchie for pointing out this technique to us and for providing initial estimates of the rejection.

6) A. Van Ginneken, Nucl. Instr. Meth. **A251** (1986) 21.

7) the rapid improvement as $y \rightarrow 1$ stems in part from the $(1-y)^2$ term in the parameterization of ref. 6.

8) P. Cooper, private communication.

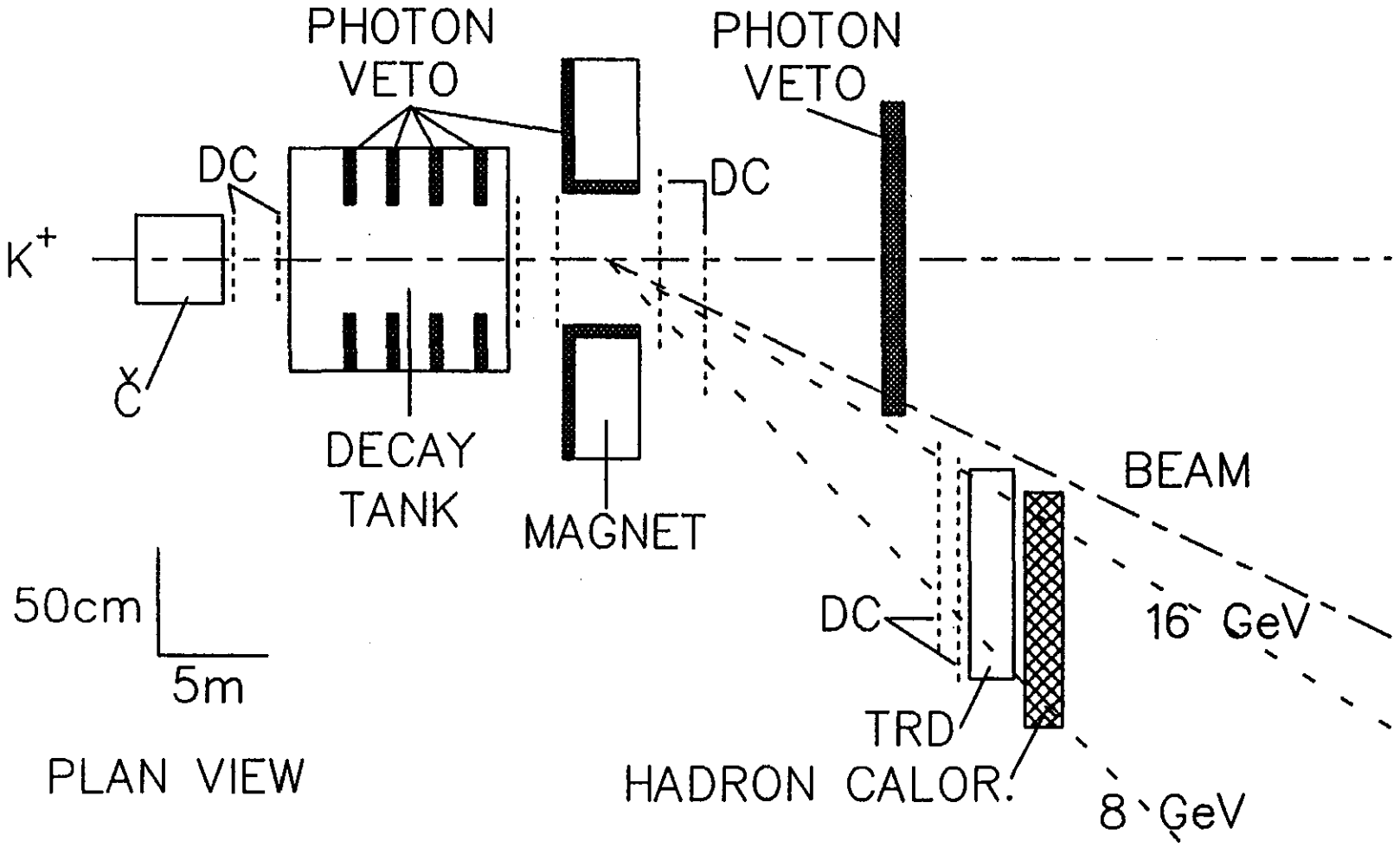

Fig. 1: Layout of the detector. Note the difference in horizontal and vertical scales.

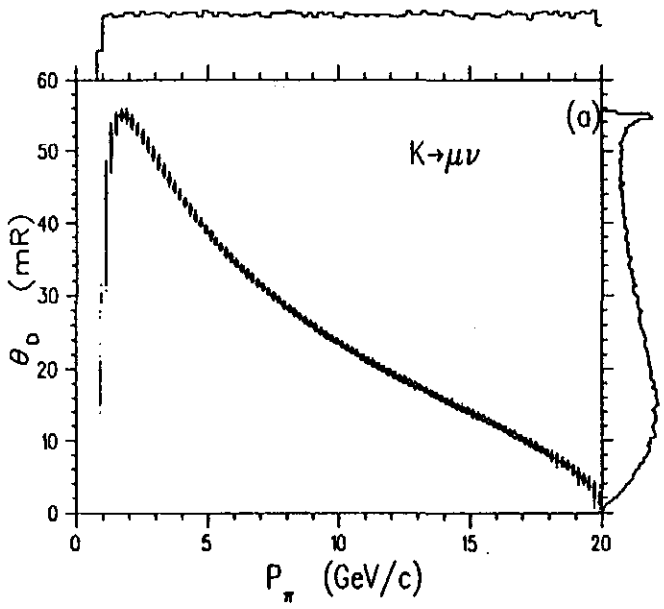

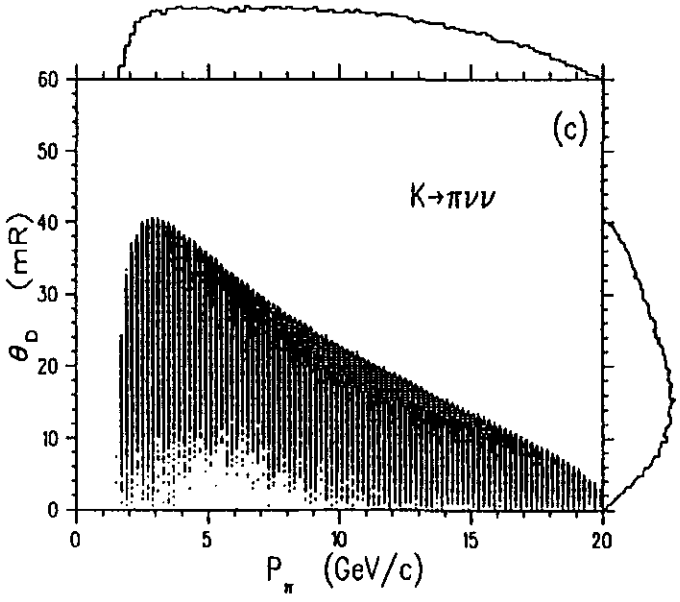

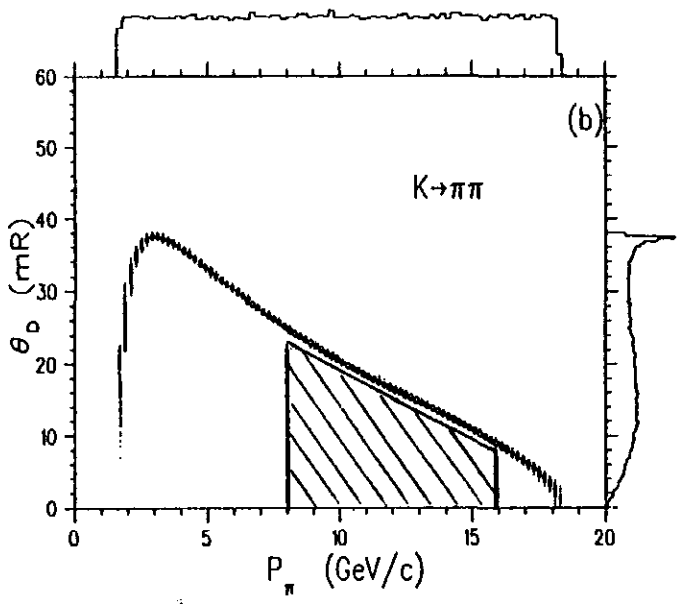

Fig. 2: Decay angle (θ_D) versus decay momentum for 20 GeV/c incident K^+. (a) $K^+ \to \mu^+\nu$, (b) $K^+ \to \pi^+\pi^0$, (c) $K^+ \to \pi^+\nu\bar{\nu}$. The signal search region is indicated as a hashed area in (b).

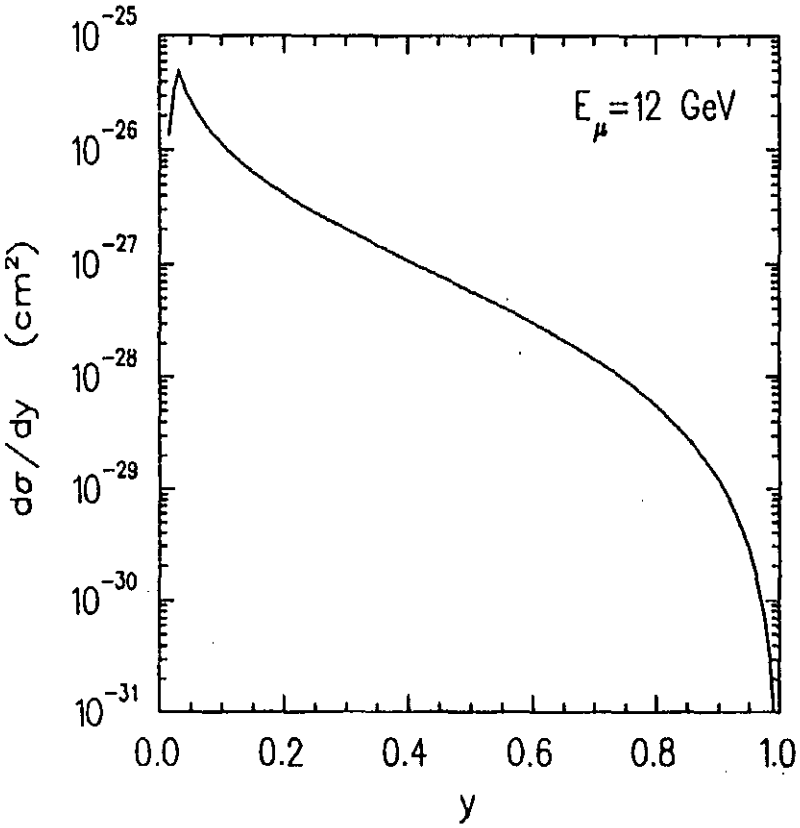

Fig. 3: Differential cross section for muon deep inelastic scattering (DIS), deduced from the parametrizations of reference 6.

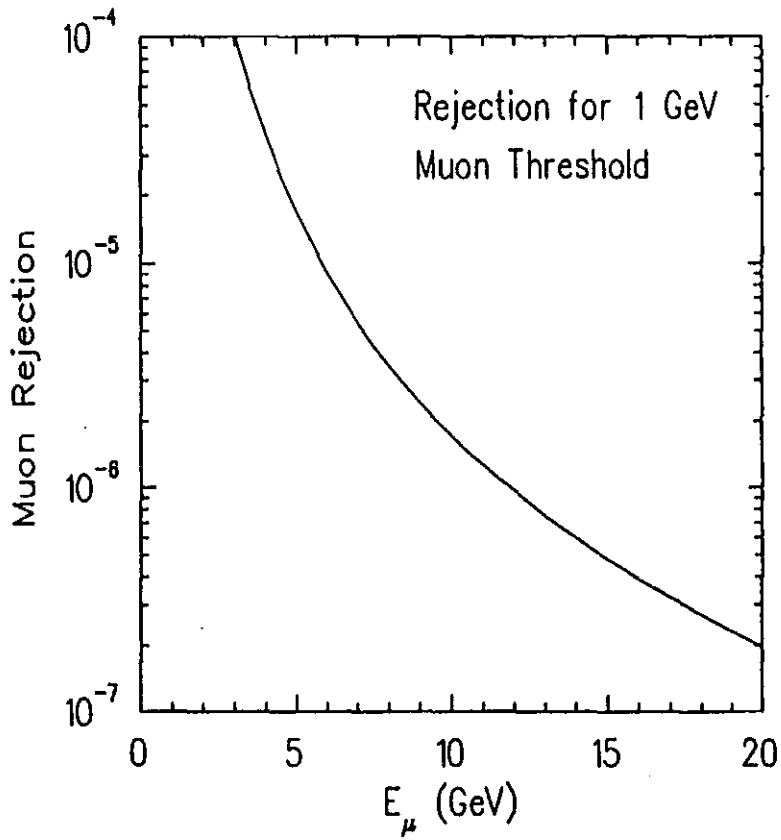

Fig. 4: Estimated muon rejection efficiency versus incident muon energy (see text).

Report of the CPT Tests working group, Physics at the Main Injector. 16-18 May, 1989 DOE/ER/3072-54

PHYSICS AT THE PLANCK SCALE: TESTS OF CPT INVARIANCE AT THE FERMILAB MAIN INJECTOR

G.D. Gollin, P.D. Meyers, and R. Tschirhart

Princeton University
Department of Physics
P.O. Box 708
Princeton, New Jersey 08544

Abstract

It is possible that CPT-violating amplitudes with sizes of order m_K / m_{Planck} contribute to processes involving K mesons. We describe several tests of CPT invariance that could be carried out at the Fermilab Main Injector. To our surprise we find that one experiment, a precision measurement of the CP-violating charge asymmetry in semileptonic K decays, can be performed with sufficient statistical accuracy to detect the presence of CPT-violating amplitudes of size m_K / m_{Planck} which generate a mass difference between K^0 and $\overline{K}^0$.

Introduction

In the context of field theories, reasonable assumptions such as Lorentz invariance and the connection between spin and statistics results in invariance of physical systems under the combined operations of charge conjugation, parity, and time reversal— CPT. Because the success of such theories provides the underpinnings of most of our current understanding of elementary particle physics, CPT invariance is generally held to be valid at current energy scales, and such an assumption has not been seriously contradicted by experiment.

Besides establishing various relationships among decay amplitudes, CPT invariance guarantees the equality of masses and lifetimes between particles and antiparticles, even if charge conjugation itself is violated. It is here that the most stringent tests of CPT are found. The most powerful of these is δm, the K^0- $\overline{K}^0$ mass difference, inferred from the measured K_L-K_S mass difference and other parameters of the neutral-kaon system to be $\delta m / m_K \leq 6 \times 10^{-19}$.[1]

With its deep connections to Lorentz invariance and other cornerstones of physics, one might not expect violations of CPT at all. Such violations may in fact occur at the Planck mass scale[2],[3] of $1.2 \times 10^{19}\ \mathrm{GeV}/c^2$ where conditions necessary for CPT symmetry (e.g. locality) might not hold. This scale is out of direct reach of current or currently foreseeable technology, so this might see.n to be a particularly unpromising

line of experimental effort. However, if CPT-violating effects do occur in the K system at a scale of $m_K/m_{Planck} = 4 \times 10^{-20}$, current limits on δm are less than two orders of magnitude from this. Of course, one could argue that a search in the neutral kaon system assumes many things, notably that the CPT violation occurs in strangeness-changing interactions. It is also possible that the appropriate scale is, say, $(m_K/m_{Planck})^2$. However, the prospect of probing Planck-scale physics is certainly a tantalizing one.

CP, T, and CPT in the Neutral K System

Mixing and ε

CP violation has only been observed in the existence of a charge asymmetry in the semileptonic decays $K_L \rightarrow \pi\mu\nu$, $K_L \rightarrow \pi e\nu$ and in the decay $K_L \rightarrow \pi\pi$.[4] The dominant source of CP violation is a T-violating asymmetry in the transition rates $K^0 \leftrightarrow \bar{K}^0$: $\Gamma(\bar{K}^0 \rightarrow K^0) > \Gamma(K^0 \rightarrow \bar{K}^0)$. This asymmetry causes both the (nonmixing) mass eigenstates, K_L and K_S, to contain slightly more K^0 than $\bar{K}^0$. Neglecting normalizations,

$$|K_S\rangle \sim (1+\varepsilon)|K^0\rangle + (1-\varepsilon)|\bar{K}^0\rangle \quad \text{and} \quad |K_L\rangle \sim (1+\varepsilon)|K^0\rangle - (1-\varepsilon)|\bar{K}^0\rangle.$$

The $\Delta S = \Delta Q$ rule requires $K^0 \rightarrow \pi^- l^+ \nu$ and $\bar{K}^0 \rightarrow \pi^+ l^- \bar{\nu}$ so the observed charge asymmetry in a K_L beam is proportional to $Re(\varepsilon)$. Note that the same charge

asymmetry would be observed in a pure K_S beam. The magnitude and phase of ε are $(2.259 \pm 0.018) \times 10^{-3}$ and $(43.67 \pm 0.13)^\circ$ respectively.[5] Since $CP(|K^0>) = |\bar{K}^0>$ and $CP(|\bar{K}^0>) = |K^0>$, the mass eigenstates are not CP eigenstates. The CP eigenstates K_1 and K_2 are

$$|K_1> \sim |K^0> + |\bar{K}^0> \text{ and } |K_2> \sim |K^0> - |\bar{K}^0>.$$

In terms of K_1 and K_2 one may write

$$|K_S> \sim |K_1> + \varepsilon|K_2> \text{ and } |K_L> \sim |K_2> + \varepsilon|K_1>.$$

Because the $|\pi\pi>$ final state from K decay must have CP = +1, a pure K_L beam will yield $\pi\pi$ decays from the beam's small K_1 component.

Direct CP Violation and ε'

A second possible source for CP violation would be the existence of a non-zero amplitude for the decay $K_2 \rightarrow \pi\pi$. It is necessary that $Amp(K^0 \rightarrow \pi\pi) \neq Amp(\bar{K}^0 \rightarrow \pi\pi)$ if the K_2 is to decay into $\pi\pi$. In particular, the quantity

$$\varepsilon' \equiv \frac{1}{\sqrt{2}} \frac{A_2 - \bar{A}_2}{A_0 + \bar{A}_0} e^{i(\delta_2 - \delta_0)}$$

must be nonzero where

$$A_0 \equiv \mathrm{Amp}(K^0 \to \pi\pi\,|_{I=0}), \quad \bar{A}_0 \equiv \mathrm{Amp}(\,\bar{K}^0 \to \pi\pi\,|_{I=0})$$
$$A_2 \equiv \mathrm{Amp}(K^0 \to \pi\pi\,|_{I=2}), \quad \bar{A}_2 \equiv \mathrm{Amp}(\,\bar{K}^0 \to \pi\pi\,|_{I=2}).$$

δ_2 and δ_0 are final state interaction phase shifts suffered by the pions moving away from the kaon decay vertex. After defining

$$\eta_{+-} \equiv \frac{\mathrm{Amp}(K_L \to \pi^+\pi^-)}{\mathrm{Amp}(K_S \to \pi^+\pi^-)} \quad \text{and} \quad \eta_{00} \equiv \frac{\mathrm{Amp}(K_L \to \pi^0\pi^0)}{\mathrm{Amp}(K_S \to \pi^0\pi^0)},$$

some algebra reveals that $\eta_{+-} = \varepsilon + \varepsilon'$ and $\eta_{00} = \varepsilon - 2\varepsilon'$. A nonzero ε' would split the values of the two η's by $3\varepsilon'$. Searches for this "direct" CP violation through measurements of $\mathrm{Re}(\varepsilon'/\varepsilon)$ are underway at Fermilab and CERN; results so far are inconclusive.[6] Since CPT invariance forces $\bar{A}_I = A_I^*$ and since the $\pi\pi$ phase shifts have been well measured, the phase of ε' is known to be $(48 \pm 8)°$. $\mathrm{Arg}(\eta_{+-})$ has been determined to be $(44.6 \pm 1.2)°$; recent results from Fermilab E731 and CERN NA31 indicate that $\mathrm{Arg}(\eta_{00})$ is within three degrees of $\mathrm{Arg}(\eta_{+-})$.[5],[6]

CPT violation parameters

Two different avenues for CPT violation suggest themselves. The first is a CP-violating, but T-conserving mixing of K^0 and $\bar{K}^0$ to produce the mass eigenstates. This corresponds to a situation where the K_S contains, for example, an excess of K^0 while the K_L contains an excess of $\bar{K}^0$. The CPT violating parameter Δ enters into the description of K_S and K_L like this:

$$|K_S> \sim (1+\varepsilon+\Delta)|K^0> + (1-\varepsilon-\Delta)|\bar{K}^0> \quad \text{and} \quad |K_L> \sim (1+\varepsilon-\Delta)|K^0> - (1-\varepsilon+\Delta)|\bar{K}^0>.$$

Note the sign switch between ε and Δ in the K_L expression. The component of Δ which is perpendicular to ε in the complex plane, $\Delta_\perp$, corresponds to a K^0 - $\bar{K}^0$ mass difference, while the component parallel to ε corresponds to a lifetime difference.[1]

A second possible route to CPT violation is through a CPT-violating relationship among the various $K\to\pi\pi$ decay amplitudes. Because $A_I - A_I^* = 2i\,\mathrm{Im}(A_I)$ and $A_I + A_I^* = 2\mathrm{Re}(A_I)$, the phase of ε' would be shifted from its value of $(48\pm8)^\circ$ by a CPT-disallowed relationship such as $\bar{A}_I \neq A_I^*$.

In terms of ε, ε', and Δ, $\eta_{+-} = \varepsilon + \varepsilon' - \Delta$ and $\eta_{00} = \varepsilon - 2\varepsilon' - \Delta$. A nonzero value of Δ will shift both η's in the same direction in the complex plane and will split the K_L and K_S semileptonic charge asymmetries. An unusual ε' phase will split the η's apart without affecting the charge asymmetries.

Experimental investigation of CPT violation

Overview

A comparison ot the semileptonic charge asymmetries for K_L and K_S decays yields information about $\mathrm{Re}(\Delta)$. $\mathrm{Arg}(\eta_{+-}) - \mathrm{Arg}(\eta_{00})$, when combined with a value of

$\mathrm{Re}(\varepsilon'/\varepsilon)$, determines the phase of ε'. $\mathrm{Arg}(\eta_{+-}) - \mathrm{Arg}(\varepsilon)$ and $\mathrm{Arg}(\eta_{00}) - \mathrm{Arg}(\varepsilon)$ provide determinations of $\varepsilon' - \Delta$ and $-2\varepsilon' - \Delta$, respectively. We will discuss an experiment to measure $\mathrm{Re}(\Delta)$. Because of the relationship between $\Delta_\perp$ and δm, the K^0 - $\bar{K}^0$ mass difference, the semileptonic rate study is the most interesting of the possible measurements. It is conceivable that physics at the Planck scale (or string compactification scale) will give rise to processes which generate a nonzero δm, of size $\delta m/m_K \approx m_K/m_{\mathrm{Planck}} = 4 \times 10^{-20}$. The current experimental limit is $\delta m/m_K < 6 \times 10^{-19}$, only a factor of 25 larger than m_K/m_{Planck}. Note that δm will be zero if CPT is conserved while Δm, the K_L-K_S mass difference, is not [$\Delta m = (3.521 \pm 0.014) \times 10^{-6}$ eV].[5]

The interpretation of a precision measurement of $\mathrm{Arg}(\eta_{+-}) - \mathrm{Arg}(\eta_{00})$ as a CPT test is complicated by the fact that the η_{+-}- η_{00} phase difference can be small, but nonzero, in a CPT-invariant universe. $\mathrm{Arg}(\eta_{+-}) - \mathrm{Arg}(\eta_{00})$ is known to be within three degrees of zero; Fermilab E773 will measure it to an accuracy of 1/2 degree in the near future. The utility of measurements considerably more precise than this would require improved measurements of the phase of ε and the value of $\mathrm{Re}(\varepsilon'/\varepsilon)$.

Re(Δ) and the semileptonic charge asymmetry experiment

The semileptonic charge asymmetry is

$$\delta \equiv \frac{\Gamma(K \to \pi^- l^+ \nu) - \Gamma(K \to \pi^+ l^- \bar{\nu})}{\Gamma(K \to \pi^- l^+ \nu) + \Gamma(K \to \pi^+ l^- \bar{\nu})}.$$

Neglecting violation of the $\Delta S = \Delta Q$ rule, the behavior of δ as a function of proper time should depend only on the relative probabilities that a beam kaon be a K^0 or a $\bar{K}^0$. Allowing for CPT violation, the charge asymmetry in a pure K_L beam will be approximately $4Re(\varepsilon+\Delta)$ while that in a pure K_S beam will be $4Re(\varepsilon-\Delta)$. Small $\Delta S = \Delta Q$ violations will not mimic CPT violation unless the $\Delta S = \Delta Q$ amplitudes are also CP violating.

If one could produce a pure K_S beam, one could measure δ_S directly and compare it to δ_L determined by the same detector exposed to a K_L beam. Since this is not possible, it is necessary to extract Δ by studying the interfence between K_S and K_L decays downstream of a target. The observed semileptonic decay downstream of a target is a function of many things: acceptance, reconstruction efficiency, magnitude and phase of ε, magnitude and phase of Δ, relative amounts of K^0 and $\bar{K}^0$ leaving the production target. We have investigated the statistical sensitivity of a possible CPT experiment at the Main Injector, leaving study of systematic difficulties for a later date. Our assumptions are naïve: our toy detector has uniform (and perfectly known) acceptance in a decay volume which is 10^{-9} seconds of proper time long. We assume there are no backgrounds to our K_{e3} signal (neglecting the copious $K_S \rightarrow \pi^+\pi^-$ mode). We assume we have a monochromatic K beam and can reconstruct the energy of the detected kaons unambigously. We generate proper time spectra for K_{e3} decays using specific values for six parameters: $|\varepsilon|$, $Arg(\varepsilon)$, $|\Delta|$, $Arg(\Delta)$, the dilution factor D (defined as the difference in the K^0 and $\bar{K}^0$ fluxes leaving the target divided by the sum of the fluxes), and the total target K flux. We jitter the contents of each bin in the time spectrum using a Gaussian distribution with $\sigma = \sqrt{n_{bin}}$ and then use MINUIT[8] to fit for the six

parameters. Note that $\Delta_\perp \approx 10^{-5}$ corresponds to $\delta m/m_K \approx m_K/m_{Planck}$[1]; we use a conservative value for D of 0.2.[9] The K yield expected in the proposed Main Injector high intensity neutral beam will be in excess of 10^9 kaons per second.[10] Here is a set of results from one of the fits, assuming 10% detection efficiency and 10^{15} kaons leaving the target.

Parameter	True value	Fit value
Target K flux	1.0×10^{15}	$1.0 \times 10^{15} \pm 1.7 \times 10^{9}$
$\|\Delta\|$	1.0×10^{-5}	$(1.05 \pm 0.20) \times 10^{-5}$
Arg(Δ)	133.6°	$(117.0 \pm 12.4)°$
$\|\varepsilon\|$	2.274×10^{-3}	$(2.280 \pm 0.002) \times 10^{-3}$
Arg(ε)	43.6°	$(43.7 \pm 0.05)°$
D	0.2	$0.2 \pm (0.2 \times 10^{-5})$

There were about 4×10^{12} (!!) detected decays in this sample. These results are typical: 10^{15} target kaons give several standard deviations of sensitivity to a CPT-violating mass difference between K and $\bar{K}$. The results of the MINUIT fits are insensitive to initial values of the trial parameters. When the fit algorithm is given an "infinite statistics" sample, the algorithm converges to the correct parameter values.

Discussion

The K^0 beam at the Main Injector will be capable of producing 2.2×10^9 kaons per second during extraction with a 50% duty factor.[10] Neglecting deadtime, this would yield 10^{15} target kaons in less than two weeks. Available K flux will not be a limiting

factor in the ability of a semileptonic CPT violation search to reach its goals. The experiment will have to overcome problems associated with running in a very high rate environment. The experiment trigger will need to reject nonleptonic kaon decays quickly without introducing significant bias in the K_{e3} sample. To be able to record trillions of semileptonic decays, it will be necessary to analyze data in realtime, storing only a small amount of information about each event. Even if each trigger can be processed in 1 μsec, with one byte per event written to tape, the full event sample will require several thousand 8mm cassette tapes.

The detector will need to be designed to eliminate systematic acceptance and reconstruction efficiency differences between the $\pi^+e^-\bar{\nu}$ and $\pi^-e^+\nu$ final states. In addition, it will probably be necessary to employ tricks involving several targets at different distances from the spectrometer to remove systematic uncertainties associated with imperfect knowledge of acceptance. Fortunately, the CPT-violating signal is an unusual time evolution of the charge asymmetry, not its value at a particular proper time. This dependence on a change in the charge asymmetry should cancel many systematic effects associated with charge-dependent efficiencies. However, the need to control systematics at the required level will be a difficult challenge, and warrants further study.

Conclusions

There is a fair chance that a CPT violation experiment can be carried out at the

Fermilab Main Injector with a level of statistical sensitivity sufficient to observe the existence of CPT-violating amplitudes of size m_K / m_{Planck}. Ample K flux will be available but the data taking rates are high, the number of events to be processed and stored in realtime is large, and strict control of systematic uncertainties crucial. However, the possible physics payoff is enormous: a first observation of the workings of the fundamental interactions at the Planck scale.

References

(1) See, for example, Cronin, J.W., "CP Violation, Status and Prospects", XXIII Cracow School of Theoretical Physics, Zakopane, Poland, June, 1983.

(2) E. Witten, private communication (1989).

(3) J. Harvey, private communication (1989).

(4) See K. Kleinknecht, "CP Violation and K^0 Decays", Ann. Rev. Nucl. Sci. 25, 1 (1976) for a review of K meson and CP phenomenology.

(5) Particle Data Group, Phys. Lett. B 204 (1988).

(6) Fermilab E731 collaboration and CERN NA31 collaboration. See reports from these groups in "CP Violation in Particle Physics and Astrophysics", Blois, France, 22-26 May, 1989, J. Tran Thanh Van, ed. (1989).

(7) V.V. Barmin *et al.*, "CPT Symmetry and Neutral Kaons", Nucl. Phys. B247, 293 (1984).

(8) MINUIT is French for midnight.

(9) A.J. Malensek, "Empirical Formula for Thick Target Particel Production", Fermilab report FN-341 2941.000 (1981).

(10) S. Childress *et al.*, "Fermilab Fixed Target Beams from the Main Injector", Fermilab report (May, 1989) and W. Molzon *et al.*, "Letter of Intent: High Precision, High Sensitivity K^0 Physics at the Main Injector", B. Winstein, contact person (June, 1989).

Studies of Lepton Flavor Violation at the New Main Injector

A. Heinson, S. Imlay, W. Molzon, J. Urheim
University of California, Irvine
K. McFarlane
Temple University

This working group studied the possibility of significantly improving the sensitivity of experiments to search for lepton flavor violation, specifically the decay $K_L^\circ \to \mu e$, using the New Main Injector. The studies concentrated on the sensitivity which could be achieved and did not consider in great detail the question of background rejection. In this report, we summarize these studies and list other considerations which must be addressed in mounting such an experiment.

As a very brief introduction, we give the basic motivation for these experiments. The decay $K_L^\circ \to \mu e$ is forbidden by conservation of the additive quantum numbers associated with electron- and muon-type leptons. Observation of this decay would be the first evidence of lepton flavor violation and would provide evidence for interactions outside the Standard Model of strong and electroweak interactions. The process is sensitive to extremely high mass scales. If it proceeds through the exchange of a virtual particle of mass M between μ and e leptons and s and d quarks, the rate is proportional to $1/M^4$. Assuming a V-A coupling of weak-interaction strength, observation of this decay at a branching ratio of 10^{-10} would imply M = 70 TeV/c^2.

The most successful experiments to date to search for lepton flavor violation in the decay of K_L° have been done at relatively low energy machines, either at BNL[1,2] with a 24 GeV/c proton beam or at KEK[3], with a 12 GeV/c proton beam. The present limits on the branching fraction for the decay $K_L^\circ \to \mu e$ is about 10^{-10}; the combined sensitivity of these experiments should be about 10^{-11} in the next year.

The lower energy accelerators have provided two advantages to doing these experiments, which we discuss in turn.

First, the available kaon flux has been higher at the lower energy machines; E791 at BNL routinely runs with 5×10^{12} protons per pulse incident

on the kaon production target every 3.2 seconds, with an estimated kaon flux close to 10^8 per pulse in a beam of approximately 75 μstr. The proton intensity available at KEK is lower (about 10^{12} protons per pulse) but with a long running period per year that experiment has achieved impressive results. It is expected that the Main Injector will be able to deliver in excess of 10^{13} protons per pulse, with a repetition rate of approximately 3 seconds and a 50% duty cycle. In addition, the accelerator in principle can run for a large fraction of the year, compared with the roughly 20 weeks available at BNL. As we show below, the available kaon flux will probably not be a limitation to the experiments, and in this regard the Main Injector is at least as good as other machines.

A second advantage of the lower energy machines has been in the ability to reject potential backgrounds, both in selecting events to record for analysis and in the physics analysis. The principal sources of such background originate from $K_L^\circ \to \pi e \nu$ decays in which the neutrino has little energy.

One background occurs if the pion decays or is misidentified as a muon. Online rejection of these events entails either some requirement that the transverse momentum of the two charged particles be approximately equal (as is done by KEK137) or an online kinematic analysis (as is done by BNL791). Offline, excellent kinematic resolution is required to reject such events; this is achieved by requiring that the particle trajectories not have kinks and that the event be consistent with a two-body decay of a K_L° originating from the production target. This background rejection power is limited by the momentum resolution of the spectrometer. The contribution to the momentum resolution due to measurement error can be made independent of the kaon beam momentum by a suitable choice of the spectrometer dimensions, scaling the length of the spectrometer by the mean kaon momentum. The contribution to the resolution due to scattering is momentum independent for equal material in the spectrometer. The longer spectrometers necessary for higher energy experiments present only small additional material from the extra gas (typically helium) in the spaces between the spectrometer elements; hence there is no large intrinsic advantage to a particular energy experiment in the kinematic background rejection.

Particle identification is important for both online and offline event selection. Online, events with a muon and electron must be selected quickly. Experiments at lower energies have an advantage in the relative ease of par-

ticle identification. Threshold gas Čerenkov counters with relatively good efficiency can be used for identifying electrons, and with an appropriate choice of gas the threshhold for muons and pions can be high enough that they are not a significant source of background in the trigger. At higher energies, other more complicated means of selecting electrons (transition radiation detectors, for example) are required. Online selection of muons has no strong energy dependence, except at muon energies much below 1 GeV/c, where the range is sufficiently short that pions become a source of background. This has limited the range of allowed muon momentum in present experiments to be above 1 to 1.5 GeV/c.

Offline, a second background arises if both the pion is misidentified as an electron and the electron is misidentified as a muon. Misassignment of particle masses then causes some of these decays to be reconstructed with a μe invariant mass at or above the K_L^0 mass. For $p_\mu >> m_\mu$, the mass shift depends only on the ratio of particle momenta and hence the energy dependance of the background is only due to energy dependence of particle misidentification. Typically, two means of electron and muon identification are required. For electrons, energy measurement in an electromagnetic shower counter is used offline to further reduce backgrounds at the analysis level. The improved fractional energy resolution at higher energy then presents an advantage for higher energy experiments. For muons, improved identification is often achieved by requiring the measured momentum to be equal to the muon energy as measured by its range in matter. This presents a particular advantage for lower energy experiments, where the muon is more easily ranged out in an absorber.

Thus, from the point of view of the available kaon flux and background rejection, there are minor advantages to slightly lower energies. The new Main Injector will be intermediate in energy between these machines and the Fermilab Tevatron or CERN SPS and may present some unique advantages to rare kaon decay experiments. In the remainder of this report, we discuss the design of an experiment at the Main Injector which will make a significant advance in sensitivity to lepton flavor violating decays of netural kaons. We set a goal of designing a spectrometer capable of achieving a sensitivity approaching 10^{-13} for two body decays. We assume that a delivered proton flux of $1 - 2 \times 10^{13}$ protons per spill will be available to the experiment.

We restrict ourselves to studies of a conventional two sequential dipole magnet spectrometer, similar to that of BNL791. The advantage in this approach is that the performance of such a device can be readily extrapolated from our experience. Others have discussed novel ideas for other geometries, which may be better suited to lower energy experiments. These include a solenoidal geometry[4]. In addition, a study[5] similar to this was done for an experiment which could be done at BNL after the booster there is commisioned.

This study is further restricted to design studies for experiments with 2-body decays of K_L^o . Other working groups and previous studies have looked at 3- and 4-body decays, especially those involving neutral pions; that work is summarized separately in this proceedings and in references contained therein.

As we will show, the limitations probably will be due to excessive rates in the various detectors. The rates originate from three categories of sources. First, there is the rate due to charged particles from kaon decays. To minimize this, one wants to minimize the flux of very low or high energy kaons (where the acceptance of the apparatus is zero). Typically, the former is more of a problem since the flux of kaons at high energies is relatively lower and the decay probability is small.

A particular advantage of the Main Injector is that a kaon beam can be produced at relatively large angle with respect to the incident proton beam with a kaon energy spectrum well matched to the acceptance of the detector. This is demonstrated in Figure 1, which shows the energy spectrum of decaying kaons in a 16 m long decay region for different targeting angles.

The curves were calculated using the parameterization of Atherton, et al.[6]. Also shown is the expected spectrum for a 24 GeV/c beam. In the momentum interval 3-20 GeV/c, where the acceptance for a spectrometer similar to the E791 apparatus is largest, the flux for the 120 GeV/c proton beam is significantly larger than that of the 24 GeV/c beam, and is peaked at higher momentum, where the acceptance is better. Furthermore, only 28% of the kaons decaying in a 16 m long decay region are below 3 GeV/c for 120 GeV incident protons, compared with 52% for the 24 GeV/c incident beam, both for 2.75° targetting angle.. The flux of kaons above 20 GeV/c, where we assume the acceptance to be zero, is larger for the Main Injector, but is not a significant contribution to the total rate in the detector.

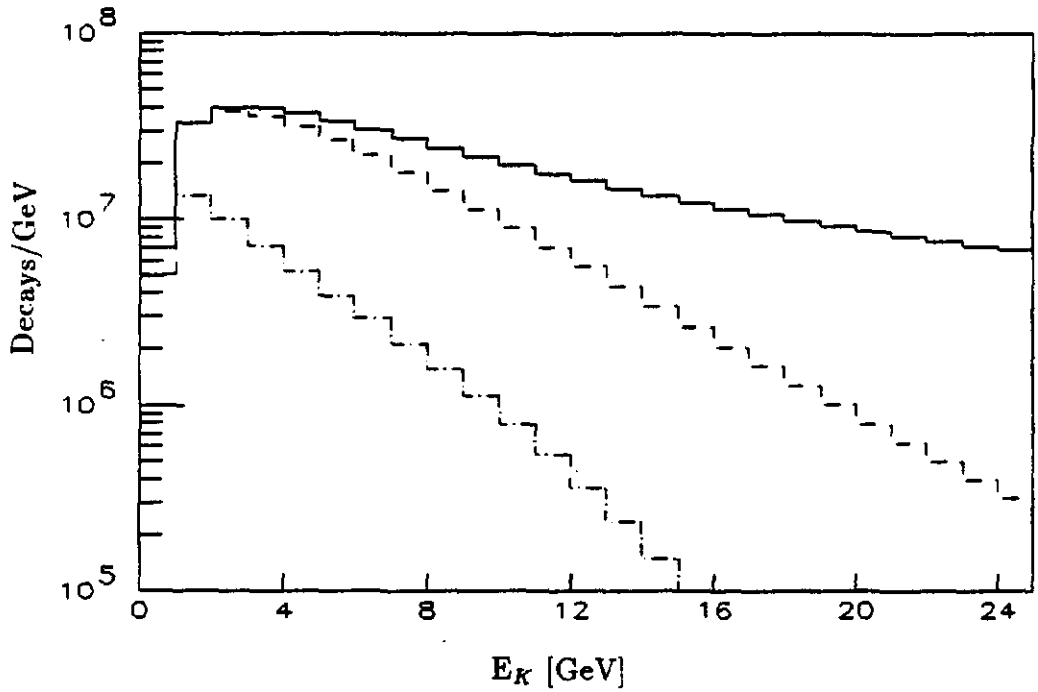

Figure 1. The energy spectrum of kaons decaying in a 16m long decay region for different incident proton energies and targetting angles: solid 120 GeV/c, 0°, dashed 120 GeV/c, 2.75°, dot-dashed 24 GeV/c 2.75°. All curves are for a 100 μstr beam and 10^{13} protons incident on a 1 absorption length beryllium target.

The second cause of excess rate in the detectors is the flux of charged particles from neutron interactions in detector elements or other material. This can be minimized by designing a beam which has a small n/K ratio or which has very little material in the path of the beam. The former method involves producing the beam at large targetting angle or preferentially absorbing neutrons in a low atomic number abosrber. The latter involves transporting the beam in vacuum through the detector and ensuring that there are no tails in the transverse beam profile to interact in detectors near the beam. In this report, we don't calculate the expected n/K ratio

(see the report of the working group on beams in this document), but presume it will be low due to the large targeting angle and the relatively long region for collimation of the beam and absorption of low energy neutrons and photons, and could be further reduced with the use of a low atomic number absorber.

The third source of excess rate in detector elements is from electronics noise. This is a concern because the detectors, particularly wire chambers, are run at low gas gains to minimize the possibility of damage, and hence are more susceptible to noise. A working group has considered detectors for high sensitivity experiments, and their report appears in this document.

We conclude that a detector similar to the E791 apparatus (but scaled up for increased acceptance) might be well matched to a kaon beam with relatively low n/k ratio at the Main Injector.

The principal limitation to present experiments has in fact been the high rates in the detector elements. For example, with 5×10^{12} protons per pulse on target the measured rates in the E791 drift chambers are $1 - 2 \times 10^7$ per one second long pulse, with rates in individual wires with the highest rates close to 10^6 per pulse. The rates are limiting in a number of ways. First, the drift chambers have been physically damaged by large, localized current being drawn. Although the current is from discharges and not the direct result of current from amplification of the tracks of ionizing particles, the discharges are induced by the large rate of ionizing particles traversing the chambers. Second, the track reconstruction efficiency, both offline and in the online triggering, has reduced efficiency at high intensities. Figure 2 shows the reconstruction efficiency as a function of the proton flux on the production target. For rates above about 5×10^{12} protons per pulse, increasing the proton flux results in a net decrease in the rate of reconstructed events.

In the case of BNL791, the source of high rate is not completely understood; rates are higher, perhaps as much as 5 times higher, than that expected from kaon decays. Some is from electronics noise, and there is evidence that some is from interactions of neutrons in the vacuum windows, helium, and the edges of the detectors nearest the beam. Improved beam design, and a better kaon to neutron ratio will be beneficial. Even with optimistic assumptions about the source of excess rates in the detectors, it is clear that improving the sensitivity by 1000 cannot be achieved by

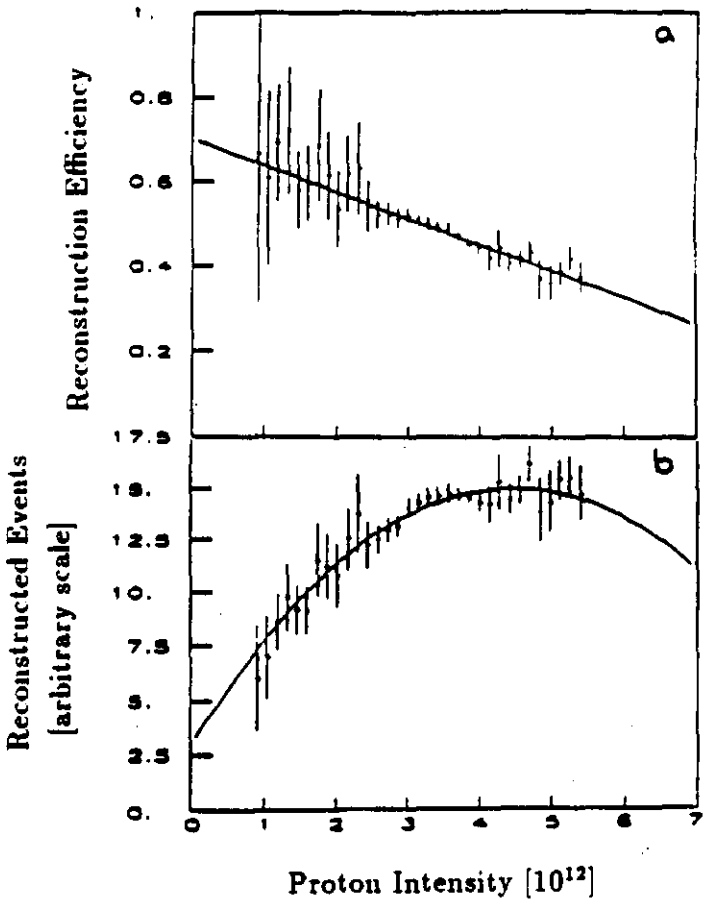

Figure 2. The reconstruction efficiency (a) and the rate of reconstructed events per time (b) versus the number of protons per spill on target for the E791 spectrometer.

simply increasing the intensity; a substantial increase in acceptance will be required.

From the perspective of minimizing the rate in the detectors, a good measure of quality of a spectrometer is the sensitivity per unit time divided by the rate in the most active detector element. The goal of a design optimization is then to maximize the acceptance while minimizing the rate in the most active parts of the detector, and the working group has concentrated on that goal.

We have studied the performance of the spectrometer while varying characteristics of the beam and spectrometer. The distance from the target to the decay region was varied, which changes both the physical size of the beam at the spectrometer for a fixed beam solid angle and the momentum spectrum in the decay region. The decay region length was varied, which also changes the size of the beam and the number of decays. The transverse detector sizes were varied to increase the acceptance, and the size of the beam (the dead region in the center of the detector) was varied to optimize the acceptance versus the rate in the detectors closest to the beam. Some means of optimization which might prove fruitful have not been tried. These include using a one arm spectrometer with detectors in the beam (*c.f.* BNL780), using a single dipole magnet with tracking in the magnet (which might be more compatible with studies of 3- and 4-body decays), and using a 2 dipole spectrometer with fields oriented in the same direction (*c.f.* KEK137).

Acceptance calculations were done using a simple Monte Carlo program. Acceptances were calculated by generating kaons with the energy distribution discussed above, simulating the decay kinematics, and tracking the decay products through the spectrometer. The acceptance criteria included, in addition to fiducial volume cuts on the detector elements, a minimum momentum requirement of 1.0 GeV/c (necessary for muon identification), a maximum momentum of 12 GeV/c (for reasons of resolution), and a momentum asymmetry requirement (useful in eliminating events particularly susceptible to background).

Figure 3 shows a schematic of the spectrometer resulting from the design optimization. We assume the momentum transfer in each analysing magnets is 300 MeV/c, and the field orientation in the two magnets are opposite. We somewhat arbitrarily limited the linear dimensions of the drift chambers to 2.8 meters. Figure 4 shows the acceptance of this spectrometer as a function of the K_L° energy. The peak acceptance occurs at about 11 GeV/c with a value of about 28% and the mean acceptance, averaged over the momentum interval 3-20 GeV/c is 14.8%. The decay probability averaged over this interval is 5.9%. With this spectrometer, 0.70% of *all* kaons produced at the target and decaying to μe would be detected. We note that in comparing acceptances of different spectrometers it is important to define the momentum interval and decay region length for which

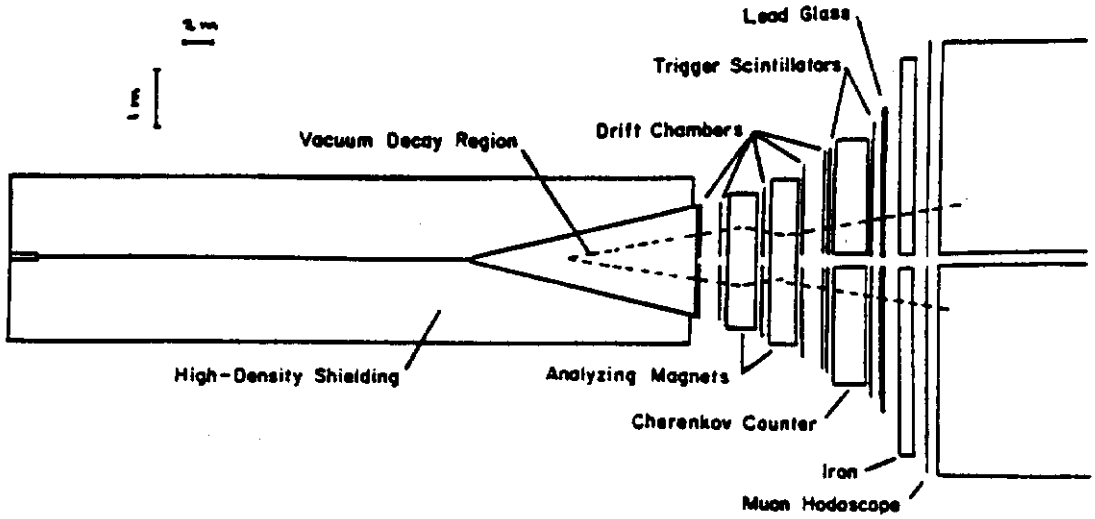

Figure 3. A plan view of the spectrometer discussed in this paper.

the acceptance is calculated.

Some idea of the potential gain of further improvements in the spectrometer can be had by understanding where events are lost. Table 1 shows a matrix with information on which acceptance criteria cause events to be lost. The rows and columns are labelled by the selection criteria. The diagonal elements of the matrix give the fraction of all decays which are lost due to only the single cut. The lower off-diagonal entries give the fraction of events lost to precisely the two cuts represented by that element of the matrix, while the upper off-diagonal elements give the (non-exclusive) fraction of events cut by at least three requirements, including the two represented by the row and column. The cuts on horizontal and vertical apertures cause the largest loss of events. Increasing either the horizontal or vertical apertures or moving the detectors closer to the beam would be most effective in increasing acceptance.

We next show several examples of the dependence of the acceptance on small changes in apparatus dimensions and other parameters. Figure 5a-c shows the acceptance versus the lower track momentum cut, the upper

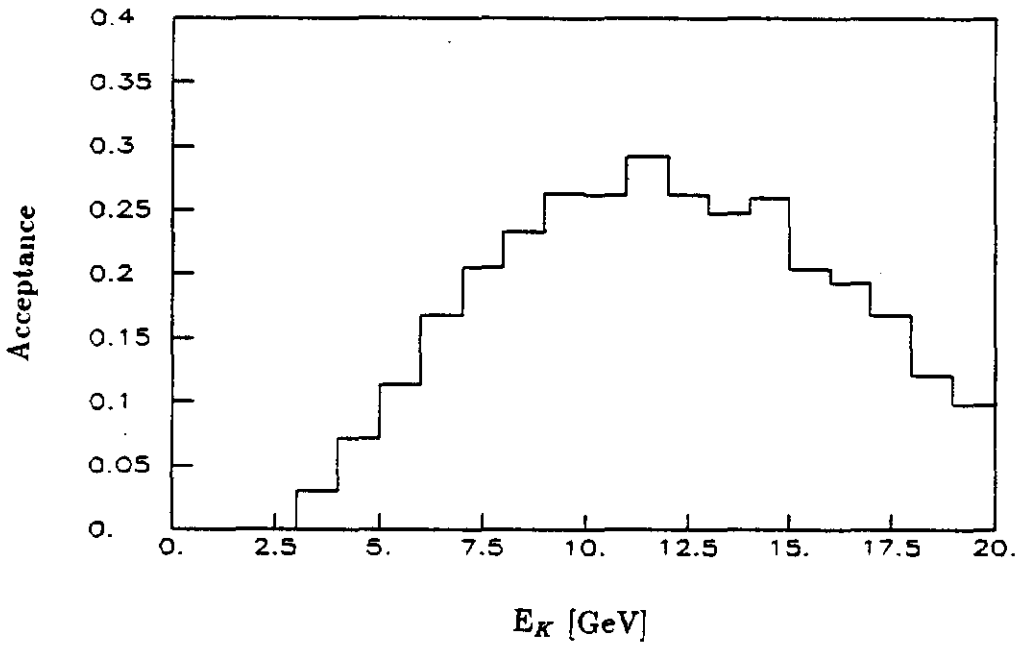

Figure 4. The acceptance of the spectrometer versus the kaon energy. The selection criteria are discussed in the text.

track momentum cut and the momentum asymmetry cut. Small variations in the limits on these parameters do not have a significant effect on the acceptance. Figure 6a-c show the acceptance versus some of the spectrometer dimensions. In each case, other closely coupled dimensions were changed appropriately. For example, in varying the vertical aperture of the first magnet, all other vertical apertures were also varied proportionally. Substantial gains in acceptance can be had by increasing the transverse dimensions of the spectrometer, but presumably with substantially increased costs. The exact choice of spectrometer dimensions would rest on an analysis of the relative costs of different configurations, the available resources, and the technical feasibility of different options.

Since the experiment as conceived would be limited by the rate in the detector elements, as discussed above, a good figure of merit is the ratio of the rate of accepted events to the rate in the most active detector elements. We define the occupancy in a detector element as the probability of a signal occuring in that element within the livetime of that element. We calculate

	1	2	3	4	5	6	7
1	**0.0**	0.9	18.2	17.4	18.7	8.8	25.4
2	0.0	**0.3**	0.9	0.5	2.7	1.2	2.6
3	0.2	0.0	**9.3**	14.7	17.6	10.8	19.2
4	0.8	0.0	6.5	**6.7**	8.0	2.5	16.7
5	0.1	0.4	4.3	0.1	**8.4**	15.4	22.5
6	0.0	0.0	0.0	0.0	3.8	**0.0**	10.5
7	1.8	0.1	0.5	1.2	1.5	0.0	**0.4**

Table 1. The matrix showing the percentage of events lost due to only one selection criteria (diagonal elements), only two criteria (lower off diagonal elements), and at least three criteria (upper off diagonal elements). The criteria are 1) minimum charged particle momentum of 1.0 GeV/c, 2) maximum charged particle momentum of 12 GeV/c, 3) vertical aperture, 4) horizontal aperture, 5) inner aperture, 6) particle crossing to opposite spectrometer arm, 7) momentum asymmetry greater than 0.6.

the occupancy for a proton flux of 10^{13} protons per 1.5 second spill. For this calculation the livetime is assumed to be 60 ns (corresponding to a 3 mm drift distance and Ar-ethane gas). The number of accepted events per hour was also calculated, assuming a 50% duty cycle. In this calculation, no running inefficiencies, or trigger and analysis inefficincies were included. In the case of E791, the net effect of these was a loss of 2-3 in sensitivity per unit time. Table 2 shows the maximum occupancy, total drift chamber rate, and number of accepted events per hour for different solid angle beams. The figure of merit quoted above is not very sensitive to the solid angle of the beam used; this could then be adjusted to achieve the desired rate and occupancy, depending on the flux of protons available. For comparison,

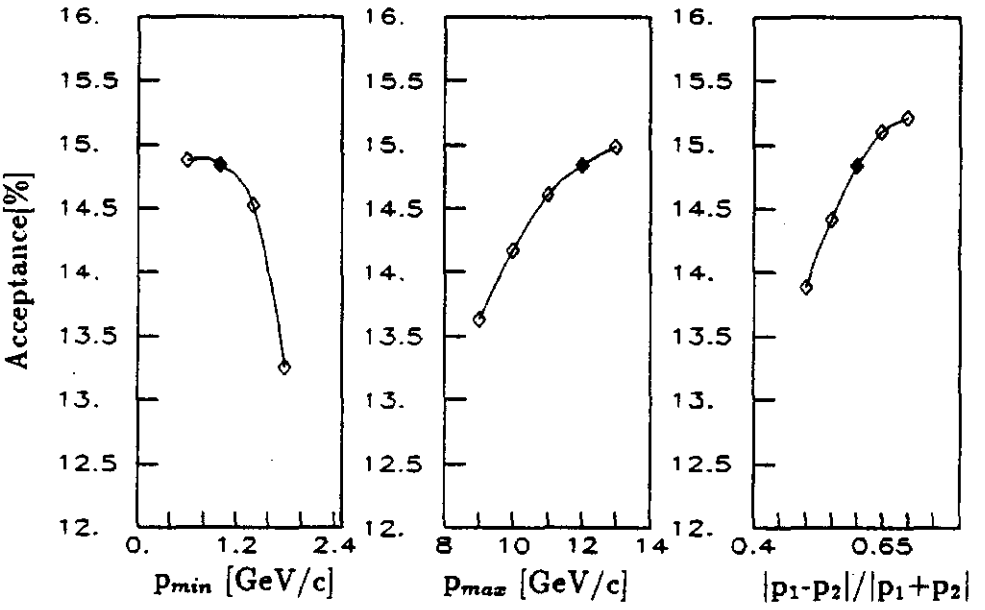

Figure 5. The spectrometer acceptance versus variations in some of the selection criteria: a) the lower particle momentum cut, b) the upper particle momentum cut, c) the momentum asymmetry cut. The symbol representing the value used in the acceptance calculated herein is darkened.

we include the calculated numbers for the E791 spectrometer and for a spectrometer which could be built at BNL with acceptance comparable to the one described here[4]. With a 17 μstr beam, the experiment at the main injector has about .75 times the random occupancy and .6 times the total drift chamber rate of an improved BNL experiment for an equivalent number of detected events per unit time. It is about a factor of eight better than BNL791.

From these results, one can speculate on what sensitivity could be achieved in a specified running time. We make the following assumptions:

- The occupancy per channel is restricted to less than 1.5%.
- The product of the accelerator and experiment running efficiencies is 60%.

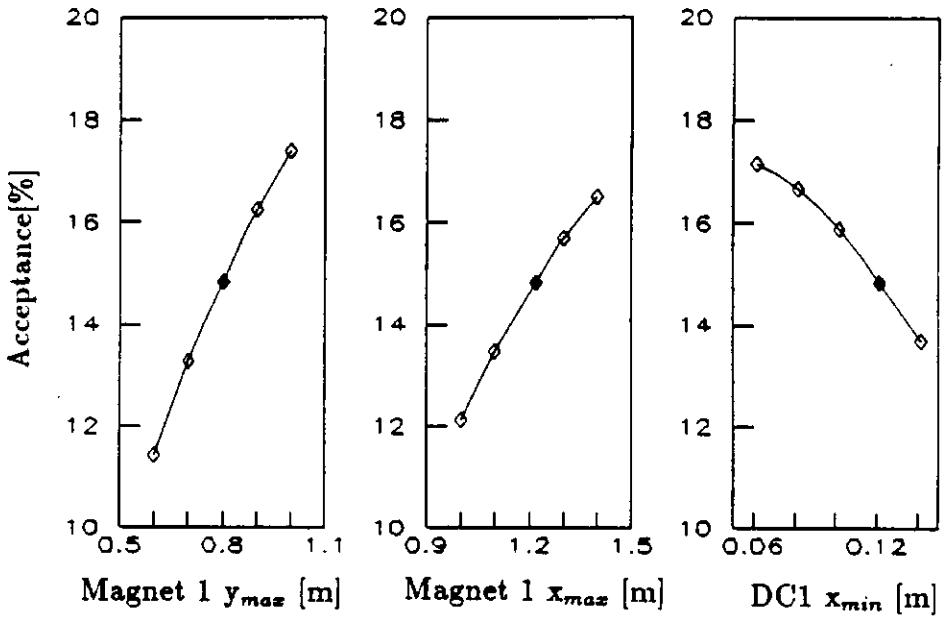

Figure 6. The spectrometer acceptance versus variations in some of the spectrometer dimensions: a) the vertical aperture of the first magnet, b) the horizontal aperture of the first magnet, c) the distance from the active region of the first drift chamber to the beam centerline.

- The total loss of sensitivity due to detector inefficiencies, trigger inefficiencies, deadtime, and analysis losses is 50%.

With these assumptions, the experiment described would detect one event per 5500 hours of running time if the brancing fraction for the decay $K_L^\circ \rightarrow \mu e$ were 10^{-13}. This could be achieved in one year of running if the accelerator ran 8 months per year.

We have not addressed the question of the resolution necessary to ensure that the experiment will be background free. A few qualitative statements can be made, based largely on the experience of BNL791. First, the design calculations for BNL791 showed that that experiment would be background free at a sensitivity of 10^{-12} or below if the dominant source of background was from $K_L^\circ \rightarrow \pi e \nu$ decays in which the pion decayed in flight and if drift chamber resolutions of 200 μm or better were achieved. Resolutions

Spectrometer	Solid Angle (ustr)	Rate ($\times 10^7$)	Occupancy (%)	Events Hour ($\times 10^9$)
Main Injector	17	1.8	1.5	6.2
Main Injector	50	4.6	3.6	14.0
Main Injector	100	8.0	6.6	21.0
BNL Upgrade	100	2.0	1.3	4.1
BNL791	100	1.1	1.3	0.7

Table 2. Measures of the rate of charged particles traversing the first drift chamber on each side of the apparatus, the maximum random occupancy in a 6 mm drift chamber cell, and the number of accepted events per hour of running for various beam solid angles.

of about 120 μm were achieved, at which point the momentum resolution is dominated by scattering rather than measurement error. The design considered here would have roughly the same amount of scattering (slightly larger due to the smaller wire pitch, and perhaps a larger, thicker vacuum window). Hence, the resolutions and backgrounds would be expected to be about the same.

However, E791 has not yet achieved the calculated momentum resolutions, and this is probably reflected in the background levels. Figure 7 shows the mass distribution of $K_L^0 \rightarrow \mu e$ candidates as a function of μe invariant mass in the region below the K mass. Also shown is a prediction of this distribution, where the pion decay and misidentification probabilities were taken directly from the data, and the effect of measurement errors is taken from a Monte Carlo simulation of the apparatus. While the curves agree reasonably well near $M_{\mu e} = 480\ MeV/c^2$, the data show an excess

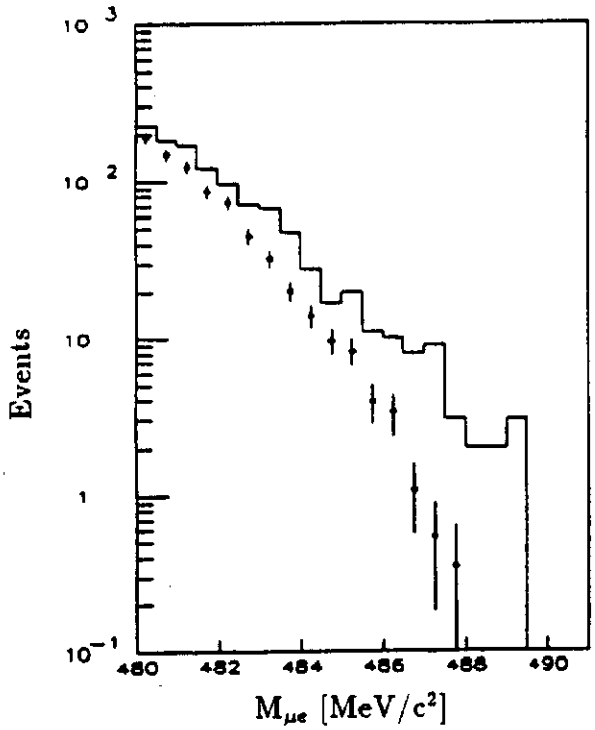

Figure 7. The mass distribution of $K_L^\circ \rightarrow \mu e$ candidates as a function of μe invariant mass in the region below the K mass for the data (solid histogram) and a prediction derived as discussed in the text (points with error bars).

at higher masses. This could be due to the worse resolution achieved in the experiment. At a sensitivity of 10^{-10} the worse resolution does not result in background, but improved resolution would be necessary for a background free experiment at a sensitivity of 10^{-13}.

In addition, the original proposal of BNL791 did not consider the background due to $K_L^\circ \rightarrow \pi e \nu$ decays in which both charged particles are misidentified. To reject this as a source of background, the probability of simultaneously misidentifying both charged particles must be less than 10^{-9}; this level of particle identification efficiency has not been demonstrated, but should be achievable.

Finally, a potential source of background originates from neutron interactions with the residual gas in the vacuum decay region. This is more a background concern for $K_L^\circ \to \mu\mu$ decays, where muon pairs can be produced in interactions more easily than can muon electron conincidences. From the absence of background in BNL791[1], where the vacuum was 40 mTorr, one can deduce that a vacuum of between .1 and 1 mTorr would probably be sufficient to eliminate interactions as a source of background. The spectrum of neutrons extends to higher energies than in BNL791, and the higher energy interactions could increase this potential background. Also, the larger acceptance of the spectrometer discussed here would increase the probability of detecting other particles produced in the interactions, which could be of use in eliminating these events.

In conclusion, the New Main Injector seems a particularly promising place to do experiments to search for lepton flavor violation in kaon decays. A kaon beam produced at relatively large angle, where the neutron flux is small, is well matched to a spectrometer design extrapolated from our experience with BNL791. It appears possible to design an experiment capable of achieving a sensitivity of 10^{-13} for the decay $K_L^\circ \to \mu e$. Assuming the dominant source of rate in detectors is from decays of neutral kaons, the probability of an extra hit in the highest rate channel of the spectrometer would not exceed 1.5%, significantly below the measured occupancy rate of BNL791. It remains to show that lepton misidentification probabilities below $10^{-4} - 10^{-5}$ can be achieved, and that sufficient kinematic resolution can be achieved to ensure a background free experiment. Details of the event selection and analysis have not been considered; these topics would must be studied prove the feasibility of such an experiment.

References

[1] R.D. Cousins *et al.*, Phys. Rev. **D 38**, 2914 (1988);
"New Experimental Limits on $K_L^\circ \to \mu e$ and $K_L^\circ \to ee$ Branching Ratios",
C. Mathiazhagan, *et al.*, Submitted to Phys. Rev. Lett.
[2] H. B. Greenlee *et al.*, Phys. Rev. Lett. **60**, 893 (1988);
S. F. Schaffner *et al.*, Phys. Rev. **D 39**, 990 (1989).
[3] T. Inagaki, *et al.*, KEK preprint 88-26.
[4] BNL791 memo KL209, S. Wojcicki.
[5] BNL791 memo KL237, S. Imlay and W. Molzon.
[6] H. W. Atherton, *et al.*, CERN Report 80-07, as parameterized by A. J. Malensek, Fermilab Reports FN-341 and FN-341-A.

DETECTOR REQUIREMENTS FOR K DECAYS

M. P. Schmidt
Physics Department, Yale University
New Haven, Connecticut 06511

Introduction

For the purposes of this workshop the subgroup on detectors for K decays chose to focus attention on one decay mode, $K_L \to \pi^0 e^+ e^-$, with discussions based on the 'reference design' detector outlined by Winstein.[1] While it is quite desirable to contemplate a detector facility for the Main Injector capable of studying several K decay modes, considerations relevant to $K_L \to \pi^0 e^+ e^-$ provide a benchmark for the potential and challenges for K decay physics at the Main Injector. The search for $K_L \to \pi^0 e^+ e^-$ has a well defined goal in the sense that Standard Model calculations suggest,[2] among other things, that a branching fraction sensitivity of about 10^{-13} may be required in order to detect the presence of a direct CP violating amplitude ($K_2^0 \to \pi^0 e^+ e^-$). This goal places serious demands on all elements of the detector, and in what follows we address several of the issues raised.

Participants in the K detector working group included: D. Anderson, J. Enagonio, A. Heinson, D. Jensen, M. Schmidt, S. Teige, R. Tschirhart, H. Wahl, C. Woody, H. Yamamoto, and T. Yamanaka.

Detector Overview

At the Main Injector the neutral kaon beam is to be derived from interactions of a 120 GeV/c proton beam. For the purposes of discussion it is assumed that the neutral beam is formed at an angle of 20 mr with a solid angle of 6 mr by 6 mr. A γ filter/neutron moderator comprised of 3" of lead and 18" of beryllium would be used giving a kaon to neutron ratio of about one at the non-zero targeting angle. About 25 m of magnetized collimation and shielding would separate the production target and the beginning of a 20 m evacuated decay region.

The neutral beam passes unimpeded through the detector (see Figure 1) which has a single large aperture dipole magnet. The momentum of charged particles is determined from trajectories

measured by drift chambers situated upstream and downstream of this analysis magnet ($\Delta p_t \sim$ 200MeV/c). The position and energy of gamma rays are determined in an electromagnetic (EM) calorimeter situated at the end of the charged particle spectrometer. Electrons are identified by transition radiation detectors (TRDs) as well as through a comparison of the energy deposited in the EM calorimeter with the measured momentum (E/p). The detector is terminated by a hadron calorimeter and muon identifier which is used to further distinguish photons and electrons from other particles. In order to have high acceptance the detector is compact along the beam ($\sim$ 10 m) and has large transverse dimensions (3 m by 3 m).

Monte Carlo calculations obtain a large acceptance for $K_L \to \pi^0 e^+ e^-$: 16% for $p_K > 15$ GeV/c, and this includes a requirement, $E_\gamma > 1$ GeV. With 3×10^{13} protons on target per 1.9 sec pulse every 3.8 sec, it is expected that there will be roughly 2 GHz each of neutrons and kaons in the neutral beam. There will then be about 130 MHz of K decays in the 20 m decay region with about 1/4 of these decays having $p_K > 15$ GeV/c. In principle 1000 hours of running would provide a sensitivity to $130 \times 10^6 \times 0.16 \times 1/4 \times 1000 \times 3600 \sim 2 \times 10^{13}$ K decays.

The detector will have to operate in a very high rate environment in order to achieve the desired sensitivity. The singles rates in the first chamber will be about 160 MHz from K decays alone, making the design of the neutral beam and transport critical. Issues of occupancy and radiation damage must be addressed for all of the detector elements.

Acceptance and Backgrounds

A class of potential backgrounds for $K_L \to \pi^0 e^+ e^-$ follows from the overlap of two decays — for example $K_L \to \pi e \nu$, with the pion misidentified as an electron, in coincidence with gamma rays from another K decay such as $K_L \to 3\pi^0$. Note that in the Main Injector experiment there will be about one K decay every 8 nsec. Without directional information from the gamma rays the event vertex is defined solely by the charged particles from the K^0_{e3} decay. Unlike the case for many backgrounds resulting from a single K decay, pseudo-events arising from the overlap of two K decays are not *a priori* excluded from the fiducial volume of reconstruction variables ($e.g.$ $m_{\gamma\gamma} \sim m_{\pi^0}, m_{\pi ee} \sim m_K, p_t^{missing} \sim 0$).

Backgrounds of this sort are minimized in a detector with excellent time resolution and high geometrical acceptance as we show in what follows. The number of signal events is

$$S = N_{\pi ee} = N_K n Br(\pi ee) A_{\pi ee},$$

where N_K is the number of K decays per pulse, n is the number of pulses, $A_{\pi ee}$ is the acceptance and $Br(\pi ee)$ is the branching fraction for $K_L \to \pi^0 e^+ e^-$. The number of background events from overlapping K decays is given by

$$B = (N_K Br(\pi e \nu) A_{\pi e})(N_K Br(3\pi^0) A_{\gamma\gamma}) n \Delta t,$$

where Δt is the time resolution, $A_{\pi e}$ is the acceptance for $K_L \to \pi e \nu$ with the pion misidentified as an electron, and $A_{\gamma\gamma}$ the acceptance for detecting *two and only two* gammas. Noting that the required rate of decays is set by the desired sensitivity and the running time:

$$N_K = \frac{N_{\pi ee}}{n Br(\pi ee) A_{\pi ee}},$$

we find that the signal to background ratio is

$$\frac{S}{B} = \frac{Br^2(\pi ee) A^2_{\pi ee}}{Br(\pi e \nu) A_{\pi e} Br(3\pi^0) A_{\gamma\gamma} \Delta t} \frac{n}{N_{\pi ee}}.$$

As the geometric acceptance of the detector increases, $A_{\pi ee}$ and $A_{\pi e}$ increase, but $A_{\gamma\gamma}$ decreases as it is less likely to miss *all* of the additional gamma rays. Thus the signal to background is proportional to the square of the geometric acceptance of the detector. For the Main Injector detector $A_{\gamma\gamma}$ is minimized by requiring a small hole (and therefore a bright beam) through a finely segmented electromagnetic calorimeter, and by surrounding the decay region with γ (-veto) detectors.

Electromagnetic Calorimeter

Perhaps the most important element of the detector is the electromagnetic calorimeter. In order to deal with the high rates and potential backgrounds anticipated in the $K_L \to \pi^0 e^+ e^-$ search a fine grained, fast, high resolution, radiation hard detector is required. If possible it is highly desirable to improve on the energy resolution ($\sim 5\%/\sqrt{E}$) and spatial resolution ($\sim$ 2 mm)

currently achieved in searches for $K_L \to \pi^0 e^+ e^-$. The estimated radiation dose of about 10 Gray (10^3 rad) per week for the worst part of the detector rules out the use of lead glass.

The detector as envisaged would be built from two layers of BaF_2 blocks, each with a depth of 10 radiation lengths, with about 15,000 blocks in all. Most ($\sim 2/3$) of the cells would have a size of 4 cm by 4 cm; in the central region around the beam hole 2 cm by 2 cm cells would be used in the first layer. The segmentation of the detector into two layers is suggested for two reasons: first to enhance the detectors capability in identifying showers of electromagnetic origin by virtue of their longitudinal development, and second to accommodate limitations in the formation of high quality BaF_2 crystals.

BaF_2 crystals are expensive, with a cost of \$7/cm^3 (cut and polished). A combination of techniques currently under investigation[3] such as lanthanum doping of the scintillator, Fabry-Perot filters, and quartz faced phototubes with solar blind (CsTe) photocathodes will be required to efficiently isolate the 'fast' ($\tau \sim 0.6$ nsec, $\lambda \sim 220$ nm) component of light from the 'slow' ($\tau \sim 625$ nsec, $\lambda \sim 310$ nm). Baseline restoring electronics might also be required. In any case it is easy to see the cost for the EM detector approaching \$30M dominated by the BaF_2. For this reason it is attractive to consider alternative scintillating and Čerenkov radiating crystals. Of particular interest are PbF_2 (@ <1/2 the cost),[4] CeF_3,[5] and 'pure' CsI.[6]

It is also useful to consider the possibility of mixing detector technologies. While it may be necessary to use BaF_2 in the central region of the detector, the demands outside this region may allow for other less expensive and hopefully less exotic solutions. Perhaps PbF_2 could be used in the outer part of the first layer, and a lead/scintillator 'spaghetti' calorimeter[7] could be used for the second layer. In addition there are other novel approaches conceivable such as those using liquid Čerenkov radiators[8] or index matched solutions containing BaF_2 powder ('slurries').[9]

These possibilities need to be considered in the context of detector specifications derived from Monte Carlo simulations of the signal and backgrou nd and the experience gained with present detectors. It is of particular importance to give serious consideration to the calibration of the EM calorimeter. This is especially true if information from the EM calorimeter is to be used on-line, for example to determine energy moments (and even an estimate of the invariant mass) for K decays

to electromagnetic final states.

Tracking Chambers

The high instantaneous rates expected in the experiment suggest the use of a tracking chamber system based on small drift cells, e.g. 'mini drift chambers'. The 160 MHz rate quoted above for the first (3 m by 3 m) chamber translates to a rate of about 1 MHz on the hottest wire assuming a 3 mm drift gap. Small chambers (1/8 m by 1/8 m) with a 3 mm square cell geometry have been reliably operated at fluxes of $\sim 3 \times 10^5$ $s^{-1}cm^{-2}$, a spatial resolution of better than 100 μm was achieved in these chambers.[10] The use of 'fast' gas mixtures with CF_4 has been explored for high rate beam chambers.[12] The high drift velocities, ~100 μm/nsec for an 80:20 Ar-CF_4 mix, that have been achieved correspond to a maximum drift time of 30 nsec and an occupancy of about 3% for the hottest wire.

Employing these techniques in large chambers presents several challenges. Undoubtedly the chambers will need to be divided (into quadrants?) or the long wires supported by some means without spoiling the resolution capabilities. The expense of CF_4 and its unknown resistance to radiation damage are concerns. It is noted that the charge collected on the hottest wire is likely to be less than a mC/cm in one run, and this is to be compared with the 1 C/cm survived by chambers operating under well controlled (clean) conditions. Experience with large chambers in the less well controlled environment of typical experiments suggest that this is not a large safety margin.

The tracking chambers would probably consist of four sense planes each: X, X', Y, and Y'. To achieve high track reconstruction efficiency a certain amount of redundancy will be necessary. As shown in the accompanying figure the system might have three chamber stations upstream of the first TRD for determining the vertex and opening angle for the e^+e^- pair, and two stations upstream and three downstream of the analysis magnet for momentum determination and tracking into the second TRD and EM calorimeter. It will also be important to minimize the material, and thereby the multiple scattering and conversions taking place, in the chambers and TRDs.

Transition Radiation Detectors

As mentioned before excellent π/e separation will be necessary to suppress backgrounds in the experiment. At the Main Injector transition radiation detection is an applicable technique. However convential TRDs are not well suited to the demands of this high intensity experiment. A convential TRD requires about 10% of a radiation length of radiator and chamber. A Xe X-ray chamber with a depth of a few cm is necessary in order to have a high quantum efficiency given that only 10-20% of the X-rays make it through the radiator to the chamber. The depth of the Xe chamber implies a collection time on the order of a microsecond and this is just too long.

A very promising direction is found in the 'fine-sampling' TRD. [11] Here a factor of 2-3 is gained in the number of observed X-rays per radiation length of detector by dividing the detector longitudinally into submodules each containing about 1/10 the number of radiating foils of a conventional TRD followed by a few mm deep Xe X-ray chamber. The smaller chamber depth implies shorter collection times, perhaps on the order of 30 nsec if a 'fast' gas mixture for the Xe chamber could be used.

It is possible that the Xe chamber could be constructed using straw tube technology. A staggered set of 4 mm diameter tubes could be used where each tube is made from a 1/2 mil carbon loaded polycarbonate (aluminized) film wrapped in 1/2 mil mylar. One meter long tubes of this kind have been successfully made in quantity. Ongoing R&D efforts will address issues such as the absorption of X-rays near the tube walls and the control of the variation of thickness of the chamber.

For the $K_L \to \pi^0 e^+ e^-$ search it is desirable to have two independent fine sampling TRD detectors, one before and one after the analysis magnet, to achieve the maximum π/e separation. The electronics required could be relatively simple — a fast amplifier/discriminator on each channel, and with the high speed detector envisaged it is possible that it could be used as a triggering element. With the combination of TRDs and EM calorimeter, a π/e separation of 10^{-7} is conceivable.

Conclusions

The Main Injector has enormous potential for extending the search for $K_L \to \pi^0 e^+ e^-$ by virtue of the high energy *and* high intensity kaon beams it can provide. However formidable experimental challenges must be met in order to realize the goal of 10^{-13} in branching fraction sensitivity. Many of the difficulties arise as a result of high rates in the detectors and are then often of common concern for detectors at the SSC. Ongoing research and development on chambers using 'fast' gas components and sampling TRDs employing straw tube chambers are of great interest. The EM calorimeter poses a somewhat more unique challenge and an aggessive R&D program is quite warranted. Finally with the present (published) limit for $K_L \to \pi^0 e^+ e^-$ at the level of a few times 10^{-8}, there will undoubtedly be much to learn from the ongoing efforts at Brookhaven (E845), CERN (NA-31), Fermilab (E731/799) and KEK (E162).

References

[1] B. Winstein, these proceedings; also "CP Violation in the Kaon System with the Fermilab Upgrade", B. Winstein, G.J. Bock, and R. Coleman, EFI 89-01.

[2] F. Gilman, these proceedings.

[3] C. Woody, these proceedings; also C. Woody et al., IEEE Transactions on Nuclear Science, *36* (1989) 536.

[4] D.F. Anderson, these proceedings and "Proposal for the Development of PbF_2 as a Very Compact and Fast Electromagnetic Calorimeter for the SSC", generic detector R&D proposal.

[5] D.F. Anderson, IEEE Trans. on Nucl. Sci. *36* (1989) 137, and W.W Moses and S.E. Derenzo, *ibid*, 173.

[6] S. Kubota et al., NIM *A268* (1988) 275.

[7] R. Wigmans, Proceedings of Snowmass '88 Summer Study.

[8] 'Tetrabromoethane as a Radiation Hard Electromagnetic Calorimeter", S. Teige, these proceedings.

[9] D.R. Winn and M. Whitmore, IEEE Trans. on Nucl. Sci., *36* (1989) 256.

[10] I.E. Chirikov-Zorin et al., NIM *A260* (1987) 142.

[11] R. Tschirhart, these proceedings; also T. Åkesson et al., from *The Feasibility of Experiments at High Luminosity at the LHC*, CERN 88-02, 31, and B. Dolgoshein, NIM *A252* (1986) 137.

[12] J. Fischer et al., NIM *A238* (1985) 249.

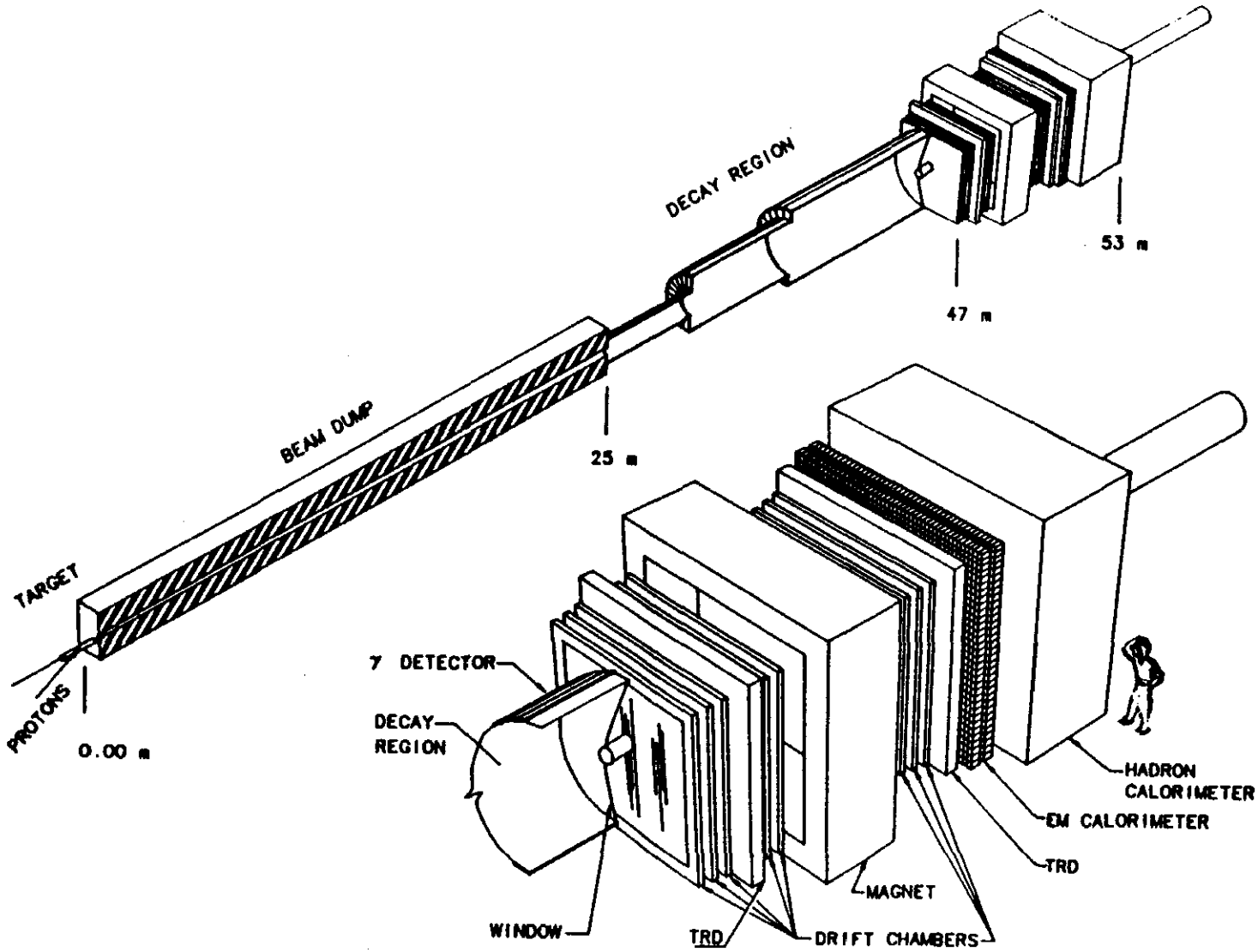

Figure 1: **MODEL KAON FACILITY AT THE MAIN INJECTOR**

Summary Report on Long Base Line Neutrino Oscillation

M.Koshiba/TOKAI University 18 May, 1989

Participants: W.Gajewsky of UC Irvine (IMB), N.Goodman of ANL (SOUDAN II), T..Haines of Maryland U (GRANDE), M.Koshiba of Tokai U (LENA), J.LoSecco of Notre Dame U (IMB), H.Ma of BNL (P-848), K.Nishikawa of Tokyo U (LENA), J.Scholz of UC Irvine (GRANDE), H.Sobel of UC Irvine (GRANDE) and L.Stutte of FNAL (ν-beam).

Discussion:

As can be expected, there immediately was an unanimous agreement on the importance and the richness of this field of study and on that it should be explored with utmost vigor.

When it comes to how and what type of detector,however, all the experimental groups are on their own.

Before summarizing the discussions, we show the table specifying the presented experiments

Table-1 $\nu_\mu \rightarrow \nu_x$ **Long-Base-Line Experiments**

Experments	Appearance or Disappearance	Dedicated Yes/No	Length for Oscill. (km)	Detector Mass (k-ton)	Min.Δm^2 $(eV)^2$
BNL P848	D and A(ν_e)	Yes	1/3/10	0.4/1.5	0.05
GRANDE	D and A	No	900	5000	0.003
IMB	D and (A)	No	550	5	0.003
LENA I/II	A	Yes	3/500	10/1000	0.003
SOUDAN	D and A(NC/CC)	No	800	1	0.3/0.07

It seems also appropriate to look at the relevant regions of the oscillation parameters as shown in the Figure. In the Figure the region (a), shaded black, is the one already excluded for (ν_μ-ν_τ) oscillation by the accelerator experiments. The region (b), shaded grey, is the one claimed to be of possible positive signal for (ν_μ-ν_τ) oscillation by KAMIOKANDE-II observation of the anomaly in the atmospheric $N\nu_\mu/N\nu_e$ ratio[1]. The +symbol indicates the optimal set of parameters to explain the effect. The region (c) is the target of Short-Base-Line Oscillation Experiments discussed in a separate study group. Δm^2 of tens of $(eV)^2$ and small mixing parameter in this region was theoretically motivated; based on the Sea-Saw mechanism, the assumed similarity in the mixing matrices of quarks and neutrinos, and the possibility of assigning ν_τ to Cosmic Dark Matter. The region (d) is the one to be investigated by Long-Base-Line Experiments of this study group. The region (e), also shaded grey, signifies the lower part of M-S-W solution of the solar ν_e deficiency as observed anew by KAMIOKANDE-II[2]. Note that the upper horizontal branch, the adiabatic solution, is excluded by the sizable flux observed above 9.3 MeV, 46% of the Standard Solar Model prediction with a spectrum not inconsistent with the bare ^8B decay spectrum. Remembering that the region (b) resulted from the observed deficiency of ν_μ's and the region (e) from the observed deficiency of ν_e's, the Sea-Saw mechanism by itself seems to suggest that the masses of ν_τ, ν_μ, and ν_e are in the range of 10^{-1}eV, arround 10^{-3}eV and smaller than 10^{-3}eV, respectively.

The task is thus how to experimentally scrutinize this region (b). The problem of neutrino oscillation being of primary importance, definitely beyond the Standard Electro-Weak Theory, a dedicated appearance experiment of best conceivable resolution is desiraole; a personal feeling hopefully to be shared by others. If we were to include the optimum parameter set at Δm^2 of about $10^{-2}(eV)^2$ in a τ-appearance experiment of (ν_μ-ν_τ), we have to consider at least 500km or more for the distance between the decay-tunnel and the detector because the ν_μ energy has to be 4 GeV or more. The divergence of the ν-

beam and the distance require a detector of not much smaller than 1Megaton fiducial mass for some 10^{20} protons on target. Furthermore, a really good μ/e discrimination capability is required since this is the first thing to use in detecting the produced τ's. If the detector had the e/γ discrimination capability it would help greatly in reducing the neutral current background. Obviously the most promissing energy region for the identification of the produced τ will be just above the production threshold. Search for the $\mu\nu\nu$- and/or

$e\nu\nu$- decay modes of the pseudo-elastically produced τ's just above the threshold will have the best chance of positively identifying the (ν_μ-ν_τ) oscillation and for this purpose the above discrimination capabilities for energies down to 1 Gev seem instrumental.

With these points in mind we look at the experiments of Table-1 presented to this study group meeting.

The experiment P-848 at BNL uses lower energy ν-beam and in this respect differs from the others. We just mention here that the results from this experiment will be very valuable to the other experimental projects which plan to use the beams of Main Injector Ring in about 4 years time.

The experiment GRANDE proposes a gigantic detector of 5 Megatonnes fiducial mass originally designed for high energy ν-astronomy. It is an imaging-water-cherenkov type detector with horizontal layers of 8"ϕ photomultipliers,PMT's,on a 6mX6m lattice. It proposes to do a disappearance experiment by observing either the neutral- to charged-current ratio or the charged current rates at two different distances. The estimated parameter region to be investigated is just about the region (d) in the figure. It has shown the expected μ-e discrimination at 20 GeV energy but some detector modifications seem

needed to improve the performance near 1 Gev. The site has been already chosen and it is neccesary to build the ν–beam in this direction.

The experiment IMB of 5 k-tonnes fiducial mass has been operating for some years and it proposes to do the oscillation experiment if the ν-beam is directed to its direction. The observation of the externally produced μ's by the beam ν_μ's in the 21.5 k-tonnes effective mass of front side rock to be compared with the internally produced events constitutes the method. The experiment so far did not show the μ-e discrimination capability and this is a drawback for τ-appearance detection. The mass is too small for the distance.

The LENA-I[3] and LENA-II have been presented elsewhere in this workshop by K.Nishikawa and we do not explain any further here except that these experiments are both the dedicated experiments; LENA-I for ν_μ-e elastic scattering and LENA-II for (ν_μ-ν_τ) oscillation in appearance mode.

The experiment SUDAN II is under construction and is of calorimeter type. When it is completed it will have 1 k-tonnes mass. The proposed method of investigating the ν-oscillation is quite similar to that of IMB but a still smaller detector mass for a longer distance is making the job more dificult.

Admittedly this report is biassed but it is hoped to be tolerated by the readers in view of the sincere desire of the reporter to eventually arrive at a clear-cut design of experiment on ν-oscillation for the parameter region where there is the only existing possible positive signal.

For the sake of record I should mention the farsighted paper by A.K.Mann and H.Primakoff on the possibility of a long-base line ν-oscillation experiment with FNAL ν-beam with 220 k-tonnes detector at 1000 km; Phys. Rev. D15 (1977) 655.

During the sessions there was an occasion for preliminary exchange of views on possible merging of GRANDE and LENA-II. As of the time of this writing there has been no further development along this line.

In conclusion we are all grateful to the FNAL organizers for this exciting opotunity of discussing vital future physics and we are indeed looking forward to the forthcoming FNAL workshop at Breckenridge in August where hopefully we can arrive at a more perspective understanding of the things to be done.

References:

1) K.S.Hirata et al., Phys. Lett. B 205 (1988) 416. The anomaly observed in the $N\nu_\mu/N\nu_e$ ratio of atmospheric neutrinos is very difficult to explain away except in terms of ν-oscillations, while in the case of solar ν_e-deficiency in the absolute flux other possibilities conceivable; lower central temperature and/or different element abundances near the core,etc.. Hence, J.Learned, S.Pakvasa and T.Weiler, Phys. Lett. 51 (1988) 79; for instance. L.V.Volkova pointed out the effect of μ-polarization on the observed ratio; a private communication and Sov. J. Nucl. Phys. 31 (1980) 784. However, the polarization effect on the above ratio is estimated to be 15% and does not eliminate the anomaly. After a careful re-evaluation of the ratio with additional data it was concluded that the anomaly still exists at 5 σ level. See, M. Takita, Doctor Thesis, Univ. of Tokyo (Feb. 1989), ICR-Report-186-89-3 and also T.K. Gaisser, T. Stanev and G. Bar, Phys. Rev. D 38 (1989) 85. The anomaly was independently confirmed also at 5 σ level by observing in the KAMIOKANDE-II data the ratio of μ-e decay vs. non-μ-e decay events among the single ring contained events.

2) K.S. Hirata et al., Phys. Rev. Lett., 63 (1989) 16. This paper not only confirmed by real-time and directional observation the longstanding solar neutrino puzzle of R. Davis Jr. but also for the first time gave energy spectrum above 9.3 MeV which is consistent with that of free ^8B decay within the statistics.

3) At the time of the study group meeting LENA-I was presented as a 10 k-tonnes detector at 50 to 100 km distance for the purpose of serving as the test experiment as well as the intermediate stage of LENA-II. Here in this text we are figuring LENA-I as an experiment on its own aiming at a precise and unambiguous determination of $\sin^2 \theta_W$. The observation of y-distributions of ν_μ- as well as anti ν_μ- scatterings off electrons using the dichromatic beam will accomplish the aim. The accuracy in the angular measurement, 0.6 degree, and the energy resolution, 0.07/sqrt.E(GeV), of the detector plays the instrumental role. It will also demonstrate the e/γ discrimination by means of observing the Cerenkov light from the first few radiation length of cascade development. The improved timing characteristics and the good single photon observsbility of the new improved type of 20"ϕ PMT's are essential here.

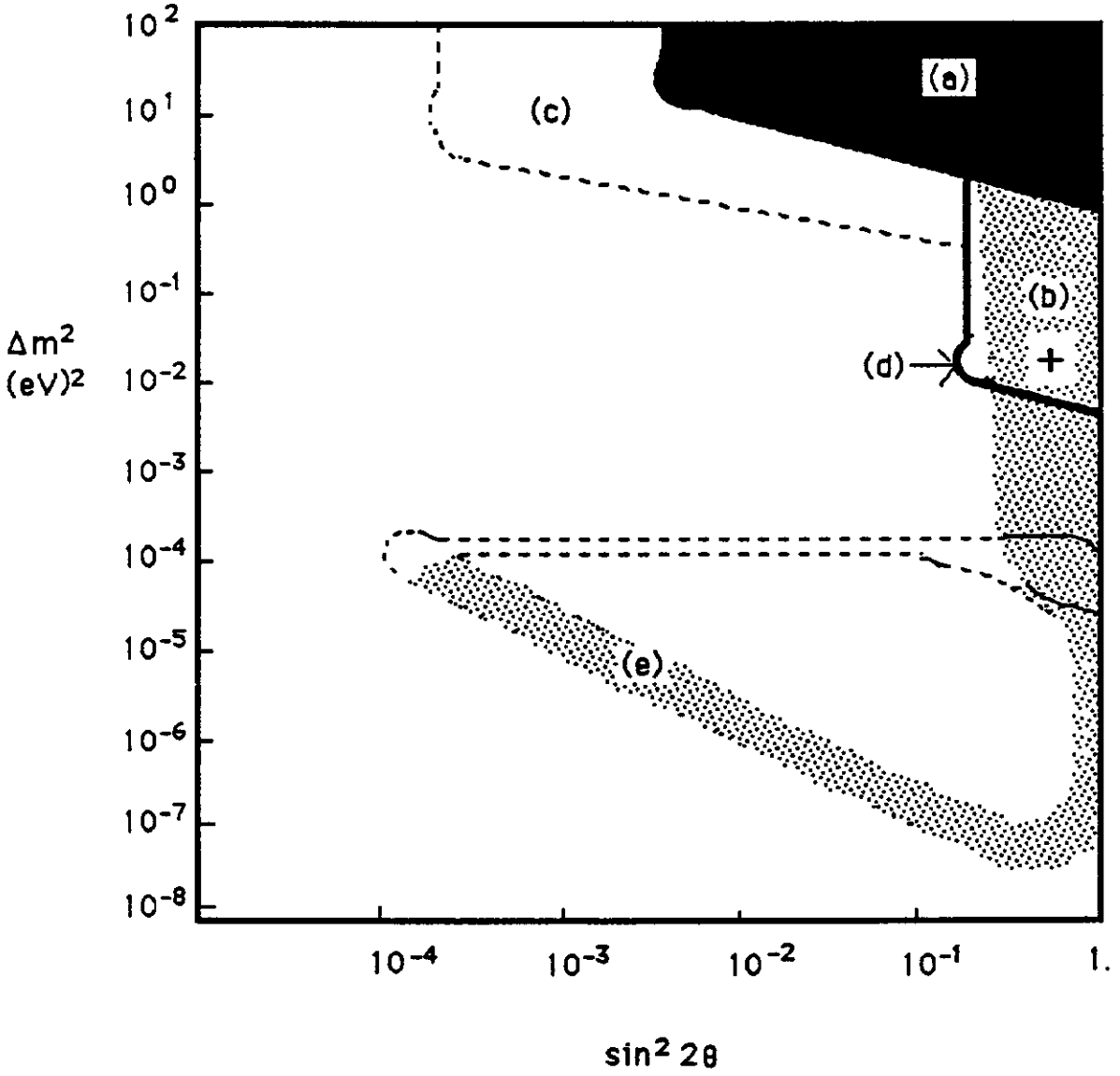
(a)
(b)
(c)
(d)
(e)
+
10^{2}
10^{1}
10^{0}
10^{-1}
10^{-2}
10^{-3}
10^{-4}
10^{-5}
10^{-6}
10^{-7}
10^{-8}
Δm^2
$(eV)^2$
10^{-4}
10^{-3}
10^{-2}
10^{-1}
1.
$\sin^2 2\theta$

REPORT FROM THE SHORT-BASELINE NEUTRINO OSCILLATIONS GROUP

N. W. Reay
The Ohio State University
Columbus, Ohio
USA

PARTICIPANTS

Bernstein[4], Brock 7, Bross[4], Childress[4], Fowler[4], Koizumi[4], Koshiba[10], Malensek[4], Marciano[1], Nishikawa[10], Peterson[5], Reay[9], Schneps[11], Seto[3], Stanton[9], Staude[2], Stefanski[4], Stutte[4], Tartaglia[7], Tzanakos[3], White[6], Willis[8].

(1) Brookhaven National Laoboratory, (2) CERN, (3) Columia University, (4) FERMILAB, (5) University of Hawaii at Manoa, (6) Los Alamos National Laboratory, (7) Michigan State University, (8) Northern Illinois University, (9) The Ohio State University, (10) Tokyo University, (11) Tufts University.

ABSTRACT:

This report from the Short-Baseline Neutrino Oscillations Working Group summarizes discussions made while studying feasibility of a high- sensitivity $\nu_\mu \rightarrow \nu_\tau$ oscillations experiment at larger δM^2. Topics covered included a possible design, various beamline locations and whether these were compatible with long-baseline experiments, a number of hardware techniques including scintillating fibers, and several possibilities for making standard-model measurements with the same apparatus.

INTRODUCTION:

The possibility of generating physics with a rapid-cycling new main injector has captured the imagination of scientists interested in such diverse topics as rare kaon decays, antiproton physics, polarization and neutrino physics. Even within subareas there is broad representation. Thus, for this workshop neutrino types were divided into groups studying long-baseline oscillations, short-baseline oscillations, electroweak and standard model measurements, and instrumentation.

However, it soon became apparent that there were strong overlaps in interest between the various neutrino groups. Instrumentation and short-baseline sections were combined from the outset; long and short baseline working groups wished to explore whether they could simultaneusly use the same beam, the short baseline group was interested in Iarocci tubes and other long-baseline instrumentation, and the electroweak aficionados argued convincingly that the combination of new low and high energy data could pin down "slow recaling of charm," the Kobayashi-

Maskawa matrix element V_{cd}, the strange sea, and $\sin^2(\theta_W)$ [1]. This report therefore will touch on several areas.

But its main focus is on a precision measurement of $\nu_\mu \rightarrow \nu_\tau$ neutrino oscillations. Many theorists [2] [3] have presented the striking hypothesis that the tau neutrino, if massive, is the only known particle which could close the universe. They employ a see-saw mechanism which relates masses of neutrinos to quark and lepton masses in the same generation. Resulting neutrino masses are so disparate that a tau-neutrino mass in the range 10-60 eV, sufficient to close the universe, could be generated and still maintain $\nu_e \leftrightarrow \nu_\mu$ oscillations in the 10^{-4} to 10^{-7} eV^2 range required by the MSW [4], [5] solution to the solar neutrino problem. The need for precision comes from the ansatz that if the two-component lepton mixing angle α is comparable to K.M. matrix quark mixing angles, $\sin^2(2\alpha)$ must be larger than 4×10^{-4}. Present 1/2% world limits determined by Fermilab experiment E531 [6] and the CERN CDHSW experiment [7] are given in Figure 1.

POSSIBLE SHORT-BASELINE DESIGN:

Reay presented as a beginning scenario the preliminary design of an experiment that could access 20 times smaller couplings in the mixing parameter and 5 times smaller δM^2, (see also Figure 1). Experimental layouts are shown in Figures 2a, 2b, and 2c. The new hybrid emulsion-electronic design used almost a ton of emulsion exposed to a double-horn focused secondary beam generated with protons from the new Main Injector. Multiple layers of emulsion were incorporated to enhance rate; and (as further discussed by N. Stanton) scintillating fiber planes and straw tube drift chambers were used to provide tracking between layers of emulsion. A field of approximately one Tesla from the existing 15 foot bubble-chamber magnet was provided to obtain the sign and P_T of tau-lepton single-prong decays and to aid in vertex reconstruction. Emulsion and tracking systems resided within a "calorimeter cave" to enhance muon and electron identification. Estimated muon efficiencies are given in Figure 3.

A typical tau neutrino emulsion interaction is shown schematically in Figure 4. Candidates for charged current interactions of tau neutrinos consist of events with no primary muon or electron which have a high P_T negative kink track with a production angle less than 15 degrees. The primary vertex is located by scanning back along emulsion tracks which match those found by the electronic spectrometer. Once an event has been located in the emulsion, the slopes of charged emulsion tracks coming from the primary can be measured using automatic techniques. A 2 millimeter "follow-down" procedure searching for negatively-charged decay "kinks" would be performed on all primary emulsion tracks with lab angles less than 15° whose slopes do not match those of any electronic detector track. Only "muon-less" kinks with a P_T greater than 0.1 GeV/c would be retained, since taus decay 69%

of the time into muonless single-prong "kinks" while most of the background is multiprong.

G. Koizumi and R. Stefanski discussed two scenarios for constructing a short-baseline experimental area. One, indicated in Figure 5, made extensive use of existing facilities, the other more expensive version established a new target area with the goal of using the present bubble chamber building for the oscillations experiment while maintaining compatibility with other neutrino experiments. A high-intensity neutrino beam design relying on a double-horn focussing system was discussed by L. Stutte [8]. The spectrum of neutrino interactions for the proposed 150 GeV beam is given in Figure 6. An offline cut on visible energy corresponding to 11 to 60 Gev in beam energy will retain 57% of these interactions while enriching the potential tau sample. The interaction rate is mind-boggling. A 7 month run (2.6×10^6 pulses at 2×10^{13} protons per pulse) with 180 liters (3/4 ton) of emulsion target would yield 132,000 software-reconstructed charged-current interactions in the 11 to 60 GeV energy range. By incorporating a center "plug" and focusing on negatives, the intense antineutrino beam shown in Figure 6 also can be generated.

Stanton and Reay also discussed both backgrounds and possible kinematic cuts which could result in significant background reductions. Possible sources of background consist of tau neutrinos coming from the primary proton beam dump, ordinary interacting tracks which elastically scatter from nucleons without leaving evidence for nuclear breakup in the emulsion, charged hyperon and kaon decays, and a variety of cases containing single prong decays of charm particles. Of these, the two most worrisome are "white star" hi-P_T elastic scattering of secondary tracks, and antineutrino production of anti-charm. The number of interactions due to real tau neutrinos coming from the proton beam dump appeared negligible, but if necessary could be reduced more than an order of magnitude by placing two main-ring dipoles at the end of the decay space, giving secondaries from the dump a 50 milliradian angular displacement.

The probability that a track would suffer a secondary single-prong large P_T "kink" interaction with no dark tracks from nuclear breakup and occuring within 2 millimeters of production appeared smaller than 10^{-6}, but there was considerable uncertainty among emulsion experts whether such scatters occured diffractively off the whole nucleus or in fact had a large component with scattering off nucleons. The latter would considerably raise the background level in the absence of additional kinematic cuts. [9].

A major contribution to background comes from anti-neutrino interactions in which a negative charm single-prong decay occurs and the primary charged-current muon or electron is missed. It is assumed that the ratio of $\overline{\nu}_\mu$ to ν_μ interactions is 4%, as in E531. In the absence of kinematic cuts, the resulting muon antineutrino

charged-current background was calculated to be 0.8×10^{-5}. If the relative yield of $\overline{\nu}_e$ is the same as the measured value of 1.5% for ν_e interactions in E531, the overall background summed over all sources totals 1.2×10^{-5}.

At this workshop kinematic cuts were suggested that could reduce the anti-charm background, as at low energies charm and taus occupy different locations of x-y space. However, the efficiency of such cuts was difficult to estimate as cuts would have to be made on incorrect values generated by assuming candidate tau kinks define the lepton direction. Other suggestions included rejection of events in which a low-energy track is "back-to-back" with the kink direction, and by eliminating events with overall P_T balance. Charged-current events mostly balance P_T while tau events mostly do not. Emulsion scanning for taus would have to be performed on all neutral-current events, plus the 5% of charged-current events without identified muons. This is 53×10^3 events, or approximately 28% of all interactions. This is a large number, and kinematic background reduction cuts will have to be investigated. Those suggested during this workshop included both E_{vis} and P_T cuts, as neutral current events have lower visible energy and more missing P_T than typical tau charged-current events. Investigations of the above cuts will be presented at Breckenridge.

The raw ratio of (found ν_τ / found charged-current interactions) is subject to a sizable upward correction before one can infer the actual fractional ν_τ interaction rate. The correction includes a variety of efficiencies and branching ratios, but a major ingredient is that the measured ratio must be increased to take into account the mean ratio of ν_τ to ν_μ cross sections, which is 0.5 for the Stutte beam. The overall correction value was computed to be 4.15.

If zero ν_τ interactions are seen over a background of $139{,}000 \times (1.2 \times 10^{-5}) = 1.67$, the 90% C.L. on the signal (assuming observed events = expected background) is 3.7 events over a denominator of 122,000 charged-current interactions (139,000 corrected for emulsion scanning efficiency):

$$R = \left(\frac{3.7}{122,000}\right) \times (4.15) = 1.25 \times 10^{-4} \qquad (1)$$

R may be interpreted in terms of a two-component representation of neutrino oscillations;

$$R = \sin^2(2\alpha) \int \rho(\frac{L}{E}) \sin^2(1.27 \delta M^2 \frac{L}{E}) d\frac{L}{E} \qquad (2)$$

where ρ gives the flux of neutrinos in terms of the variable (L/E), L is the neutrino flight path in meters, E the neutrino energy in MeV and δM^2 in $(eV)^2$. For large δM^2 the oscillation length is small compared to the variation in neutrino flight

length, and the (L/E) integral has an approximate value of 0.5. Thus, the overall sensitivity is 2.5 x 10^{-4} at the 90% CL. The corresponding plot of $\sin^2(2\alpha)$ sensitivity versus δM^2 is given in Figure 1.

COMPATIBILITY OF SHORT- AND LONG-BASELINE EXPERIMENTS:

A major topic of concern was whether long and short baseline experiments could use a common neutrino beam. V. Peterson discussed the use of Dumand as a long-baseline detector, and K. Nishikawa presented a proposed detector based on the Kamioka design. Both had dip angles due to the curvature of the earth of 5-20° with respect to Fermilab, as shown in Figure 8, and would require new beam facilities constructed at significant downward angles. If any short baseline experiment were to make use of the same beam it would have to be constructed underground, and the overall additional cost to insure compatibility appeared to be in excess of $20 million. On the positive side, it appeared that the Koshiba-Nishikawa oscillation design could also be used for a precision measurement of neutrino-electron scattering. This possibility is quite interesting and should be pursued vigorously.

INSTRUMENTATION:

Discussions of instrumentation proved to be more fruitful. W. Fowler showed that the 15 foot Bubble Chamber magnet coils and cryostat used in the oscillation layout were packaged with the original intent of being produced at Argonne National Laboratory and transmitted as a single unit to Fermilab. He averred that relocating the coils would require very little disassembly.

Bross presented the present status and future prospects for scintillating fibers both as a tracking adjunct to emulsion target experiments or as a totally electronic target. Glass fibers have a density of 2.6 g/cm^3 and diameters as small as 20 microns. The hit density presently is approximately 4 photo-electrons/mm for short fibers, but the attenuation length is less than 40 cm without much hope of significant upgrades. Plastic is lighter (1.0 g/cm^3), and has a similar number of photo-electrons for 1 meter lengths of 200 micron diameter fibers. It was noted that a several ton totally electronic target would have in excess of a billion fiber-meters at a current cost of 10 cents per meter, and would show events in only two dimensions, as opposed to three for emulsion. Bross also suggested lowering cost by using an amalgam of lead and fibers, but such a design would require extensive monte carlo studies.

The consensus appeared to be that with present technology fiber targets were prohibitively expensive and could not replace emulsion. However, Bross felt that an aggressive R & D program on plastic fibers could increase their photoelectron "hit" density by an order of magnitude to 25/mm, and that the attenuation length

could be increased from 1 to perhaps 3 meters. These improvements would occur through the combined effects of small improvements such as increasing intrinsic efficiency by using large Stokes shift single-dopants to reduce both attenuation and cross-talk, and improving light piping by achieving better polish and cladding. The Hamamatsu readout intensifiers also could be cooled to reduce background noise. It is hoped that Fermilab will undertake such a program; it would have significant benefits for a wide variety of experimental approaches.

Seto discussed the proposed Brookhaven Nation Laboratory long-baseline oscillation experiment, which was based on extensive experience with construction and inexpensive readout of Iarocci limited-streamer tubes. This technique, which was also addressed by Tzanakos (another expert from the same experiment), looked particularly promising for use in the extensive short-baseline calorimetric coverage. One of the main issues was cost; more tubes would be required per unit area of coverage than if use were made of conventional proportional wire chambers. Plans were formulated to continue the study of muon and electron detection at Breckenridge.

MEASURING STANDARD MODEL PARAMETERS:

A discussion of whether short-baseline experiments could be used to measure interesting electroweak parameters was made in a joint session of oscillation and electroweak groups. As these experiments could see short distance decays, they could also study charm production. As the production of anti-charm is a significant oscillation background, such studies would be required even if there were no additional benefits. Brock stressed that the "slow rescaling" of charm production was a limiting systematic error in extracting $\sin^2(\theta_W)$ from data on deep inelastic scattering of neutrinos. This parameter is related to the ratio of total neutral (NC) to charged-current (CC) processes. The simple parton model used to describe the data assumes that all quarks are massless, whereas the charm quark, being heavy, has a reduced CC production cross section at present day energies. The measured (NC/CC) ratio therefore is too large and must be decreased. Unfortunately, the onset of charm production as E_ν rises above threshhold is not well understood, and this uncertainty causes a systematic error which may be represented by the size of errors in the charm quark mass M_c used to characterize threshhold behavior. It appeared that present errors of $\pm$ 0.4 GeV/c^2 could be reduced by more than a factor of five in the proposed oscillation effort.

Other areas of interest include studies both of the Kobayashi-Maskawa matrix element V_{cd} and of the magnitude and shape of the strange sea. Present studies take advantage of the fact that production of charm from valence quarks is Cabibbo suppressed. Thus, production of charm by neutrinos at high energies is almost equally divided between valence and sea quarks, while anti-charm production by

antineutrinos is only from sea quarks. It is assumed that opposite-sign dimuons occur via CC reactions in which a charm particle is produced and subsequently undergoes a muonic decay. The types of charm particles produced and their muonic branching ratios are used as inputs to a rather complicated procedure in which the shape of charm "slow rescaling," the strange sea shape, magnitude and evolution with Q^2 and the Kobayashi-Maskawa matrix element V_{cd} are extracted in a highly correlated fashion. W. Marciano presented the following simplified quark model of deep inelastic scattering for purposes of discussion:

$$\frac{d\sigma(\nu \rightarrow charm)}{dxdy} = \frac{G_F^2 MEx}{\pi}\left([u(\xi) + d(\xi)] \mid V_{cd} \mid^2 + 2s(\xi) \mid V_{cs} \mid^2\right)$$

where $\xi = x + M_c^2/2M\nu$, x is the usual Feynmann variable, $\nu = E_{had}/e_\nu$ and M_c is the previously-mentioned charm quark mass. "Slow rescaling" is given by using ξ rather than x in the quark distributions. "u" and "d" are mixtures of valence and sea quark distributions, while "s" represents the strange sea. Simply put, charm production must occur at a larger x because of the heavy charm-quark mass. Overall suppression of the cross-section by helicity factors was not taken into account in order to simplify the exposition and the factor of 2 multiplying the strange sea was derived from exact SU(3).

Since s(x) falls rapidly with increasing x, at the lower neutrino energies of the oscillation experiment the minimum x requirement for charm production would considerably reduce the magnitude of charm production by neutrinos from the strange sea. This in turn would make the KM matrix element V_{cd} both more prominent and less correlated with other fitting parameters. Also, slow rescaling in principle would be easier to study at low energies where the charm cross-section changes rapidly, though a caveat was expressed that the slow rescaling parameter M_c might be partially masked by the sharp threshhold energy requirement for producing charm mesons and baryons. (ed. comment - this caveat subsequently was shown not to be a problem). Brock discussed the possibility that a combined effort of new low and high energy neutrino experiments could reduce all systematic errors to the point where one possibly could approach the holy grail limit of a 1% measurement of $\sin^2(\theta_W)$. This truly is an exciting possibility.

In summary, the short Main Injector Workshop made the short-baseline $\nu_\mu \rightarrow \nu_\tau$ oscillation experiment seem almost a reality. The possibility of a measurement at the $2_\bullet \times 10^{-4}$ level was combined with discussions of a variety of cuts which might reduce background, experimental techniques by which such a measurement could be implemented, and with possibilities for precision measurements of electroweak parameters. Participants looked forward to the longer Breckenridge Workshop at which many of the issues raised in this Workshop could be addressed in more detail.

References

[1] The above statements are based on calculations and presentations to this conference by R. Brock, as well as a presentation to the short-baseline working group by B. Marciano.

[2] H. Harari, Phys. Lett. B216, 413 (1989).

[3] W. Marciano, rapporteur's talk at Conference on New Directions in Neutrino Physics, Fermilab, (1988).

[4] L. Wolfenstein, Phys. Rev. D17, 2369 (1978).

[5] S. P. Mikheyev and A. Yu. Smirnov, Sov. J. Nucl. Phys. 42, 913 (1985).

[6] N. Ushida, *et al.*, Phys. Rev. Lett. 57, 2897 (1986).

[7] F. Dydak, *et al.*, Phys. Lett. **134B**, 281 (1984).

[8] Future Options for Fermilab Fixed Target Beams, p. 65.

[9] P803 oscillation collaborators plan to make a re-measurement of kink backgrounds during early 1990 in an exposure to a pion beam at KEK.

[10] A. Gauthier, Ph.D. thesis, The Ohio State University, 84 (1987). Results were corrected slightly to include better estimates of the contribution from quasi-elastic scattering.

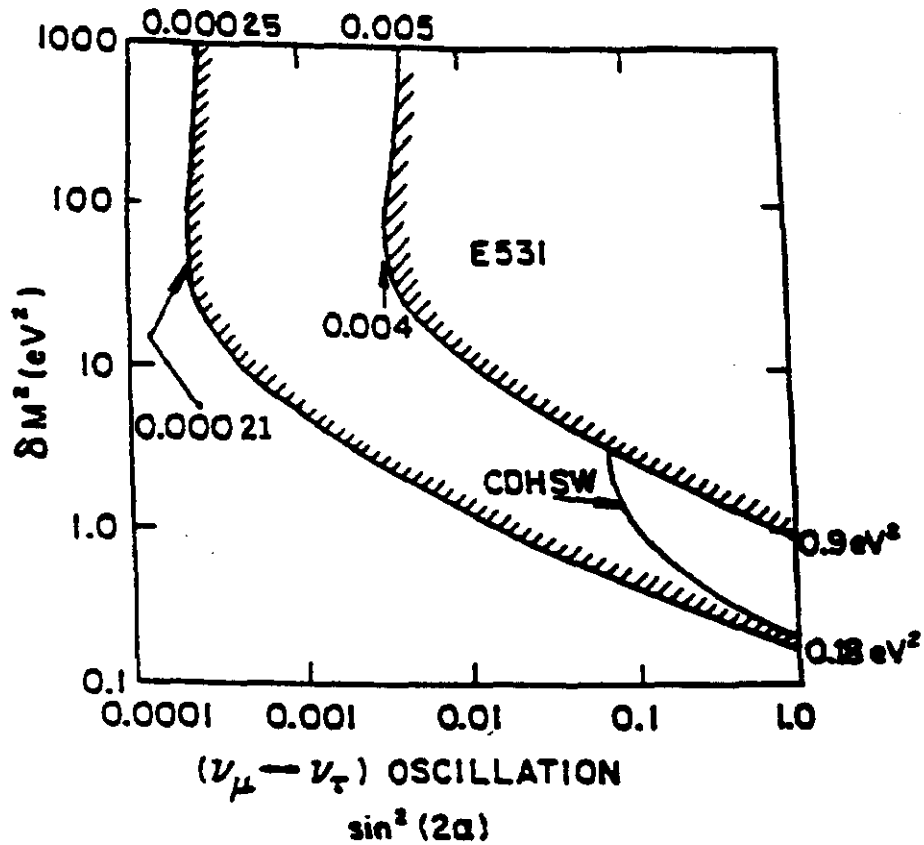

FIGURE 1: δM^2 versus $\sin^2(2\alpha)$ plane showing the previous limits for $\nu_\mu \rightarrow \nu_\tau$ oscillation superposed on improved limits which could be obtained from the new experiment. The regions to the right of the appropriate curves are excluded at the 90% confidence level.

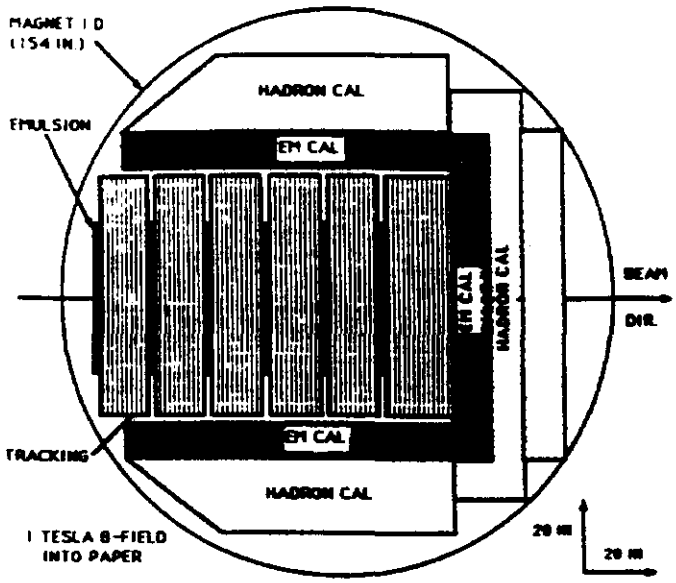

SCINTILLATOR COUNTERS DOWNSTREAM OF ALL EMULSION MODULES AND IN ALL CALORIMETERS NOT SHOWN. MOST MUONS IDENTIFIED BY RANGE AND P.H. IN THE CALORIMETERS. RANGE WALL DOWNSTREAM OF COILS FOR CENTRAL HIGH-ENERGY MUONS NOT SHOWN.

NEUTRINO OSCILLATION EXPERIMENT
PLAN VIEW

FIGURE 2a

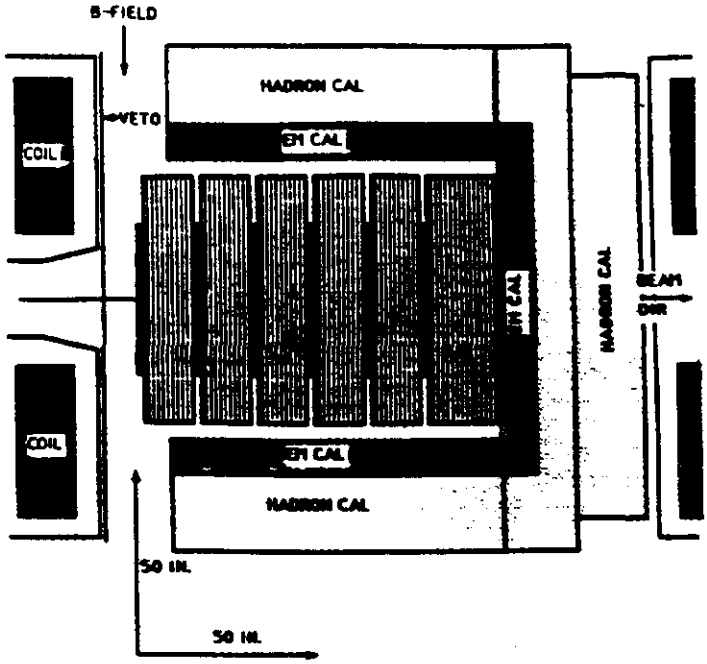

NEUTRINO OSCILLATION EXPERIMENT
ELEVATION VIEW

FIGURE 2b

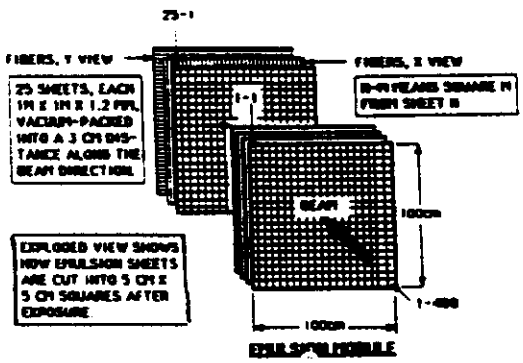

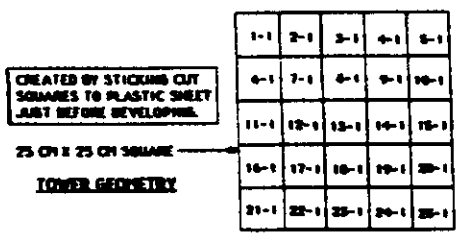

EMULSION PLUS SCINT. FIBER MODULE

FIGURE 2c

FIGURE 2: a) Plan view of experiment; b) Elevation view of layout of experiment; c) Detail of emulsion and scintillating fibers which indicates how tower geometry will be created in order to speed scanning.

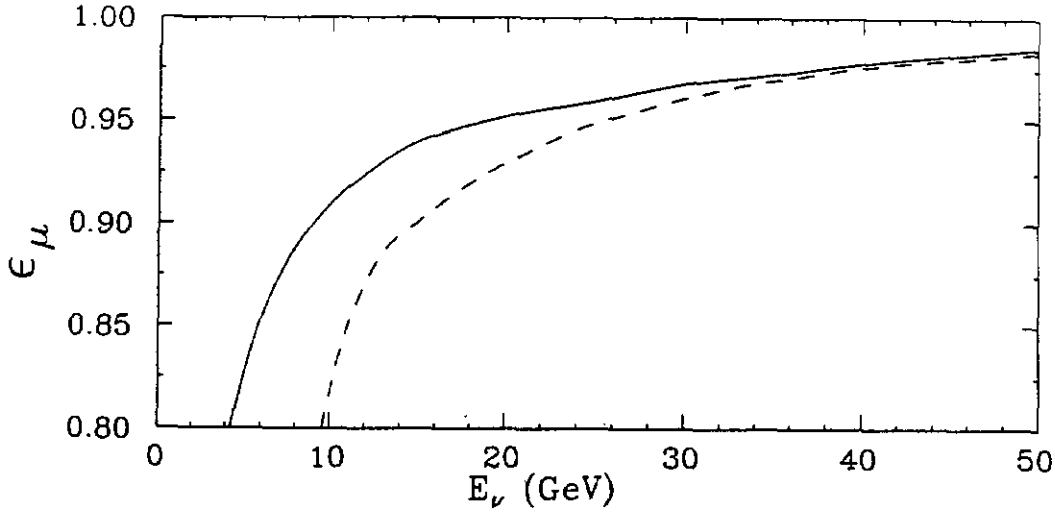

FIGURE 3: Average muon detection efficiency as a function of neutrino energy for μ^- from all charged current events (solid), and for μ^+ from anticharm production by antineutrinos (dashed); note the suppressed zero.

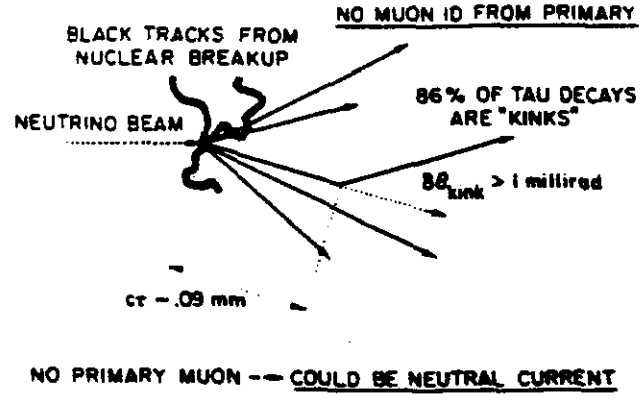

FIGURE 4: Schematic picture of a ν_τ interaction. Note the heavily-ionizing tracks from nuclear breakup, the absence of an identified muon from the interaction vertex and a short decay-length "kink" with a large P_T.

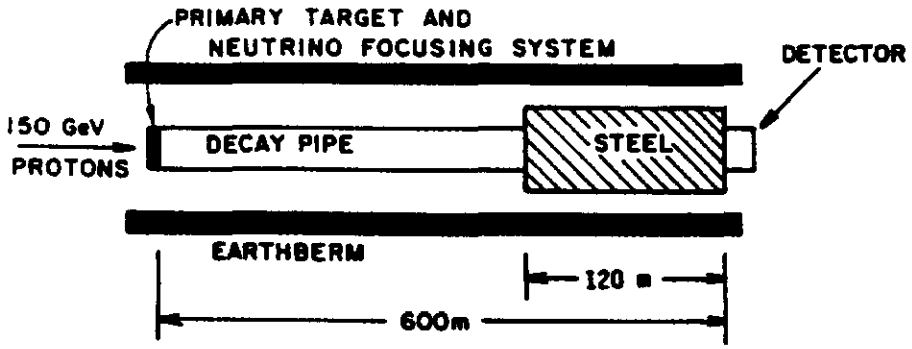

FIGURE 5: Layout of proposed neutrino beam line showing the location of the proposed oscillation experiment.

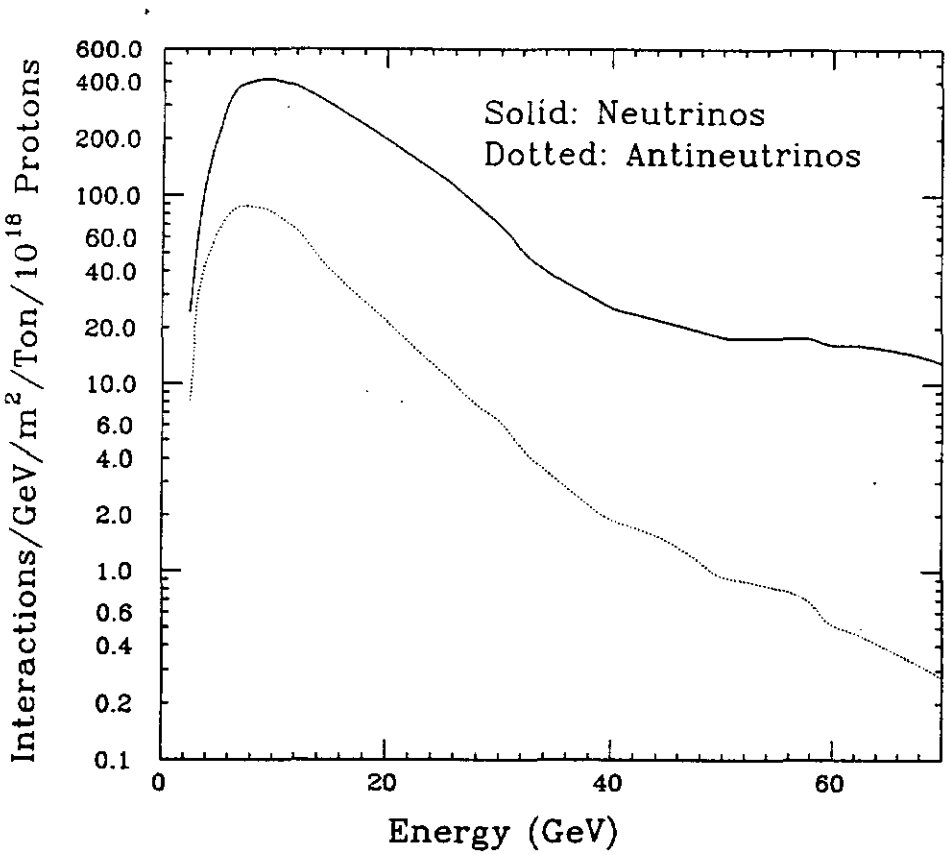

FIGURE 6: Charged-current event rate for the 150 GeV high-flux neutrino (solid line) and antineutrino (dased line) beams. The calculations assume a 400 meter decay pipe, 120 meter shield and a double-horn focusing system.

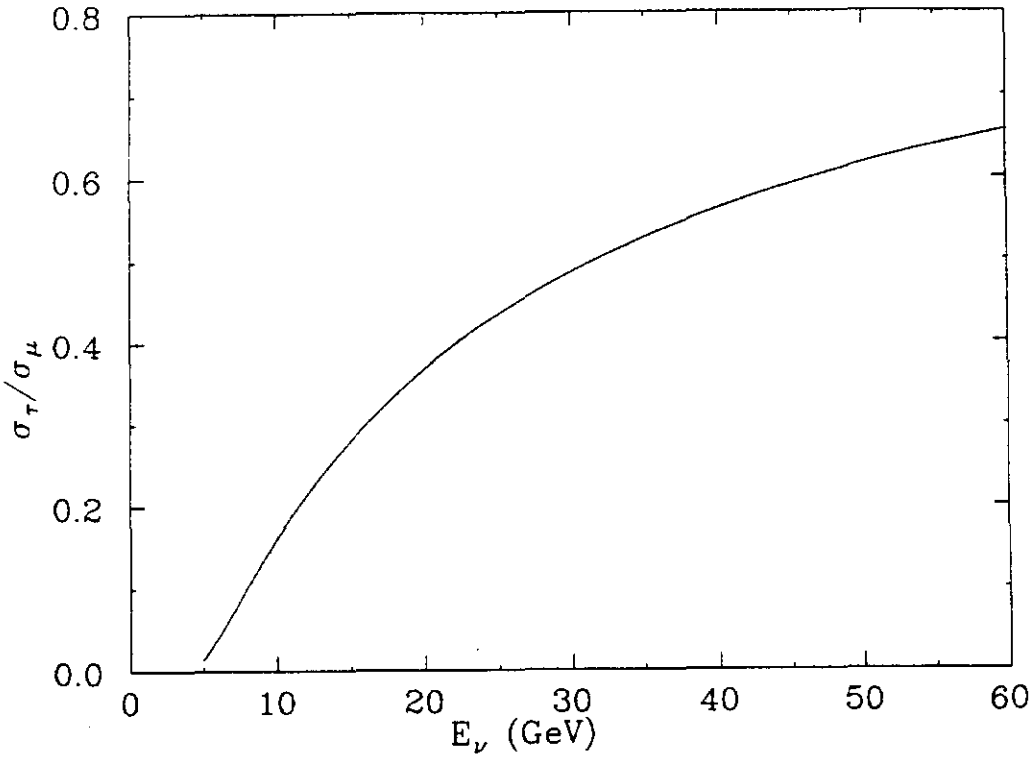

FIGURE 7: The ratio of ν_τ/ν_μ cross-sections displayed as a function of incident neutrino energy. These curves have been corrected for the contributions of quasi-elastic and Δ^{++} production processes.

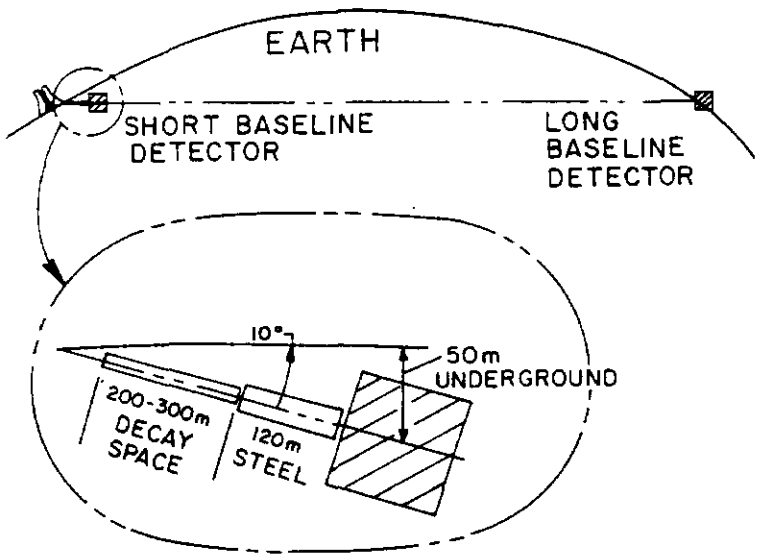

FIGURE 8: A schematic view of various suggested very-long-baseline oscillation experiments showing the large size of the dip angle due to the curvature of the earth.

Summary of Working Group on Electroweak Tests and Structure Functions with Neutrinos at the Main Injector

R. Bernstein
Fermi National Accelerator Laboratory

Participants: R. Bernstein, R. Brock, W. Marciano, N.W. Reay, L. Stutte

The Main Injector will be the most intense high-energy neutrino source ever constructed: more than forty times the number of $\nu_\mu N$ and an order-of-magnitude increase in the number of $\nu_\mu e$ scatters compared to previous Tevatron runs are available for typical runs and detectors.[1] This Working Group focused on the possibilities for a precise measurement of $\sin^2\theta_W$ in two different ways: first, through $\nu_\mu e$ scattering and second, through an emulsion experiment, designed to search for $\nu_\mu \rightarrow \nu_\tau$ oscillations. The second choice could address the slow-rescaling issue and possibly perform its own precise measurement of $\sin^2\theta_W$.

Improved measurements of $\sin^2\theta_W$ are central for an improved understanding of the Standard Model and for any search for physics beyond it. Determinations of $\sin^2\theta_W$ through the defining relation $\sin^2\theta_W = 1 - M_W^2/M_Z^2$ will be the most precise; however, as pointed out by many authors[2], comparisons of $\sin^2\theta_W$ measured in different processes provide valuable information: the values obtained may be compared and requiring consistency both searches for and sets limits on new physics.

One important channel for measuring $\sin^2\theta_W$ is $\nu_\mu e$ scattering through a determination of $\sigma(\bar{\nu}_\mu e)/\sigma(\nu_\mu e)$. The CHARM II experiment [3] is expected to have errors of ± 0.005. This measurement will be limited by flux normalization and any significant improvement will be difficult. A different method of studying the process is to study the y-distribution ($y = T_e/E_\nu$):

$$\frac{d\sigma}{dy} = \rho^2 \frac{{G_F}^2 m_e E_\nu}{2\pi}\left[(g_V \pm g_A)^2 + (g_V \mp g_A)^2(1-y)^2 + O(\frac{m_e}{E_\nu})\right] \qquad (1)$$

where the upper(lower) signs refer to ν_μ ($\bar{\nu}_\mu$) scattering. This approach was used in BNL-734 [4]which has published $\sin^2\theta_W = 0.195 \pm 0.018 \pm 0.013$ based on 250 events. The copious neutrino flux of the Main Injector makes it possible to envisage a dichromatic run with 1000 events for a 300 ton detector in one six-month run; here one could use the properties of the

dichromatic beam to determine y instead of measuring $\theta_e^2 \propto (1-y)$. Such a sample could determine $\sin^2\theta_W$ to $\pm 2\%$.[5]

FNAL P-803 [6] proposes to study $\nu_\mu \rightarrow \nu_\tau$ oscillations using an emulsion target. The emulsion technique was originally designed to study charm-production and lifetimes; its superior vertex resolution and tracking capabilities will be used in the oscillation experiment to search for τ-decay. The Working Group explored the possibility of using the charm-detection capabilities of such a detector to attack a significant uncertainty that has plagued old deep-inelastic scattering measurements: charm-production from d, s quarks in the nucleon. The determination of $\sin^2\theta_W$ from[7]

$$R_\nu = \frac{\sigma(\nu_\mu, NC)}{\sigma(\nu_\mu, CC)} = \rho^2\left[\frac{1}{2} - \sin^2\theta_W + \frac{5}{9}\sin^4\theta_W(1+r)\right] \qquad (2)$$

($r = \sigma(\bar{\nu}_\mu, CC)/\sigma(\nu_\mu, CC)$) is affected because the charged-current denominator has a contribution of $\approx 7\%$ from charm-production ($E_\nu > 30GeV$) while the neutral-current denominator is free of this flavor-changing process. The calculation of the rate is difficult because of the heavy charmed quark; we must include the effect of its mass, and neither the mass to be used nor the method of inclusion is clear. "Slow-rescaling," which makes the substitution $x \rightarrow x(1 - m_c^2/Q^2)$, has been used in the past, where m_c is a parameter in the model. The standard choice [2] $m_c = 1.5 \pm 0.3$ leads to an error of ± 0.0041 on $\sin^2\theta_W$. However, there is little experimental evidence to support this choice: the best data come from opposite-sign dimuon production from neutrinos, which involves the same process, and the best measurement comes from CCFR[8]: $m_c = 1.3 \pm 0.6$ which would effectively double the slow-rescaling error and yield a total error[9] of ± 0.01 instead of the ± 0.0066 quoted in [2]. These larger errors would radically change quoted limits on the top-quark mass (through a comparison of $\sin^2\theta_W$ measured in deep-inelastic scattering to the collider determinations) and greatly weaken any checks that can be made. Hence any method of attacking this problem could be of great use. The emulsion method, which can detect charm states, could measure the charm-production cross-section *vs.* E_ν and possibly pin down the m_c parameter as well as check the slow-rescaling *ansatz*. Brock and Marciano have estimated that a determination at 10 GeV could be performed to $\pm 0.1 GeV/c^2$. The difficulty arises in extrapolating from the Main Injector energies to those of old deep-inelastic experiments whch are typically a factor of six higher. This method has considerable potential, however, and more study is underway.

The idea of determining $\sin^2\theta_W$ within the emulsion experiment was also addressed. Here, charm-production is not a significant problem (the cross-section is much smaller because of the threshold for charm-production). However, other difficulties present themselves: punchthrough in neutral-current showers could fake charged-current events, mixing the numerator and denominator of R_ν. There are also a variety of errors in any R_ν measurement which contributed approximately $\delta(\sin^2\theta_W) \pm 0.004$ to old high-energy measurements, such as the quark-to-antiquark content of the nucleon, higher-twist, and other QCD effects. These

effects must be carefully evaluated at the neutrino energies and Q^2 of the Main Injector before errors are quoted but the idea is certainly promising and will be pursued. As part of these studies, the idea of determining V_{cd} through a measurement of D^o-production normalized to all charged-current events will be examined; the ratio is proportional to V_{cd}^2 times a branching-ratio times a slow-rescaling turn-on.

One fascinating possibility is a dedicated facility which sees both Main Injector and Tevatron beams. Such a facility would have an enormous reach in x and Q^2 and statistics of several million events. Brock has pointed out that different targets could be used in different runs in order to map out the A-dependences. Such a program would include studies of Λ_{QCD} and higher-twist effects, both of which are of considerable and obvious interest. The importance of such a systematic study of structure functions was stressed last year at Snowmass[10] and this subject will be pursued at Breckenridge.

A Tagged-Neutrino Beam[11] has been studied at the Tevatron; the experiment would produce ν_μ, ν_e, and their antiparticles through the decays of the K_L. A tagging spectrometer would determine the neutrino species event by event by detecting the associated hadron and lepton. Such an experiment could determine $\sin^2\theta_W$ to ± 0.004 or less in a manner largely free of slow-rescaling errors and other QCD effects. The experiment requires the fixed-target flux increase from the Main Injector to be viable. For this Working Group, it was determined that the statistics at a low-energy version, with 150 GeV protons, were insufficient: we could expect $2000(\nu_\mu + \bar{\nu}_\mu)/10^{20} pot/kTon$ in a tagged configuration. If we relaxed the requirements of a tagger the rate would go up by at most a factor of eight.

In conclusion, there is considerable promise in $\nu_\mu e$ scattering and emulsion techniques to study $\sin^2\theta_W$ with high-intensity neutrino beams at the Main Injector. The data may both improve old measurements and provide new ones of considerable precision. The idea of a dedicated neutrino facility which would study structure functions and their A-dependence over an enormous energy range is of great importance and must be carefully studied.

References

[1] R. Brock, this Conference.

[2] U. Amaldi *et al.*, Phys. Rev. D36(1987) .1385 and references therein.

[3] K. DeWinter *et al.*, NIM A278(1989) 670.

[4] K. Abe *et al.*, Phys. Rev. Lett. 62(1989) 1709.

[5] K. Abe, F. Taylor, and D.H. White, BNL-32247 (microfiche), submitted to Snowmass Summer Study 1982: 165.

[6] N. W. Reay, this Conference.

[7] J.E. Kim *et al.*, Rev. Mod. Phys. 53(1981) 211.

[8] C. Foudas *et al.*, submitted to Phys. Rev. Lett.

[9] A detailed study of the errors in Deep-Inelastic Determinations of $\sin^2\theta_W$ is R. Brock, "Deep-Inelastic Determinations of $\sin^2\theta_W$," Talk Presented at New Directions in Neutrino Physics at Fermilab, September 1988.

[10] Wu-Ki Tung *et al.*, Snowmass 1988, FNAL-CONF-89/26.

[11] R. Bernstein, Neutrino Physics in a Tagged-Neutrino Beam, FNAL-CONF 89/34 and "A New Method of Determining $\sin^2\theta_W$ in Deep-Inelastic $\nu_\mu N$ Scattering," Talk Presented at XII International Workshop on Weak Interactions and Neutrinos, Ginosar, Israel.

Experiments with Antiprotons
Summary of the Working Group's Activities

Petros A. Rapidis
Fermilab

Our group[1] did not consider only experiments that are feasible with the present Antiproton Source at Fermilab. We also examined the possibilities that are opened by the increased antiproton production rate when the Main Injector becomes operational, as well as experiments that may involve new machines, or modifications to the existing or proposed accelerators. We viewed our discussions as a preparation for a more serious consideration, to take place in the Workshop on Physics at Fermilab in the 1990's to be held at Breckenridge, Colorado in August.

Most of the physics issues are discussed in G. Smith's contribution to this conference[2]; as a result I will focus my remarks on the more technical issues that were raised:

Charmonium Production in $p\bar{p}$ Collisions and Related Topics

There was consensus that this rich field of physics can be adequately studied in the Accumulator with the E760 apparatus[3] and its internal hydrogen gas jet target. Extensions to the E760 program, e.g. the search for states that decay to $\phi\phi$ (glueball search), or for bound states of hadrons[4]

(cryptoexotics), have already been considered. The limitation will be the lowest momentum that antiprotons can be decelerated to in the Antiproton Accumulator. It is expected that this lowest momentum will be less than 2 GeV/c, thus the available mass range starts from a value less than 2.4 GeV/c^2 and extends to 4.3 GeV/c^2.

Charmed Baryon Production

The exclusive production of charmed baryon-antibaryon pairs in proton-antiproton collisions was proposed as a clean way to study these elusive states. There are two alternative ways to do this : either by installing in the Main Injector an extraction channel for antiprotons with energies in the range of 10 to 25 GeV (note that such an extraction line has to point 'backwards' in relation to a proton extraction line) or by installing an internal gas jet target in the Main Injector.

In the former case, one could extract antiprotons at the same time that the fixed target program, that uses protons from the Main Injector, is running. This implies an interleaved version of running, with a portion of the protons of the Main Injector being used for antiproton production, as well as periodic exclusive use of the Main Injector for antiproton acceleration and extraction. Such a scenario would mean a reduction of approximately 50% in the intensity of the protons available from the Main Injector for fixed target running.

In the latter case, one should at least make allowances for :

i. *Good vacuum.* With the proper practices a vacuum of the order of 5×10^{-9} Torr or better can achieved. This assumes a clean and pre-baked vacuum chamber but not one that can be baked in situ.

ii. *A modest stochastic cooling system:* a betatron cooling system will counteract the transverse emitance blowup caused by Coulomb scattering in the gas jet.

iii. *Long straight sections - interaction region.* A charmed baryon experiment has a size similar to experiments at the Brookhaven AGS, i.e. 15 meters long. If one wants to consider the possibility of studying bottomonium production[5] then the apparatus will be some 30 meters long ('Serpukhov' size). The currently envisioned long straight sections (26 meters long) do not seem adequate for such a use.

If one takes into account the fact that the use of the Main Injector as a storage ring with an internal gas target implies the exclusive use of that machine for the duration of such an experiment, one sees that this choice is problematical. Nevertheless the lessons of the Main Ring tunnel and of the Accumulator, i.e. that both machines had to accommodate interaction regions that were not part of their original design, point to the prudence of allowing for such interaction areas ahead of time.

CP Violation in Hyperon-Antihyperon Pair Production and Low Energy Antiproton Physics

Both of these rather different areas share a common characteristic, that is they need a new low energy antiproton machine to be carried out. In

particular the CP Violation experiment involves the detection of $\Lambda\bar{\Lambda}$ through the decay $\Lambda \rightarrow p\,\pi$. This decay sequence is identified by reconstructing the decay vertex. A small beam pipe (diameter of the order of a centimeter) would be ideal.

Even though, no one from our group was an atomic physicist, we recognized that experiments with extremely low energy antiprotons (e.g. gravitational properties of antiprotons, precision atomic spectroscopy with antihydrogen) may be very interesting. A design effort for an RFQ deceleration system, to bring antiprotons down to an energy of a few KeV, was initiated [6].

Polarized Antiprotons

The Spin Splitter Collaboration has been studying the possibility of polarizing the antiprotons circulating in a storage ring[7]. The question of whether a polarizing apparatus could be incorporated in an antiproton storage ring at Fermilab was addressed by Y. Onel and S. Hsueh [8]. A detailed study to incorporate such a scheme in the Accumulator is under way.

Conclusions

Antiproton physics has an inter-disciplinary flavor that goes beyond the realm of the usual high energy physics regime. It was the feeling within our working group that if sufficiently interesting experiments can be proposed, then a new opportunity will exist at Fermilab. We look forward to Breckenridge, where we hope that the discussions will lead to detailed and concrete proposals for experiments.

References

1 P. Ferreti-Dalpiaz (INFN Ferrara), D. Hertzog (U of Illinois, Champaign), E. Menichetti (INFN Torino), A. Nathan (U of Illinois, Champaign), D. Peaslee (U of Maryland), P. Rapidis (Fermilab), J. Rosen (Northwestern U), and G. Smith (Penn. State U). S. Hsueh (Fermilab), F. Mills (Fermilab), and Y. Onel (Iowa State U) also participated in part of the discussions.

2 G. Smith, *Antiproton Physics up to 120 GeV,* this conference.

3 Fermilab Proposal No. 760, *A Proposal to Investigate the Formation of Charmonium States Using the Antiproton Accumulator Ring,* Fermilab-Ferrara-Genova-Irvine-Northwestern-Penn State-Torino Collaboration, approved December 1985.

4 J. Rosen, *Heavy Hadronic Molecules*, AIP Conf. Proc. No. 185, ed. S.U. Chung, p. 611.

5 We expect that $\sigma(p\bar{p} \rightarrow \Upsilon) / \sigma(p\bar{p} \rightarrow \psi) \cong (m_\psi / m_\Upsilon)^8 \cong 10^{-4}$. Since E760 with a luminosity of 10^{32} $cm^{-2}s^{-1}$ expects a few 10^4 events, it seems unlikely that a bottomonium experiment will succeed. In any case, the required beam momentum is 68 GeV/c; the design for the Main Injector allows for a maximum momentum of 75 GeV/c for continuous operation.

6 P. Zhou and F. Mills, *RFQ for Decelerating Anti-Proton Beams*, Fermilab, unpublished, to be presented in the Workshop on Physics at Fermilab in the 1990's at Breckenridge, Colorado, 1989.

7 H. Kreiser, Y. Onel, et al., *Polarized Antiprotons with the Spin Splitter*, in Proceedings of the European Particle Accelerator Conference, Rome, June 7-11, 1988, ed. by S. Tazzari, Vol. 2, p. 848, World Scientific, Singapore 1989.

8 S. Y. Hsueh, *A Second Solenoid*, Fermilab, unpublished, October 1988.

REPORT FROM THE POLARIZATION GROUP OF THE FERMILAB INJECTOR WORKSHOP‡

E. Berger, Argonne National Laboratory
G. Glass, Texas A&M University
K. Imai, University of Kyoto, Japan
L. Jones, University of Michigan
A. M. T. Lin, University of Michigan
S. R. Mane, Fermilab
A. Meschanin, Serpukhov, USSR
Y. Onel, University of Iowa
J. Roberts, Rice University
S. Hsueh, Fermilab
L. Teng, Fermilab
D. Underwood,* Argonne National Laboratory
A. Vasiliev, Serpukhov, USSR

20 July 1989

ABSTRACT

The group considered physics, accelerator, and polarized source issues. Most of the physics study was concerned with what significant and unique experiments could be done if polarized protons could be accelerated in the main injector and eventually in the Tevatron.

---

‡ Work supported in part by the U.S. Department of Energy, Division of High Energy Physics, Contract W-31-109-ENG-38.

* Reported by D. G. Underwood.

Physics Issues

One issue of great concern at present is the spin content of the proton. The EMC experiment with polarized muons and polarized proton target has shown that not all the spin of the proton is carried by quarks.[1] It is important to measure the angular momentum contribution from gluons, which could be as large as 5 units of angular momentum.[2-4] Experiments using polarized protons on polarized protons are the most direct way to learn about the gluon spin distribution.[2-5]

It is known from the EMC polarized muon experiment and the SLAC-Yale polarized electron experiment that at large x most of the spin of the proton is carried by the leading quark. We can use this leading quark as a color-charged and polarized probe to study the contributions of gluons at smaller x which have a big influence on the overall spin content of the proton. There may be partial cancellations of gluon spin contributions and orbital angular momentum of constituents. There may be significant contributions from strange quarks. In any case, we would like to directly measure the polarization of gluons as a function of x.

The way in which polarized protons can best be used to probe the gluon polarization varies with the energy. The use of the main injector beam at 120 GeV in a fixed target experiment could be problematical if we want to understand effects using low order QCD calculations. The optimum experiment here seems to be the creation of a J/ψ state through an intermediate χ state which is formed at Q^2 of about 10 GeV^2 from two gluons (Fig. 1). The spin projection states of the χ will be populated differently, depending on the polarization of the gluons.

With higher energy polarized beam accelerated through the Tevatron, one can do fixed target direct gamma experiments. The QCD Compton diagram (Fig.

2) provides one of the cleanest measurements of gluon polarization. If the away side jet (or a leading pion from the jet) is measured in addition to the gamma, we have the x dependence. At a given x the observed asymmetry is simply the product of the two quark and gluon polarizations and a QCD calculated scattering asymmetry, which is about 0.6.

With 1.8 TeV in the c.m. colliding polarized p on unpolarized $\bar{p}$, one has an extra handle on extracting physics signals of supersymmetry[6,7] or distinguishing left and right handed currents in W production.[6,7] A number of studies which were done on polarization physics at SSC are in an AIP conference proceedings.[6] Some of the more exciting physics, as mentioned above, might be more easily searched for at energies lower than the SSC, such as collider energy, due to the shrinkage of the parton distributions at high Q^2.

We also discussed possible experiments with ~ 100 GeV neutrons polarized by small angle scattering in a secondary beam, and plans to do single spin experiments with a polarized gas jet internal target at UNK at ~ 3 TeV.

Accelerator Issues

The primary reason for wanting to accelerate polarized beam rather than obtaining polarized beam in some other way is to get high intensity. The present 200 GeV polarized proton and polarized anti-proton beam at Fermilab operated at about 10^7 per 20 second spill during the last running period. This beam utilized the parity violating decay of Λ° and $\bar{\Lambda}^0$. The beam may be upgraded to 10^8/spill and 600 GeV. A similar beam, POLEX, proposed at UNK at Serpukhov may operate at 10^9/spill at 2.5 TeV, but this would require targeting 10^{14} primaries/spill.[8]

We see an opportunity for intensities of 10^{10} immediately and perhaps much more eventually by using the Fermilab main injector to accelerate beam from a polarized source.

Polarized protons have been accelerated at the Argonne ZGS, Brookhaven AGS, KEK PS, Los Alamos LAMPF, Saclay Saturne, TRIUMF, Indiana IUCF, etc. Unfortunately, the spin resonances are more difficult to manage at higher energies with the resonance jumping techniques. An elegant way to deal with these resonances by means of what are now called Siberian snakes was proposed in 1977.[9] A snake is a set of spin precession magnets, typically arranged to give 180° net precession but no net bend or displacement of the beam. This technique is highly developed in principle, if not in practice, especially with the recent advent of powerful tracking codes. In simplest form, the use of two snakes 180° apart gives a spin tune of 1/2 independent of energy. The first tests in an accelerator were begun during this Main Injector workshop at the Indiana IUCF.

Studies of particular relevance to the Main Injector an Tevatron are a Fermilab technical memo[10] by L. Teng, which may be included in these proceedings, and the papers presented at the Siberian Snake Workshop in conjunction with the VIII International Symposium on High Energy Spin Physics,[11] now published.

The simplest configuration would use two snakes on opposite sides of the ring (Fig. 3). One would be of type I with net precession axis along the beam (all fields perpendicular to the beam). The other would be of type II having net precession axis in a radial direction. We have an explicit example of a snake of each type which would be appropriate for the main injector in straight sections of 26 m long and 180° apart. These snakes would be made up of conventional magnets quite similar to the main injector dipoles,[12] having the same peak field at maximum energy, same size coil ends, etc. The apertures must be larger than the 5 cm M.I. dipoles, approximately 8 to 10

cm. One could make 16 magnets of the type I snake of one length and all 12 magnets of the type II snake of another length.

Below some energy such as 50 GeV these would be used as partial snakes and ramped with the machine to minimize the orbit bump. Above this energy they would be full (180°) snakes at constant field.

If there are not two straight sections exactly 180° apart in the injector, then snakes which are not pure type I or type II must be used. Solutions to this problem have been found by G. Steffan,[6] and we have computer programs to search for snake solutions given particular requirements.

One would want to measure the polarization after each type of accelerator, linac, booster, main injector, etc. Three new polarimeters for high energy were developed for the present Fermilab polarized beam in Experiments 581/704.[2,4] Their performance is essentially energy independent as shown in Fig. 4.

One of our primary motivations for wanting to accelerate polarized beam in the main injector is to get higher intensity than secondary beams. However, existing polarized proton sources for accelerators cannot provide as much intensity as unpolarized sources. Typical polarized sources at BNL-AGS, KEK-PS, and LAMPF can provide about 10 micro-amps of H^-. Given the time structure of acceleration cycles, this leads to about 3×10^{10}/second at high energy. Many improvements are underway. There is a new source being installed at LAMPF. Investigations are being done at BNL and elsewhere on ultra-cold storage of polarized protons. A Russian prototype source may provide two milliamps of H^+ in pulsed mode.

It seems prudent at present to investigate time sharing of the main injector. One possibility would be to put polarized beam in one or two of the six booster fills needed to fill the main injector. This would avoid long

time delays between extractions of polarized beam and would not seriously affect the average intensity.

Many issues remain to be studied. It is possible that spin correction magnets might be required in transfer lines. For example, from linac to booster, from booster to main injector, from injector to Tevatron, and from Tevatron to experiments. This is because these lines have both vertical and horizontal bends intermixed with quadrupoles. The extreme symmetry of the existing polarized beamline would probably not be required because the accelerated beam has much smaller phase space.

We need to find a computer tracking code to study these issues quickly and flexibly. One possibility is a version of DECAY TURTLE with spin tracking for dipoles and quadrupoles (non-linear). We have used various versions of this for many years. One problem is the specification of the beam phase space as a source for the program. It has also been suggested that CINCH be used.

Summary

One of the big assets of Fermilab is the experience of various groups in developing techniques for physics experiments such as di-muon, di-hadron, direct photon, jets, charm decays, etc. All of these are important in exploring the spin degrees of freedom. In many cases, the experimental set-ups exist. It seems sensible therefore to extract polarized beam, both at 120 GeV from the main injector and at 800 + GeV from the Tevatron, to existing beamlines. Perhaps eventually polarized protons will also prove useful in collider experiments.

Fermilab is in a unique position to do measurements of gluon spin distributions and QCD checks by using polarized protons at high energy.

1) The straight sections in the injector open up the possibility of using snakes which are needed to accelerate polarized beam to high energy.
2) At 120 GeV we could do physics and prove the principles of snakes for Tevatron, HERA, SSC, ...
3) Polarized beam at higher intensity than the MP beam would extend the range of experiments now planned for E-704, E-678, ...
4) We can now consider polarized proton experiments at 120 GeV, Tevatron fixed target, and Collider.

We thank Fermilab and the organizers of the Main Injector Workshop for providing the opportunity for our discussions and for their hospitality.

REFERENCES

1) J. Ashman et al., (European Muon Collaboration), Phys. Lett. B206, 364 (1988).

2) VIII Int. Symposium on High Energy Spin Physics, AIP Conf. Proc. 187, Particles and Fields 37, (1989).

3) Probing Gluon Polarization in Hadronic Direct Photon Production, E. Berger and J. Qiu, ANL-HEP-PR-88-64.

4) Proceedings of the Symposium on Future Polarization Physics at Fermilab, June 1988.

5) Single-Spin Production Asymmetry from the Hard Scattering of Pointlike Constituents, D. Sivers, ANL-HEP-PR-89-32.

6) Polarized Beams at SSC, AIP Conference Proceedings No. 145, Particles and Fields 34 (1985).

7) Spin Physics at Short Distances, Craigie, Hidaka, Jacob, and Fernard, Phys. Rep. 99 (1983).

8) POLEX Proposal, Serpukhov

9) Ya. S. Derbenev and A. M. Kondratenko, 10th Int. Conf. on High Energy Accelerators, Vol. 2, 70 (Protvino 1977); Ya. S. Derbenev et al. Particle Accel. 8, 115 (1978).

10) Polarized Beams in Tevatron, L. Teng FNAL-TM-1559-Revised

11) Workshop on Snakes and Accelerated Polarized Beams, AIP Conf. Proc. 187, Particles and Fields 37, (1989).

12) Conceptual Design Report, Fermilab Upgrade: Main Injector

FIGURE CAPTIONS

Figure 1 — J/ψ production from two gluons with an intermediate χ state. The asymmetry using longitudinally polarized beam and target would be dominated by the polarization of gluons of $x \approx .2$. Constraints on helicities by intermediate states would give a mass dependent asymmetry. This would be useful at 120 GeV or 800 GeV.

Figure 2 — The QCD Compton diagram. Direct γ experiments with polarized beam and polarized target provide a clean way to measure the gluon spin distribution (polarized structure functions) of the proton.

Figure 3 — Schematic of the proposed main injector ring. There are six straight sections of 26 meters, two of these approximately 180° apart could be used for the two Siberian snakes.

Figure 4 — Polarimeters for high energy have been developed and tested in E-581/704.

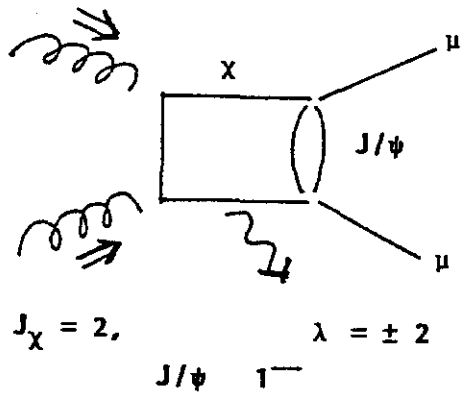

Figure 1

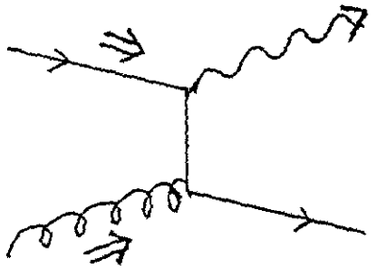

$$A_{LL} = \Delta G \quad \Delta Q \quad \hat{A}_{LL}$$

Figure 2

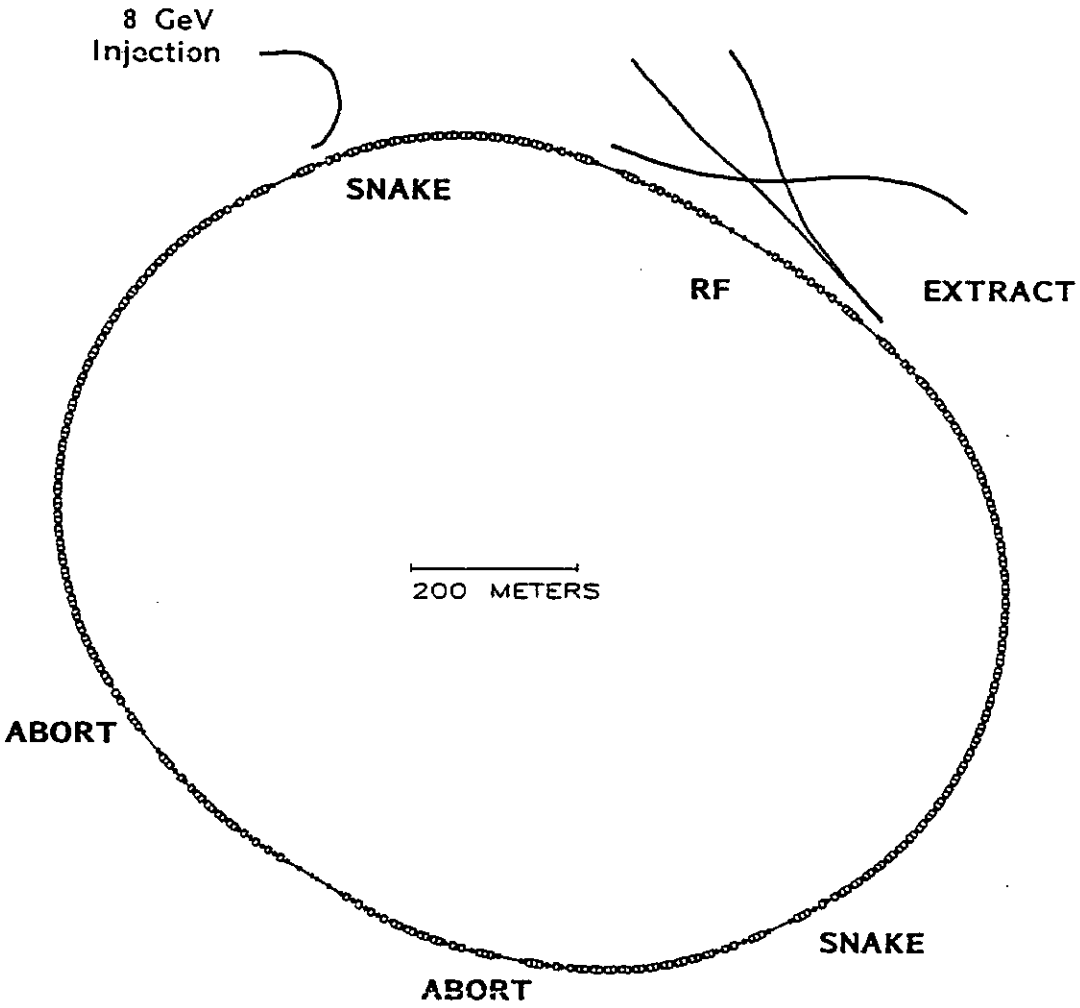
8 GeV
Injection
SNAKE
RF
EXTRACT
200 METERS
ABORT
SNAKE
ABORT

Figure 3

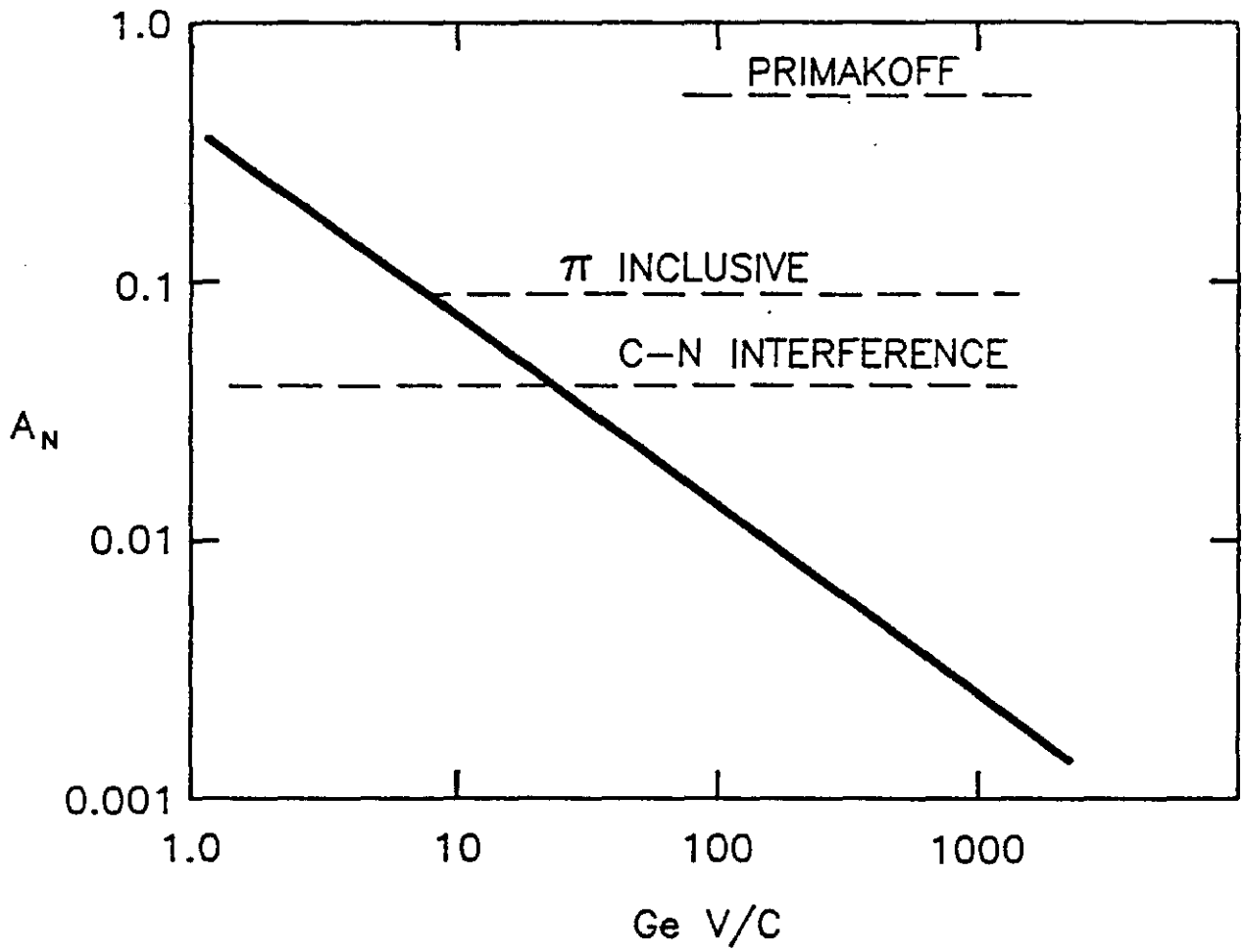
1.0
0.1
0.01
0.001
A_N
PRIMAKOFF
π INCLUSIVE
C—N INTERFERENCE
1.0
10
100
1000
Ge V/C

Figure 4

III.
Contributed Papers

Neutrino Oscillation Experiment In DUMAND II employing a Neutrino Beam from the Fermilab 150 GeV Injector

John G. Learned and Vincent Z. Peterson
Department of Physics and Astronomy
University of Hawaii

for the
DUMAND Collaboration

abstract

It is proposed that a unique neutrino oscillation experiment can be performed employing a new neutrino beam produced by the proposed 150 GeV main injector at Fermilab. DUMAND II, planned for full operation by summer 1993, could observe of the order of 2200 events in a 6 months run. Both contained events (300 NC and CC) and throughgoing muons (1900) would be observed. The contained events give a beam normalization check, while the muon rate would be sensitive to muon neutrino disappearance. The L/E range is unchallenged (6000km/20GeV), and is sensitive to δm^2 down to about 0.001 eV^2. This encompasses possible oscillations from ν_μ to ν_τ, as suggested from recent underground experiments, and from flipped SU(5) models. Such oscillations would result in easily detected deficits of muons (50% of expected flux). It may be possible to discriminate between oscillation to ν_τ versus oscillation to ν_e via the ratio of throughgoing muons to contained events, versus energy.

11 July 1989
HDC-5-89

submitted to the Proceedings of the Workshop on
Physics at the Main Injector
Fermilab, 18 May 1989

Introduction

The idea of using neutrino beams from accelerators to search for neutrino oscillations is not at all new, having been around for 20 years or so, but has recently received renewed interest. One major source of this interest is due to the reported deficit of low energy neutrinos in underground experiments designed to study proton decay. The deficit occurs most prominently in the ratio of μ/e events in the published Kamiokande data[1] in the range of 200 – 700 MeV. This was interpreted in Ref. 2 as possibly due to muon neutrinos oscillating to tau neutrinos, with essentially full mixing and a δm^2 in the range of 0.03 – 0.4 eV^2. The suggestion is bolstered by deficits in both the IMB data and Frejus data (see references in Ref 2) which, while not statistically significant in themselves, do all show less muon events than expected. On the other hand, all these data involve the comparison of the μ/e ratio observed to that calculated, which leaves the concern that the dicrepancy might be simply a problem in calculating the neutrino fluxes and interaction rates.

Further interest in this range of oscillations comes from theory, however, in the flipped SU(5) model of Nanopoulos et al.[3], which yields masses in exactly this range. One need hardly take more space pointing out the physics value of such measurements.

It is quite difficult to probe the range around δm^2 of 0.001– 0.1 eV^2. In terms of distance divided by energy, the oscillations depend upon $\sin^2(1.27(\delta m/eV)^2(L/km)/(E/GeV))$, and the value of L/E suggested by the Kamiokande data is > 24 km/GeV. One sees that on-site accelerator experiments are not practical, while long distance experiments have been limited by inadequate flux. As we shall see, the proposed injector can give a remarkably good signal in DUMAND at a distance of about 6000 km. With an effective beam energy peaking around 30 GeV, the $L/E \cong 200$ km/GeV to DUMAND gets into a new region of sensitivity, down to a $\delta m^2 = 0.001$ eV^2. This goes ten times further than the exploration possible with IMB or other relatively nearby detectors.

One may ask why this range cannot be explored with cosmic ray neutrino fluxes. The answer is that the underground and underwater experiments measuring muon flux versus zenith angle have difficulty exploring this range because of the problem of contamination of the event sample near the horizon by scattered or misfit downgoing muons. A second limitation is simply due to statistics (the total world collection of underground upcoming mucns from cosmic ray neutrinos is about 1000 events at present, from the entire lower hemisphere). DUMAND can in fact (uniquely) explore the near horizontal region in zenith angle [4], but the cosmic ray neutrino induced muon flux in the near horizontal direction is dominated by 100 GeV neutrinos, whereas with the accelerator beam we can explore a region with about 1/10 the mean of the cosmic ray neutrino energy. Moreover, as usual, having a beam of known energy spectrum, direction, and timing gives a much cleaner measurement than using the cosmic rays.

And, if an effect should be observed, it can be easily followed up by modifying beam conditions in order to resolve the oscillation parameters.

Experiment

The Fermilab NUADA program was employed to estimate the neutrino flux at IMB, in runs made by Linda Stutte. The results are shown in column 2 of Table I, showing the event rate per 2.5 GeV bin, scaled to the 2×10^6 ton contained event volume of DUMAND II. The run assumed a two horn configuration, 400 m decay tunnel and 150 GeV protons. We assume a beam of 3×10^{13} protons per pulse at a rep rate of 20 pulses per minute for 100 useful hours per week, over a 6 months run, and a flux of 70% of the program calculation. The NUADA program calculated interaction rate was also corrected for neutral current events and applies to the total visible energy (from Cherenkov radiating particles). While the assumption of a dedicated 6 month run is surely optimistic, dividing the beam 3 ways over the same period still leaves us with a healthy total of >700 events.

The beam from Fermilab (location 42° N, 88° W) would have to be pointed downwards, 29.5° below the horizon, 1.7° North of West to intersect the DUMAND site (19° N, 153° W). The Neutrinos would arrive, coming upwards at a zenith angle of 119.5°. This is close to the zenith angle for maximum effective area for DUMAND II (26,000 m^2), for muons of greater than 20 GeV. The distance from Fermilab to DUMAND II along a cord of the earth is 6283 km (59° along a great circle). The beam spot radius at DUMAND would be about 10 km from π decay and 80 km from K decay, at 20 GeV initial energy. The pointing precision of previous Fermilab beams has been less than 1/10 of the spot size. We thus anticipate no problem in targeting the DUMAND II detector, though care is certainly required.

Fermilab beam monitoring would employ traditional techniques, and could be accomplished to at least ±15%. A more precise monitoring would employ the ratio of throughgoing muons to contained events, as discussed below. Limitations due to systematic errors need study, but we estimate them to be similar to the statistical errors below.

We have not yet employed the Monte Carlo program to study the trigger threshold of DUMAND II for these relatively low energy contained interactions (the DUMAND design was optimized for through going muons). However, we estimate that sufficient light will be generated for high efficiency to be achieved for <50 GeV. Initially the importance of the detection of contained events is mainly as a beam monitor, giving a check that the surveying is correct and that flux calculations at least approximately accurate. A threshold of 50 GeV for contained events would yield, according to Table I, 300 events in a 6 month run, for roughly a 6% beam normalization (statistical). Note that the

contained events would include neutral current (NC) and charged current (CC) interactions, including those from τ's, if oscillations are significant.

For fast extraction, the background counting rate in DUMAND II drops by at least 10^3, and if one employs RF structure, perhaps much more. Since we expect a total of 3600 cosmic ray neutrino induced muons per year in DUMAND II from the entire lower hemisphere, the number coming from within 1^o of the direction of Fermilab, and within the few millisecond spill time (duty factor of order 10^{-3}), is completely negligible. The background for contained events from the Fermilab beam, for which we do not yet know the angular resolution, will be larger. The background due to cosmic ray neutrino interactions within DUMAND II will be small, but we must look at the background induced by cosmic ray muons.

The use of a common time reference from the Global Positioning System can give us relative times to the nanosecond level.

The physics would come from the measurement of the throughgoing muon rate, which is presented in Table I, in columns 4 and 5. Again, while we need to study the details with the Monte Carlo program, it is clear that since 20 GeV is needed for a muon to traverse DUMAND in the near horizontal direction, we can expect a signal at the level of 1900 events in the proposed run. Oscillations at the level suggested by the Kamioka data would manifest themselves in a 50% deficit in this number, which would be obvious after a run of only one week. The integral fluxes from Table I are plotted in Figure I.

If a deficit is seen in the muon rate, then we must seek to discriminate between the possibilities of oscillation to ν_e or ν_τ. DUMAND II would not have much chance to observe τ production directly, but would count τ events along with the other contained ν events (CC and NC). If the oscillation is to ν_τ, then not only will the the muon flux will be depleted, but the contained event rate will be somewhat depleted due to the reduced ν_τ crossection, especially at the lower energies (eg. 30% at 50 GeV). The other case, of oscillation to ν_e, would not suffer that deficit. Depending upon the value of δm^2, however, matter oscillations could complicate the situation. It remains to do detailed Monte Carlo studies of these different cases to determine the extent of the capability of DUMAND II to resolve the situation.

Conclusions

We have taken a quick look at the potential for detecting neutrinos from the proposed Fermilab 150 GeV injector in DUMAND II and find, remarkably, that the muon neutrino signal would be eminently

detectable. The experiment would cleanly probe a unique region in δm^2 a factor of >100 below present accelerator based limits, down to about 0.001 eV^2, and could cleanly detect the presence of oscillations causing muon neutrino disappearance.

If signals of oscillation are detected then various measures may be taken to discriminate between oscillation to electron or tau neutrinos, but more work is needed by the DUMAND Collaboration to determine the limits of sensitivity.

It may also be that the potential distance measurement (to about 1 m), via time of flight, may have interest for geodesy. Certainly the calibration of DUMAND II survey and event angle reconstruction would be of great use as well.

The biggest technical problems seem to be the cost of the 30 degree downward bend, and the decay pipe required to send neutrinos towards DUMAND. There may also be environmental concerns about the beam dumping in the ground water, which concerns need exploration.

Followup experiments with DUMAND could be considered in which the beam conditions are varied and/or lower energy sensitivity could be optimized in the detector via increased phototube density. In a more fine grained detector one could discriminate between hadronic and electromagnetic showers in order to pin down the source of oscillation (by carrying out a ν_e appearance experiment).

Acknowledgements

Thanks to Linda Stutte of Fermilab for running the flux prediction program. Useful discussions were had with Wojciech Gajewski, Matthew Jaworski, Bob March, Sandip Pakvasa, Leonidas Resvanis, Art Roberts, and Xerxes Tata. Lou Voyvodic made us aware of the injector's potential for neutrino detection at great distances.

References

(1) Hirata, K.S., et al., Phys Lett. 205B, 416 (1988).
(2) Learned, J.G., Pakvasa, S., and Weiler, T.J., Phys. Lett. B 207, 79 (1988).
(3) Leontaris, G.K., and Nanopoulos, D.V., Phys. Lett. 212B, 327 (1988).
(4) DUMAND II Proposal, HDC-2-88, August 1988.

Table 1

Neutrino Rates in DUMAND II from proposed Fermilab 150 GeV injector for hypothetical 6 months run. Columns 2 and 3 are for events contained in DUMAND. "Integ rate" means integral of rate above that energy. Stated energy is in middle of bin. For contained events it represents visible energy. The last two columns show the expected rate of muons with at least that energy at entering surface of the DUMAND array.

Energy GeV	Cont Evt Rate /2.5 GeV	Integ C E Rate	μ Rate /2.5 GeV	Integ μ Rate
1.25	1975.8	12430.1	89.2	4435.1
3.75	1499.6	10454.3	237.4	4345.9
6.25	1261.3	8954.7	337.2	4108.5
8.75	1115.1	7693.4	389.5	3771.3
11.25	982.8	6578.2	406.0	3381.8
13.75	822.8	5595.4	401.3	2975.8
16.25	947.3	4772.6	365.2	2574.5
18.75	537.3	3825.3	322.1	2209.3
21.25	627.1	3288.0	288.3	1887.2
23.75	449.5	2660.9	246.0	1598.9
26.25	268.6	2211.4	222.5	1352.9
28.75	324.7	1942.8	200.9	1130.4
31.25	483.2	1618.1	157.2	929.5
33.75	228.7	1134.8	112.6	772.2
36.25	138.7	906.2	93.7	659.6
38.75	193.5	767.5	74.5	565.9
41.25	113.3	574.0	55.2	491.5
43.75	47.8	460.7	46.6	436.3
46.25	53.2	412.9	42.1	389.6
48.75	32.0	359.7	38.1	347.6
51.25	26.8	327.8	36.2	309.5
53.75	26.4	301.0	34.1	273.3
56.25	30.0	274.6	31.7	239.2
58.75	25.3	244.6	29.0	207.5
61.25	24.9	219.3	26.3	178.5
63.75	24.3	194.4	23.7	152.2
66.25	17.1	170.1	21.7	128.5
68.75	19.6	153.1	19.6	106.8
71.25	21.7	133.4	17.0	87.2
73.75	17.2	111.7	14.5	70.2
76.25	17.0	94.5	12.2	55.7
78.75	10.5	77.6	10.5	43.5
81.25	13.6	67.0	8.9	33.0
83.75	9.6	53.4	7.3	24.1
86.25	11.9	43.8	5.6	16.8
88.75	8.2	31.8	4.2	11.2
91.25	6.8	23.6	3.2	6.9
93.75	6.3	16.7	2.1	3.8
96.25	5.4	10.4	1.2	1.6
98.75	5.0	5.0	0.4	0.4

Figure 1

Integral neutrino event rate in DUMAND II versus energy. Solid line: number of muons with more than that energy at the surface of DUMAND II. Dashed line: contained events versus total visible energy. Numbers are for hypothetical 6 month run with 3×10^{13} PPP, a 20 PPM rep rate, a 400 m decay tunnel, and two horn focussing.

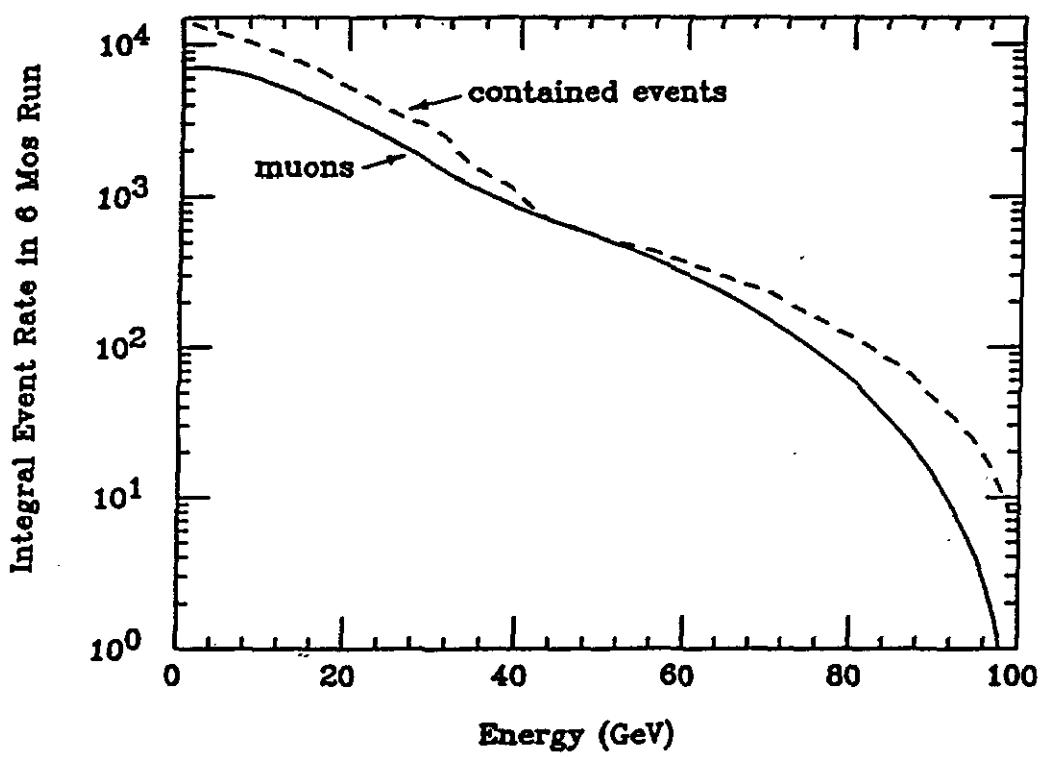

LENA ; A LONG BASE LINE EXPERIMENT ON ν-OSCILLATION

M. Koshiba , K. Nishikawa , H. Suda , Y. Watanabe

Department of Physics, Tokai University,Tokyo, Japan,151

Inst. for Nuclear Study, University of Tokyo, Tokyo, Japan, 188

Department of Physics, Kobe University, Kobe, Japan, 657

Department of Physics, Tokyo Inst. of Tech., Tokyo, Japan, 152

An appearance experiment on ν oscillation, especially τ–lepton detection, has been examined. The projected Main Injector Ring of FNAL offers an excellent oppotunity to study unexplored Δm^2 below $10^{-2}eV^2$ region.

Aims of the experiment

The final goal of the experiment is to build a LENA of 1M-tonnes fiducial mass at 500 to 1,000km from the high energy neutrino source of FNAL-Main-Injector-Ring in order to study; (1) ν-oscillation, in the form of appearance experiment, down to the hitherto unexplored Δm^2 region around or below $10^{-2}eV^2$, (2)supplementary to 1), the atmospheric ν interaction by the high statistics data: ca.14,000 upward-moving μ and 100,000 contained events annually, (3) possible heavy relic particles accumulated in the sun with a factor of more than 1000 increase, compared to any existing devices, in sensitivity, (4) high energy ν-astronomy with a sensitive area of $35,000m^2$ and with an angular resolution of 1 degree or better, (5) very high energy primary γ–ray point sources with excellent background rejection of cosmic ray hadronic showers.

Detector

General characteristics

The proposed detector is an imaging water Cerenkov detector .One of the differences from KAMIOKANDE, for example, is in the surface density of photomultipliers, PMTs, 1 per $9m^2$ rather than 1 per $1m^2$, and in the installation site, on surface rather than underground. In order to achieve a really large size for moderate cost, we consider a photo-cathode coverage of 2.2% for LENA. This choice will degrade the energy resolution

but retains the muon-electron discrimination capability which is crucial in order to study ν-oscillation by appearance methods. The vertex reconstruction accuracy is expected to be a sigma of 30cm or better, due to improvements achieved on PMT design in its time jitter and in its single photoelectron detection capability. We propose to divide the experiment into two phases, LENA-I and LENA-II. LENA-I with about 10K-tonnes of fiducial mass will be placed in the existing FNAL ν beam line to investigate the ν_μ-e elastic scattering to obtain an ambiguous determination of $\sin^2\theta_W$ with a dichromatic beam. It will also serve as the test experiment for LENA-II. LENA-II with 1M-tonnes of fiducial mass will use the proton beam of energy 120 to 150 GeV from the projected Main Injector Ring of FNAL and will be placed at 500 to 1,000km from the target to do the appearance experiment on ν_μ-oscillation in the Δm^2 region down to $0.005eV^2$ for $\nu_\mu \rightarrow \nu_\tau$ and to $0.001eV^2$ for $\nu_\mu \rightarrow \nu_e$. Both of the detectors will be surround by anti-counter modules, also of water Cerenkov type, on top and at sides. In high energy γ-ray astronomy, these modules act as total absorption energy-flow detectors, while the main detector act as μ-monitor covering the entire area.

Expected performances

Directional and energy measurement

A Monte Carlo study shows that the accuracy in direction is seen to be better than 1 degree. There is no justification for improving the accuracy still further because of the unknown emission angle of the secondary μ in the high energy ν-interaction. For energy measurements,scaling from KAMIOKANDE by the photocathode coverage, we expect to have the accuracies;11% for 1GeV electron or γ, 8% for stopping μ's, and 40% for charged π's of energy larger than 1 GeV.

Muon/Electron Discrimination

The discrimination between μ and e is based on the cascade shower development by the latter. The process produces a large number of low energy electrons/positrons which are deflected by Coulomb multiple scattering and emit Cerenkov light more diffuse way than

in μ case. The probability for erroneously assigning a μ-event as an electron event can be made 0.1% or less for 60% acceptance of 1Gev electrons.

Neutrino beam and Rates

For the rate calculation, we assume 150 GeV proton energy and $5x10^{19}$ protons can be delivered on target per year. The detector is 1M-tonnes, placed at a distance of 500km. We considered two kinds of ν-beam lines, double horn and dichromatic system (secondary momentum is 15GeV/c with 30% momentum byte), both with a decay pipe of 1000m. Table I shows expected rates and possible signatures with an assumption of maximal mixing ($\sin^2 2\theta=1.0$) and $\Delta m^2>0.005$ eV^2 case.

Table

	Horn beam	Dichromatic beam
Total ν_μ charged current events	130,000	10,000
Total ν_τ charged current events	9,000	700
<<Possible signals>>		
Single ring e-events(from τ->e$\nu\nu$ decay)	770	
μ or e with large missing energy		100 (μ or e)

Signal and backgrounds

We note the following points for ν_τ charged current interaction.

(1) Due to the mass of τ , the fraction of quasi elastic τ-production is large compared to that of ν_μ or ν_e interactions. Also most of the incident energy is carried by τ-lepton. As a result, the hadron multiplicity of the event is smaller for ν_τ charged current events than that for ν_μ or ν_e reactions and about 2/3 of the energy will be carried by final state ν's. (2) If π^0 is produced, charged pions will most likely be produced with it for the energy spectrum under consideration. The only exception is due to coherent π^0 production in neutral current interaction at a level of $<10^{-3}$ of the total cross section. (3) μ's are relatively easy to be identified, even in a multi-particle final state. These points motivated us to try ,at

least for the first step, to look for ν_τ charged current interaction by looking for (1)single electron events due to quasi elastic τ production followed by τ->e$\nu\nu$ decay in the horn ν beam or (2) μ or e productions with large missing energy in dichromatic beam. As of this writing, the signal and background situation in the horn beam, listed in Table, is as follows. In one year running with maximum mixing and Δm^2>0.005eV^2, the expected signal is 410 events where expected background events is 273 events. We are studying a possibility to distinguish e from π^0 by looking at the difference in the early stage of the shower developments using PMT timing information. The possible Δm^2 and mixing angle parameter space which can be explored in LENA is shown in Figure.

Cosmic ray background for LENA-II is indeed severe amounting a rate of 5Mhz of top-module firing, 5khz per module. This implies on the average, 0.75 top-module will fire during the main detector coincidence width of 150nsec. However a study shows that the experiment tenable. (One of the purpose of LENA-I is to experimentally verify these conjectures.)

Detection of pure gamma-ray event

The selection rely entirely on the number of muons contained in the shower. MC-simulation of the LENA response to the electromagnetic and hadron showers shows the instrumental role played by the main detector as the muon-monitor covering the entire area.

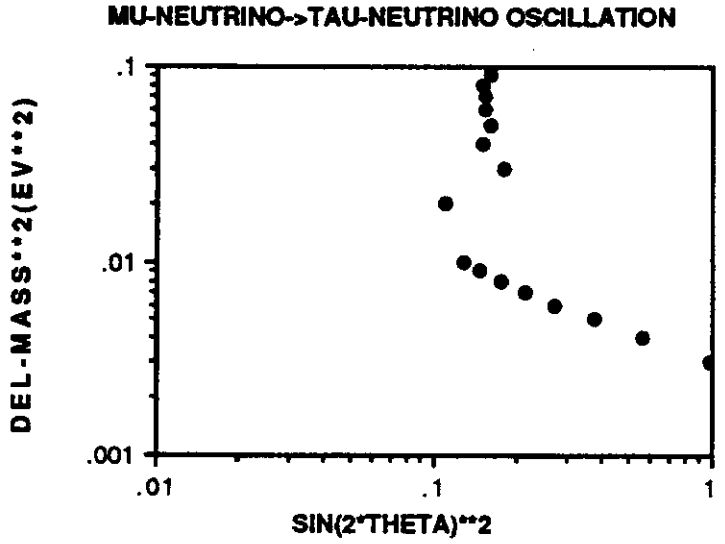

Soudan 2 as a long baseline neutrino detector

Maury Goodman
Argonne National Laboratory
Argonne, Illinois

Abstract

In a nine month run with a 150 GeV proton beam and a conventional double horn neutrino beam aimed at the Soudan 2 detector, a search could be made for neutrino oscillations in the mode $\nu_\mu \rightarrow \nu_\tau$. If evidence for oscillations is not found, new limits could be set extending the Δm^2 excluded region from .3 eV^2 to .004 eV^2 at 90% confidence level.

Introduction

Long baseline neutrino oscillation experiment was first suggested in 1977.[1] A sensitive new experiment is considered in this workshop and is motivated by three factors: The possible observation of neutrino oscillations by the Kamioka ν_e/ν_μ ratio,[2] the near completion of the 1 kiloton Soudan 2 nucleon decay detector,[3] and the proposed new injector at Fermilab which could be a source of large neutrino fluxes with relatively low energy.[4]

ν Beam

The present plan for Fermilab neutrino beams from the injector is to use 150 GeV primary energy protons and a double horn similar to the one used by many previous Fermilab wide band beam neutrino experiments. Linda Stutte has run NUADA, the Fermilab neutrino beam generator, for a Soudan 2 sized detector located 810 km from Fermilab. The resulting neutrino flux and event rate are shown as a function of energy in Figures 1 and 2.

Neutrino Oscillations

The probability for a neutrino to oscillate goes as

$$P_{\nu_a \rightarrow \nu_b} = sin^2 2\theta \cdot sin^2(1.27 \cdot \Delta m^2 \cdot \frac{L}{E}) \qquad (1)$$

where L is the distance of flight in kilometers, Δm^2 is in $(eV)^2$ and E in GeV.

If ν_μ's oscillate into ν_τ's, then 82% of them will appear in the Soudan 2 detector as neutral current events. The hadronic showers will be contained in the Soudan 2 detector for at least 50% of the neutrino events. I then assume that Soudan 2 will have 100% separation between neutral current and charged current events. This requires determining the presence or absence of a muon from the main vertex. The granularity of Soudan 2 makes it well suited for such a study. The average event energy will be about 30 GeV, so for most of the y region, this will be true. For very low y, a correction will have to be made for muons which do not come out of the shower. It should be possible to accurately make this correction with the help of a monte carlo.

The assumption is that all of the $\nu_\tau's$ will appear as neutral currents, except the $18\%\tau^- \rightarrow \mu^-$ branching fraction. Thus measurement of the correct ratio, $.31 \pm .01$ is evidence against neutrino oscillations, and measurement of too many neutral current events is evidence for neutrino oscillations. The sensitivity in Δm^2 depends on the distance the beam goes and the

energy, while the sensitivity to $sin^2(2\theta)$ goes with statistics. For an injector beam with 3×10^{13} protons every 2.9 seconds and 100 hours of beam per week for nine months, Soudan 2 would have 78 analyzable events. The 90% confidence limits we could set in the absence of oscillations are shown in figure 3. Only statistical errors are included.

With an average energy of about 30 GeV, about 5% of ν_τ interactions would be the quasielastic channel $\nu_\tau n \rightarrow \tau^- p$, and in 35% of these, the τ would decay into a single high angle electron or muon. These events would be rather unlikely in the absence of oscillations, and a positive result for ν_τ's in the nc/cc or disappearance part of the experiment should be accompanied by the appropriate number of such events. Our ability to reject hadrons versus electrons at 15GeV should be better than 100 to 1.

Disappearance experiment

There would also be a large number of muons coming in the front of the detector from charged current interactions in the rock. The rate of these muons is

$$n_\mu = 1.0 \times 10^{-12} GeV^{-2} \int_0^\infty dE_\nu E_\nu^2 n(E_\nu) \tag{2}$$

The two E_ν factors come from the cross section and muon range both proportional to the neutrino energy. In the same running period, with an area of $40m^2$, we would expect 964 muons. Our trigger and reconstruction efficiency should be very high. Only the lowest energy several percent would range out within our detector. With good accelerator timing and angular information, cosmic background will be negligible. Ranging and multiple scattering would give some indication of the energy distribution. However, I have just calculated the neutrino oscillation limits based on the total rate. This is given in figure 3. The accuracy with which one detector can do a ν_μ disappearance experiment depends on the systematic knowledge of the absolute flux. If the flux is known to 5%, the best $sin^2(2\theta)$ limit that could be reached would be .083. The number of neutrino interactions in the detector will help normalize the expected number of upstream μ's.

SSC Beam DUMP

The SSC beam dump is another possible source of neutrinos for long baseline type experiments.[5] The SSC will need two dumps for single turn beam elimination. In principle they could be aimed anywhere. There will be a prompt flux of $\nu's$ from charm decays for the 83 kilometer ring, or 276 microsecond long pulse. Volkova[6] gives the flux of neutrinos per square meter per proton on target from charmed particle decay at a distance from an accelerator:

$$10^{-15}(0.415 log E_p - 1)\frac{10^3 km^2}{L} E_p \cdot \int_{\frac{E_\nu}{E_p}}^{0.71} (1-x)^{0.4}(\frac{5}{3} - 3x^2 + \frac{4}{3}x^3) x dx dE_\nu \tag{3}$$

for Λ_c decays and a similar equation from D's. This equation is valid for the "central" region. For the 20 TeV Texas SSC beam with 1.27×10^{14} protons, I calculate the neutrino event rate would be .023 neutrinos interacting in our detector per spill. Using equation 2, we would also have 19 muons from neutrinos interacting in front of the detector. Equation 2 will slightly overestimate the muon flux because muon range is no longer proportional to energy above several TeV. We would see about 1/3 of the muons in one event frame, since we would have about 80 microseconds to see the events. The other 2/3 would be during the deadtime. $\nu_\tau's$

would be perhaps 1% of the flux, but would not be distinguishable. Based on CDF experience, one might expect about 100-200 dumps per year or a few neutrino events and several thousand muons.

Optimum Distance from FNAL

It may be that a double horn beam is built along the present direction of the neutrino beam line for an emulsion experiment.[7] A natural question would be the optimum distance of a detector for a disappearance type experiment. A comparison for various distances is given in figure 8 for a $40m^2$ detector. These plots show statistical errors only. The true $sin^2(2\theta)$ limit comes from the systematic knowledge of the flux in the beam. If the beam is only known to 5%, the practical limit on $sin^2(2\theta)$ is .083. Thus the best location for a detector would be 1000 kilometers. In fact, the problems of pitching down a neutrino beam and then digging a site for the emulsion experiment would probably dictate the distance of the detector. However the nearness of the proposed Sudbury Neutrino Observation detector to the present neutrino beamline should make that direction a very promising one to aim the beam. The limit which could be set by the $240m^2$ Sudbury detector in a ν_μ disappearance experiment is included in Figure 3.

Conclusion

The Soudan experiment together with a run of the wide band beam at the injector could investigate new regions of the mixing parameter and mass difference in a neutrino oscillation experiment. Other experiments at this conference could do similar experiments, including Lena 1, Lena2, Grande, and IMB. The Sudbury experiment which is located near the direction of the present neutrino beam line, could do a good disappearance experiment, but would not be able to distinguish neutral current and charge current events as Soudan 2 could. A long baseline neutrino oscillation experiment should be on the physics agenda of the Fermilab main injector.

References

1. Mann & Primakoff, Phys. Rev. D15, 655 (1977).
2. K. S. Hirata et al., Physics Letters **B205**, 416 (1988).
3. D. S. Ayres, "The Soudan 2 Experiment", submitted to the Proceedings of the 10th Workshop on Grand Unification, Chapel Hill, North Carolina, April 1989.
4. S. Holmes, these proceedings, and L. Stutte, these proceedings.
5. SSC Conceptual Design, SSC-SR-2020, March 1986.
6. L.V. Volkova, Il Nuovo Cimento Vol 8C, 5, September 1985. p 552.
7. N. Reay, these proceedings.

Figure 1. 150 GeV double horn νflux at Soudan 2

Figure 2. Neutrino event energy spectrum. In a nine month run with the injector, we could expect 156 events, and do neutral current/charged current separation on 78 of them.

Figure 3. 90% CL upper limits which could be set by Soudan 2 in the appearance and disappearance experiments, and by Sudbury in a disappearance experiment.

Figure 4. Statistical sensitivity for a 40 m^2 detector at 4 distances. Systematic effects would limit the closer detectors.

Figure 1
Neutrino Flux at Soudan 2

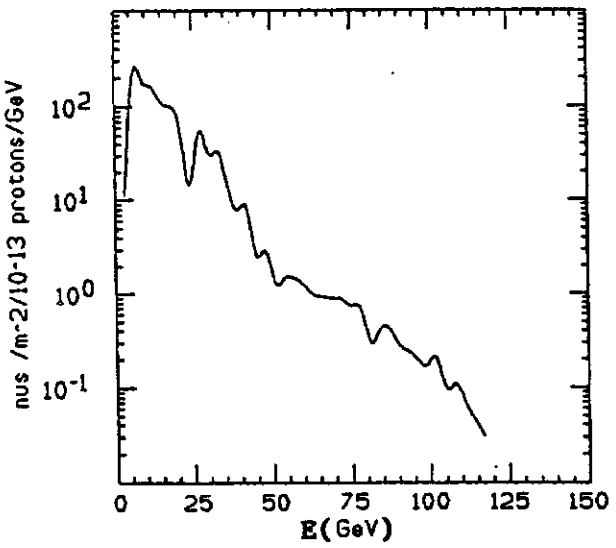

Figure 3
delta m squared limits

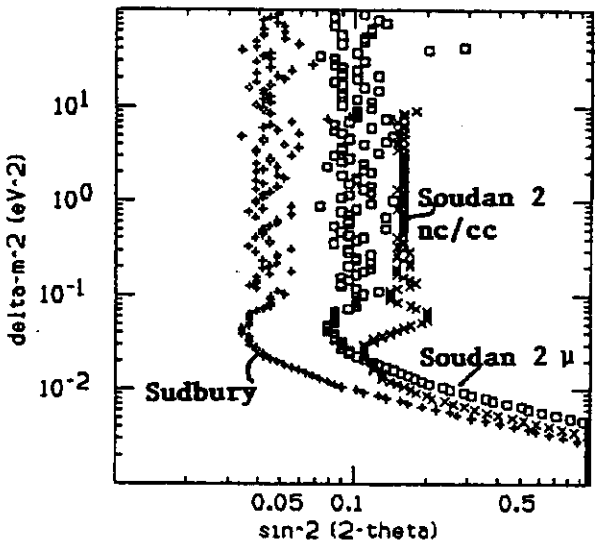

Figure 2
Neutrino Event energy spectrum

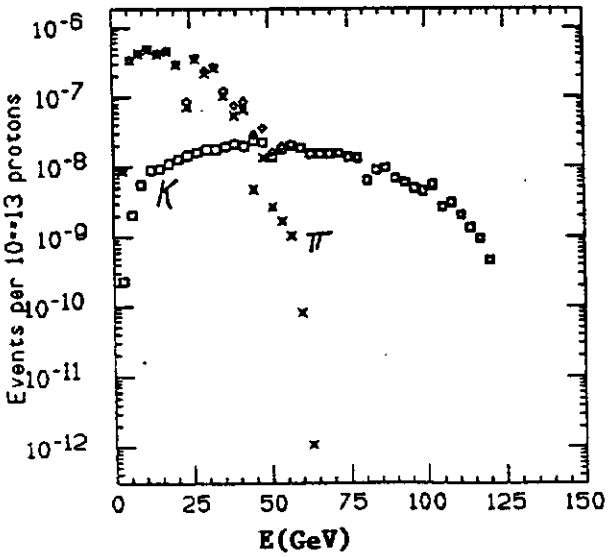

Figure 4
90% CL limits For 10,100,1000,5000 km

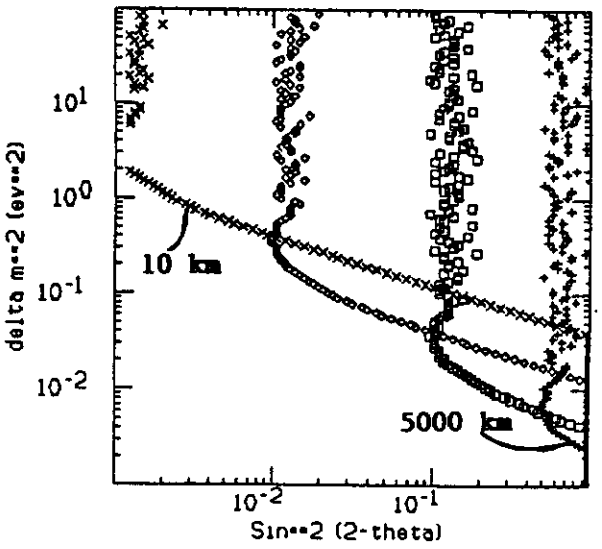

A LONG BASELINE NEUTRINO OSCILLATION EXPERIMENT USING THE IMB WATER CERENKOV DETECTOR

R. Becker-Szendy, C.B. Bratton, D. Casper, S.T. Dye, W. Gajewski, M. Goldhaber, T.J. Haines, T.W. Jones, D. Kielczewska, W.R. Kropp, J.G. Learned, J.M. LoSecco, S. Matsuno, C. McGrew, L.R. Price, F. Reines, J. Schultz, H.W. Sobel, L.R. Sulak, R. Svoboda.

The University of California, Irvine
Cleveland State University
The University of Hawaii, Manoa
University College, London
Warsaw University
The University of Notre Dame
Boston University
The University of Maryland

Presented by W. Gajewski UCI

INTRODUCTION

The high intensity neutrino beam from the Main Injector at FNAL presents an opportunity to conduct a long baseline ν_μ oscillation experiment. Some indication of such oscillations have been reported by underground proton decay detectors[1]. An analysis of these reports, and of other existing experimental limits, performed in ref (2), led some authors to a range of neutrino mass differences and mixing angles, which would be implied by these results. The predictions of a GUT model derived from string theory, flipped SU(5)*U(1), point to a similar mass hierarchy and mixing in the lepton sector[3].

If these indications are true, there is an opportunity to observe ν_μ disappearance or ν_τ appearance at distances of the order of several hundred miles. Experiments of this type have been discussed for some time, however, the proposed Fermilab Main Injector provides realistic conditions for their realization.

In this paper we discuss the advantages of using the existing and well understood IMB detector as the target of such a long baseline neutrino experment. The primary goal would be to resolve the ambiguities implied by an observed deficit of muon neutrinos coming from the atmosphere, by replacing

that beam with a well understood and controlled accelerator beam traveling a known path. For the FNAL-IMB configuration the distance allows exploration of the square-mass difference range 2 orders of magnitude below the regions currently available to accelerator experiments. For atmospheric neutrinos the L/E ratio is 10km/0.4GeV=25. The beam from FNAL to IMB also has this ratio equal to 580km/23GeV=25.

FEATURES OF THE IMB DETECTOR

The detector is situated in a salt mine (600 m underground) at Grand River (Ohio) at a latitude of 41.44 N and a longitude of 81.17 W. The FNAL injector has a latitude of 41.50 N and a longitude of 88.15 W. The great circle angle between the beam source and the detector is 5.23^{o} (91.3 mrad), and the linear distance is 581 km.

The detector consists of a rectangular volume of ultraclear water (size: 17m x 17.5m x 23m) viewed on its surface by 2048 8" Hamamatsu photomultiplier tubes with 2'x2' waveshifter plates mounted on them. Such a design provides a sensitivity of 0.8 photoelectrons collected per 1 MeV energy deposited by charged particles in water. The trigger threshold of 20 MeV is far below the requirements for the Fermilab experiment. The background rate of atmospheric muons of 2.7 Hz with the dead time of 3.5 ms per trigger provide a comfortable live time of 99%. The absolute time of every trigger is measured by WWVB clock to the accuracy of 1 ms. A local crystal provides a relative timing with the accuracy of 3us. These clocks provide sufficient precision to make gating of the accelerator spill unnecessary.

The detector provides some identification of leptons produced in neutrino interactions. Sixty percent of the negative muons stopping in the detector produce a decay electron signal. Muons with an energy above about 2 GeV produce patterns of lit tubes visually distinguishable from patterns produced

by electrons. Below such energies, more elaborate methods of pattern analyses provide distinction between showering and nonshowering particles with a reliability of about 95%.

Tracks of π^o are clearly resolved from electron tracks up to energies of 500 MeV, when tracks of individual gammas are separated by more than 30^o. Above this energy, some identification is possible with the confidence diminishing with increased energy. That fact is inherent to all detectors with limited spatial resolution, and as it is discussed later, limits the search for τ appearance.

NEUTRINO BEAM AND THE EVENT RATE AT IMB DETECTOR

The FNAL neutrino beam flux at IMB has been calculated using the FNAL version of the NUADA program (the beam layout and the preliminary computation were provided by L. Stutte, then the program was installed at UCI). Atherton's parameterization for pion production and two horn focussing were employed. The neutrino energy spectrum and the beam profile are shown in Fig 1. The integrated flux is $6200/m^2/10^{13}$ppp and its mean energy is 16 GeV. Such a beam produces 1.8 CC+NC interactions per hour in the volume of the IMB detector. This corresponds to 4400 interactions in a half year (25 weeks, 100 hours per week). A sample of this size assures 1.5% statistical accuracy, which is probably better than systematic uncertainties. The energy spectrum of muons from CC interactions is shown in Fig 2. As one can see, this spectrum has a low energy tail, where identification of muons is more difficult.

In addition to the contained events, the detector collects muons produced by neutrino interactions in the surrounding salt. The effective target mass for interactions producing muons, which would enter the detector through the west wall, can be roughly estimated from the formula:

$$V\rho = \frac{S < E_\nu > < y > \rho}{\frac{dE}{dx}\ \rho}$$

It is important to notice, that the effective target mass depends on the type of matter only through the dE/dx parameter, which does not vary much from one type of "rock" to another. Nevertheless, the geological profile of the mine in the vicinity of the detector is well known from existing drilling.

With $S=300m^2$, $< E_\nu >$ = 23 GeV (the mean weighted by cross section), $<y>=0.5$ and $dE/dx=1.6$ MeV/g one gets the mass of 21.6 kton from the above formula. A more realistic Monte Carlo calculation gives an effective mass of 23.7 kton for all neutrino induced muons entering the detector. This target mass provides 4.8 muon tracks per hour (12000 per half a year).

Entering tracks produce a pattern of early tubes with large pulse height, the so called "entry spot", which makes them easily distinguishable from contained interactions.

SEARCH FOR NEUTRINO OSCILLATIONS

The first indication of muon neutrino oscillations would be their disappearance from the beam. One can look for such disappearance in two different ways, each of them with different systematic limitations:

1. One can measure the ratio of the number of muons entering the detector from the surrounding rock to the number of contained interactions. The contained events serve as a measure of the total neutrino flux, while entering muons serve as a measure of the muon neutrino abundance in the beam. The number of entering muons can be predicted from the known structure of the rock in the vicinity of the detector (200m to the west, and 25m below and above).

2. The muon neutrino content can be measured directly from the fraction of contained events classified as muons. This parameter suffers from a smaller statistical accuracy and depends on muon identification for contained events. Different detectors, depending on their density of the light sensors, have different lower energy limit, below which muon tracks cannot be separated from the others. Here the IMB has an advantage over the other proposed detectors, in its sensitivity and in its electronics, which makes it possible to also identify muon decay electrons with high efficiency.

Of the two methods, the ratio in the first one has a smaller statistical error, and it seems to also have the least systematic one. The major source of its systematic uncertainty is the misassignment of contained and entering events. In spite of the fact, that both numbers in this ratio are sensitive to the shape of the neutrino spectrum, this dependence is reduced in the ratio.

Assuming that the systematic uncertainties are smaller than the statistical (which does not need to be the case), after half a year of observation, if the number of entering muons is in agreement with the expectations, one can set the limits on the muon neutrino mass difference and mixing angle shown in Fig 3.

The ratio in the second method seems to have more systematic uncertainties, but since it is automatically measured with the first one, it may be considered complementary.

In addition to the search for neutrino disappearance, it would be extremely interesting to look for the appearance of τ neutrinos. A very appealing signature of such oscillations would be observation of electrons from τ decays in the contained sample. In spite of the fact that the IMB detector has high light collection sensitivity, such analysis seems to be very

difficult, and not very promising. The main difficulty is due to the uncertainties in distinguishing between electron and π^0 tracks. The extent to which this difficulty limits the search for τ appearance, requires further detailed Monte Carlo studies.

The proposed experiment requires a dedicated neutrino beam line from the Main Injector towards the IMB detector. Such a beam line has to go underground with the inclination of 46 mrad. This means that the end of the decay tunnel, 0.5 km long, will at a depth of about 25 m. Positioning there another neutrino detector, for instance the emulsion chamber with its tracking system, would create some interesting advantages for both experiments. It would allow a joint effort to build the common neutrino beam line. The emulsion experiment would profit from the additional shielding of 25 m overburden, and the IMB experiment would benefit from information on the beam profile and its spectrum.

CONCLUSION

A high intensity neutrino beam from the Fermilab Main Injector opens new, exciting possibilities for the investigation of neutrino oscillations on very long base lines. This information is of basic importance for the further development of Grand Unified Theories. Such studies require detectors with a very large target mass. The existing and continuously operating IMB detector has the location, active mass and sensitivity optimal for performing such an experiment.

REFERENCES

1. K.S. Hirata et al., Phys. Lett. B205, 416, (1988) (Kamiokande)
C. Arpesella, Proc. XXIV Int. Conf. on HEP, Munich, 1988, p 1298 (Frejus). W. Gajewski, ibid p 1305 (IMB).

2. J.G. Learned et al. Phys. Lett. B207, 79, (1988),
V. Barger and K. Whisnaut, Phys. Lett. B209, 365, (1988).

3. G.K. Leontaris and D.V. Nanopoulos, Phys. Lett. B212, 327, (1988).

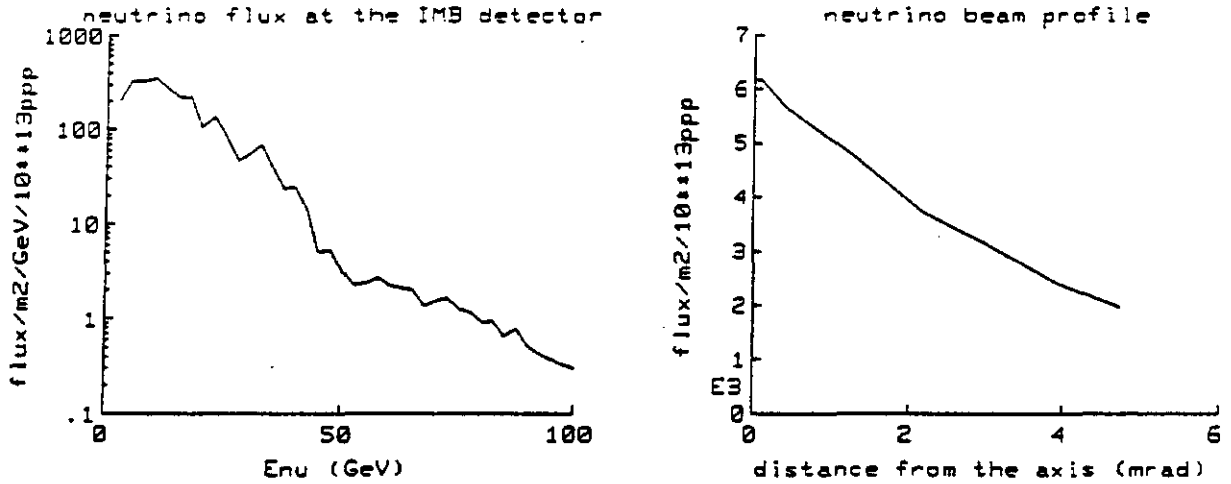

Fig. 1. Neutrino energy spectrum and beam profile at IMB detector

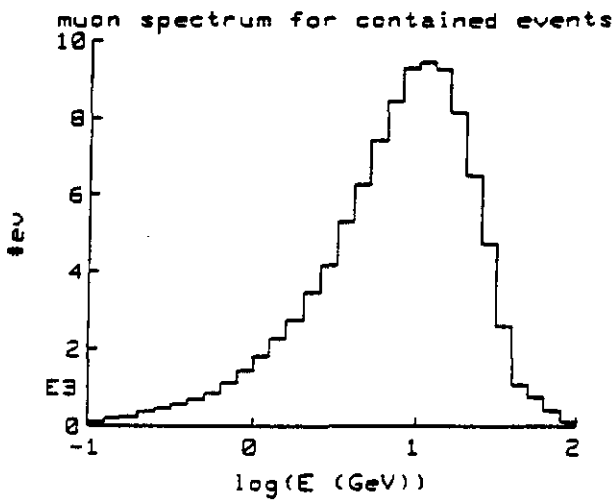

Fig. 2. Muon energy spectrum for contained events

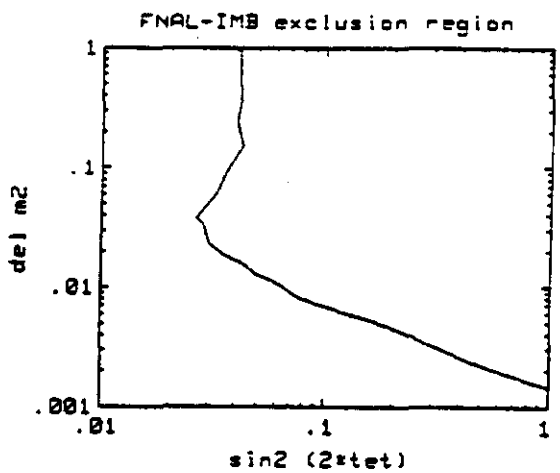

Fig. 3. The exclusion region in δM^2 versus $\sin^2(2\theta)$ plane which can be obtained by FNAL-IMB oscillation experiment

STUDY OF SLOW RESCALING IN NEUTRINO SCATTERING WITH THE PROPOSED FERMILAB MAIN INJECTOR

Raymond BROCK

Department of Physics and Astronomy
Michigan State University, East Lansing, MI 48824

The possibility of studying the means by which heavy quarks are produced from light quarks for neutrino scattering is discussed. The emphasis here is on the determination of the slow rescaling parameter, m_C, by using proposed Fermilab Phase II "Main Injector" (MI) upgrade.

Introduction

Because of the increased role that processes such as light quark→charmed quark transitions play in precision experiments, the reliability of the tools used to calculate the cross section for this process has become an important subject. The means by which this transition has been described to date is through a modification of the Parton Model called "slow rescaling"[1]. A possible detector for the MI neutrino area is one in which neutral charmed mesons might be detected with high efficiency. It therefore seems reasonable to ask whether data from such a detector could provide new information on the production of heavy particles in neutrino scattering. This information might include details of low Q^2 production of heavy particles alone, or it might conceivably rule on the advisability of relying on the slow-rescaling *ansatz* itself.

The analyses in which this issue has recently been recognized as being important are those of determining $\sin^2\vartheta_W$ in the comparison of deep-inelastic neutral current to charged current rates in neutrino scattering. The attempt to keep the total uncertainty at the few % level has failed without better understanding of this process, as the uncertainty associated with slow rescaling alone is more than 2%. The average error in $\sin^2\vartheta_W$ due to this uncertainty is roughly $6\%\cdot(m_C - 1.5)\cdot\sin^2\vartheta_W$ [2] and is therefore a considerable limitation in this measurement using the currently acceptable ranges of $m_C = 1.5\pm0.3\text{-}0.4$ GeV/c^2. There have been a few imprecise attempts at measuring the allowable variation on m_C in opposite-sign dimuon experiments (although no results are published yet). This is a measurement which is complicated by a number of correlated quantities, all poorly known: the amount of strange sea, the sorts of charmed hadron final states and their branching ratios, the assumptions inherent in charmed particle fragmentation, and the Kobayashi-Maskawa mixing parameters.

While the MI WBB is at low energy, the ability to see the development of particular, identifiable charm final states *from threshold* could rule, once and for all on the correctness of the slow rescaling ideas and, in addition, possibly make a definitive measurement of the parameter m_C. If the scheme is acceptable[3], then the uncertainty on m_C could possibly be determined in a more convincing manner than is possible from dimuon final states, and retroactively applied to the existing world data on $\sin^2\vartheta_W$. We can get an idea of what this situation might be at the MI through a simple calculation. Figure 1 shows the shape of the excitation curve for charm production by neutrinos using the cross section for charm production of

$$\sigma_{charm}(E_\nu) = \int\int dxdy(1-y+\frac{xy}{\xi})$$
$$\times\{\sin^2\vartheta_C[\xi u(\xi)+\xi d(\xi)]+\cos^2\vartheta_C 2\xi s(\xi)\}$$
$$\times\theta(\xi-1)\theta(W^2-1.8^2)$$

where ξ is the "slow rescaling variable" defined as $\xi=x_{Bj}+\frac{m^2_c}{2M\nu}$. Also shown on this figure is the situation where there is only "fast rescaling", namely, the abrupt turn-on of the charm channel with available center-of-mass energy. As an illustration, the excitation is calculated for two choices of m_C, 1.5 GeV/c^2 and 1.6 GeV/c^2. Note that this small deviation is roughly 4-5 times smaller than that allowed by data[4], and 3 times smaller than the historical variation applied in most $\sin^2\vartheta_W$ analyses[5]. In order to reject this 100 MeV/c^2 excursion around the assumed central value to 3σ, roughly 700 charm events would be required. The data point shown is representative of a data set of this magnitude where six equally populated bins from below to far above threshold were used. This is not an unreasonable number of neutral charmed particle events for the MI WBB. Such a measurement might be an extremely important contribution to this puzzle.

---

[1] R.M. Barnett *PR D14* (1976) 70; J. Laplan and F. Martin *NP 115* (1976) 333, and R. Brock *PRL 44* (1980) 1027.

[2] U. Amaldi *et al*, *PR D36* (1987) 1385 , R. Brock, "Deep Inelastic Neutrino Measurements of $\sin^2\vartheta_W$ ", to be published in *Proceedings of the New Directions in Neutrino Physics at Fermilab*, September, 1988.

[3] The acceptability of this method would depend on the degree to which one could control the understanding of the Q^2variation of this mass as well as the next-to-leading order QCD effects in the strange quark distributions from the MI energies up to the energies at which the neutral current experiments were performed. This could be an experimental problem as the uncertainties in running the mass may be overshadowed by other uncertainties in such an experiment. More work should be carried out in this regard to understand this point.

[4] W. Smith, for the CCFRR collaboration, private communication and unpublished preprint. B. Strongin, for the FMMF collaboration, unpublished thesis from Massachusetts Institute of Technology. Both experiments fit for m_c and find uncertainties that are in the range of ±0.5.

[5] see Brock in reference 2.

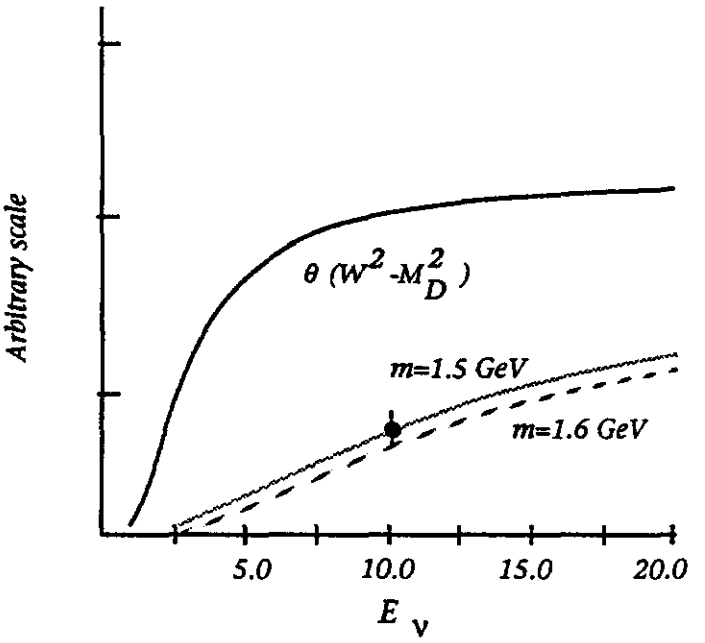

Figure 1. Excitation shapes for charm production as a function of neutrino energy. The solid curve is the threshold for "fast rescaling", with no threshold enhancement beyond that of requiring that there be enough mass in the final state to produce a charmed meson plus a nucleon. The gray curve is for slow rescaling with m_c=1.6 GeV/c^2 and the dashed curve is for m_c=1.5 GeV/c^2. The representative data point giving an indication of the error is placed under the assumption that the correct value is m_c=1.5 GeV/c^2 and that there are 130 charm events in 6 bins.

ν_μ+e→ν_μ+e SCATTERING WITH THE PROPOSED FERMILAB MAIN INJECTOR

Raymond BROCK

Department of Physics and Astronomy
Michigan State University, East Lansing, MI 48824

The possibility of studying ν_μ+e→ν_μ+e elastic scattering with the determination of $\sin^2\vartheta_W$ through measurement of y using the proposed Fermilab Phase II "Main Injector" upgrade is discussed.

Introduction

The classical neutral current reaction among Standard Model possibilities is the process ν_μ+e→ν_μ+e. Experimentally, this is a particularly difficult reaction to study both because of its small cross section and significant backgrounds. Interest in this reaction in recent years has not abated in spite of the small number of events in the world because of the increasing need for a very precise determination of $\sin^2\vartheta_W$. While the traditional determination of $\sin^2\vartheta_W$, that of using deep inelastic scattering, is very precise statistically it is less so from a theoretical perspective due to the need to rely on the parton model in a decidedly non-scaling regime. With an concerted effort, it may be possible to determine $\sin^2\vartheta_W$ using the ν_μ+e→ν_μ+e reaction and that is being attempted at CERN with the CHARM II collaboration. This experiment is very difficult as the precision required places emphasis on the relative antineutrino-neutrino flux normalization required to measure the quantity

$$\frac{\sigma(\overline{\nu}_\mu e)}{\sigma(\nu_\mu e)}$$

This measurement is being done in the wide-band beam of the CERN PS which is comparable to the old Fermilab beams. There is a significant background to this reaction from coherent π^0 and γ production which have larger cross sections at high energies than the signal and traits similar to the signal. Low energy beams are not so plagued with this background. An additional complication to the ratio method employed at CERN is the extreme precision required for the relative flux determination. Such demands are difficult in a NBB, and are likely to require heroic efforts in a WBB. The only other prospect for a high statistics determination of $\sin^2\vartheta_W$ from this reaction is the proposed liquid Argon detector at LANL. The enormous flux available at the Main Injector obligates new thinking about possibilities not seriously considered previously for precision measurements of $\sin^2\vartheta_W$ using the ν_μ+e→ν_μ+e reaction.

Cross sections

The cross section for $\nu_\mu e$ elastic scattering is simply expressed as a function of y as

$$\frac{d\sigma}{dy} = \frac{G^2 m_e E_\nu}{2\pi}[A + B(1-y)^2]$$

where $y = \frac{E_e}{E_\nu}$ and the A and B coefficients are simple functions of the chiral couplings for vector and axial vector matrix element contributions.

reaction	A	B
$\nu_\mu e \rightarrow \nu_\mu e$	$(g_V^e + g_A^e)^2$	$(g_V^e - g_A^e)^2$
$\overline{\nu_\mu} e \rightarrow \overline{\nu_\mu} e$	$(g_V^e - g_A^e)^2$	$(g_V^e + g_A^e)^2$
$\nu_e e \rightarrow \nu_e e$	$(g_V^e + g_A^e + 2)^2$	$(g_V^e - g_A^e)^2$
$\overline{\nu_e} e \rightarrow \overline{\nu_e} e$	$(g_V^e - g_A^e)^2$	$(g_V^e + g_A^e + 2)^2$

Since $g_V = -\frac{1}{2} + 2\sin^2\vartheta_W$ and $g_V = -\frac{1}{2}$, then

reaction	A	B
$\nu_\mu e \rightarrow \nu_\mu e$	$1 + 4\sin^4\theta_W - 4\sin^2\theta_W$	$4\sin^4\theta_W$
$\overline{\nu_\mu} e \rightarrow \overline{\nu_\mu} e$	$4\sin^4\theta_W$	$1 + 4\sin^4\theta_W - 4\sin^2\theta_W$
$\nu_e e \rightarrow \nu_e e$	$1 + 4\sin^4\theta_W + 4\sin^2\theta_W$	$4\sin^4\theta_W$
$\overline{\nu_e} e \rightarrow \overline{\nu_e} e$	$4\sin^4\theta_W$	$1 + 4\sin^4\theta_W + 4\sin^2\theta_W$

Figure 1 shows each of the A and B coefficients as a function of $\sin^2\vartheta_W$. If the differential cross section could be determined, the coefficients of the flat and $(1\text{-}y)^2$ components could give a measure of $\sin^2\vartheta_W$. This has been successfully attempted only once.[1] The relation among y, θ_e, and E is as follows:

$$\theta^2 = \frac{2m_e}{E_e}(1 - y)$$

Since $y < 1$, the maximum $E_e\theta^2$ is 1MeV-mrad^2. For an electron energy typical of the 400 GeV-era accelerator-neutrino beams such as 20GeV, the angle is limited to about 7 mrad which is extremely small. For a much lower electron energy, the requirements on the angle are much less. Figure 2 shows the electron angle as a function of energy at various values of y. For the Main Injector beam with an average interacting energy of approximately 15 GeV and an average electron energy of 5-7 GeV, the electron angle is bounded from above by about 15 mrad, which may be practical. A study was done in 1982[2] on just this possibility of measuring the ratios of the A and B coefficients. Figure 3 shows the ratio of coefficients showing that they are quite sensitive to $\sin^2\vartheta_W$ for $\nu_\mu e$ scattering. A method of determining the $\sin^2\vartheta_W$ with no flux-dependence would be to fit the differential cross section, measure A and B and, determine $\sin^2\vartheta_W$ from the ratio[3]. The premium is on good y resolution.

Resolutions

The resolution in y is easily expressed as a function of angle and energy. For an angular resolution of the form $\sigma(\theta) = \frac{\alpha(mrad)}{\sqrt{E_e}}$ and an energy resolution expressed in the form $\frac{\sigma(E_e)}{E_e} = \frac{\beta}{\sqrt{E_e}}$ we can write:

$$(\delta y)^2 = \frac{E_e\theta_e^{\,2}}{m_e^2}(\alpha)^2 + \frac{E_e\theta_e^{\,2}}{4m_e^2}\theta_e^{\,2}(\beta)^2$$

$$\delta y = \sqrt{\left(\frac{E_e\theta_e^{\,2}}{m_e^2}\right)\left[\alpha^2 + \frac{\theta_e^{\,2}}{4}\beta^2\right]}$$

$$\delta y = \sqrt{\left(\frac{2(1-y)}{m_e}\right)\left[\alpha^2 + \frac{m_e(1-y)}{2E_e}\beta^2\right]}$$

The detector challenge is clearly to make the angular resolution for low energy electrons as good as possible. As an example of feasibility, we can consider some extremes. We choose the worst possible angular resolution to be that of the Brookhaven E734 apparatus (which was actually quite good!) $\sigma(\theta_e) = \frac{12mrad}{\sqrt{E_e}}$ and the best possible angular resolution to be half of this. For the worst-case energy resolution, we choose $\frac{\sigma(E_e)}{E_e} = \frac{20\%}{\sqrt{E_e}}$ and the best to be $\frac{\sigma(E_e)}{E_e} = \frac{15\%}{\sqrt{E_e}}$. Figures 4 and 5 show the range in y resolution for each of these contributions and the quadratic combination.

One unique possibility at the Main Injector would be the construction of a narrow band beam. y could now be defined as the familiar ratio of E_e/E_ν and the resolution function is now independent of the angular resolution and the driving uncertainty becomes the beam energy spread. The y resolution for the beam contribution is

$$\delta y = y\sqrt{\frac{\beta^2}{E_e} + \gamma^2}$$

where $\gamma \equiv \frac{\delta E_\nu}{E_\nu}$ is the fractional beam spread, which we assume here to be σ=4 GeV. Figure 6 shows the y resolution for the two possible energy resolution extremes comparing the beam-determined y with that of the detector-determined (meaning θ_e) y . Clearly, the beam-resolution is much better than the detector-resolution except at high y where, even for the worst-case angular resolution, the detector determination is better. The two methods compliment one another nicely, and, if used in the same detector would result in a nearly flat y resolution.

In reference 2, it is stated that a 2% measurement is possible with 1000 events, which may be feasible feasible with a dichromatic beam at the MI. Whether such a narrow energy spread is possible is perhaps problematical and should be studied. However, given the manner in which uncertainty in energy factors into the determination of y and the possibility that the high y region could be determined better with an angle measurement, it is still possible that considerable relaxation in δE_ν could be acceptable without sacrificing the necessary low-y capability.

---

[1] The Brookhaven neutrino experiment E734 is the only experiment which has successfully measured the two pieces of the cross section to determine $\sin^2\vartheta_W$. They did not determine y, but rather measured θ_e^2 . From this they extracted $\sin^2\vartheta_W$ = 0.195±0.018±0.013 as reported in K.Abe et al., *PRL 62* (1989) 1709.

[2] K. Abe, F.E. Taylor, and D.H. White "Measurement of Neutrino and Antineutrino Elastic Scattering as a Test of the Standard Model", page 165, Proceedings of the 1982 DPF Summer Study On Elementary Particles and Future Facilities, 1982, R. Donaldson, R. Gustafson, and F. Paige, eds.

[3] See reference 3 for details of resolution effects on the ratio.

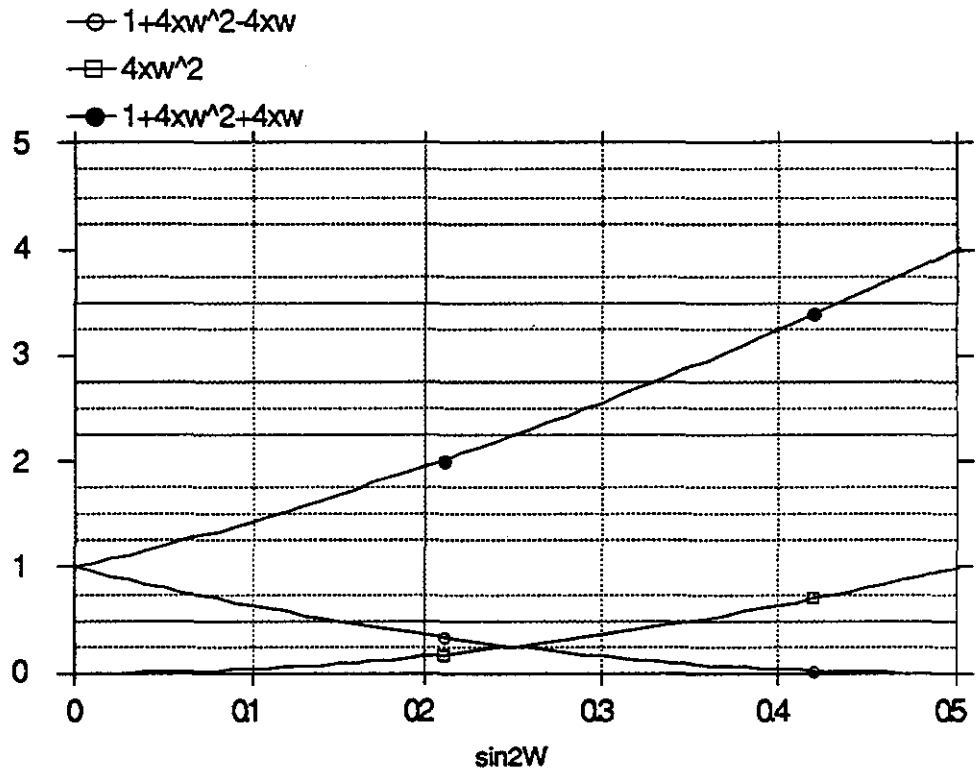

Figure 1. *Neutrino-electron elastic scattering y-coefficients.*

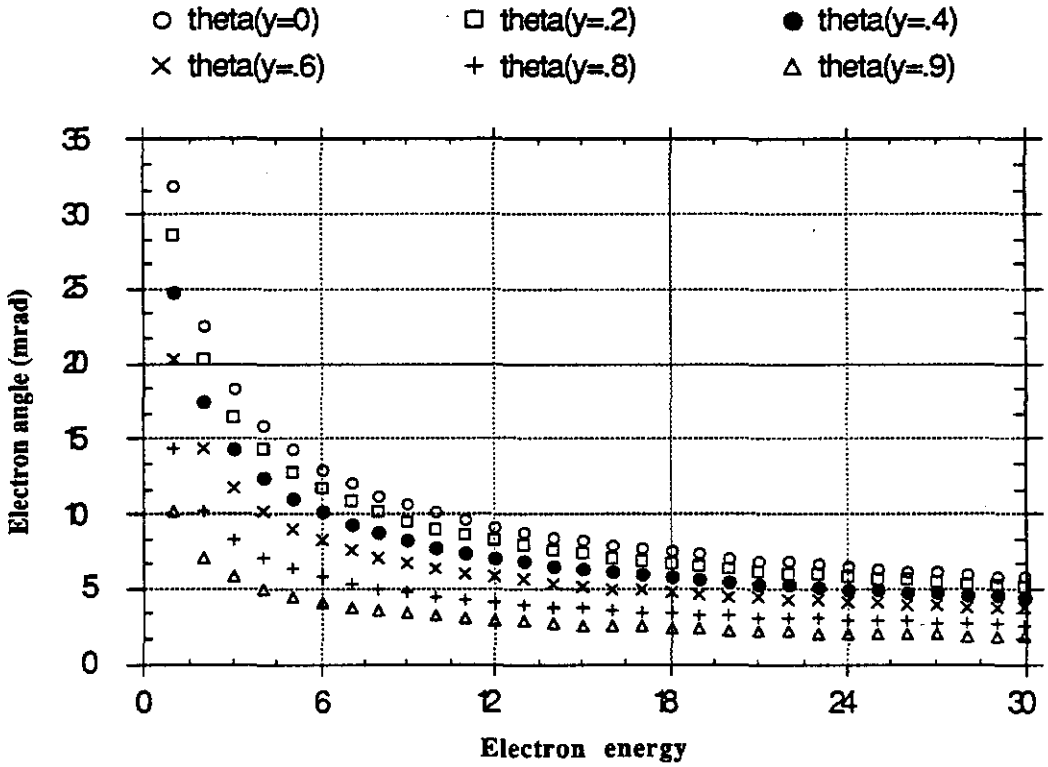

Figure 2. *Electron angle for neutrino-electron elastic scattering.*

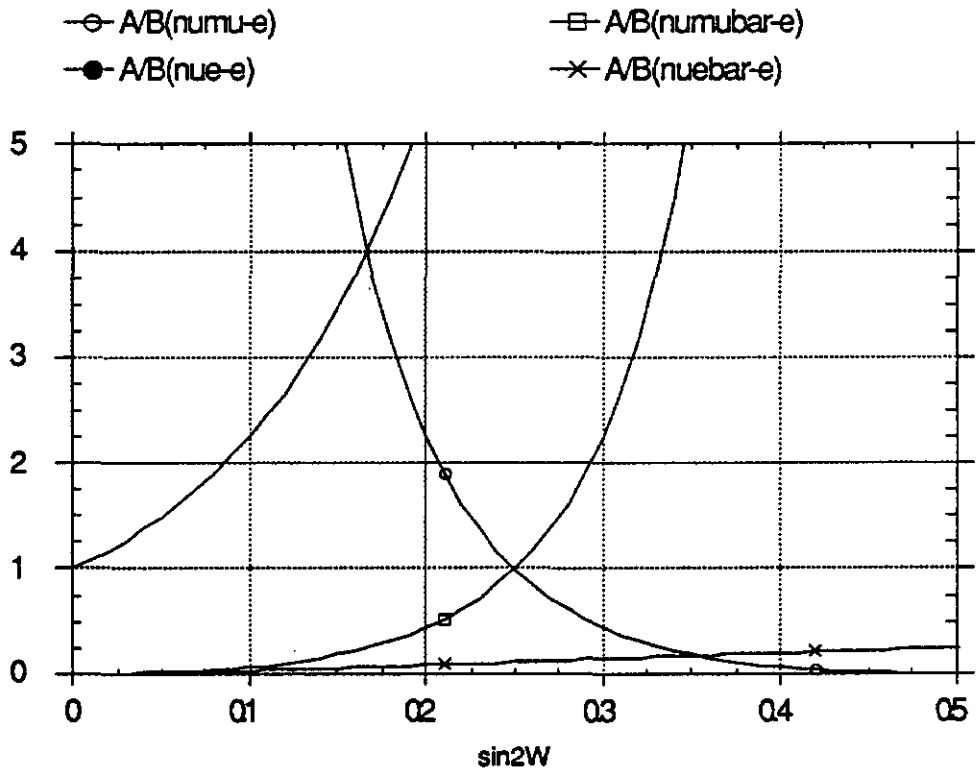

Figure 3. *Ratio of y-coefficients for neutrino-electron elastic scattering.*

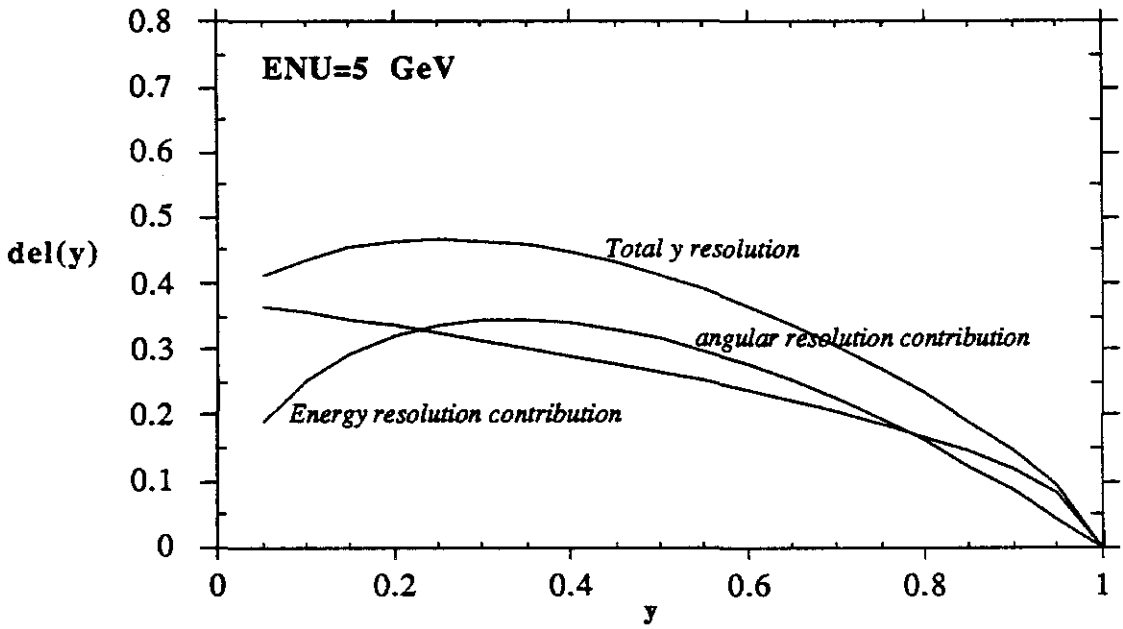

Figure 4. *y-resolution contributions for "best" angle and "worst" energy resolutions.*

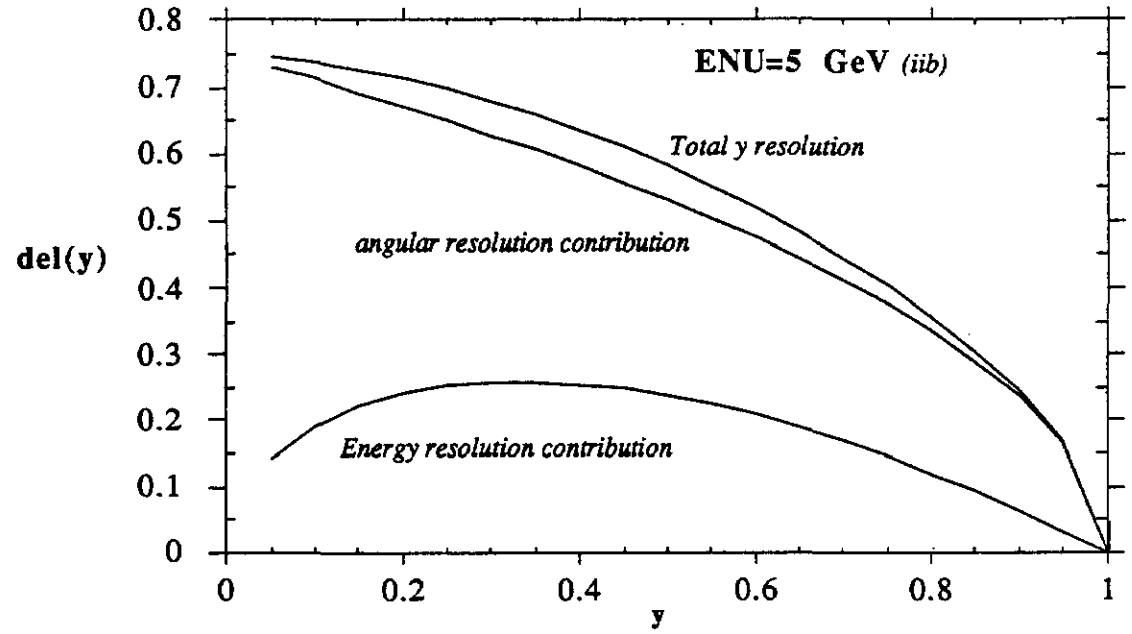

Figure 5. y-resolution contributions for "worst" angle and "best" energy resolutions.

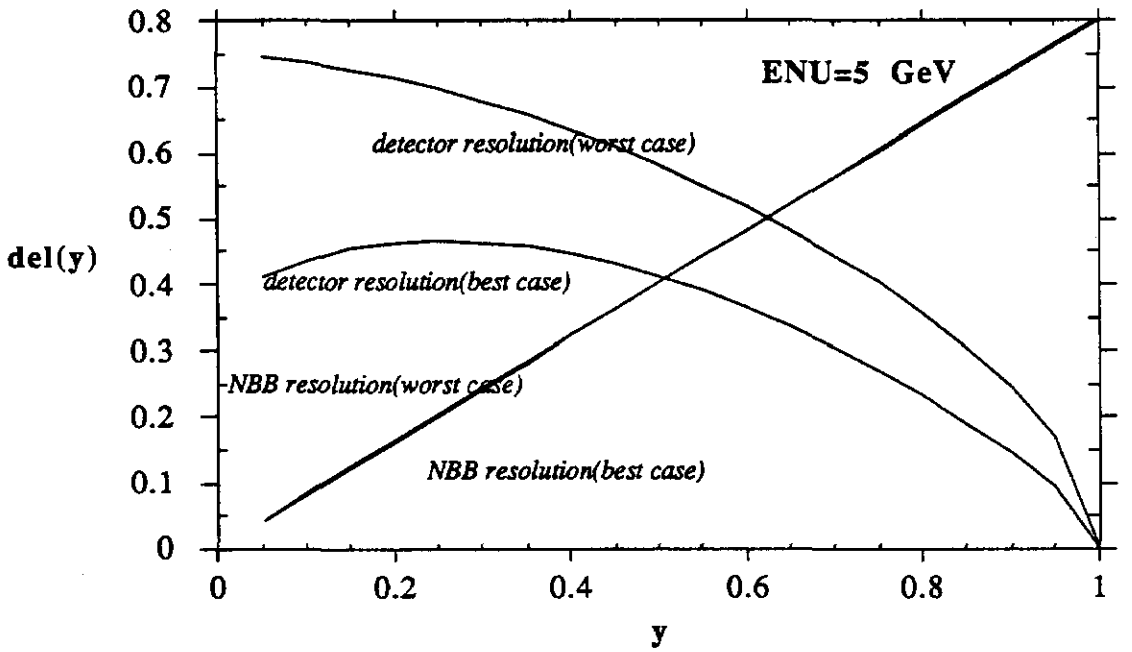

***Figure 6.** y-resolutions detector-induced compared with beam-induced.*

Measurement of ϵ'/ϵ at Main Injector

Hitoshi Yamamoto

Enrico Fermi Institute, University of Chicago,Chicago,IL,60637.

Abstract Possibility of measuring the CP violation parameter ϵ'/ϵ to a precision of 5×10^{-5} at the proposed Main Injector is investigated. Based on the experiences gained at the experiment E731 at Fermilab, sizes of major backgrounds, systematic as well as statistical errors are extrapolated to the Main Injector enviroment. We find no fundamental obstacles in attaining the stated precision.

Introduction The parameter ϵ'/ϵ (actually the real part of it) can be extracted by measuring the following double ratio:

$$R \equiv \frac{\Gamma(K_L \to \pi^+\pi^-)/\Gamma(K_S \to \pi^+\pi^-)}{\Gamma(K_L \to 2\pi^0)/\Gamma(K_S \to 2\pi^0)} \approx 1 + 6\mathrm{Re}(\frac{\epsilon'}{\epsilon}).$$

Currently, the experiment E731 has a sample of about 300K $K_L \to 2\pi^0$ events on tape, and substantially more for other three decay modes. This corresponds to a final statiscal error in R of 3×10^{-3} (5×10^{-4} in ϵ'/ϵ). A preliminary analysis based on 20% of the data indicates that the total systematic error can be controled to a level less than the statistical error. The question we address here is wheter we can measure it 10 times more precisely ($\sigma_R = 3 \times 10^{-4}$) at the Main Injector.

The statistically required number of observed $K_L \to 2\pi^0$ decays is 3×10^7. Assuming an acceptance of 0.1 and using $\mathrm{Br}(K_L \to 2\pi^0) = 0.001$, the corresponding number of K_L decays is 3×10^{11}. The model beamline/detector described by B. Winstein[1] has a 20m decay region with a 36 mr^2 beam size, and can collect the above statistics in about 6 hours. Therefore, the intensity is more than enough, and we can give away the yield in exhcange for a better control of systematics (e.g. by making the beam size smaller and well collimated, and by limitting the fiducial decay region).

A Brief Rview of E731 In E731, two parallel K_L beams were employed to control various systematics, where a regenerator alternated between the two beams every spill to supply a coherently generated K_S beam. In this way, any variations in gains, efficiencies, and deadtimes of the detector, which would have affected K_S and K_L differently, cancel to a good accuracy. Also, the momentum dependence of regeneration amplitude is such that the final kaon momentum spectrum is similar for K_S and K_L.

Table 1 shows the major backgrounds for E731. The backgrounds in charged modes are small and are not expected to be a problem for the Main Injector setup, provided that electron and muon identifications are adequate.

mode	source	level
$K_{S,L} \to \pi^+\pi^-$	$K_{e3}, K_{\mu 3}$	small
$K_L \to 2\pi^0$	$3\pi^0$	0.35 %
	X-over from K_S beam	4%
$K_S \to 2\pi^0$	incoherent K_S	2.5%

Table 1 Backgrouynd levels in E731

The $3\pi^0$ background for $K_L \to 2\pi^0$ creeps in when two of the six photons of a $3\pi^0$ decay are lost either by merging with another photon cluster or by escaping the detector undetected. By further improving the coverage of photon vetoes and improving the granularity of calorimeter, it seems quite feasible to reduce it to less than 0.1 %.

The regenerator generates incoherent K_S's as well as coherent K_S's. The incoherent K_S's are generated with a finite P_t^2, and result in the X-over background under $K_L \to 2\pi^0$ and the incoherent background under $K_S \to 2\pi^0$. Since the signals are selcted by requiring the center of energy of photons to lie inside the beam area, these backgrounds are roughly proportional to the beam size. They are by far the largest backgrounds; we will will use narrower beams together with a fully active regenerator to reduce these incoherent backgrounds.

A Case Setup for Main Injector We will take the following parameters as a case study of an ϵ'/ϵ experiment at the Main Injector:

1. Beam size: 2 mr^2 $\times$ 2 beams. Targetting angle 20 mr.
2. A totally active regenerator at 20m from the calorimeter.
3. Energy range $15 < E_K < 50$ GeV.
4. Length of decay region: 4m (K_S life time = 1.4m at 25 GeV).

Then the rate of K_L decay in the decay region will be

$$3 \times 10^7 \text{Hz} \cdot \frac{2\text{mr}^2}{36\text{mr}^2} \cdot \frac{4\text{m}}{20\text{m}} = 3.7 \times 10^5 \text{Hz}.$$

This leads to a running time of 500 hours to accumulate the goal of 3×10^{11} inclusive K_L decays.

At this point, the $K_S \to 2\pi^0$ yield is 50 times more than $K_L \to 2\pi^0$ yield. This would result in a large X-over background for K_L; thus, we will use a 3-interaction-length absorber in the K_S beam to reduce the yield ratio down to 2.5. The totally active regenerator is expected to reject virtually all of the inelastic part of the incoherent backgrounds. The fraction of inelastic component is estimated to be 80% for K_L and 60% for K_S. Assuming the P_t^2 distribution of incoherent K_S to be independent of kaon energy (which is a good approximation), the above numbers leads to 0.25% for the X-over background under K_L and 0.35% for the incoherent background under K_S.

The incoherent background can be estimated to about 5% of itself (or better) without much difficulty. Thus, the systematic error in the double ratio R will be 1.3×10^{-4} for the X-over background and 1.8×10^{-4} for the incoherent background under K_S. Even though these are barely acceptable, a further reduction of these backgrounds is desirable.

We will now turn our attention to rates and accidentals. The number of kaons going through the regenerator is 5×10^6/sec, and about the same for neutrons. This results in a rate of one interaction every 100ns; which is high but not unmanageable.

There will be 5×10^6 K_L decays within the detector including all kaon momenta; some of them will overlap with a potential signal event causing them to be rejected. As long as the probability of getting rejected by accidental overlap is the same for K_S and K_L modes, it does not affect the measurement of the double ratio. For example, isolated hits in a photon veto counter do not cause a problem. However, since the accidental events mostly originates from the K_L beam, the illumination of accidental hits is not symmetric between K_S and K_L beams. Thus, the acceidental overlap at the calorimeter could affect the K_S and K_L modes differently to the extent that the two beams are not exactly on top of each other. Clearly, it is important to reduce the accidnetal hits on the calorimeter by vetoing on the counters that do not affect K_S and K_L differently (e.g. photon vetoes). The timing resolution of the calorimeter must be as good as possible, and that for the photon vetoes be well matched (not too slow, not too fast) to reject the accidental overlaps which are not resolvable by the calorimeter timing. For the charged modes, similar considerations are in order for the tracking system.

These asymmetry between K_S and K_L needs to be carefully studied by a simulation. For E731, the effect was shown to be of order 0.1% or less. Since the beams are smaller and closer together for the Main Injector setup, it seems reasonable to expect that the asymmetry is much less. If it turns out to be non-zero, a correction can be made to the double ratio.

The rate of reconstructable $K_L \to 2\pi^0$ decays within the fiducial region of kaon energy and decay vertex is about 20Hz, and that for $K_S \to 2\pi^0$ is 50Hz adding up to slightly less than 100 Hz. This rate will be increased by $2\pi^0$ decays outside the

fiducial region, $3\pi^0$ and $\pi^+\pi^-\pi^0$ decays. An on-line processor that selects four-cluster events and calculates masses and decay verteses is in order. The $\pi^+\pi^-\pi^0$ decays can be rejected by requiring no tracks. The charged 2π modes have twice as big branching fractions as corresponding neutral modes, and also the detection efficiencies for the charged modes are expected to be a few times larger. If the charged mode triggering rate turns out to be too high, it could be prescaled by a factor of a few. The other charged mode decays of K_L — $K_{\mu 3}, K_{e3}$ and $\pi^+\pi^-\pi^0$ — need to be rejected by an muon identification (μ-wall), by an electron identication (a TRD is a good candidate, or by an on-line E/P cut), and by an on-line mass calculation. Thus, both in neutral and charged modes, it is crucial to have fairly sophisticated on-line trigger processors. All in all, it seems possible to keep the total triggering rate to a few KHz.

In conclusion, we have looked at backgrounds and rate problems in an experiment at the proposed Main Injector to measure ϵ'/ϵ to 5×10^{-5}. No unmanageable problems have been found. However, further studies are needed to estimate the systematic errors caused by uncertainties in acceptances, energy scale, and non-linearities.

References

1. B. Winstein, in this proceedings.

K_S^o EXPERIMENTS AT THE MAIN INJECTOR

Gordon B. Thomson

Rutgers University

In this talk I will consider what experiments would be interesting to do at the Main Injector on decays of K_S^o mesons, or using the interference between K_S^o and K_L^o mesons. The decays I will cover will be $K_S^o \rightarrow \pi^o e^+ e^-$, K_S^o and $K_L^o \rightarrow \pi^o \mu e$. The interference experiments are those for decays to $\pi^+\pi^-\pi^o$, $3\pi^o$, and $\pi^o e^+ e^-$.

The first question about any K_S^o or interference experiment is: how close to the target can you observe kaon decays. I took the hyperon magnet for P796 at Fermilab (the follow-up experiment to E621) and scaled it to a 125 GeV/c proton beam, while keeping the same flux of kaons per incident proton. Greg Bock's talk on kaon beams will include a description of the result. The important points are that it takes 1.25 m to sweep away the proton beam with a 35 kGauss field, and another 1.25 m to absorb the protons. So the magnet ends up being 2.5 m long, and has quite a bad fringe field. I left another meter to let the fringe field die away (although perhaps one could do better here) to total 3.5 m to the beginning of the decay region. For the average kaon, at x=0.2, this is about 2.75 K_S^o lifetimes.

For a detector, I took the design we are planning for P796, shown in Fig. 1. After a 40 m long decay region, there follow three MWPC's, a magnet with a 1.6 GeV/c p_T kick, and three more MWPC's to measure the charged particles' momenta. An electromagnetic calorimeter catches the gamma rays (and charged particles to provide e/π identification), and a separate plug

calorimeter fills the hole left in the main calorimeter for the beam to pass through. The beam goes through the entire detector either in vacuum, or in helium bags. The acceptance of this detector is high: over 90% for most p and z bins above x=0.1. To modify it for the Main Injector, simply compress it longitudinally by a factor of 6.

Based on our experience in E621, and Monte Carlo calculations we have done for P796, with the Main Injector we would reach the space charge limit for 2 mm wire spacing MWPC's at a proton beam intensity of 5×10^{11} protons/minute, at a targeting angle of 18 mrad. The single event sensitivity for $K_S^o \rightarrow \pi^o e^+ e^-$ would be about 8×10^{-12}. It is worth noting that at the Tevatron, because the decay region would start at about 0.5 τ_S, one could reach a single event sensitivity of 1×10^{-12}.

To study CP violation in K_S^o decay (that is, measure η_{+-o} and η_{ooo}) using interference between K_S^o and K_L^o, it is also important to get as close to the target as possible. The sensitivity of a Main Injector experiment is about 3 times worse that of a Tevatron experiment, all other things being equal. The higher flux at the Main Injector is of no use for these decays.

The technique we used to in E621 measure η_{+-o} was to use two targets, one at the entrance to the hyperon magnet, and the other 3 K_S^o lifetimes upstream of there. We split the proton beam in two parts, and struck both targets simultaneously. We learned that, although we put 95% of the beam on the upstream target, only 7% of the rate in the spectrometer came from that target. The flux of K_L^o's from the upstream target was within a factor of 2 of that from the downstream target. This suggests that if we struck only the upstream target, we could stand a beam flux of 1×10^{14} protons/minute, which is 1/6 of what the Main Injector is designed to deliver. This would yield a single event sensitivity of 1×10^{-11} for $K_L^o \rightarrow \pi^o \mu e$ or $\pi^o e^+ e^-$. I

should add that the simple spectrometer I have described is probably insufficient to eliminate backgrounds to reach $1x10^{-11}$ for $K_L^o \rightarrow \pi^o \mu e$. The necessary additions to make a viable spectrometer would probably reduce the acceptance considerably. Since the decay $K_L^o \rightarrow \mu e$ is sensitive to pseudoscalar and pseudovector couplings and $K_L^o \rightarrow \pi^o \mu e$ is sensitive to scalar and vector couplings, I suspect it will be worth while looking into just how to do this experiment.

The same geometry of striking only an upstream target is how one would look for interference in K_S^o and $K_L^o \rightarrow \pi^o e^+ e^-$. The K_L^o amplitude is the sum of three terms: direct CP violation, indirect CP violation, and a CP conserving one. To disentangle these three contributions, phase information may be necessary, so the interference experiment (which measures the magnitude and phase of the amplitude ratio) will be important. Figure 2 is a graph of the number of decays per unit proper time vs. the proper time, for a pure K^o beam, assuming that $\eta_{\pi ee} = 6x10^{-3}\, e^{i\pi/4}$. The horizontal arrow shows the 1-event level for the experiment we are discussing. If the decay region covered the $6\tau_s < t < 14\tau_s$ region, the deviation from exponential behavior might be seen. Here we are sampling part of about 10^{13} K_S^o decays (for $t > 0.5\tau_s$), and will need a proton beam intensity of $1x10^{14}$ protons/min.

In summary, we have adopted the philosophy of having a simple detector, scaled from existing apparatus and rates, and concluded that the really unique contribution of the Main Injector is in the K_S^o - K_L^o interference region, rather than in pure K_S^o decays. The experiments that seem the most interesting to me are a measurement of interference in $\pi^o e^+ e^-$ decays, and a search for the separate lepton number nonconserving decay, $K_L^o \rightarrow \pi^o \mu e$.

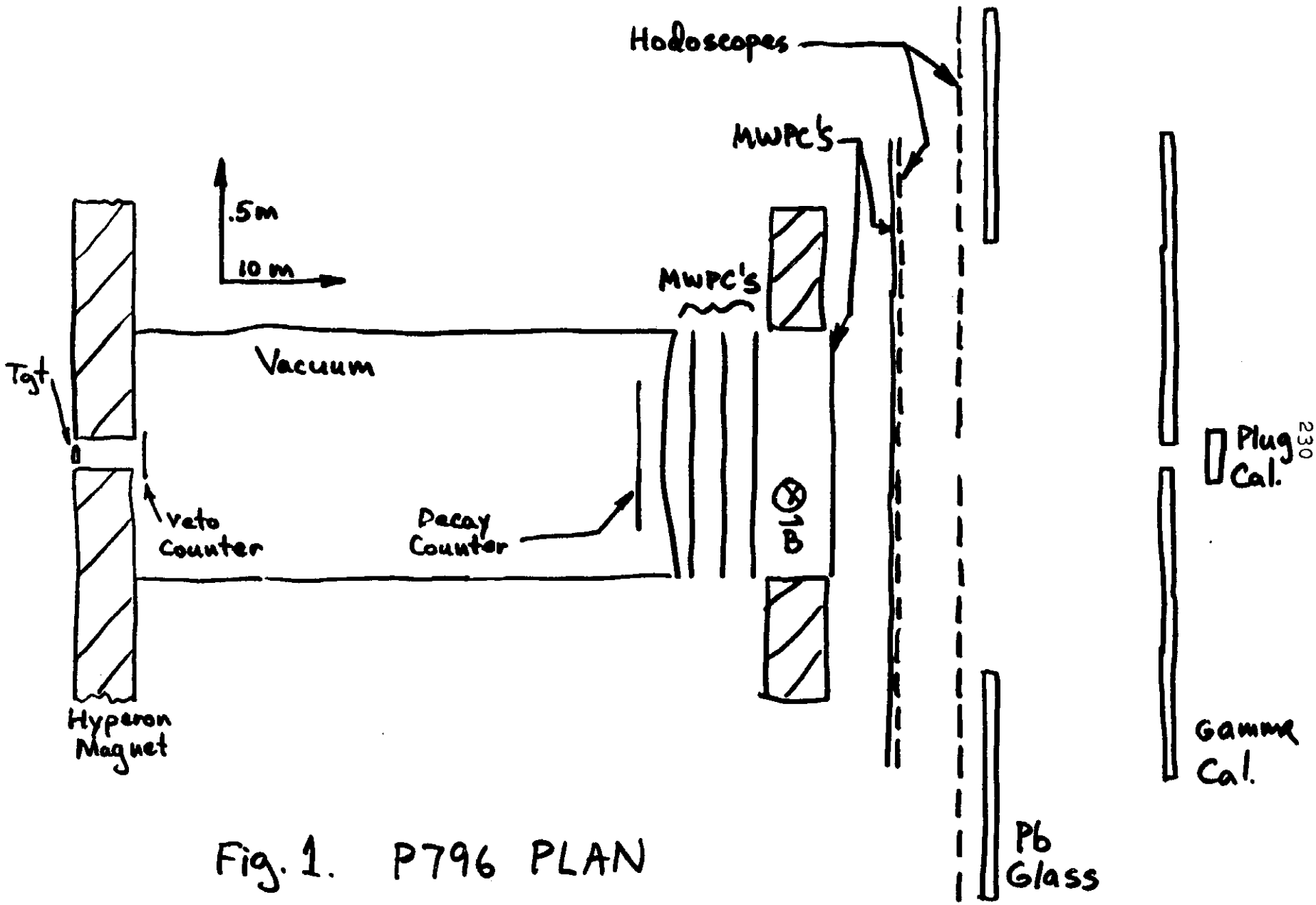

Fig. 1. P796 PLAN

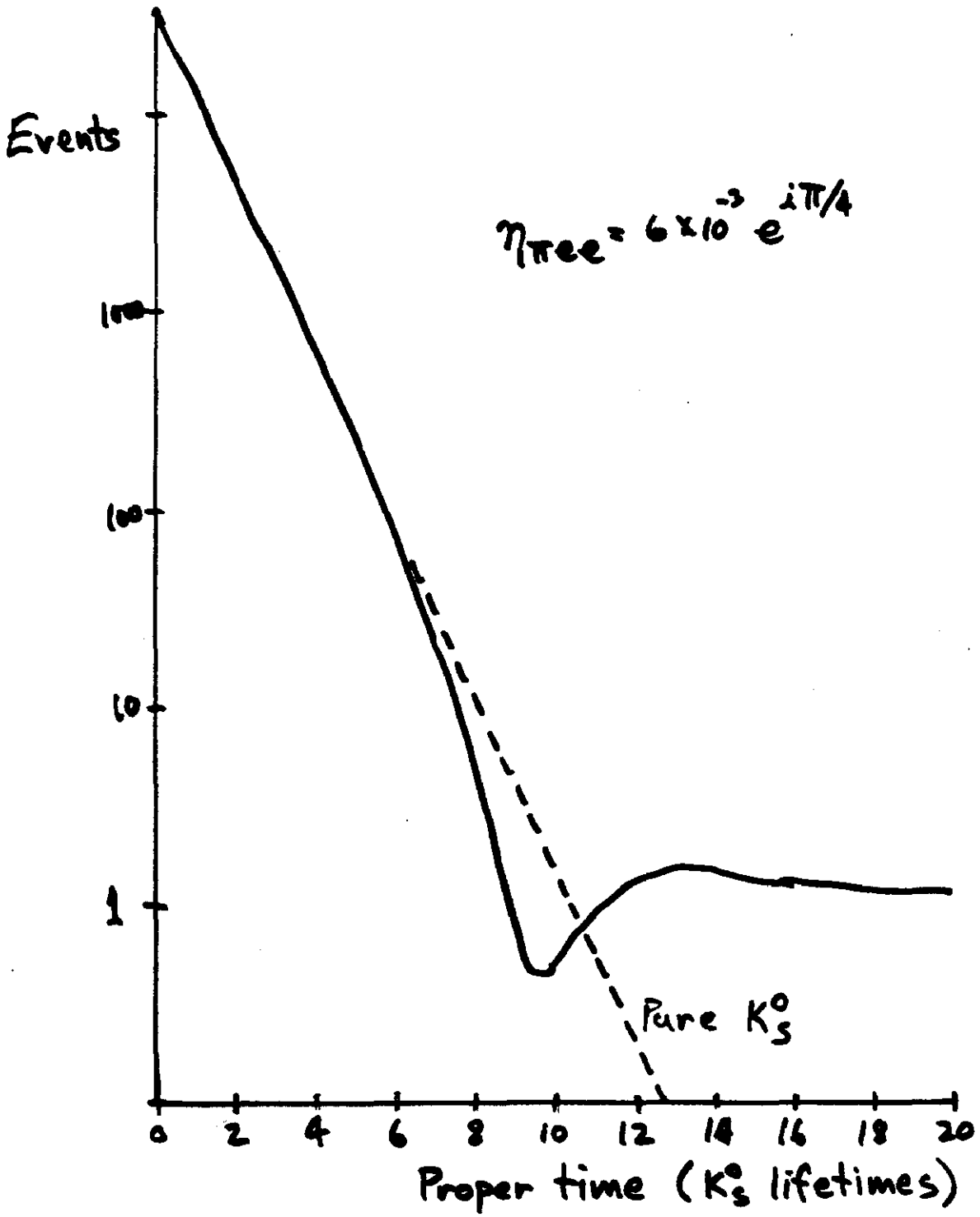

Fig. 2. $\frac{dN}{dt}$ for $K^0 \to \pi^0 e^+ e^-$

BACKGROUNDS FOR $K_L \rightarrow \pi^0 e^+ e^-$

Taku Yamanaka
Fermilab
P.O.Box 500, Batavia, IL 60510

Abstract

In the Fermilab Tevatron experiment E799, the major backgrounds for $K_L \rightarrow \pi^0 e^+ e^-$ will be K_L Dalitz decay or radiative Ke3 decay with an overlapped accidental cluster, which are at a level of 5×10^{-12}. These are also expected to be the major background sources in the Main Injector $K_L \rightarrow \pi^0 e^+ e^-$ experiment.

Backgrounds in General

Backgrounds for $K_L \rightarrow \pi^0 e^+ e^-$ can come from a K_L decay with a combination of a) missing particles (mostly γ's), b) particle misidentification (π/e), and c) overlay with accidental clusters. The background level is given by :

$$BG = \prod_i BR_i \prod_j \pi/e_j \frac{A(bkg)}{A(\pi^0 e^+ e^-)} [R_{accid}], \qquad (1)$$

where BR_i are the branching ratios involved, π/e_j is the probability of misidentifying a pion as an electron, A(bkg) is the acceptance of the background, $A(\pi^0 e^+ e^-)$ is the acceptance of the signal. If accidental photons are involved, then R_{accid} is the rate of the accidental photons.

Backgrounds for E799 at Fermilab

The background levels were estimated for E799 which will measure the branching ratio of $K_L \rightarrow \pi^0 e^+ e^-$ at the FNAL Tevatron[1]. The parameters used for the estimates are : $30 < E_K/\text{GeV} < 150$, 59m decay volume, four drift chambers with 110μm resolution, lead glass calorimeter with a resolution of $1.5+5/\sqrt{E}$ %, and a transition radiation detector (TRD) with a π/e rejection of 10^{-2}. The lead glass and the spectrometer give another π/e rejection of 10^{-2} from E/p. The full-blown Monte Carlo for the E731 ε'/ε analysis was used for the background simulation. Special events which were triggered randomly during the E731 run were overlayed on Monte Carlo events to simulate the backgrounds which involve accidental clusters in the glass. The accidental probabilities at 2×10^{12} protons per pulse are

0.12 (>=1 cluster) and 0.024 (>=2 clusters).

In the analysis, the following kinematics were required; four clusters in the calorimeter, two tracks in the chamber system, $125\text{MeV/c}^2 < m_{\gamma\gamma} < 145\text{MeV/c}^2$, $489\text{MeV/c}^2 < m_{ee\gamma\gamma} < 507\text{MeV/c}^2$, $m_{ee} > 150\ \text{MeV/c}^2$ (to reject π^0 Dalitz decay), and $P_t^2 < 100(\text{MeV/c})^2$. The mass resolution for $\gamma\gamma$ and $ee\gamma\gamma$ are 5MeV/c^2, and P_t^2 has σ of $20(\text{MeV/c})^2$. The overall acceptance for the signal is 10%.

The background levels are summarized in Table 1 under column E799. The numbers with unequal sign give the upper limit with 90% CL. The major backgrounds are K_L Dalitz decay or radiative Ke3 associated with overlapping accidental clusters, which give the background level of $5.3\text{x}10^{-12}$ and $2.2\text{x}10^{-12}$, respectively.

Background Level at the Main Injector

The background levels at the Main Injector can be roughly estimated by scaling the ones for E799 as follows.

$$BG_{MI} = BG_{E799}\, r_{\Delta E}^3 \prod_{all\ \pi} (r_{\Delta E} r_{TRD})[r_{\Delta t}\, r_{acc}], \qquad (2)$$

where BG_{MI} and BG_{E799} are the background levels at the Main Injector and E799, and r_k ($k=\Delta E, TRD, \Delta t, acc$) are the ratios of parameters between the Main Injector experiment and E799. ΔE is the energy resolution of the calorimeter at the typical e/γ energy, *TRD* is the π/e rejection factor of the TRD, Δt is the timing resolution of the detector, and *acc* is the rate of accidentals. Here, we will assume that the Main Injector experiment has the same geometrical acceptance ratio between the background and signal as E799.

The photon energy resolution, ΔE, can contribute to reduce the backgrounds in cube, because of three cuts on $m_{\gamma\gamma}$, $m_{ee\gamma\gamma}$, and P_t^2. It also contributes to π/e rejection by the E/p resolution. A better TRD can help to further improve the π/e rejection factor. The accidental probability can be reduced by improving the timing resolution of the detector, Δt. It can also be reduced by detecting the particles associated with the accidentals. If most of the accidental photons are coming from $3\pi^0$ decays, detecting at least one of the six photons will in principle eliminate accidental photons from this source.

At E799, the energy resolution of lead glass for a typical e/γ energy is about $1.5+5/\sqrt{15}=2.8\%$. If we use BaF_2 for the Main Injector and assume the resolution of $1+1.5/\sqrt{E}$ % and the average e/γ energy of 5GeV, then it gives an energy resolution of 1.7%. The π/e rejection of the TRD can be improved from 10^{-2} to $5\text{x}10^{-3}$. The timing resolution of the detector (especially the calorimeter) can be reduced from 20ns to 1ns. Let us also assume that we manage to control the accidental rate increase by a factor of 10 even

though the kaon rate goes up by two orders of magnitude. By plugging $r_{\Delta E}$=1.7/2.8=0.6, r_{TRD}=5x10^{-3}/10^{-2}=0.5, $r_{\Delta t}$=1/20, and r_{acc}=10 in equation (2), we can calculate the background levels at the Main Injector. The estimated values are listed in Table 1 under the Main Injector column.

The main background is K_L Dalitz decay with one accidental, which is 5.8x10^{-13}. The ee$\gamma\gamma$ mass is slightly higher than the kaon mass because of the additional gamma, and we are looking at the tail of this peak. The energy resolution is crucial for this background. Other potential backgrounds are K_{e3} and radiative K_{e3} decays with 1 or 2 accidentals, which are order of 10^{-13}.

From this rough estimate, we conclude that the energy resolution of the calorimeter has to be better than 1+1.5/$\sqrt{E}$ %, the π/e rejection factor of the TRD has to be better than 5x10^{-3}, the timing resolution has to be better than 1ns, and the accidental rate compared to the kaon rate has to be less than 10 times smaller than E799.

It should be noted that these extrapolations are only good to orders of magnitude, and more detailed Monte Carlo studies will be done at workshop at Breckenridge in August.

Reference

1. Y.Wah and T.Yamanaka, A Proposal to Search for the Rare Kaon Decay Mode $K_L \rightarrow \pi^0 e^+ e^-$, FNAL proposal (1988)

Table 1. Summary of backgrounds

Mode	ΠBR	#π	#acc	E799	Main Injector
$K_L \to \pi^0\pi^0$, $\pi^0 \to e^+e^-\gamma$	1.2×10^{-5}	0	0	$<8.7\times10^{-14}$	$<1.9\times10^{-14}$
$K_L \to \pi^0\pi^0$, $\pi^0 \to e^+e^-e^+e^-$	3.0×10^{-8}	0	0	$<3.7\times10^{-13}$	$<8.2\times10^{-14}$
$K_L \to \pi^0\pi^0$, $\pi^0 \to e^+e^-\gamma$, $\pi^0 \to e^+e^-\gamma$	1.4×10^{-7}	0	0	$<3.3\times10^{-12}$	$<7.3\times10^{-13}$
$K_L \to \pi^+\pi^-\pi^0$, (e^+e^-)	1.2×10^{-1}	2	0	$<9.9\times10^{-14}$	$<2.0\times10^{-15}$
$K_L \to \pi^+\pi^0e^-\nu$, (e^+)	6.2×10^{-5}	1	0	$<1.6\times10^{-13}$	$<1.0\times10^{-14}$
$K_L \to e^+e^-\gamma + \gamma_{acc}$ or $K_L \to e^+e^-\gamma + 2\gamma_{acc}$	1.7×10^{-5}	0	1	5.3×10^{-12}	5.8×10^{-13}
$K_L \to \pi^+\pi^-\gamma + \gamma_{acc}$, (e^+e^-)	4.0×10^{-5}	2	1	1.1×10^{-17}	1.1×10^{-19}
$K_L \to \pi^+e^-\nu\gamma + \gamma_{acc}$, (e^+)	1.9×10^{-2}	1	1	2.2×10^{-12}	7.1×10^{-14}
$K_L \to \pi^+e^-\nu + 2\gamma_{acc}$, (e^+)	3.9×10^{-1}	1	2	$<8.0\times10^{-12}$	$<2.6\times10^{-13}$

BACKGROUND ESTIMATE FOR $K_L \to \pi^0\mu^+\mu^-$ WITH A MAIN INJECTOR FIXED TARGET BEAM AND DETECTOR

K. Lang
Physics Department
Stanford University, Stanford, CA 94305

Y. W. Wah
The Enrico Fermi Institute and The Department of Physics
The University of Chicago, Chicago, IL 60637

A high sensitivity search for the as yet unobserved neutral kaon decay mode $K_L \to \pi^0\mu^+\mu^-$ provides an attractive avenue to explore 'direct' CP violation. It complements the effort in searching for $K_L \to \pi^0 e^+e^-$. These processes have been studied theoretically[1-6] and their branching ratio predictions range from i) for $K_L \to \pi^0 e^+e^-$, $\sim 10^{-9}$ to $\sim 10^{-11}$, ii) for $K_L \to \pi^0\mu^+\mu^-$, $\sim 10^{-10}$ to $\sim 10^{-12}$. Typically the muonic decay channel is suppressed by about a factor of five compared to that of the electronic channel mostly due to phase space.

Present experimental limits[7-9] are: B.R. $(K_L \to \pi^0 e^+e^-) < 4 \times 10^{-8}$ and B.R. $(K_L \to \pi^0\mu^+\mu^-) < 1.2 \times 10^{-6}$.

Here we estimate some of the principal sources of background assuming the 'Reference' beam and detector[10] for the measurement. Other assumptions include: 1) an 1000 hours run with 6×10^{13} integrated kaon flux; 2) acceptance of 0.2 with a fiducial decay length of 20m and with kaon energy >15 GeV. We emphasize that the detector should have superior 1) momentum resolution (maybe with two analyzing magnets); 2) vertex resolution; 3) $\pi/\mu/e$ identification (TRD; electromagnetic and hadronic calorimeter); 4) high rate and finely segmented EM calorimeter and 5) photon vetos hermeticity.

The background to $K_L \to \pi^0\mu^+\mu^-$ could be classified into two categories: (1) due to overlaps of an accidental π^0 with other copious kaon decay modes with two tracks reconstructed as muons; (2) $K_L \to \pi^+\pi^-\pi^0$ decay with both $\pi^+\pi^-$ decay in flight to muons.

The first category background is dominated by the following three cases, (i) $K_L \to \pi^{\pm}\mu^{\mp}\nu + \pi^0_{accid}$; (ii) $K_L \to \pi^+\pi^- + \pi^0_{accid}$, and (iii) $K_L \to \pi^+\pi^-\gamma + \gamma_{accid}$ with the pions either decayed or misidentified as muons. The contribution from case (i) could be estimated by the product of the following factors:

B.R. $(K_L \to \pi\mu\nu)$	= 0.27
B.R. $(K_L \to 3\pi^0)$	= 0.21
Acceptance $(K_L \to \pi\mu\nu)$	= 0.20
Acceptance (π^0 from $K_L \to 3\pi^0$)	= 10^-4
π/μ rejection assumed (from calorimeters)	= 10^{-5}
Kinematics + geometric rejection	= 10^{-6}
Time resolution $\tilde{}$ 1.5ns	= 1.5×10^{-9}
Integrated kaon flux[2]	= 3.6×10^{27}

The above corresponds to about 60 events.

The second category background could be considered by three cases, namely (i) both pions decay before the tracking system; (ii) both pions punch through the calorimeter, and (iii) one pion decays and the other one punches through. With the assumption that π/μ rejection is $\sim 10^{-5}$, then case (ii) is negligible with respect to the other two. The related background with pion decays within the tracking system (between chambers and inside magnets) need a realistic simulation and is not considered here.

The background contribution from case (i) is then:

Probability of first pion decays to muon	= 0.05
Probability of second pion decays to muon	= 0.05
Kinematics rejection with mass mis-assignment	= 5×10^{-5}
Vertex resolution rejection	= 10^{-4}

B.R. $(K_L \to 3\pi)$	= 0.27
Acceptance	= 0.20
Integrated kaon flux	= 6×10^{13}

The above corresponds to about 4 events.

For case (iii), the contribution is:

Probability of pion decays to muon	= 0.05
Probability of pion punch through	= 10^{-5}
Kinematics rejection with mass mis-assignment	= 7×10^{-3}
Vertex resolution rejection	= 10^{-3}
Acceptance	= 0.20
B.R. $(K_L \to 3\pi)$	= 0.27
Integrated kaon flux	= 6×10^{13}

The above corresponds to about 11 events.

Assuming B.R. $(K_L \to \pi^0 \mu^+ \mu^-) \sim 10^{-11}$, this 1000 hr data run yields a 100 events signal. A detailed background simulation would be needed to address many open questions, e.g. the needed realistic performance and other potential background sources. The challenge to achieve π/μ rejection of 10^{-5} and kinematic rejection of 10^{-6} is of most concern.

REFERENCES

1. J.F. Donoghue, B.R. Holstein, and G. Valencia, Phys. Rev. D35, 2769 (1987).
2. G. Ecker, A. Pich, and E. deRafael, Nucl. Phys. B303, 665 (1988).
3. C.O. Dib, I. Dunietz, and F. Gilman, Phys. Rev. D39, 2639 (1989).
4. F. Flynn and L. Randall, Phys. Lett. B216, 221 (1989).
5. T. Morozumi and H. Iwasaki, KEK Preprint TH-206 (Apr 1988).
6. L.M. Sehgal, Phys. Rev. D38, 808 (1988).
7. L.K. Gibbons et al., Phys. Rev. Lett. 61, 2661 (1988).
8. G.D. Barr et al., Phys. Lett. 214B, 303 (1988).
9. A.S. Carroll et al., Phys. Rev. Lett. 44, 525 (1980).
10. B. Winstein, G. Bock, and R. Coleman, University of Chicago Preprint EFI-89-01 (Jan 1989); Fermilab document 'Fermilab Fixed Target Beams from the Main Injector' (May 1989).

A Study of Electromagnetic Calorimeters by EGS

Hitoshi Yamamoto

Enrico Fermi Institute, University of Chicago,Chicago,IL,60637.

Abstract Electromagnetic showers in a transparent block-type calorimeter have been studied using EGS[1]. It is shown that there are compensating effects between leakage and light attenuation both in non-linearity and energy resolution. Also, related considerations on some of new materials for calorimetry are given.

Introduction What we are concerned here is an electro-magnetic calorimeter which is sampled at the back end by a photomultiplier or an alternative photo-sensitive device. In such a calorimeter, non-linearity is often dominated by shower leakage off the back and light attenuation through the block. Also, longitudinal shower fluctuation contributes substantially to final energy resolution (comparable to or dominating photo-electron statistics). In order to study these effects quantitatively, we have simulated showers in a lead-glass calorimeter[2] using EGS program.

Electron Shower Simulation The inputs are longitudinal size of block (z_0), attenuation coefficient per radiation length (α), and the electron energy (E GeV). The transverse dimension of the block is assumed to be infinite. Electrons enter the block perpendicular to the front face and each path of charged particle is weighted by Cerenkov light output:

$$1 - \frac{1}{\beta^2 n^2}.$$

where β is the velocity of the charged particle, and n is the index of refraction of the lead-lgass (=1.64). For a given event, the total amount of light reaching the end $I(E, \alpha, z_0)$ is then given by

$$I(E, \alpha, z_0) = \int_0^{z_0} f(z) \exp(-\alpha(z_0 - z)) dz$$

where f(z) is raw light output as a function of z. For a completely transparent block of infinite length, no non-linearity was observed within statistical error (less than 0.1%). Even for such an idealized case, the simulation predicts an intrinsic light fluctuation which is well parametrized by $1.4\%/\sqrt{E}$.

To the extect the leakage off the back can be neglected, the closer the shower to the front end, the more light is attenuated. Thus, one expect less light per GeV for

smaller energy showers. Fig.1 shows the light output normalized to the ideal case of perfect transparency and full containment:

$$< I(E, \alpha, z_0) > / < I(E, 0, \infty) >,$$

where the bracket indicates average over showers. The drop near $E = 0$ is due to the above mentioned effect due to the motion of shower max as a function of E. The leakage causes the slow decrease as a function of E for $z_0 = 16X_0$ and for low values of α. The curve is nearly flat for $E > 10$ GeV, $\alpha > 3.8\%$, and $z_0 = 16X_0$; this is caused by compensation of leakage and light attenuation. In fact, the compensation of the two effects is much more dramatic in energy resolution.

The fluctuation of mean shower depth is of order 1 radiation length for electrons (it is larger for photons); thus, this fluctuation coupled to the attenuation results in fluctuation in amount of light collected. Also, the longitudinal fluctuation results in fluctuation of leakage off the back. Since the leakage is expected to be larger when the shower fluctuates closer to the back, the two effects tend to compensate each other.

Fig. 2 shows the energy resolution as function of E, α, and z_0. The photo-electron statistics (typically 0.5 to 1 photo-electrons per MeV) is not included. The curves are not smooth due to the statistics of shower generation. The effect of the compensation is clearly seen; e.g. for $z_0 = 16X_0$, the best resolution for 20 GeV is obtained for α of about 3.4% rather than for better transparencies. Thus, there is an optimum block length for given attenuation and energy. If both attenuation and length can be chosen at will, however, the best resolution is always obtained for $\alpha = 0$ and $z_0 = \infty$.

Photon Showers A photon shower is a pair of electron showers generated at a depth d, where d is distributed exponentially with mean depth of $9/7\ X_0$. This results in a larger longitudinal shower fluctuation than for electrons; thus, the leakage-attenuation compensation is different for photons; quantitative study of optimization for photon energy resolution has not been completed. The deeper shower also means that the amount of light per GeV for photon is greater than for electrons (assuming that leakage is small). Fig. 3 shows the ratio of electron response to photon response for $z_0 = 20X_0$. For the same energy, the light output of photon is typically a few percent larger than for electron.

New Materials PbF_2 has been attracting renewed attentions[3] as a dense Cerenkov material for calorimetry. It has a short radiation length (0.98 cm) and relatively cheap. An EGS simulation was performed to estimate the light output of PbF_2, and the result is shown in Table 1 together with corresponding numbers for lead-glass (F-2).

	X_0(cm)	n	total path (cm)	#γ/GeV/eV
Pb-glass	3.13	1.64	717/GeV	33.3K
PbF_2	0.98	1.86	310/GeV	18.9K

Table 1

The total path of charged particles in a 1 GeV shower is shorter for PbF_2 due to its density; accordingly, the light output per unit band width (ev) for PbF_2 is about 60% of lead-glass. The useful band width of PbF_2, however, is much larger than lead-glass, which is expected to more than compensate its low unit light yield. If PbF_2 can be manufactured with good transparency (about 1% per radiation length) and if it withstands high radiation, then it could be a good contender for the next generation of calorimeter material.

The same consideration of non-linearity and resolution as given above can be applied to new scintillating materials such as BaF_2 and pure CsI etc. For the scintillators, however, the transverse size of shower was found to be 20 to 30% larger than for Cerenkov material of same Moliere radius. This is because the velocity of particles away from the shower core is more likely to be below Cerenkov threshold, while there is no such suppression for scintillation light.

References

1. R. Ford and W. Nelson, SLAC-210 (1978).
2. Schott F-2. This study was conducted as a part of the analysis for E731 at Fermilab. See J. R. Patterson, PhD thesis, University of Chicago, 1990 (unpublished).
3. D. Anderson, in this proceedings.

Figures

1. Light output normalized to the ideal case of perfect transparency and full containment, plotted for various values of attenuation coefficient α and block length z_0.
2. Energy resolution without including the photo-electron statistics.
3. Ratio of the light yield of electron shower to that of photon shower of the same energy ($z_0 = 20X_0$).

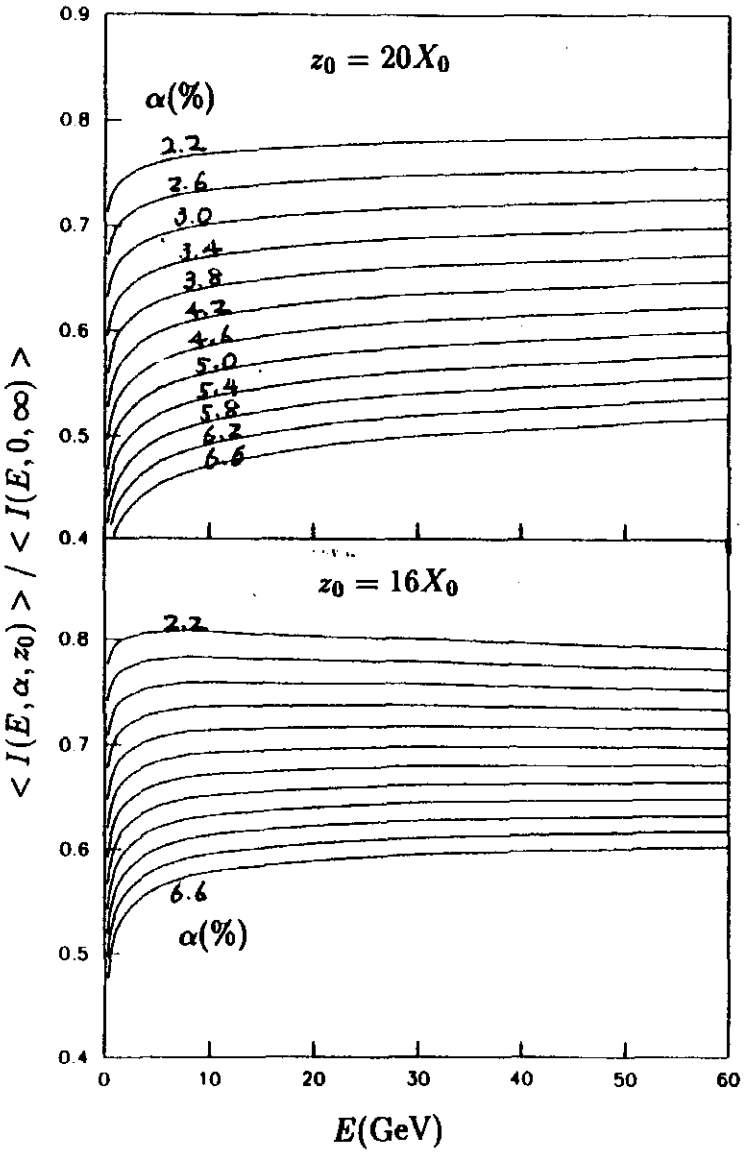
$z_0 = 20X_0$
$\alpha(\%)$
2.2
2.6
3.0
3.4
3.8
4.2
4.6
5.0
5.4
5.8
6.2
6.6
$z_0 = 16X_0$
2.2
6.6
$\alpha(\%)$
$< I(E,\alpha,z_0) > / < I(E,0,\infty) >$
E(GeV)

Fig. 1

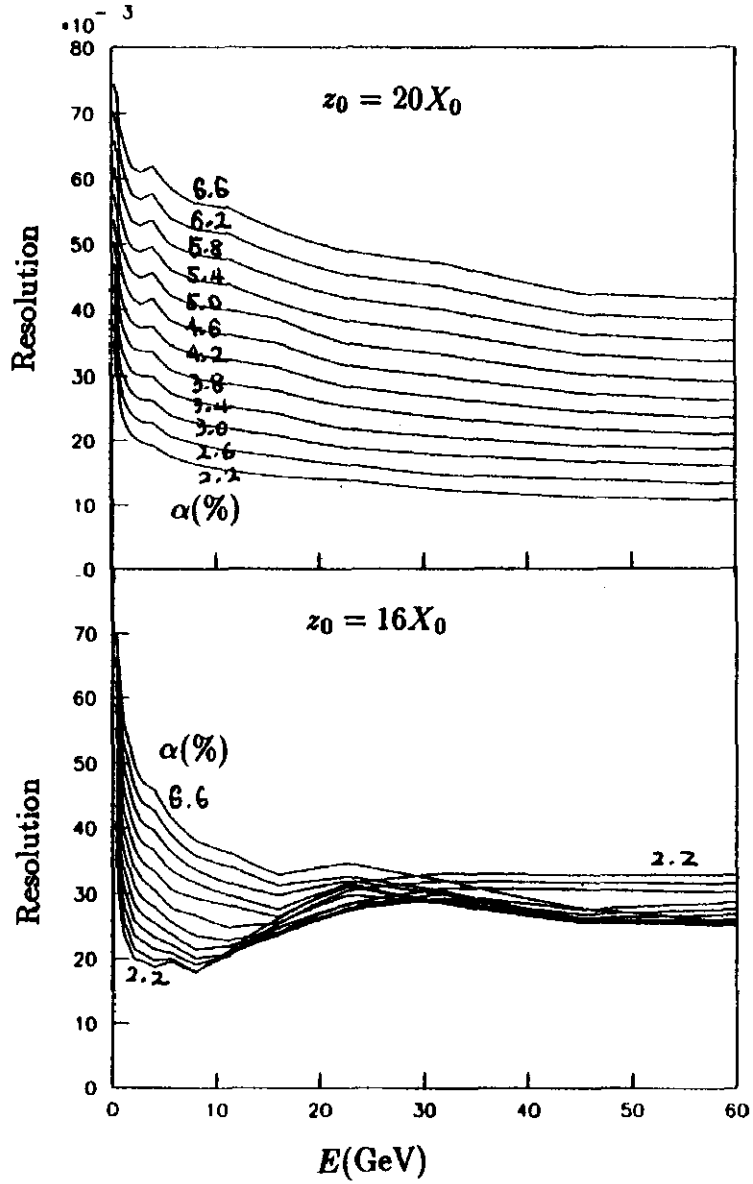
$\cdot 10^{-3}$
$z_0 = 20X_0$
6.6
6.2
5.8
5.4
5.0
4.6
4.2
3.8
3.4
3.0
2.6
2.2
$\alpha(\%)$
$z_0 = 16X_0$
$\alpha(\%)$
6.6
2.2
2.2
Resolution
Resolution
E(GeV)

Fig. 2

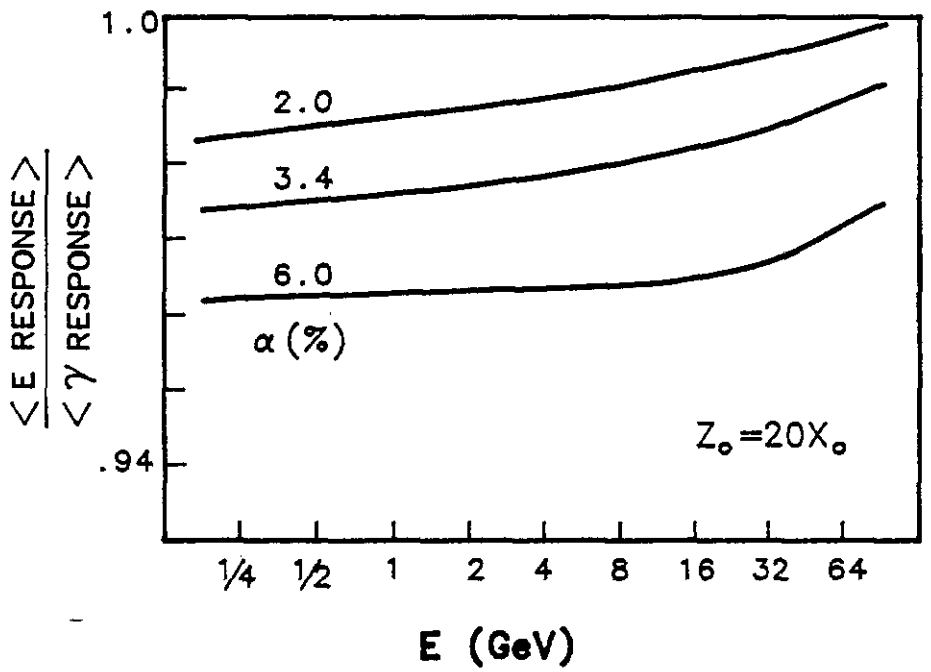
1.0
.94
2.0
3.4
6.0
α (%)
$Z_o = 20X_o$
$\frac{\langle E \text{ RESPONSE} \rangle}{\langle \gamma \text{ RESPONSE} \rangle}$
¼ ½ 1 2 4 8 16 32 64
E (GeV)

Fig. 3

TETRABROMOETHANE AS A RADIATION HARD ELECTROMAGNETIC CALORIMETER

S. Teige

Department of Physics and Astronomy, Rutgers—The State University of New Jersey, Piscataway, New Jersey 08854

Abstract

I have identified a liquid with radiation length and transmission properties similar to lead glass. If this material proves suitable it will be possible to achieve the energy resolution of lead glass without the difficulties associated with radiation damage.

Liquid Cerenkov Radiators

I have been investigating high density liquids for use as Cerenkov radiators. If a suitable liquid material could be identified there are many possible advantages to be gained. For example, radiation damage in typical Cerenkov radiators is associated with the solid state of the material. Liquids may have much higher intrinsic radiation hardness, giving a large factor in the useful life of a detector. It may also prove possible to replace or chemically purify a liquid while the detector is operating. This could, in principle, give such a detector an infinite lifetime. This long lifetime would allow a main injector experiment to survive long enough to probe rare processes or make high precision measurements of CP-violation parameters.

Kusumegi *et al.* investigated a saturated solution of thallium salts in water as a possible material. Their results [1] were somewhat disappointing because they could not produce a solution of sufficient clarity to achieve good energy resolution. The radiation length of the

solution they obtained was 2.57 cm. Using current prices [2] the cost of this material is $8.30 per $cm^2 \cdot$ radiation length. Thallium compounds are extremely toxic so containment and disposal costs will be considerable.

Work in Progress

I have identified tetrabromoethane (also known as acetylene tetrabromide), $(CHBr_2)_2$, as a promising candidate and have begun to investigate its properties. Tetrabromoethane is produced by exposing acetylene (a common welding gas) to bromine. Tetrabromoethane is available in industrial quantities since it is used commercially in the production of Dacron. I have obtained a sample of this material and have made transmission measurements. Its density is 2.964 grams/cc and its radiation length is 4.0 cm. When bought in lots larger than 170 Kg its price is $ 0.049 /($cm^2 \cdot$ radiation length).

Figure 1 shows the transmission of the material taken right after I got the sample. The fresh material was also treated by exposing it to metallic zinc for 24 hours. It was suspected that any free bromine in solution would form zinc bromide (a colorless crystal) and would therefore be removed from solution. The improvement in the transmission is evidence that this is the case. (see Fig. 2) This is a particularly attractive feature of this material. A simple tube filled with zinc gauze connected to by a pump to the detector could be used in an operating detector to remove free bromine generated by radiation disassociation of the tetrabromoethane. The method of manufacturing this material also suggests a method for removing bromine. It would be easily possible to bubble acetylene through a column connected to the detector thereby forming compounds similar to tetrabromoethane and removing the free bromine.

The sample I examined, when fresh, was not visibly discolored. After a few weeks the sample was examined again and found to be somewhat brown. Su Yumin [3] has examined the causes of this deterioration and determined that it can be dramatically reduced by the addition of a small quantity of a free radical scavenger, 1,3,di-*tert*-butyl-2-hydroxy-5-methyl-benzene, also known as BHT. The conclusion as to the cause of the deterioration was to an accumulation of free bromine molecules and radicals. Another component of the deterioration was the accumulation of polymers created by reactions of the fragments produced when bromine was removed from the tetrabromoethane. It was claimed that this process produced a cloudy discoloration. I have not observed this effect and it is claimed to take place on a time scale of several years. The addition of BHT also suppresses this deterioration mechanism. Addition of methylal, a known polymerization suppressant, may also help. Several other methods for color stabilization have also been suggested. [4]

I am in the process of evaluating these procedures. The results of Su Yumin are encouraging. It was reported that the material could be stabilized and remain nearly colorless for as long as two years.

Conclusion

The possibility of constructing large, low cost, radiation hard electromagnetic calorimeters based on liquid Cerenkov radiators is being investigated. Some promising results have been obtained and interesting avenues for future investigation have been identified. The possibility of repairing radiation damage in an operating detector is particularly attractive for a main injector calorimeter.

References

[1] A. Kusumegi and K. Kondo, Nucl. Instr. and Meth. **177** (1980) 605, A. Kusumegi *et al.* Nucl. Instr. and Meth. **185** (1981) 83, A. Kusumegi *et al.* Nucl. Instr. and Meth. **196** (1982) 231

[2] The prices in the current Kodak catalog are $112.50 for 100 grams of thallium formate and $363.00 for 100 grams of thallium malonate. Kusumegi *et al.* used pure thallium formate as did I when I estimated the cost. When bought in large quantities the price may be significantly reduced.

[3] Su Yumin, Tianjin Daxue Xuebao No.2 (1988) 91.

[4] Published information on this topic is difficult to come by since most of the work has been done by private corporations for profit. I have found information in the form of abstracts of patent applications. The suggestion of using styrene oxide to stabilize tetrabromoethane comes from US patent 3876712 (John H. Rains,Ethyl Corp.). The idea of using epichlorohydrin, epibromohydrin or propylene oxide is from West German patent DE 1443641 (Herbert Jenkner, Chemische Fabrik Kalk).

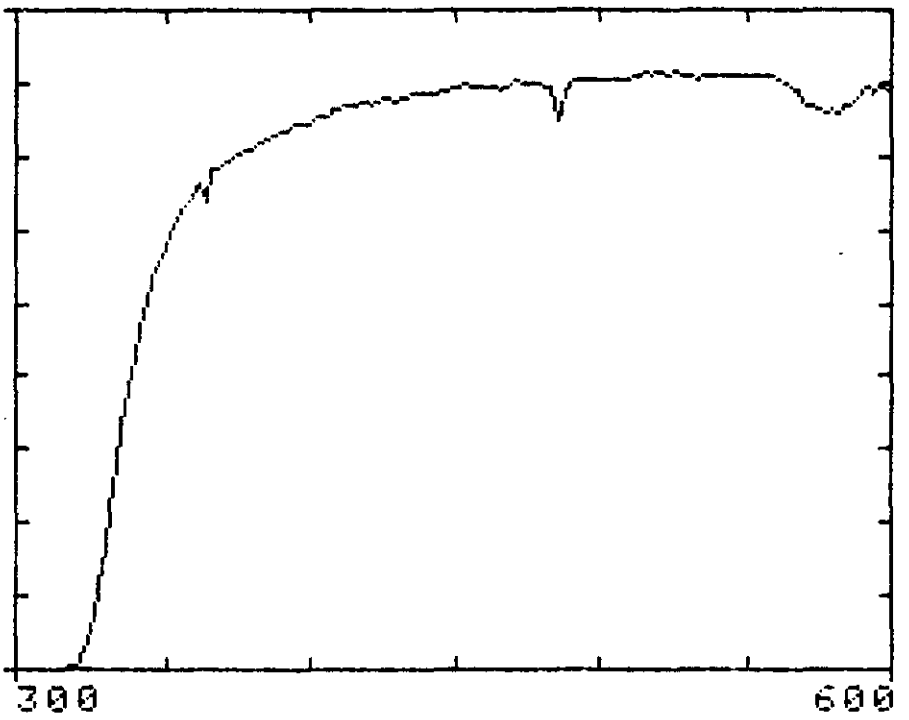

FIG. 1. The transmission of practical grade tetrabromoethane. horizontal scale is in nanometers, vertical scale is arbitrary but the value in the flat region is believed to be near 100%

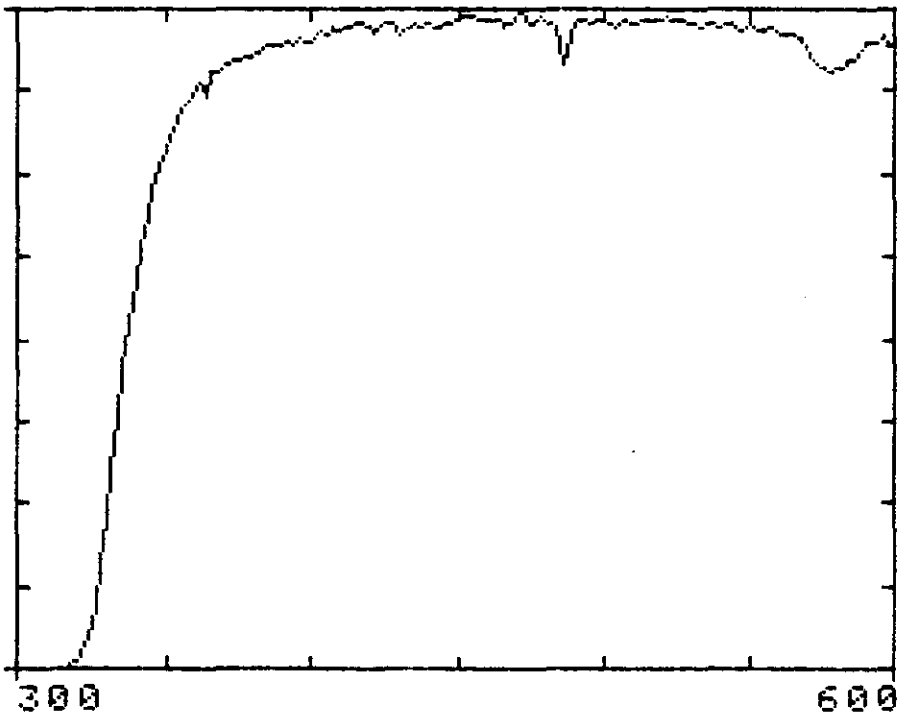

FIG. 2. The transmission of practical grade tetrabromoethane after being exposed to metallic zinc for 24 hours. I believe that the free bromine in the sample reacted with the zinc to form zinc bromide and so was removed from solution.

UM – HE – 89 – 20
June 27, 1989

Studies of Neutron Polarization Phenomena with 120-150 GeV Protons

LAWRENCE W. JONES*

University of Michigan
Ann Arbor, MI 48109

Abstract

It is proposed to have a neutral beam line from the new Main Injector to study and utilize polarized neutrons.

The polarization of neutrons is an area of strong interactions on which up until now, there is absolutely no data at multi-GeV energies. Such studies are made possible by utilizing a phenomenon first discussed by Schwinger;[1] in the scattering of neutrons from a nuclear target there is almost 100% polarization at angles where the nuclear scattering amplitude (which is almost purely imaginary) and the "Coulomb" amplitude (scattering of the neutron magnetic moment by the nuclear charge; a purely real amplitude) are equal. Such a scattering process thus provides both an effective polarizer and a convenient analyzer for neutrons. Neutron detection using an ionization calorimeter is a familiar technique, which has improved with better knowledge of calorimeter characteristics in recent years.

It is well known that hyperons are produced in proton collisions at high energy with surprisingly large polarization; up to about 30% in the case of Λ°, for example.[2] However no comparable measurement for neutrons has ever been undertaken. Neutrons are of course copiously produced in proton collisions at high energy; from inelastic interactions of protons on any nuclear target the leading baryon is a neutron about 25% of the time. Moreover the neutron spectrum is reasonably hard; from measurements at 400 GeV[3] it can be crudely fit to $(1\text{-}x)^2$, when integrated over $p_\perp$.

The program which would be attractive to pursue with the proposed new Main Injector is therefore as follows:

First, the Schwinger Effect should be verified in neutron scattering utilizing a double scattering experiment. This would involve production of a pencil neutron beam at about 0° by the protons of 120-150 GeV on a Be target, and subsequent analysis of this polarization by a second scattering. The neutrons would then be detected with an ionization calorimeter behind a position-sensitive neutron conversion vertex detector.

Second, neutrons produced inclusively by protons of 120-150 GeV on nuclear targets (*e.g.* Be) would be studied. Here the secondary neutron beam would be defined with a collimator and the the polarization studied with a single scatter from uranium. The calorimeter would flag each neutron energy; production angles would be varied by steering the incident proton beam onto the target, so that neutron polarization could be mapped vs E_n, $p_{\perp n}$.

Third, if the neutron polarization is comparable to that of Λ°, a polarized neutron beam would be established. Using this beam, polarization experiments could be carried out on np total cross sections, elastic scattering, and production processes, analogous to the program of proton experiments in E704, E706, and discussed for a polarized beam in the Main Injector.

Fourth, if this program is successful and if interesting physics develops, an extension to such a polarized neutron beam from 900-1000 GeV protons from the Tevatron could be considered.

The requirements on the Laboratory for this program are quite modest. They are dominated by the need for a 600-1000 meter straight beam line from the proton target. This, however, is a very modest line; for most of its length it would be simply a buried pipe. The end station and two or three intermediate sites would need be only 10-20 feet in cross sectional dimensions and 50-100 feet long. Neutron detection requires only a good calorimeter of a few tons preceded by a vertex detector. The beam should be transported mostly in vacuum. The most critical beam elements will be the collimators, which may have apertures as small as one or two mm and lengths of up to 2 meters of iron. They must be remotely controlled to permit precise alignment. Spin rotation may be achieved

easily using regular dipoles; a field integral of 5.13 Testa-meters perpendicular to the spin direction will rotate the neutron spin 180°, independent of neutron energy.

If the neutron beam is found to be polarized as much as are lambdas, a polarized neutron beam could then be produced as follows: A 120 GeV proton beam of about 2 x 10^{13} per pulse would strike a target at about 12 mr. The secondary neutron beam would then be produced at $p_\perp$ of about 1 GeV/c for E_n of 70 to 100 GeV, and a polarization (average) of about 15%. The flux of polarized neutrons utilized will then depend on the solid angle; with a rectangular aperture of 5 mr x 10 mr, the neutron flux in this window would be about 8 x 10^8 neutrons.

The motivations for focusing on the Main Injector for this program are the following: A calorimeter resolution of Δ E/E $\cong$ 50% $\sqrt{E}$ is readily achieved, corresponding to about 5% at 100 GeV. At much lower energies the poorer resolution becomes a limit to the accuracy with which P is measured. Also, at lower energies the physics is more muddled with other "soft" phenomena. However, at higher energies the beam line required, especially for the double scattering needed to study the Schwinger Effect, becomes difficult and more expensive. The polarizing/analyzing power of the Schwinger Effect is proportional to $(1\text{-}\rho^2)^{-1}$, where ρ is the ratio of real to imaginary amplitudes in NN scattering. This ratio passes through 0 at about 100 GeV, although even ρ of 0.2 results in a loss of only 4% in analyzing power.

The concept for this experiment grew out of discussions with J. Rosen, and his "Design of a High Energy Polarized Neutron Beam for NAL," a supplement to E-27. Our group developed a Fermilab proposal P-579, submitted in January 1978. Many details are contained in that proposal together with related addenda and responses to the Program Committee and laboratory management.

* Supported by the U.S. National Science Foundation.

Summarized below are a few useful relationships germane to this discussion.

Neutron-Uranium total Cross section at 100 GeV:	$\sigma(\mathrm{nU}) = 3.3 \times 10^{-24}\ \mathrm{cm}^2$
Differential n-U elastic scattering cross section at 0°:	$\left(\frac{d\sigma_e}{d\Omega}\right)_0(\mathrm{nU}) = 1.72 \times 10^{-18}\ \frac{\mathrm{cm}^2}{\mathrm{sr}}$
Neutron interaction mean free path in uranium:	$\lambda(\mathrm{nU}) = 120\ \mathrm{g/cm}^2$
Fraction of incident neutron flux scattered per sterad by a $(1/2)\lambda$ U scatterer:	$\frac{0.3}{\sigma}\left(\frac{d\sigma_e}{d\Omega}\right)_0 = 1.55 \times 10^5\ \mathrm{sec}^{-1}$
Transverse momentum for maximum polarization in n-U elastic scattering:	$p_{\perp 0} = \frac{4\pi\alpha Z\mu_n}{m_n\sigma(\mathrm{nU})} \cong 2.0\ \mathrm{MeV/c}$
Scattering angle corresponding to $p_{\perp 0}$ for 100 GeV neutrons:	$p_{\perp 0}/100\ \mathrm{GeV} = 20\mu$ radians
Relative scattering angle:	$q = p_\perp/p_{\perp o}$
Polarization vs $p_\perp$ away from $p_{\perp 0}$:	$P = \frac{2q}{(1+q)^2}(1+\rho^2)^{-1}$

REFERENCES

1. J. Schwinger, Phys. Rev. 73, 407 (1948). J. Rosen "Design of a High Energy Polarized Neutron Beam for NAL," Supplement to Proposal E-27.
2. G. Bunce, et al., Phys. Rev. Lett. 36, 1113 (1976), K. Heller, et al., Phys. Lett. 68B, 480 (1977).
3. L. W. Jones, et al., Proceedings of the X International Symposium on Multiparticle Dynamics, Goa, India (1980) p. 684.

IV.
List of Registrants

Proceedings of the Workshop on Physics at the Main Injector

List of Registrants

Areti, V. Hari	Fermilab
Barnes, Peter D.	Carnegie-Mellon University
Bernstein, Robert	Fermilab
Bjorken, James D.	Fermilab
Bock, Gregory	Fermilab
Brock, Raymond L.	Michigan State University
Bross, Alan D.	Fermilab
Brown, Charles N.	Fermilab
Bryman, Douglas	TRIUMF
Carrigan, Richard	Fermilab
Charlton, Gordon	U.S. Department of Energy
Childress, Sam	Fermilab
Coleman, Richard	Fermilab
Dimitroyannis, Dimitri	University of Maryland
Dugan, Gerald	Fermilab
Enagonio, Janice	Fermilab
Ferretti-Dalpiaz, Paola	University of Ferrara
Fowler, William	Fermilab
Gajewski, Wojciech	University of California, Irvine
Garbincius, Peter	Fermilab
Gilman, Frederick J.	Stanford University
Glass, George	Texas A & M University
Gollin, George	Princeton University
Goodman, Maury	Argonne National Laboratory
Heinson, Ann	University of California, Irvine
Holmes, Stephen	Fermilab
Imai, Kenichi	Kyoto University
Jensen, Douglas A.	University of Massachusetts
Jones, Lawrence W.	University of Michigan
Koizumi, Gordon	Fermilab
Koshiba, Masatoshi	Tokai University
Kycia, Thaddeus F.	Brookhaven National Laboratory
Lang, Karol	Stanford University
Lin, Ali M.T.	University of Michigan
Littenberg, Laurence S.	Brookhaven National Laboratory
Ma, Hong	Brookhaven National Laboratory
MacLachlan, James A.	Fermilab
Malensek, Anthony J.	Fermilab

Marciano, William J.	Brookhaven National Laboratory
Marlow, Daniel	Princeton University
McFarlane, W. Kenneth	Temple University
Menichetti, Ezio A.	INFN, Torino
Molzon, William	University of California, Irvine
Moore, Craig	Fermilab
Nezrick, Frank A.	Fermilab
Nishikawa, Koichiro	INS, University of Tokyo
Peaslee, David C.	University of Maryland
Pruss, Stanley	Fermilab
Rameika, Regina	Fermilab
Rapidis, Petros	Fermilab
Read, A. Lincoln	Fermilab
Reay, Neville W.	Ohio State University
Ritchie, Jack L.	University of Texas at Austin
Roberts, Jay	Rice University
Rosati, Marzia	McGill University
Rosen, Jerome	Northwestern University
Schmidt, Michael P.	Yale University
Schneps, Jack	Tufts University
Schultz, Jonas	University of California, Irvine
Seto, Richard	Nevis Laboratories
Shoemaker, Frank C.	Princeton University
Smith, Gerald A.	Penn State University
Sobel, Henry W.	University of California, Irvine
Stanton, Noel	Ohio State University
Staude, Arnold	CERN/University of Munich
Stefanski, Raymond	Fermilab
Stutte, Linda	Fermilab
Swallow, Earl C.	Elmhurst College/University of Chicago
Tartaglia, Michael	Michigan State University
Tschirhart, Robert	Princeton University
Tzanakos, George	Columbia University
Underwood, David	Argonne National Laboratory
Urheim, John	University of Pennsylvania
Wah, Yau W.	University of Chicago
Wahl, Heinrich	CERN
White, D. Hywell	Los Alamos National Laboratory
Winstein, Bruce D.	University of Chicago
Yamamoto, Hitoshi	Enrico Fermi Institute
Yamanaka, Taku	Fermilab
Yamanouchi, Taiji	Fermilab
Zioulas, George	McGill University